UNIVERSITY OF LATVIA

FACULTY OF CHEMISTRY

Doctoral thesis

Artūrs Zariņš

FORMATION, ACCUMULATION AND ANNIHILATION OF RADIATION-INDUCED DEFECTS AND RADIOLYSIS PRODUCTS IN ADVANCED TWO-PHASE CERAMIC TRITIUM BREEDER PEBBLES

Supervisor: Leading researcher, Dr. chem. Gunta Ķizāne

Scientific advisors: Dr. chem. Arnis Supe

Dr. rer. nat. Regina Knitter

RIGA

2018

ABSTRACT

Advanced lithium orthosilicate (Li_4SiO_4) pebbles with additions of lithium metatitanate (Li_2TiO_3) as a secondary phase are suggested as a potential candidate for the tritium breeding in future nuclear fusion reactors. In this doctoral thesis, for the first time the formation, accumulation and annihilation of radiation-induced defects (RD) and radiolysis products (RP) in the Li_4SiO_4 pebbles with various contents of Li_2TiO_3 are analysed and described under the simultaneous action of 5 MeV accelerated electrons and high temperature. To exclude the effects from technological factors, which could affect the formation and accumulation of RD and RP in the Li_4SiO_4 pebbles during irradiation, the influence of the noble metals, the pebble diameter, the grain size and the chemisorption products on the radiolysis is analysed and evaluated.

Key words: *Nuclear fusion, tritium breeding, lithium orthosilicate, lithium metatitanate, radiation-induced defects, radiolysis products.*

TABLE OF CONTENT

ABBREVIATIONS

ATR	Attenuated total reflectance
CFC	Carbon fibre composite
CFQ	Clear fused quartz
CL	Cathodoluminescence
D	Absorbed dose
DEMO	Demonstration fusion power plant
DTA	Differential thermal analysis
E_a	Activation energy
EDX	Energy dispersive X-ray spectrometry
ESR	Electron spin resonance spectrometry
EXOTIC	EXtraction Of Tritium In Ceramic
EU	European Union
FTIR	Fourier transform infrared spectrometry
G	Radiation chemical yield
GC	Gas chromatography
HCCB	Helium Cooled Ceramic Breeder
HCCR	Helium Cooled Ceramic Reflector
HCLL	Helium Cooled Lithium Lead
HCPB	Helium Cooled Pebble Bed
HICU	High neutron fluence Irradiation of pebble staCks for fUsion
ICP-OES	Inductively coupled plasma optical emission spectrometry
ITER	International Thermonuclear Experimental Reactor
JET	Joint European Torus
KALOS	KArlsruhe Lithium OrthoSlicate
LL	Lyoluminescence
LLCB	Lithium Lead Ceramic Breeder
MCS	Method of chemical scavengers
NIF	National Ignition Facility

P	Dose rate
PBA	Pebble Bed Assemblies
PIE	Post irradiation examination
p-XRD	Powder X-ray diffractometry
Q	Fusion energy gain factor
RAFM	Reduced activation ferritic martensitic steel
RD	Radiation-induced defects
RL	Radioluminescence
RP	Radiolysis products
SEM	Scanning electron microscopy
T	Temperature
TBM	Test Blanket Module
TBR	Tritium breeding ratio
TG	Thermogravimetry
TSL	Thermally stimulated luminescence
Tokamak	Russian acronym: ТОроидальная КАмера с МАгнитными Катушками
VV	Vacuum vessel
WCCB	Water Cooled Ceramic Breeder
W7-X	Wendelstein 7-X
XPS	X-ray photoelectron spectrometry
XRF	X-ray fluorescence spectrometry
XRL	X-ray induced luminescence
α	Radiolysis degree
β	Heating rate
ΔB_{pp}	Peak-to-peak line-width of ESR signal

INTRODUCTION

Lithium orthosilicate (Li_4SiO_4) and lithium metatitanate (Li_2TiO_3) in the form of ceramic pebbles have been developed as two of the most promising candidates for the tritium breeding in future nuclear fusion reactors [1]. The main task of the lithium-containing ceramic breeder pebbles is to produce and release tritium, nevertheless the ceramic breeder pebbles must be able to withstand the harsh operation conditions of the nuclear fusion reactor. Under the operation conditions of the nuclear fusion reactor, the ceramic breeder pebbles will be exposed to an intense neutron flux (up to 10^{18} n m^{-2} s^{-1}), ionizing radiation dose rate (up to 1 kGy s^{-1}), a high magnetic field (up to 7-10 T) and elevated temperature (up to 1190 K) [2-5]. The previous long-term neutron-irradiation experiments, such as PBA (Pebble Bed Assemblies) [6] and EXOTIC (EXtraction Of Tritium In Ceramics) [7-9], already confirmed that both the Li_4SiO_4 pebbles and the Li_2TiO_3 pebbles will perform sufficiently well under the expected operation conditions of the nuclear fusion reactor. However, it has also been reported [6] that the mechanical properties of the Li_4SiO_4 pebbles need to be improved, while the Li_2TiO_3 pebbles require a higher enrichment with lithium-6 isotope to increase the tritium production. The tritium breeding ratio (TBR) should be higher than 1.10 to ensure the tritium self-sufficiency of the nuclear fusion reactors, which will operate with a closed tritium-deuterium fuel cycle [10].

The advanced Li_4SiO_4 pebbles with additions of Li_2TiO_3 as a secondary phase are proposed as an alternative candidate for the tritium breeding in the nuclear fusion reactors in order to combine the advantages of both phases within one single tritium breeding ceramic [11]. The preliminary studies indicate that the advanced Li_4SiO_4 pebbles with additions of Li_2TiO_3 have acceptable properties for the tritium breeding: high lithium density, improved mechanical properties [11], appropriate melting temperature [12], good tritium release characteristics [13-15], low neutron activation behaviour [16] and chemical compatibility with structural materials [17]. While the re-melting and lithium re-enrichment studies [18] revealed that the recycling of the advanced Li_4SiO_4 pebbles, without a deterioration of the material properties, is possible using a melt-based process.

Problem. To develop a new two-phase chemical composition for the advanced ceramic tritium breeder pebbles, it is a critical issue to investigate and compare the behaviour of the Li_4SiO_4 pebbles with various contents of Li_2TiO_3 under the simultaneous action of radiation, temperature and magnetic field. Previous short and long-term neutron-irradiation studies [6-9, 19-23] showed that under such conditions various processes, like lithium burn-up, nuclear reactions, ionization, atomic displacements, radiation-induced processes (radiolysis) and phase

transitions, can take place and thus affect the phase composition and the microstructure, as well as the thermal and mechanical properties of the ceramic breeder pebbles. The accumulated radiation-induced defects (RD) and radiolysis products (RP), which are induced in the ceramic breeder pebbles by neutrons and ionizing radiation, can interact with the generated tritium and strongly influence the tritium diffusion and release processes. Previously, it has been reported [23] that the accumulation of RD and RP can increase the tritium retention up to 30 %. Most crucial are electron type RP, such as colloidal lithium (Li_n) particles, which can interact with the generated tritium and form thermally stable lithium tritide (LiT). The correlation between the tritium release and the thermal annealing of the accumulated RD and RP has been reported and described for various lithium-containing compounds by several authors [20-26], and it has been assumed that the recombination processes of RD and RP can trigger the tritium de-trapping from the ceramic breeder pebbles.

Solution. Additional research is required to investigate the formation, accumulation and annihilation of RD and RP in the Li_4SiO_4 pebbles with various contents of Li_2TiO_3 considering the simultaneous action of radiation, temperature and magnetic field. Such research is necessary to determine the parameters, which characterise the radiation stability, to evaluate the high-temperature radiolysis processes and to predict the possible tritium release temperature range of the advanced Li_4SiO_4 pebbles with additions of Li_2TiO_3 as a secondary phase. While to exclude the effects from technological factors, which could affect the formation and accumulation of RD and RP in the advanced Li_4SiO_4 pebbles during irradiation, it is essential to analyse and evaluate the influence of (1) the noble metals – platinum (Pt), gold (Au) and rhodium (Rh), (2) the pebble diameter, (3) the grain size, and (4) the chemisorption products of carbon dioxide (CO_2) and water (H_2O) vapour on the radiolysis.

The **aim of this doctoral thesis** was to investigate and describe the formation, accumulation and annihilation of RD and RP in the Li_4SiO_4 pebbles with various contents of Li_2TiO_3 under the simultaneous action of radiation and high temperature for the first time. In addition, the influence of various technological factors on the formation and accumulation of RD and RP in the Li_4SiO_4 pebbles was analysed and evaluated.

This doctoral thesis was aimed to evaluate a new two-phase chemical composition for the advanced ceramic breeder pebbles, which could be afterwards used as an alternative candidate for the tritium breeding in future nuclear fusion reactors. In this doctoral thesis, the flux of high energy accelerated electron beam (with energy up to 5 MeV and dose rate up to 35 kGy s^{-1}) was used instead of neutron irradiation to introduce RD and RP in the Li_4SiO_4 pebbles with various contents of Li_2TiO_3, while avoiding nuclear reactions and thereby the formation of radioactive

isotopes. The irradiation temperature (up to 1285 K) was chosen in order to reach conditions comparable to the operation conditions of the nuclear fusion reactors. The influence of external magnetic field on the formation and accumulation of RD and RP during irradiation was not analysed, since it is expected that the magnetic field does not change the qualitative composition of RD and RP, but only affects the formation probability of primary RD [27].

To achieve the aim of this doctoral thesis, the following **tasks** were proposed:

1) analysis of the formation and accumulation of RD and RP in the Li_4SiO_4 pebbles with various contents of Li_2TiO_3 under action of 5 MeV accelerated electrons to estimate and compare the parameters, which characterise the radiation stability,
2) study of the thermal stability and annihilation of the accumulated RD and RP in the irradiated Li_4SiO_4 pebbles with various contents of Li_2TiO_3 to predict the possible tritium release temperature range,
3) investigation of the behaviour of the Li_4SiO_4 pebbles with various contents of Li_2TiO_3 under the simultaneous action of 5 MeV accelerated electrons and high temperature to evaluate and described the high-temperature radiolysis processes,
4) evaluation of the influence of the noble metals (Pt, Au and Rh) with a sum content of up to 300 ppm on the radiolysis of the advanced Li_4SiO_4 pebbles with additions of Li_2TiO_3 as a secondary phase,
5) study of the influence of the pebble diameter and the grain size on the high-temperature radiolysis processes of the reference Li_4SiO_4 pebbles (without additions of Li_2TiO_3),
6) estimation of the factors, which can influence the formation and radiolysis of the chemisorption products of CO_2 and H_2O vapour, lithium carbonate (Li_2CO_3) and lithium hydroxide (LiOH), on the surface of the reference Li_4SiO_4 pebbles (without additions of Li_2TiO_3).

In this doctoral thesis, the formation and accumulation of paramagnetic RD and RP in the Li_4SiO_4 pebbles with various contents of Li_2TiO_3 under action of 5 MeV accelerated electrons were analysed by electron spin resonance (ESR) spectrometry. The thermal stability and annihilation of the accumulated RD and RP were investigated by ESR spectrometry (using stepwise isochronal annealing method) and thermally stimulated luminescence (TSL) technique. The accumulated optically active RD and RP (also called as colour centres) were studied by diffuse reflectance spectrometry. By using the method of chemical scavengers (MCS), the accumulated electron type RD and RP were only analysed in the irradiated reference Li_4SiO_4 pebbles (without additions of Li_2TiO_3), due to the low solubility of the Li_2TiO_3 phase [28]. The phase transitions were studied by powder X-ray diffractometry (p-XRD) and Fourier transform

infrared (FTIR) spectrometry, while the microstructural changes were investigated by scanning electron microscopy (SEM) coupled with energy dispersive X-ray (EDX) spectrometry.

The scientific novelty. In this doctoral thesis, for the first time the formation and accumulation of RD and RP in the advanced Li_4SiO_4 pebbles with additions of Li_2TiO_3 as a secondary phase were analysed and described considering the simultaneous action of 5 MeV accelerated electrons and high irradiation temperature. To predict the possible tritium release temperature range, the thermal stability and annihilation of the accumulated RD and RP in the irradiated advanced Li_4SiO_4 pebbles with additions of Li_2TiO_3 were studied. Additionally, the influence of various technological factors (the noble metals, the pebble diameter, the grain size and the chemisorption products) on the formation and accumulation of RD and RP in the advanced Li_4SiO_4 pebbles was evaluated and described.

The practical significance. The scientific findings of this doctoral thesis can be used both by the producers of the ceramic tritium breeder pebbles and by the manufactures of the solid breeder test blanket concepts. The obtained results can also be used for future studies of the advanced Li_4SiO_4 pebbles with additions of Li_2TiO_3 as a secondary phase, for example the next short and long-term neutron-irradiation experiments, in-pile and out-of-pile tritium release studies etc. In addition, the obtained results of this doctoral thesis can be used for the next studies in the field of radiation chemistry and radiochemistry.

Publications. The scientific findings of this doctoral thesis have been summarised in five articles, which have been published in *Journal of Nuclear Materials* (Impact Factor: 2.048, Q1, Scopus and Web of Science) and *Fusion Engineering and Design* (Impact Factor: 1.319, Q1, Scopus and Web of Science). The obtained results have been presented in more than thirty international and local scientific conferences. The full list of the published articles and the attended conferences is shown in Appendix 1.

Acknowledgments. I would first like to express my deepest gratitude to the supervisor of this doctoral thesis, leading researcher, Dr. chem. Gunta Ķizāne and to the scientific advisors Dr. chem. Arnis Supe and Dr. rer. nat. Regina Knitter for guidance and support during these years. I would also like to acknowledge Dr. chem. Juris Avotiņš for his valuable comments and suggestions for this doctoral thesis.

Special thanks to all colleagues, supervised students, local and international cooperation partners, who helped to realise this doctoral thesis. The experimental and technical support of colleagues from the Latvian Institute of Organic Synthesis (Dr. chem Larisa Baumane), the University of Latvia, Institute of Chemical Physics (Līga Avotiņa, Jānis Čipa, Oskars Valtenbergs, Raimonds Meija, Valentīna Kinerte, Gennady Ivanov, Dr. chem. Aigars Vītiņš,

Dr. chem. Elīna Pajuste and Dr. chem. J. Tiliks Jr.), the University of Latvia, Faculty of Chemistry (Dr. chem. Agris Bērziņš and Prof. Andris Actiņš), the University of Latvia, Institute of Solid State Physics (Dr. phys. Laima Trinklere and Aleksejs Zolotarjovs), the Riga Technical University, Institute of Inorganic Chemistry (Dr. habil. sc. ing. Jānis Grabis and Ints Šteins), the Kaunas University of Technology, Institute of Materials Science (Prof. Sigitas Tamulevičius and Dr. Mindaugas Andrulevičius) and the Karlsruhe Institute of Technology, Institute for Applied Materials (Matthias H.H. Kolb and Oliver Leys) is gratefully acknowledged.

The work was performed in the frames of the University of Latvia financed project No. Y9-B044-ZF-N-300, "Nano, Quantum Technologies, and Innovative Materials for Economics". The research was supported by the Baltic-German University Liaison Office by the German Academic Exchange Service (DAAD) with funds from the Foreign Office of the Federal Republic Germany. The research was part-funded by the Ministry of Education and Science (the Republic of Latvia).

1. LITERATURE REVIEW

The nuclear fusion reactors, which will operate with a closed tritium-deuterium fuel cycle, have a potential to be used for the commercial electricity production, however there are several crucial scientific and technological challenges, which need to be solved [29]. One of the most important issues for future burning plasma machines, for example DEMO (Demonstration fusion power plant), is to ensure the tritium self-sufficiency. Therefore, in International Thermonuclear Experimental Reactor (ITER) several concepts of Test Blanket Modules (TBMs) will be tested [30-32] to verify and compare the proposed tritium breeding concepts and to study the functional and structural materials under real operational conditions of the nuclear fusion reactor.

Presently the Li_4SiO_4 pebbles (produced by a melt-spraying process and containing 2.5 wt% excess of silicon dioxide (SiO_2) [33]) and the Li_2TiO_3 pebbles (produced by an extrusion-spheronisation-sintering process [34]) are accepted as two of the most promising candidates for the tritium breeding in the European Union (EU) developed solid breeder TBM concept. Nevertheless, the advanced Li_4SiO_4 pebbles with additions of Li_2TiO_3 as a secondary phase are under development as an alternative candidate for the tritium breeding [11, 32]. In combining these two phases, Li_4SiO_4 and Li_2TiO_3, it is anticipated to obtain the advanced two-phase ceramic breeder pebbles with improved mechanical properties, without losing benefits of a high lithium density, appropriate melting temperature, acceptable radiation stability, low neutron activation behaviour and good tritium release characteristics.

Until now, the radiolysis of the advanced Li_4SiO_4 pebbles with additions of Li_2TiO_3 as a secondary phase was not analysed. Therefore, to develop and evaluate a new two-phase chemical composition for the advanced ceramic tritium breeder pebbles, it is a crucial issue to study the formation, accumulation and annihilation of RD and RP in the Li_4SiO_4 pebbles with various contents of Li_2TiO_3 under the simultaneous action of radiation, temperature and magnetic field. The long-term neutron-irradiation experiments, such as PBA, EXOTIC and HICU[1] [35], are expensive and require several years of planning, preparation and post irradiation examination (PIE) in addition to several years of irradiation. Therefore, the short-term irradiation studies with various types of radiation are very important to determine the parameters, which characterises the radiation stability, to evaluate the high-temperature radiolysis processes and to predict the possible tritium release temperature range of the advanced Li_4SiO_4 pebbles with additions of Li_2TiO_3 as a secondary phase. Previously, the formation and accumulation of RD and RP in the Li_4SiO_4 and Li_2TiO_3 ceramics under action of various types of radiation (neutrons, gamma rays,

[1] HICU - High neutron fluence Irradiation of pebble staCks for fUsion

X-rays, accelerated electrons, high-energy ions etc.) have been studied and described separately by several groups of researchers [19-24, 27, 36-46].

In this chapter, the background, theoretical principles, technical design and proposed tritium breeding concepts of the nuclear fusion reactors are further described. The EU developed solid breeder TBM concept and the proposed tritium breeding ceramics are characterised. The formation and accumulation of RD and RP in the Li_4SiO_4 pebbles and in the Li_2TiO_3 pebbles under various types of radiation are described. Finally, the factors, which can influence the radiolysis of the Li_4SiO_4 pebbles, are shortly discussed.

1.1 Nuclear fusion reactors

The ITER ("The Way" in Latin), which is currently under construction in Cadarache, France [47], is an international fusion research and engineering project with the main purpose to create a transition from plasma physics experimental research into power-producing nuclear fusion reactors. Thirty-five nations – the EU member states, India, Japan, China, Russia, South Korea and the United States, are collaborating in order to build and operate ITER, which will be the largest tokamak[2] type nuclear fusion reactor, when it will start to operate. It is expected that the ITER project will contribute to the design of DEMO, which will be a prototype for the commercial-scale nuclear fusion reactors. For now, the technical design of DEMO has not been formally accepted and therefore detailed operational conditions are not yet available [48].

1.1.1 Background

One of the most crucial problems of this century is to solve the energy supply, which is a result of the rapidly growing demands and consumption of energy. Fossil fuels (oil, gas and coal) are the major energy sources, which are used in the world today [49]. However, the fossil fuel reserves will decrease rapidly in near future, and therefore alternative energy sources will be required to meet growing demands for electricity. Significant progress has been made to develop various renewable energy technologies, such as biofuel, biomass, geothermal, hydropower, solar energy and wind power, however there are still challenges to generate large electricity quantities by these technologies. In additions, the renewable energy technologies have low efficiency levels and heavily depend on weather, for example solar energy and wind power. Nevertheless, electricity can also be produced by nuclear fission reactors, but the obtained nuclear wastes are highly radioactive and long-lived, and the public acceptance of the nuclear fission technology is low.

[2] Russian acronym. Токамак - ТОроидальная КАмера с МАгнитными Катушками

Therefore, alternative energy sources are currently being actively searched and one of such alternatives is the nuclear fusion, which can offer relatively clean and safe energy with minimal amount of short-lived radioactive waste. Currently, the nuclear fusion research is entering in a new development phase with the construction of ITER and with the conceptual designing of DEMO. If the ITER and DEMO projects will be successful, it will lead to the planning of the first generation of commercial-scale electricity producing nuclear fusion reactors.

1.1.2 Principles of nuclear fusion

In nuclear fusion energy is released by a reaction in which two or more atomic nuclei come close enough to form one or more different atomic nuclei and neutrons or protons. The essential condition for the nuclear fusion reaction is the requirement that the nuclei of reacting species overcome electrostatic Coulomb repulsions. The nuclear fusion reactions, such as proton-proton reactions, take place within the Sun and other stars, because the nuclei of reacting species are brought close together by intense pressure and temperature, which is produced by gravity. On Earth, there are several scientific and technological challenges, how to realise the nuclear fusion reactions, as they need a very high temperature, sufficient particle density and confinement time.

It has been identified that the most efficient nuclear fusion reaction from all possible reactions is the fusion reaction between two isotopes of hydrogen, tritium and deuterium (Eq. 1.1), and this reaction could be used in the nuclear fusion reactors [50]. In this doctoral thesis, the symbols D and T will be used for deuterium and tritium, instead of ^{2}H and ^{3}H.

$$T + D \rightarrow {}^{4}He + n + 17.6\ MeV \quad (1.1)$$

The tritium-deuterium nuclear fusion reaction has a higher efficiency and probability in comparison to other nuclear fusion reactions, for example deuterium-deuterium and tritium-tritium reactions (Eqs. 1.2-1.4). Nevertheless, to gain the required conditions for the nuclear fusion reaction, the temperature of tritium-deuterium plasma must be around 10^{8} K. The plasma is one of the four fundamental states of matter, and basically it is a gaseous mixture of negatively charged electrons and highly charged positive ions.

$$D + D \rightarrow T + p + 4.0\ MeV \quad (50\ \%) \quad (1.2)$$

$$D + D \rightarrow {}^{3}He + n + 3.3\ MeV \quad (50\ \%) \quad (1.3)$$

$$T + T \rightarrow {}^{4}He + 2\ n + 11.3\ MeV \quad (1.4)$$

From the above mentioned, it follows that the nuclear fusion reactors have two major challenges: (1) the heating of the tritium-deuterium fuel up to the required temperature, and (2) the confinement of the obtained tritium-deuterium plasma. There are several approaches, how

to realise nuclear fusion reactions, for example magnetic and inertial confinement (Fig. 1.1). In the magnetic confinement, the charged particles are confined by a strong magnetic field for a sufficient time with a high plasma particle density and temperature in order to allow charged particles to interact. While in the inertial confinement, the small pellets with the tritium-deuterium fuel are compressed using lasers to produce the necessary conditions for the fusion ignition, and then the fuel reacts in the very short time before the pellet is blown apart.

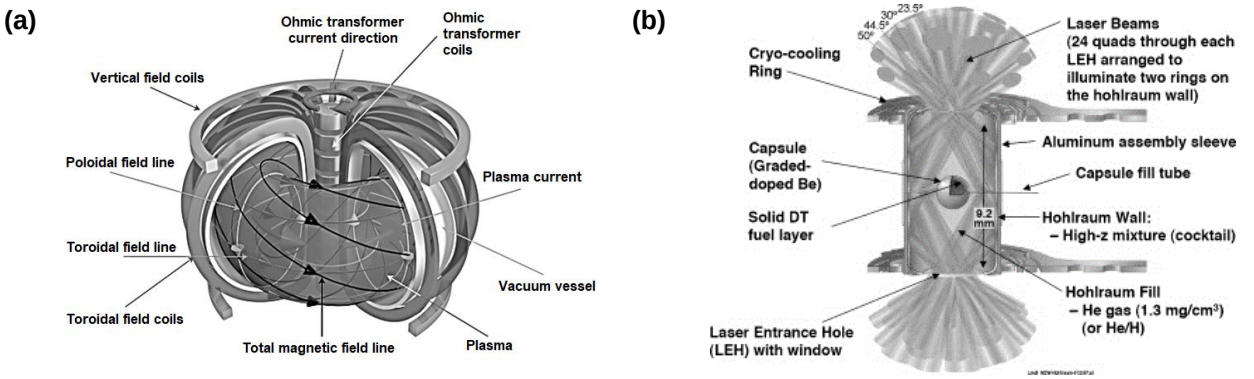

Fig. 1.1 Example of (a) tokamak type magnetic confinement in toroidally shaped vacuum vessel with a D-shaped cross-section and (b) inertial confinement of fuel capsule with laser beams [51, 52].

The largest operational inertial confinement device is located in the National Ignition Facility (or shortly NIF) in the United States. The integrated fusion ignition experiments in the NIF were started in 2010 [53].

Currently, the two main types of the toroidal devices, which are used for the plasma magnetic confinement, are tokamaks and stellarators (Fig. 1.2). In a tokamak type device, a set of coils is placed around the doughnut-shaped plasma chamber and the magnetic field is produced by toroidal and poloidal coils. While the construction of a stellarator type device is more complicated as extra helical coils surround the plasma chamber in order to provide the additional twist to the magnetic field or the twisting magnetic field is produced entirely by external non-axisymmetric coils. Since the tokamak type device is technical more simply to build, it is presently the leading candidate for future commercial nuclear fusion reactors.

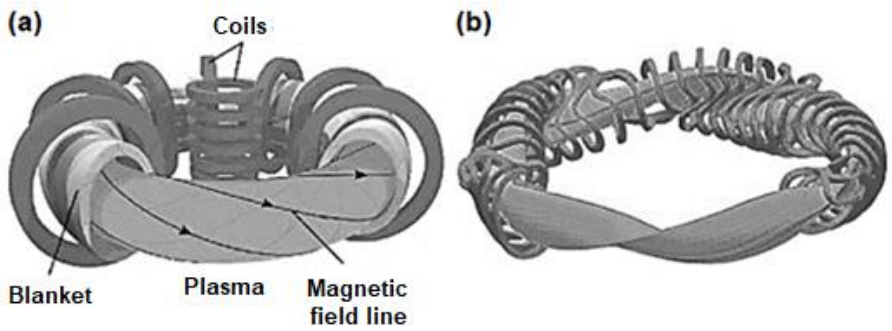

Fig. 1.2 Schematic representation of (a) a tokamak and (b) a stellarator [54].

The tokamak type nuclear fusion reactors, which should certainly be mentioned, are Joint European Torus (JET) in the United Kingdom, ASDEX Upgrade (Axially Symmetric Divertor

Experiment) in Germany, JT-60 in Japan, Tore Supra in France, Tokamak Fusion Test Reactor (TFTR) in the United States and ISTTOK (Instituto Superior Técnico Tokamak) in Portugal. For now, the JET is the largest and most powerful tokamak type nuclear fusion reactor in the world (major radius: 3 m, plasma volume: 100 m^3, magnetic field: up to 4 T) and the only tokamak type device, which can operate with the tritium-deuterium fuel [55]. Presently the JET is acting as a test facility to study the ITER technologies and plasma operating scenarios. In 1997, 16 MW of fusion power was obtained in the JET (with heating power 26 MW), which corresponds to an energy gain factor (Q) of 0.65. The Q is the ratio between produced power in the nuclear fusion reactor and required powder to maintain plasma in steady state. The Q value equal to 1 can be achieved when the produced fusion power in the nuclear fusion reactor is equal to the required power for plasma heating.

The stellarator type nuclear fusion reactors, which should be mentioned, are Wendelstein 7-X (W7-X) in Germany, Helically Symmetric Experiment (HSX) in the United States and Large Helical Device (LHD) in Japan. The W7-X is the world's largest stellarator type nuclear fusion reactor (major radius: 5.5 m, plasma volume: 30 m^3, magnetic field: up to 3 T), and its main purpose is to show the viability of the stellarator type devices for future commercial nuclear fusion reactors [56]. The first hydrogen plasma experiments in the W7-X were done on 3 February 2016.

1.1.3 Technical design of ITER

The nuclear fusion reactions in ITER will be realized in a tokamak type reactor, which will use poloidal and toroidal magnetic fields to contain and control the obtained tritium-deuterium plasma [57]. ITER will be the world's largest tokamak type device (plasma radius: 6.2 m, plasma volume: 840 m^3, magnetic field: up to 11 T), when it will start to operate. The main goals of the ITER project are: (1) to demonstrate the feasibility of nuclear fusion power, (2) to obtain the Q value equal to 10, (3) to validate and compare the proposed tritium breeding TBM concepts, and (4) to evaluate and develop the functional and structural materials for DEMO and other future commercial nuclear fusion reactors. However, it needs to be highlighted that the generated heat in ITER will not be used to generate electricity.

The technical design of ITER is schematically shown in Fig. 1.3, a. The main components are marked with arrows, while for the scale note the human (in blue lab coat) under the reactor core. The construction of the ITER Tokamak Building was started in 2010, and it is expected that access for first assembly activities will be available in 2019. The photo from the construction site of the ITER Tokamak Building is shown in Fig. 1.3, b. Presently the first

plasma experiments in ITER are planned in 2025, while the experiments with tritium-deuterium plasma are expected to start in 2035.

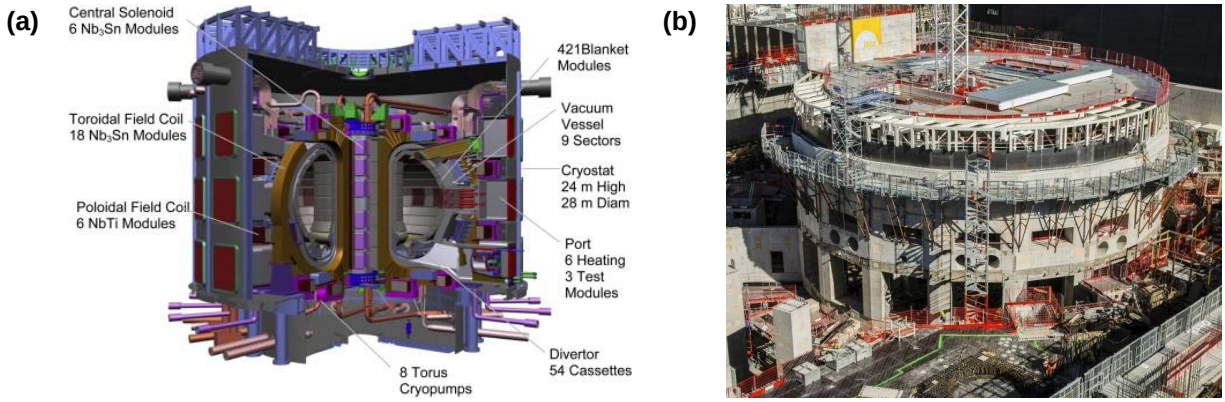

Fig. 1.3 (a) Cross-section cutaway of ITER with marked main components and (b) photo from the construction site of the ITER Tokamak Building (April 9, 2018) [47, 58].

The vacuum vessel (VV) is the central part of ITER, and its main function is to provide a hermetically sealed container in which the tritium-deuterium plasma will be obtained. In the VV, the obtained plasma will be confined by powerful magnetic fields in the torus shape, which will be produced by superconducting toroidal and poloidal field coils. The cryostat surrounds the VV and the superconducting magnets to provide a super-cool vacuum environment. The VV will be covered with blanket modules to protect the structural materials and the magnets from plasma, neutron and heat interactions. While the divertor will be used to remove heat, helium, dust and other impurities, which may form in the VV during operation.

The first wall of the ITER VV will be made of bulk beryllium (Be) and Be coated inconel tiles [59], while the divertor will be made from tungsten (W) tiles. This combination of Be and W, as plasma facing materials, was selected in order to gain a large operational flexibility and the capability to handle the large particle and heat fluxes. Previously, the carbon fibre composite (CFC) tiles and the CFC tiles coated with W were also considered as plasma facing materials for the divertor [60], however the present design of ITER excludes the use of carbon containing materials, due to potential risk of the accumulation and radioactivity of tritium.

The equatorial and upper port plugs of ITER will be used to provide access for the remote handling operations, diagnostic, heating and vacuum systems. During later stages of the ITER project, the accepted six tritium breeding TBM conceptions will be simultaneously tested and verified in three equatorial ports (No. 2, 16 and 18) [61-64]. In each equatorial port, two TBM-sets will be mechanically attached in a TBM frame. The Helium Cooled Pebble Bed (HCPB) TBM and the Helium Cooled Lithium Lead (HCLL) TBM, proposed by the EU, will be tested in the equatorial port No. 16. The Water Cooled Ceramic Breeder (WCCB) TBM, proposed by Japan, and the Dual Coolant Lithium Lead (DCLL) TBM, proposed by the United States and

supported by South Korea, will be installed in the equatorial port No. 18. The Helium Cooled Ceramic Breeder (HCCB) TBM, proposed by China, and the Lithium Lead Ceramic Breeder (LLCB) TBM, proposed by India and supported by Russia, will be tested in the equatorial port No. 2. Currently, it is planned that the installation of the TBM systems in ITER will be done during the first shutdown period following the first plasma experiments. The first wall of the TBM will act as a plasma facing component, and therefore it must withstand high particle and heat loads.

1.1.4 Tritium breeding concept

ITER will be the first nuclear fusion reactor, which will be equipped with a complete closed deuterium-tritium fuel cycle [65]. The schematic block diagram of the inner deuterium-tritium fuel cycle is shown in Fig. 1.4. With a fusion power around 500 MW, ITER will need to fuse up to 76 g of tritium per day, this value was calculated assuming that the tritium burn-up fraction is 0.3 % [66]. The tritium-deuterium fuel will be introduced into the ITER VV by a gas or pellet injection system. Since only a small fraction of the injected tritium will burn-up in the fusion reaction (<1 %), the un-burned tritium-deuterium fuel afterwards will be pumped out from the VV and recycled. The un-burned fuel will be separated from helium, which is produced during the tritium-deuterium nuclear fusion reaction (Eq. 1.1), and mixed with fresh tritium and deuterium and reinjected into the VV.

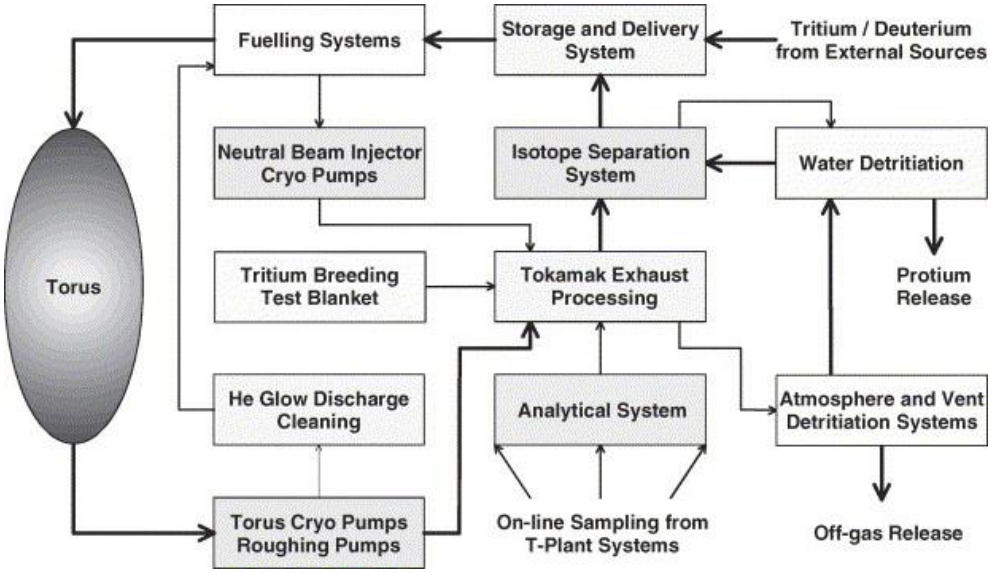

Fig. 1.4 The block diagram of the ITER inner deuterium-tritium fuel cycle [66].

Deuterium can be extracted from sea water, while the tritium resources on Earth are very limited, due to its short half-life (around 12.3 years [67]). In nature, tritium is produced by high-energy cosmic rays in the upper atmosphere (Eq. 1.5), however its natural abundance is too low to be economically exploited. Tritium decays into helium-3 by emission of an electron and anti-

neutrino, also known as β^- decay (Eq. 1.6). The electron, which is emitted by tritium, has an average kinetic energy around 6 keV, and it can only travel about 6 mm in air before it loses ability to cause ionizations.

$$^{14}N + n \rightarrow T + {}^{12}C - 4.3\ MeV \quad (1.5)$$

$$T \rightarrow {}^{3}He + e^- + \bar{\upsilon}_e + 18.6\ keV \quad (1.6)$$

For the ITER operation it is planned that tritium will be taken from the global inventory. Presently around 100 g of tritium are produced per year in a CANDU[3] pressurized heavy water (D_2O) reactor, due to neutron capture in its coolant and moderator [68]. While DEMO and other future nuclear fusion reactors will be required to produce their own tritium, not relying on any external source. Therefore, in future nuclear fusion reactors, it is planned to produce tritium by neutron reactions with various lithium-containing compounds (Eqs. 1.7 and 1.8) [69]. Naturally occurring lithium is composed of two stable isotopes, lithium-6 (7.5 %) and lithium-7 (92.5 %) [70]. The cross-section of $^{6}Li(n,\alpha)T$ reactions (940.4 barns) is significantly higher than the cross-section of $^{7}Li(n,n'\alpha)T$ reaction (0.024 barns), and therefore the tritium breeder will be enriched with the lithium-6 isotope to increase the tritium production.

$$^{6}Li + n \rightarrow T + {}^{4}He + 4.8\ MeV \quad (1.7)$$

$$^{7}Li + n \rightarrow T + {}^{4}He + n - 2.9\ MeV \quad (1.8)$$

The exact state of material, shape, size, chemical and phase composition of the tritium breeder will depend on the specific design of the TBM concept. The solid breeder concepts, the HCPB TBM, the WCCB TBM and the HCCB TBM, will use Li_4SiO_4 pebbles or Li_2TiO_3 pebbles as the tritium breeder and Be pebbles as a neutron multiplier (Eq. 1.9). While the liquid breeder concepts, the HCLL TBM and the DCLL TBM, will use the liquid lead-lithium (Pb-Li) alloy as both tritium breeder and neutron multiplier (Eq. 1.10). Whereas the LLCB TBM will use Li_2TiO_3 pebbles as the tritium breeder and the liquid Pb-Li alloy as a neutron multiplier and additional tritium breeder.

$$^{9}Be + n \rightarrow 2\ {}^{4}He + 2\ n + 2.5\ MeV \quad (1.9)$$

$$^{208}Pb + n \rightarrow {}^{207}Pb + 2\ n - 7.38\ MeV \quad (1.10)$$

As mentioned above, the EU has developed two TBMs concepts, the HCPB TBM and the HCLL TBM, and both of them will use reduced activation ferritic martensitic (RAFM) steel as a structural material, EUROFER97 steel, and pressurized helium as a coolant for heat extraction (helium pressure: up to 8 MPa, inlet/outlet temperature: 570 K/770 K) [71-74]. The nominal chemical composition of the EUROFER97 steel is 8.9 wt% chromium (Cr), 0.4 wt% manganese,

[3] CANDU reactor - Canada deuterium uranium reactor

0.2 wt% vanadium, 0.1 wt% W, 0.1 wt% carbon and 0.1 wt% tantalum, balanced by iron (Fe). In the HCPB TBM concept, the tritium breeder, the Li_4SiO_4 pebbles or the Li_2TiO_3 pebbles, and a neutron multiplier, the Be pebbles, layers will be separated by the EUROFER97 steel cooling plates, and the formed tritium from the TBM will be extracted by helium flow. The cross-section of the HCPB TBM is shown in Fig. 1.5. While in the HCCL TBM concept, the liquid Pb-Li eutectic will circulate slowly through the TBM to carry the formed tritium outside the reactor for the extraction.

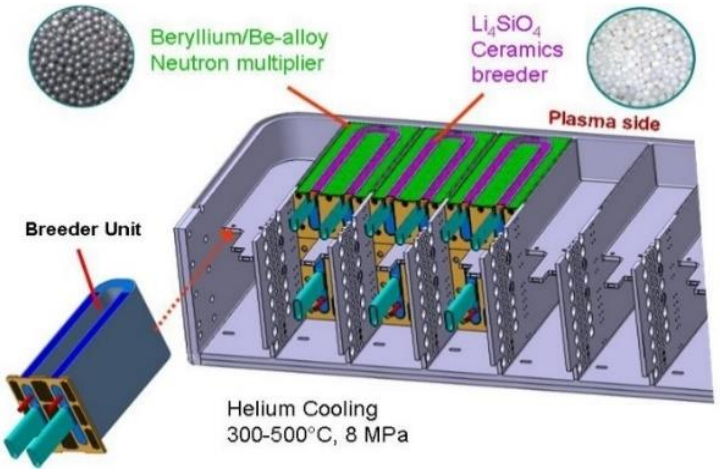

Fig. 1.5 The cross-section of the HCPB TBM *(author: F. Cismondi, KIT).*

In the HCPB TBM concept, the Li_4SiO_4 pebbles with 2.5 wt% excess of SiO_2 (diameter: 0.25-0.63 mm) are accepted as the reference tritium breeder material, while the Li_2TiO_3 pebbles (diameter: 0.6-1.2 mm) are considered as a "back-up" solution [1]. To ensure the tritium self-sufficiency of a nuclear fusion reactor, it is planned to enrich the Li_4SiO_4 pebbles with the lithium-6 isotope up to 40 % and the Li_2TiO_3 pebbles up to 70 % [3]. The Be pebbles with diameter around 1 mm (produced by a rotating electrode method) are accepted to be used as a neutron multiplier, nevertheless Be intermetallic compounds (also known as beryllides), such as $Be_{15}Ti$ [75], $Be_{12}V$ [76] and $Be_{13}Zr$ [77], are also studied as an alternative candidate.

1.2 EU proposed tritium breeding ceramics

The main task of the lithium-containing ceramic breeder pebbles inside the HCPB TBM is to produce and release tritium, nevertheless the ceramic breeder pebbles must be able to withstand the harsh operation conditions of the nuclear fusion reactor: an intense neutron fluence (up to 10^{18} n m^{-2} s^{-1}), ionizing radiation dose rate (up to 1 kGy s^{-1}), a high magnetic field (up to 7-10 T) and elevated temperature (up to 1190 K) [2-5]. The ceramic breeder pebbles also need to possess a series of properties: low neutron activation behaviour, long-term thermo-mechanical stability and chemical compatibility with the EUROFER97 steel. The fabrication process of the ceramic breeder pebbles needs to be economically and ecologically sensible, while the recycling

process must enable the recovering of the lithium-6 isotope and the removal of radioactive isotopes, which may form in the ceramic breeder pebbles under action of neutrons.

Previously, various lithium-containing compounds, such as Li_4SiO_4, Li_2TiO_3, lithium aluminate ($LiAlO_2$), lithium zirconate (Li_2ZrO_3) and lithium oxide (Li_2O), have been considered as possible solid-state candidates for the tritium breeding [78, 79]. The neutron activation is not a concern for Li_2O, Li_4SiO_4 and Li_2TiO_3, while for Li_2ZrO_3 and $LiAlO_2$ it is a major problem, due to the activation of zirconium (Zr) and aluminium (Al). The highest lithium density has Li_2O, however it has also the greatest sensitivity to moisture. The tritium release performance of Li_2O, Li_4SiO_4, Li_2TiO_3 and Li_2ZrO_3 are acceptable, while the tritium release characteristics of $LiAlO_2$ are poor. Therefore, as a compromise, Li_4SiO_4 and Li_2TiO_3 in the form of ceramic pebbles have been internationally accepted as two leading candidates for the tritium breeding in the solid breeder TBM concepts [1]. The pebble form has been selected to avoid thermal stress and irradiation cracking and to obtain a good packing factor in the TBM with complex geometry.

The previous long-term neutron-irradiation experiments, such as PBA and EXOTIC [6-9], already confirmed that both the Li_4SiO_4 pebbles with 2.5 wt% excess of SiO_2 (reference candidate) and the Li_2TiO_3 pebbles ("back-up" solution) will perform sufficiently well under the excepted operation conditions of the HCPB TBM in ITER. Apart from the higher lithium density of Li_4SiO_4, S. van Til et al. [6] reported that the Li_4SiO_4 pebbles contain more cracks and pores, which could be a benefit in the terms of the tritium production and release, while the Li_2TiO_3 pebbles have a higher mechanical strength, but they require a higher enrichment with the lithium-6 isotope to increase the tritium production. Therefore, the advanced Li_4SiO_4 pebbles with additions of Li_2TiO_3 as a secondary phase were proposed by R. Knitter et al. [11] as an alternative candidate for the tritium breeding in the nuclear fusion reactors in order to combine the advantages of both phases into one single tritium breeding ceramic. Presently the advanced Li_4SiO_4 pebbles with additions of Li_2TiO_3 have only been investigated by a few groups of researchers, and thus there is a gap in the theoretical and practical knowledge about this ceramic.

In the following, the fabrication and properties of the Li_4SiO_4 pebbles with excess of SiO_2, the Li_2TiO_3 pebbles and the advanced Li_4SiO_4 pebbles with additions of Li_2TiO_3 as a secondary phase are described separately.

1.2.1 Li_4SiO_4 pebbles with excess of SiO_2 – reference candidate

The Li_4SiO_4 pebbles with 2.5 wt% excess of SiO_2 have a high thermal stability (eutectic melting point: at around 1298 K [80]), sufficient mechanical properties (average crush load: 8-10 N [11]), good tritium release characteristics (main tritium release: at around 400-600 K) [81]

and chemical compatibility with the EUROFER97 steel [82]. The neutron activation behaviour of the Li_4SiO_4 pebbles is strongly influenced by the metallic impurities, such as cobalt (Co), Al and Pt [83], which can be introduced in the Li_4SiO_4 pebbles by the fabrication process or by raw materials, and therefore all possible contaminations sources needs to be carefully considered. Due to the excess of SiO_2, the pebbles have two crystalline phases, 90 mol% monoclinic Li_4SiO_4 as the primary phase and 10 mol% orthorhombic Li_2SiO_3 as a secondary phase [84]. The excess of SiO_2 is added to increase the mechanical stability (crush load) of the Li_4SiO_4 pebbles [85] and to minimize grain growth [11].

Concerning the fabrication method of the Li_4SiO_4 pebbles, several fabrication routes have been developed in order to produce ceramics with various characteristics (microstructure, grain size, porosity, density, crush load etc.), for example solid-state reaction [86], sol-gel [87], wet chemical [88], spray-drying [89], plasma synthesis [90], melt-based methods [91, 92] etc.

In the EU, a melt-spraying process, which is a simple and cost-efficient semi-industrial technique (200-300 kg per year [84]), is used for the fabrication of the Li_4SiO_4 pebbles with excess of SiO_2 [11]. The illustration of the melt-spraying process is shown in Fig. 1.6, a. In addition, a melt-spraying process can also be used to reprocess the neutron-irradiated Li_4SiO_4 pebbles by direct re-melting without an additional wet-chemical recycling step, however this process cannot be used to remove any activated impurities. It was clearly demonstrated by R. Knitter and B. Löbbecke [33] that the properties and the microstructure of the Li_4SiO_4 pebbles are not influenced by direct re-melting.

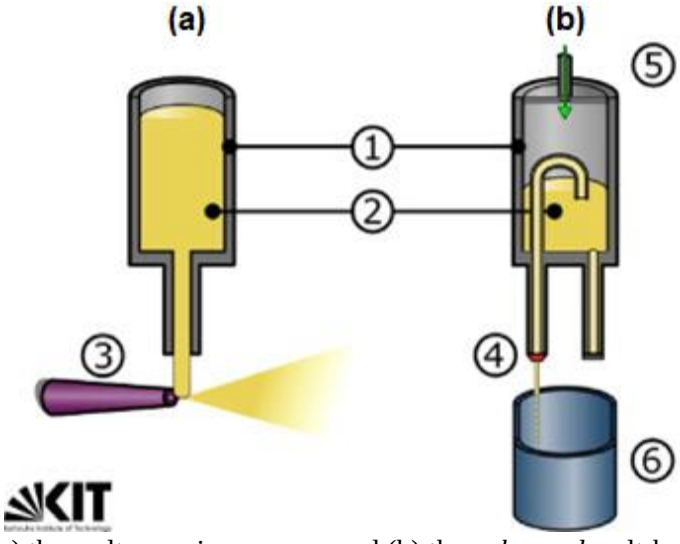

Fig. 1.6 Illustration of (a) the melt-spraying process and (b) the *enhanced* melt-based process [93].

For the fabrication of the Li_4SiO_4 pebbles with excess of SiO_2, lithium hydroxide monohydrate ($LiOH \cdot H_2O$) and SiO_2 powders are used as raw materials. The mixture of raw materials is heated in a Pt alloy crucible (1) up to 1720 K, and then the formed melt (2) is sprayed in dry air (3) to obtain pebbles. Due to the excess of SiO_2 and the rapid cooling during a

melt-spraying process, the fabricated pebbles have two main crystalline phases, Li_4SiO_4 as the primary phase and lithium orthodisilicate ($Li_6Si_2O_7$) as a secondary phase. The high-temperature phase, $Li_6Si_2O_7$, is metastable at room temperature and decomposes during thermal treatment. After thermal treatment (e.g. up to 1220 K for 1 week in air atmosphere), the fabricated pebbles consist of Li_4SiO_4 as the primary phase and Li_2SiO_3 as a secondary phase.

The chemical processes, which occur during the melting process of raw materials and the thermal treatment of the fabricated Li_4SiO_4 pebbles with excess of SiO_2, can be represented by the following reactions:

$$LiOH \cdot H_2O \rightarrow LiOH + H_2O\uparrow \quad (1.10)$$

$$4\ LiOH + SiO_2 \rightarrow Li_4SiO_4 + 2\ H_2O\uparrow \quad (1.11)$$

$$10\ LiOH + 3\ SiO_2 \rightarrow Li_4SiO_4 + Li_6Si_2O_7 + 5\ H_2O\uparrow \quad (1.12)$$

$$Li_6Si_2O_7 \rightarrow Li_4SiO_4 + Li_2SiO_3 \quad (1.13)$$

Previously, Li_2CO_3 powder had also been considered as a raw material for the fabrication of the Li_4SiO_4 pebbles with excess of SiO_2, however during the melting process a large amount of gaseous CO_2 was generated (Eq. 1.14) and the obtained Li_4SiO_4 pebbles had un-satisfactory characteristics (high porosity etc.) [91]. In addition, the melting process of $LiOH \cdot H_2O$ and SiO_2 powders is easier to control, despite the release of gaseous H_2O.

$$2\ Li_2CO_3 + SiO_2 \rightarrow Li_4SiO_4 + 2\ CO_2\uparrow \quad (1.14)$$

The fabricated Li_4SiO_4 pebbles with excess of SiO_2 have a very broad size distribution (from 10 μm to 1500 μm), due to the spraying process with dry air flow. The diameter of the obtained Li_4SiO_4 pebbles depends on the flow rate of the melt and the air jet. Optimizing the fabrication conditions, a pebble yield of up to 50 wt% with the required pebble size (between 250 μm and 630 μm) can be achieved.

To provide a narrower pebble diameter distribution and a higher pebble yield, an *enhanced* melt-based process was designed by M. H.H. Kolb et al. [93]. The illustration of the *enhanced* melt-based process is shown in Fig. 1.6, b. In this process, the mixture of raw materials, $LiOH \cdot H_2O$ and SiO_2, is heated up to 1720 K in a Pt-Rh alloy crucible (1) and a melt (2) is obtained. The formed liquid (3) is then released through a Pt-Au alloy nozzle (4) with a diameter around 300 μm to form droplets, which are quenched into liquid nitrogen (6) to obtain pebbles. To adjust the velocity of the flowing melt, synthetic air (pressure: 200-1000 mbar) can be applied as pressure gas (5) on a melt.

R. Knitter et al. [84] analysed the surface and the microstructure at the chemically etched cross-section and the crystallisation of the fabricated Li_4SiO_4 pebbles with various diameters

(Fig. 1.7). It was suggested that the cracks on the surface of the Li_4SiO_4 pebbles are caused by the rapid quenching and by the collisions of the obtained pebbles during the fabrication process. In contrast, the pebbles with diameter below 50 μm are crack free, transparent and optically amorphous, due to the extremely rapid cooling during the fabrication process. Depending on the pebble size and the fabrication conditions, three different microstructures (granular, dendritic and amorphous) were found. It was assumed that by adjusting the thermal treatment, the thermo-mechanical behaviour of the fabricated Li_4SiO_4 pebbles might be improved.

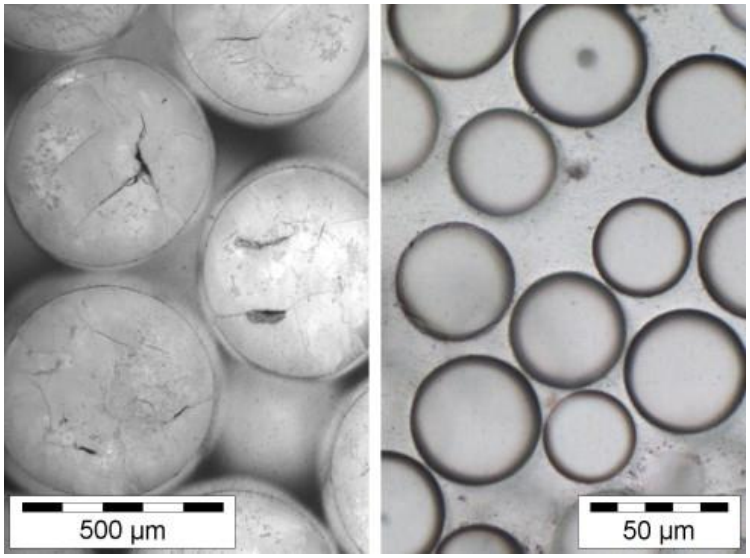

Fig. 1.7 Optical micrographs of the fabricated Li_4SiO_4 pebbles with excess of SiO_2 (left – the pebbles with diameter around 500 μm; right – the pebbles with diameter smaller than 50 μm) [84].

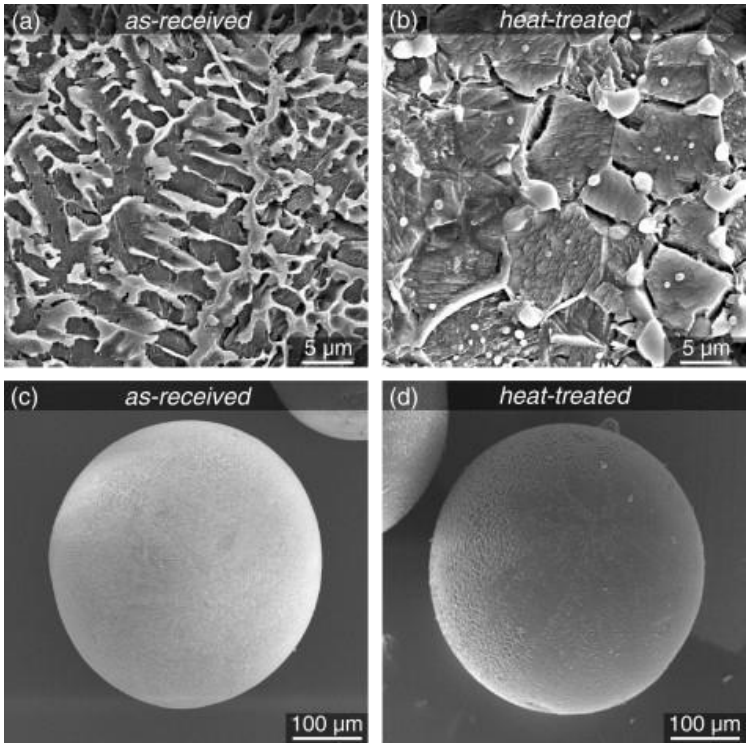

Fig. 1.8 Microstructure of the fabricated Li_4SiO_4 pebbles with excess of SiO_2 before and after thermal treatment up to 1220 K for 1 week in air atmosphere (a and b – the chemically etched cross-section; and c and d – the pebble surface) [94].

M. Kolb et al. [94] analysed the surface and the microstructure at the chemically etched cross-section of the Li_4SiO_4 pebbles with excess of SiO_2 before and after thermal treatment up to 1220 K for 1 week in air atmosphere (Fig. 1.8). The fabricated pebbles have a dendritic microstructure with dark grey Li_4SiO_4 as the primary phase and light grey $Li_6Si_2O_7$ as a secondary phase. While after thermal treatment, the dendritic grains transform into a sinter-like microstructure and the Li_4SiO_4 phase is displayed in dark grey colour with inclusions of smaller, light grey grains of Li_2SiO_3 as a secondary phase. The grains of a secondary phase are located at the triple points of the primary phase grains or within the grains of the primary phase.

The surface analysis of the Li_4SiO_4 pebbles with excess of SiO_2 before and after thermal treatment showed that CO_2 may accumulate in contact with air atmosphere [94] and is only released at temperatures >770 K [84]. The CO_2 on the surface of the Li_4SiO_4 pebbles mainly accumulates as chemisorption product, Li_2CO_3 (Eq. 1.15) [95]. Traces of Li_2CO_3 on the surface of the Li_4SiO_4 pebbles were observed in depths less than 1 μm. The formed Li_2CO_3 layer thickness on the surface of the fabricated pebbles was less than 5-7 nm, while after thermal treatment the thickness increased enormously. The formation of Li_2CO_3 layer on the surface of the Li_4SiO_4 pebbles probably occurs due to a handling, storage and too slow cooling rate after thermal treatment in contact with air atmosphere.

$$Li_4SiO_4 + CO_2 \rightarrow Li_2CO_3 + Li_2SiO_3 \quad (1.15)$$

The chemisorption process of CO_2 on the surface of the Li_4SiO_4 pebbles with excess of SiO_2 can be catalysed by air humidity (Eqs. 1.16 and 1.17) [96], and therefore small amounts of LiOH, $LiOH \cdot H_2O$ and absorbed H_2O may also accumulate. According to G. Ran et al. [97], adsorbed and chemisorbed H_2O from the surface of the Li_4SiO_4 pebbles is released in four steps at around 360 K, 400 K, 500 K and 670 K.

$$Li_4SiO_4 + H_2O \rightarrow 2\ LiOH + Li_2SiO_3 \quad (1.16)$$

$$2\ LiOH + CO_2 \rightarrow Li_2CO_3 + H_2O \quad (1.17)$$

1.2.2 Li_2TiO_3 pebbles – "back-up" solution

The Li_2TiO_3 pebbles have good tritium release characteristics and appropriate mechanical, thermal and chemical properties [1, 3, 6, 98], however they have a smaller lithium density in comparison to the L_4SiO_4 pebbles and therefore require a higher enrichment with the lithium-6 isotope. The Li_2TiO_3 exhibits high temperature polymorphism and can exist in three solid modifications: α, β and γ form [12]. The α-Li_2TiO_3 (cubic, disordered) form is metastable and transforms at around 570 K into the β-Li_2TiO_3 form. The β-Li_2TiO_3 form is monoclinic and transforms into the γ-Li_2TiO_3 (cubic) form at around 1470 K. The transitions enthalpies between

these forms have been measured by H. Kleykamp [99]. T. Hoshino et al. [100] detected the mass decrease of the Li_2TiO_3 ceramic with time, due to the evaporation of lithium under a hydrogen atmosphere at high temperatures. To compensate this mass decrease, the Li_2TiO_3 pebbles with an excess of lithium ($Li_{2+x}TiO_{3+y}$) were developed as an advanced tritium breeding material for the WCCB TBM concept, which was proposed by Japan [101].

In the EU, an extrusion and spheronization process followed by sintering was used for the fabrication of the Li_2TiO_3 pebbles and is described in detail in several articles [34, 102]. This process consists from several steps: (1) preparation of the Li_2TiO_3 powder and a paste, (2) shaping by extrusion with subsequent spheronization, and (3) sintering of the Li_2TiO_3 green pebbles. The obtained Li_2TiO_3 pellets and pebbles are shown in Fig. 1.9.

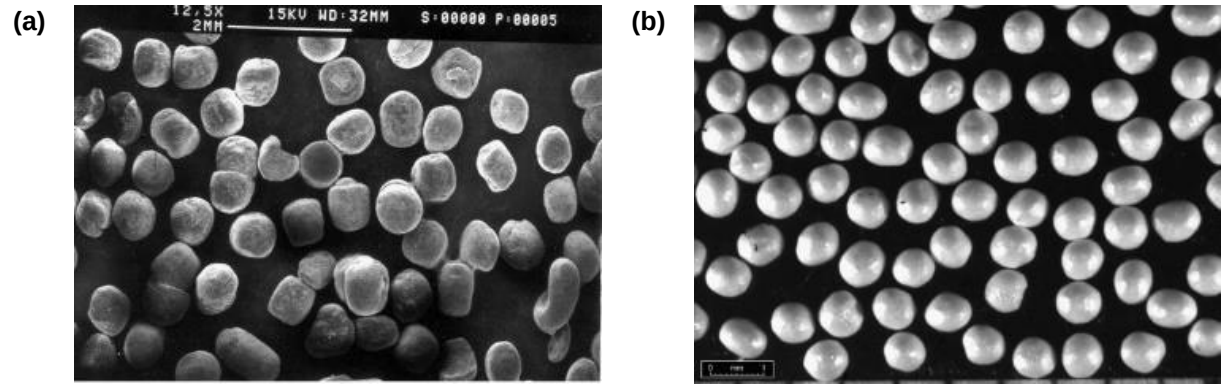

Fig. 1.9 Surface microstructure of (a) the Li_2TiO_3 pellets fabricated by the extrusion process and (b) the Li_2TiO_3 pebbles formed with a spheronization plate [102].

The sintering temperature is a key parameter to adjust the microstructural characteristics of the fabricated Li_2TiO_3 pebbles. After sintering up to 1230 K, the Li_2TiO_3 pebbles can be obtained with a density up to 90% of the theoretical density[4]. The crush load of the obtained Li_2TiO_3 pebbles (diameter: 0.8-1.2 mm) was in range from 38 to 66 N.

Previously, the Li_2TiO_3 pebbles were also produced by a direct-wet process [102-105], however additional work was required to optimize the parameters of this process and to improve the density of the produced pebbles. The direct wet process involves several steps: (1) dissolving of the Li_2TiO_3 powder in hydrogen peroxide (H_2O_2) using citric acid as the chelating agent, (2) condensing the solution, (3) dropping the condensed solution into a solvent to form gel-spheres, (4) drying and calcinations of the gel-spheres, and (5) sintering to improve the pebble properties. At the best conditions, the density of the Li_2TiO_3 pebbles was around 80-85% of the theoretical density, while the sphericity of the fabricated pebbles was low, and the grain size was larger than 5 μm.

[4] Theoretical density of Li_2TiO_3 (β-form): 3.43 g cm^{-1}

1.2.3 Advanced Li_4SiO_4 pebbles with additions of Li_2TiO_3 – alternative candidate

The first articles about the fabrication and development of the advanced Li_4SiO_4 pebbles with additions of Li_2TiO_3 as a secondary phase were published by R. Knitter et al. [11] and O. Leys et al. [106]. An *enhanced* melt-based process (Fig. 1.6, b) is adapted for the fabrication of the advanced Li_4SiO_4 pebbles with additions of Li_2TiO_3 at the Karlsruhe Institute of Technology (Germany), however the present KALOS (KArlsruhe Lithium OrthoSlicate) facility has temperature limitations, and therefore the maximum content of Li_2TiO_3 is limited to around 35-40 mol%, due to the high melting temperature of the Li_2TiO_3 phase[5]. For the synthesis, $LiOH \cdot H_2O$, SiO_2 and titanium dioxide (TiO_2) are used as raw materials. Due to the additions of TiO_2 and the rapid cooling during the fabrication process, the α-Li_2TiO_3 (cubic, disordered) form is obtained as a secondary phase in the advanced Li_4SiO_4 pebbles (Eq. 1.18). During thermal treatment (e.g. up to 1220 K for 3 weeks in air atmosphere), the α-Li_2TiO_3 form is transformed into the β-Li_2TiO_3 (monoclinic) form.

$$2\ LiOH + TiO_2 \rightarrow Li_2TiO_3 + H_2O\uparrow \qquad (1.18)$$

M. H.H. Kolb et al. [93] found that Pt particles can be released from a Pt alloy crucible, due to the exposure to the molten raw materials or synthesis products at high temperatures. O. Leys et al. [18], using inductively coupled plasma optical emission spectrometry (ICP-OES), detected elevated contents (up to 300 ppm) of the noble metals (Pt, Au and Rh) in the advanced Li_4SiO_4 pebbles with additions of Li_2TiO_3 as a secondary phase, due to the surface corrosion of a Pt-Rh alloy crucible and a Pt-Au alloy nozzle. The concentration of the noble metals in the advanced Li_4SiO_4 pebbles with additions of Li_2TiO_3 was measured after multiple re-melting, and it was observed that the accumulation rate of the noble metals slows down after each re-melting step. It is assumed that the amount of the noble metals, which can dissolve in the Li_4SiO_4-Li_2TiO_3 melt during an *enhanced* melt-based process, may eventually reach a saturation point.

M. H.H. Kolb et al. [107] also showed that an emulsion method can easily be adapted for the fabrication of the advanced Li_4SiO_4 pebbles with additions of Li_2TiO_3. The emulsion method allows to cover the full compositional range. However, this method consists from several stages: (1) the slurry preparation, (2) the fabrication of the gel-spheres, and (3) the calcination and sintering of the fabricated gel-spheres to obtain dense pebbles.

The fabricated advanced Li_4SiO_4 pebbles with additions of Li_2TiO_3 as a secondary phase are spherically shaped, and both crystalline phases are fully separated by grain boundaries (Fig. 1.10). In the advanced Li_4SiO_4 pebbles with Li_2TiO_3 contents up to 25 mol%, light grey grains of a secondary phase are very small and homogeneously distributed as inclusions between

[5] Melting temperature of Li_2TiO_3: 1823 K

the dendrites of the primary phase, which appear dark-grey. For the advanced pebbles with contents of Li_2TiO_3 higher than 25 mol%, the Li_2TiO_3 phase is the dominant crystal, taking a dendritic shape, and the Li_4SiO_4 phase fills in the gaps between the Li_2TiO_3 dendrites, indicating a reverse crystallization order. After thermal treatment (e.g. up to 1220 K for 3 weeks in air atmosphere), the grain size of the Li_4SiO_4 phase slightly increases, while the grains of Li_2TiO_3 as a secondary phase are still very small and homogeneously distributed as inclusions.

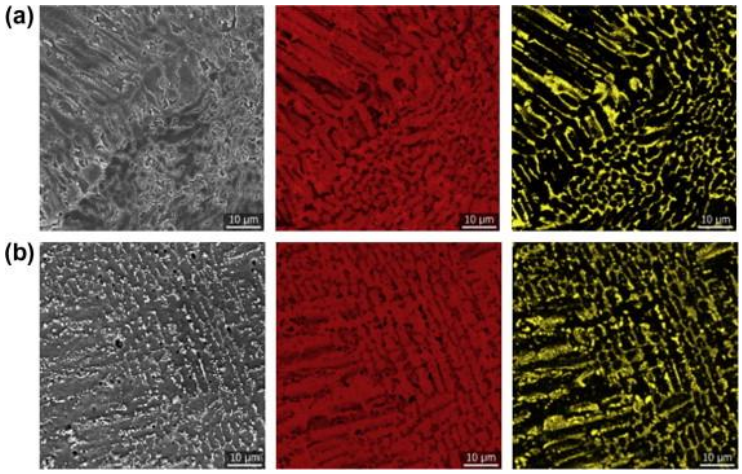

Fig. 1.10 Microstructure and element mapping of silicon and titanium at the chemically etched cross-section of the advanced Li_4SiO_4 pebbles with 15 mol% Li_2TiO_3 as a secondary phase (a) before and (b) after thermal treatment up to 1220 K for 3 weeks in air atmosphere (left – SEM image; middle – silicon distribution; right – titanium distribution) [11].

The optimum content of Li_2TiO_3 has yet to be evaluated; nonetheless the advanced Li_4SiO_4 pebbles with additions of Li_2TiO_3 as a secondary phase have improved mechanical properties in comparison to the reference Li_4SiO_4 pebbles with 2.5 wt% excess of SiO_2 (Fig. 1.11). In general, it is clearly visible that the crush load of the advanced Li_4SiO_4 pebbles increases with increasing content of Li_2TiO_3. The compressive crush load tests involve a continuously increasing load imposed onto the single Li_4SiO_4 pebble between plates until they break, after which the crush load is determined.

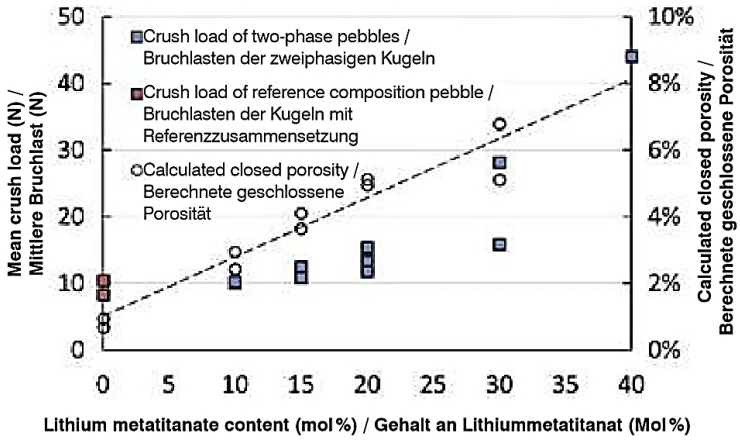

Fig. 1.11 Average crush load values and calculated closed porosity of the Li_4SiO_4 pebbles with various contents of Li_2TiO_3 [106].

Previously, it was reported that the crush load of the Li_4SiO_4 pebbles depend on various factors: moisture, falling distance during the fabrication process [93], closed porosity [106], pebble diameter [108], plate material [109] etc. Therefore, the large standard deviation of the results is very common for the ceramic pebbles and can be attributed to small differences in the pebble microstructure including intrinsic defects, minor variations in the pebble size or in the chemical and phase composition, as well as different orientations of the pebbles between the plates during the compression test.

1.3 Radiation-induced processes in ceramic tritium breeder pebbles

As mentioned above, the lithium-containing ceramic breeder pebbles under the operation conditions of the HCPB TBM in ITER will be subjected to an intense neutron and ionizing radiation, a high magnetic field and elevated temperature. The electron and hole type RD and RP in the ceramic breeder pebbles during irradiation are formed in equal amounts [36] and are mainly created by the neutron-induced nuclear reactions, $Li^6(n,\alpha)T$ and $Li^7(n,n'\alpha)T$ [23], and gamma rays [110]. The energy of charged particles is lost, when the tritium and α particles are slowed down in the crystal structure, through inelastic interactions (leads to ionization and excitation of atoms and molecules) or elastic collisions (leads to atomic displacements). While gamma rays interact with matter in three ways: (1) photoelectric effect (from 0.01 to about 0.5 MeV), (2) Compton scattering (from around 0.3 MeV to 8 MeV), and (3) electron-positron pair formation (from 5 MeV to 100 MeV). The secondary electrons (also called as σ-rays), which are produced in all these processes, usually have enough energy to produce ionization and excitation themselves, while from the excited and ionized atoms and molecules primary RD are formed. The formation of secondary RD and chemically stable RP occurs due to the aggregation of primary RD.

In the following, the radiolysis of the Li_4SiO_4 pebbles with excess of SiO_2 and the Li_2TiO_3 pebbles is described. Finally, the factors, which can influence the formation of RD and RP in the Li_4SiO_4 pebbles, are shortly discussed.

1.3.1 Radiolysis of Li_4SiO_4 pebbles with excess of SiO_2

As described above, the thermally treated Li_4SiO_4 pebbles with excess of SiO_2 have two crystalline phases, monoclinic Li_4SiO_4 as the primary phase and orthorhombic Li_2SiO_3 as a secondary phase. The crystal structure of monoclinic Li_4SiO_4 and orthorhombic Li_2SiO_3 is shown in Fig. 1.12. Previously, the radiolysis of the Li_4SiO_4 and Li_2SiO_3 ceramics has been analysed and described separately by several groups of researchers [19, 20, 22, 27, 36-40, 46, 90, 110-

112]. Both phases, Li_4SiO_4 and Li_2SiO_3, have chemical bonds [≡Si–O^- Li^+], and therefore the formation mechanisms and the structure of the formed RD and RP will be similar in both cases. On the basis of these considerations, the radiolysis of a secondary phase, orthorhombic Li_2SiO_3, in the Li_4SiO_4 pebbles will not be discussed separately in this doctoral thesis.

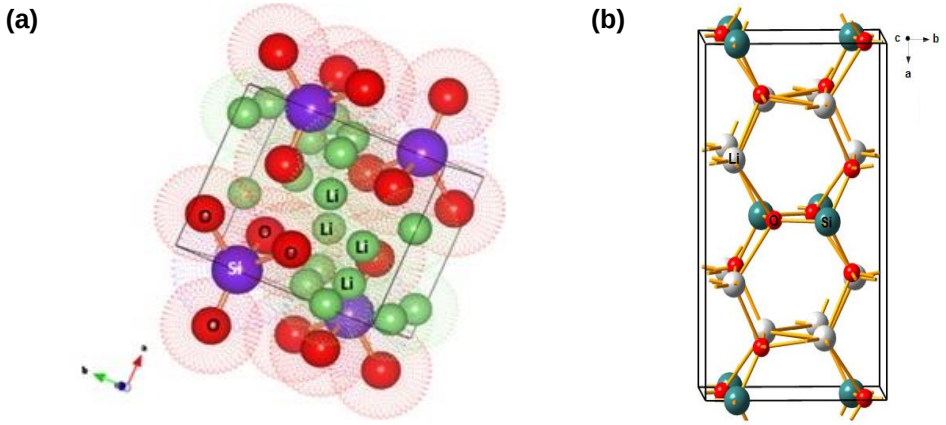

Fig. 1.12 Crystal structure of (a) monoclinic Li_4SiO_4 and (b) orthorhombic Li_2SiO_3 [110, 113].

The fabrication process and thermal treatment of the Li_4SiO_4 pebbles with excess of SiO_2 represents a determining step as it governs their chemical and phase composition, density, microstructure and hence their irradiation performance. The accumulation curves of electron type RD and RP in the five kinds of the Li_4SiO_4 pebbles under action of gamma rays at around 310 K are shown in Fig. 1.13. As suggested above, the electron and hole type RD and RP forms in equivalent amounts, and therefore only one type of the accumulated RD and RP in the Li_4SiO_4 pebbles was analysed to evaluate and compare the radiation stability.

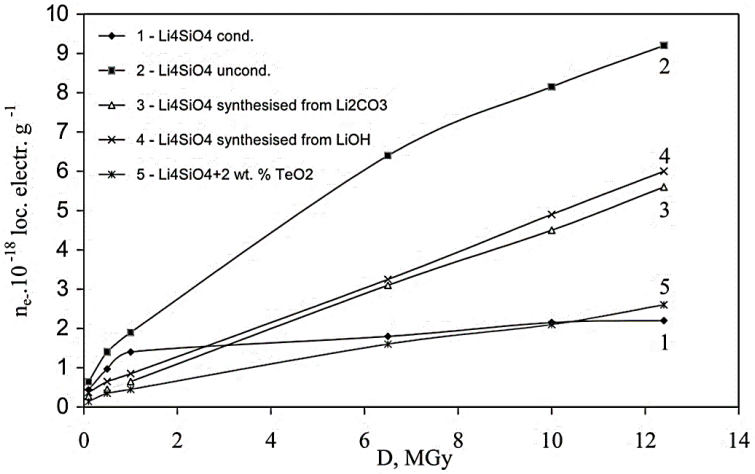

Fig. 1.13 Accumulation curves of electron type RD and RP in the five kinds of the Li_4SiO_4 pebbles with 2.0 wt% excess of SiO_2 under action of gamma rays at around 310 K (1 - the thermally treated pebbles up to 1270 K for 2 weeks in air; 2 - the un-treated pebbles; 3 - the pebbles, which were fabricated from Li_2CO_3; 4 - the pebbles, which were fabricated from LiOH; 5 - the pebbles with 2 wt% additions of tellurium dioxide (TeO_2)) [37].

The mechanism of the radiolysis is the same for the Li_4SiO_4 powders, pebbles or pellets; only the quantitative parameters of the radiolysis are different [40]. The accumulation of RD and

RP takes place through two stages. In the first stage, primary RD localise mainly on intrinsic defects (vacancies, vacancy aggregates, interstitials etc.) and extrinsic defects (impurity atoms), while in the second stage, the radiolysis of the basic matrix occurs. The thermal treatment decreases the number of intrinsic defects, which may remain in the Li_4SiO_4 pebbles with excess of SiO_2 after the fabrication process, and therefore the thermally treated pebbles usually have a higher radiation stability in comparison to the un-treated pebbles.

A. Abramenkovs et al. [23] and J. Tiliks et al. [36, 37, 40] reported that the radiolysis of Li_4SiO_4 can be divided into three main stages: (1) physical stage, (2) physico-chemical stage, and (3) chemical stage. It has been assumed that the primary electron and hole type RD, in the first stage of the radiolysis, are formed due to the dissociation of triplet excitons on oxygen ions (sometimes also called as L-centres) [23]. The dissociation of L-centres leads to the formation of HC_2 centres (≡Si-O· or SiO_4^{3-}) and E' centres (≡Si· or SiO_3^{3-}). The symbol "≡" represents three bonds to three oxygen atoms in the crystal structure and "•" is un-paired electron. In this doctoral thesis, the formation of L-centres, E' centres and HC_2 centres (also called as non-bridging oxygen hole centre or shortly NBOHC) was described by simplified reactions (Eq. 1.19-1.22).

$$SiO_4^{4-} \rightsquigarrow [SiO_4^{4-}]^* \textit{ (L-centre)} \quad (1.19)$$

$$[SiO_4^{4-}]^* \rightarrow SiO_4^{3-} \textit{ (HC}_2\textit{ centre)} + e^- \quad (1.20)$$

$$[SiO_4^{4-}]^* + e^- \rightarrow SiO_3^{3-} \textit{ (E' centre)} + O^{2-} \quad (1.21)$$

$$[SiO_4^{4-}]^* \rightarrow SiO_3^{3-} \textit{ (E' centre)} + O^- \quad (1.22)$$

In the second stage of the radiolysis, secondary RD, such as peroxide radicals (≡Si-O-O·), and chemically stable molecular compounds – RP, are generated (Eqs. 1.23-1.28). The major RP are colloidal lithium (Li_n) particles, elementary silicon (Si_n) particles, molecular oxygen (O_2) and various compounds with silanol (≡Si-Si≡), disilicate (≡Si-O-Si≡) and peroxide (≡Si-O-O-Si≡) bonds. The Li_n localises as particles of two kinds – small particles with size below 1 μm and large particles with size higher than 1 μm.

$$n\ Li^+ + n\ e^- \rightarrow Li_n \textit{ (colloidal lithium)} \quad (1.23)$$

≡Si· *(E' centre)* + ·Si≡ → ≡Si-Si≡ *(silanol bond)* (1.24)

≡Si· + ·O-Si≡ *(HC_2 centre)* → ≡Si-O-Si≡ *(disilicate bond)* (1.25)

$$≡Si\text{-}O\cdot + \cdot O\text{-}Si≡ \rightarrow ≡Si\text{-}O\text{-}Si≡ + ½\ O_2 \quad (1.26)$$

$$≡Si\cdot + O_2 \rightarrow ≡Si\text{-}O\text{-}O\cdot \textit{ (peroxide radical)} \quad (1.27)$$

$$≡Si\text{-}O\text{-}O\cdot + \cdot Si≡ \rightarrow ≡Si\text{-}O\text{-}O\text{-}Si≡ \textit{ (peroxide bond)} \quad (1.28)$$

In the third and final stage of the radiolysis chemical reactions between RP proceed and chemical compounds, such as Li_2O and SiO_2, are formed (Eqs. 1.29 and 1.30).

$$4\ Li_n + n\ O_2 \rightarrow 2n\ Li_2O \quad (1.29)$$

$$Si_n + n\ O_2 \rightarrow n\ SiO_2 \quad (1.30)$$

In previous studies [19, 20, 22, 27, 36-40, 46, 90, 110-112], the radiolysis of the Li_4SiO_4 pebbles, pellets and powders was analysed by various physical and chemical methods. The main physical methods, which can be used to study the formation and accumulation of RD and RP, are ESR spectrometry, TSL technique, radioluminescence (RL), cathodoluminescence (CL), X-ray induced luminescence (XRL) and ion-induced luminescence methods, p-XRD, Raman, FTIR and diffuse reflectance spectrometry. The chemical methods, such as the MCS and lyoluminescence (LL) technique, are sample destructive methods and are based on the difference of redox properties of hole and electron type RD and RP in acid containing solvents. The gaseous RP, such as molecular O_2, can be detected and analysed by gas chromatography (GC).

It was determined that the Li_4SiO_4 pebbles with excess of SiO_2 have a good radiation stability [37]. The radiation chemical yield (G) of RD and RP and the radiolysis degree (α) were selected as the main comparable parameters of the radiation stability. The radiation chemical yield (also called as radiolytic yield) is the number of a particular species, such as electron or hole type RD and RP, produced per 100 eV of energy loss of the charged particles or a high energy electromagnetic radiation. The radiolysis degree (sometimes also called as decomposition degree) is the percentage proportion of the decomposed molecules/ions versus the initial number of molecules/ions before irradiation. In the Li_4SiO_4 pebbles with 2.0 wt% excess of SiO_2, the radiation chemical yield of electron type RD and RP is 0.1 - 0.4 localised electrons per 100 eV and the radiolysis degree is 0.1-1 mol% after irradiation up to 1000 MGy absorbed dose.

1.3.2 Radiolysis of Li_2TiO_3 pebbles

The radiolysis of the Li_2TiO_3 powder, pellets and pebbles was investigated and described by several authors [21, 24, 37, 40, 41-45]. However, extensive researches with the chemical methods (the MCS and LL technique) are limited in literature, due to the low solubility of Li_2TiO_3 in acid solutions [28]. Therefore, the formation and accumulation of RD and RP in the Li_2TiO_3 ceramics were analysed only by physical methods, for example ESR spectrometry, TSL, RL, CL, XRL and ion-induced luminescence techniques etc.

V. Grismanovs et al. [41] and J. Tiliks et al. [37], using ESR spectrometry, detected the formation and accumulation of electron and hole type RD, namely E' centres (TiO_3^{3-}) and HC_2 centres (TiO_3^-), in the Li_2TiO_3 pebbles and pellets during irradiation (Fig. 1.15). The ESR signal with a g-factor at around 2.003 was related to E' centres, while the ESR signals with

g-factors at about 2.010 and 2.016 were attributed to HC_2 centres. The formation of Li_n particles was not detected up to 500 MGy absorbed dose.

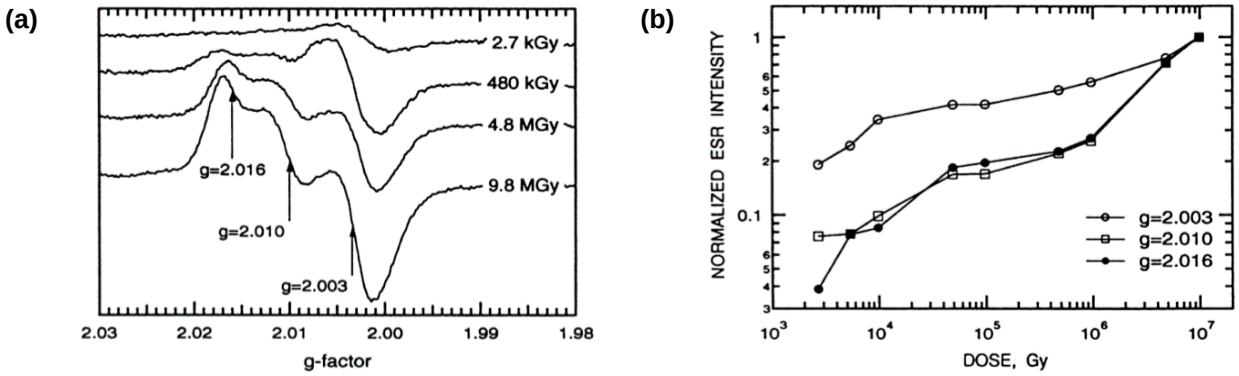

Fig. 1.15 (a) ESR spectra of the Li_2TiO_3 pellets after irradiation with gamma rays at room temperature and (b) the normalized intensities of ESR signals as a function of the absorbed dose [41].

It was reported that the Li_2TiO_3 pebbles have a very high radiation stability [37]. The radiation chemical yield of RD is approx. 10^{-2} defects per 100 eV and the radiolysis degree is around 10^{-3} mol% after irradiation up to 500 MGy absorbed dose. In this doctoral thesis, the formation of E' centres and HC_2 centres in the Li_2TiO_3 pebbles was described by simplified reactions (Eqs. 1.31-1.34).

$$TiO_3^{2-} \rightsquigarrow [TiO_3^-]^* \quad (1.31)$$

$$[TiO_3^-]^* \rightarrow TiO_3^- \textit{ (}HC_2\textit{ centre)} + e^- \quad (1.32)$$

$$[TiO_3^-]^* + e^- \rightarrow TiO_3^{3-} \textit{ (E' centre)} \quad (1.33)$$

$$[TiO_3^-]^* \rightarrow TiO_2^- + O^- \quad (1.34)$$

1.3.3 Factors influencing the radiolysis

The influence of various factors on the formation and accumulation of RD and RP in the Li_4SiO_4 ceramics was analysed and described by several authors [19, 23, 27, 36, 37, 111, 112]. It was suggested that the formation and accumulation of RD and RP only slightly depends on the irradiation type and dose rate, while the neutron fluence, metallic impurities, humidity, magnetic field, irradiation temperature and atmosphere can significantly affect the concentration of the accumulated RD and RP. The influence of these factors on the radiolysis of the Li_4SiO_4 ceramics is further discussed separately.

Irradiation temperature. It was reported that the high irradiation temperature can significantly decrease the concentration of the accumulated RD and RP in the Li_4SiO_4 pebbles, due to the thermally stimulated recombination processes. Previously, the accumulated RD, such as E' centres (≡Si· or SiO_3^{3-}), HC_2 centres (≡Si-O· or SiO_4^{3-}) and peroxide radicals (≡Si-O-O·), in the neutron-irradiated Li_4SiO_4 pebbles were annihilated between 400 K and 600 K [20].

G. Kizane et al. [19] reported that during irradiation at temperatures >900 K, the accumulation of primary and secondary RD in the Li_4SiO_4 pebbles does not occur and only thermally stable RP can form, for example small and large Li_n particles, molecular O_2, Li_2SiO_3 etc.

Neutron fluence. G. Ran et al. [112] reported that by increasing the fluence of thermal neutrons the annihilation behaviour of the accumulated paramagnetic RD in the Li_4SiO_4 ceramic becomes more complicated, and it is most likely related to the formation of secondary RD or various RP, for example small and large Li_n particles. From previous research by F. Beuneu et al. [114], it is known that the small Li_n particles with sizes below 1 μm recombine at around 570-620 K, while the large Li_n particles with sizes higher than 1 μm decompose at about 670-870 K.

Magnetic field. The external magnetic field strongly influence the formation of primary RD in the Li_4SiO_4 pebbles, and it has been suggested that this effect is related to the spin transformation of a primary exciton (singlet ↔ triplet process) [27]. The primary excitons (L-centres) can form in either singlet state (deactivation without decomposition) or triplet state (deactivation with the formation of electron and hole type RD). Since primary RD, E' centres and HC_2 centres, are created due to the dissociation of L-centre, the triplet → singlet state transformation can reduce the formation probability of primary RD.

Humidity. The humidity can increase the concentration of the accumulated RD and RP in the Li_4SiO_4 ceramic up to several times [36]. It has been assumed that the formation of ≡Si-OH and LiOH on the surface of the Li_4SiO_4 ceramic occurs (Eq. 1.35), and thereby during irradiation the radiolysis of ≡Si-OH, LiOH and adsorbed H_2O proceeds (Eqs. 1.36-1.40).

$$\equiv Si\text{-}O\text{-}Li + H_2O \rightarrow \equiv Si\text{-}OH + LiOH \quad (1.35)$$

$$\equiv Si\text{-}OH \rightsquigarrow \equiv Si\text{-}O\cdot + \cdot H \quad (1.36)$$

$$\equiv Si\text{-}OH \rightsquigarrow \equiv Si\cdot + \cdot OH \quad (1.37)$$

$$LiOH \rightsquigarrow Li\text{-}O\cdot + \cdot H \quad (1.38)$$

$$LiOH \rightsquigarrow Li\cdot + \cdot OH \quad (1.39)$$

$$H_2O \rightsquigarrow H\cdot + \cdot OH \quad (1.40)$$

Metallic impurities. The additions of polyvalent transition metal ions, such as Fe^{3+}, Cr^{3+} and lead (Pb^{4+}), can significantly reduce the concentration of the accumulated RD and RP in the Li_4SiO_4 ceramic during irradiation [36, 23]. The simplified reaction of polyvalent metal ion with electron is shown in Eq. 1.41.

$$Me^{n+} + e^- \rightarrow Me^{(n-1)+} \quad (1.41)$$

2. EXPERIMENTAL

In this chapter, the investigated samples are described, including their fabrication methods and preparation process for the irradiation. The irradiation procedure of the samples and the used equipment is specified. The applied methods of characterisation are described, including the measurement parameters and the mathematical processing of the obtained data.

2.1 Investigated samples

In this doctoral thesis, three types of the advanced Li_4SiO_4 pebbles with different contents of Li_2TiO_3 as a secondary phase were investigated together with the reference Li_4SiO_4 pebbles with 2.5 wt% excess of SiO_2 (Table 2.1). The reference Li_4SiO_4 pebbles (0 mol% Li_2TiO_3) consist of two crystalline phases, Li_4SiO_4 as the primary phase and Li_2SiO_3 as a secondary phase, and they are the present reference tritium breeder material for the EU proposed HCPB TBM concept [1]. The advanced pebbles were produced by an *enhanced* melt-based process at the Karlsruhe Institute of Technology (Germany), while the reference pebbles were fabricated by a melt-spraying process at the Schott AG (Mainz, Germany). The chemical composition of the fabricated pebbles was confirmed by ICP-OES and X-ray fluorescence (XRF) spectrometry at the Karlsruhe Institute of Technology [18, 83]. To achieve an operation relevant microstructure and phase composition, the fabricated Li_4SiO_4 pebbles with various contents of Li_2TiO_3 were thermally treated up to 1220 K for 3 weeks in air atmosphere.

Table 2.1 Specification of the investigated Li_4SiO_4 pebbles with various contents of Li_2TiO_3.

Sample	Pebbles	Phase composition			Pebble diameter, µm
		Li_4SiO_4, mol%	Li_2TiO_3, mol%	Li_2SiO_3, mol%	
#1.1	Reference	90	0	10	250-900[6]
#1.2	Advanced	90	10	0	500-1000
#1.3	Advanced	80	20	0	500-1000
#1.4	Advanced	70	30	0	500-1000

Influence of the noble metals on the radiolysis. During a fabrication campaign, several batches of the advanced Li_4SiO_4 pebbles with additions of Li_2TiO_3 as a secondary phase were produced by an *enhanced* melt-based process, and the chemical composition of the fabricated pebbles was analysed by ICP-OES at the Karlsruhe Institute of Technology. Three types of the advanced Li_4SiO_4 pebbles with similar chemical composition, but with different contents of the noble metals (Pt, Au and Rh) were selected and marked as Sample #2.1, #2.2 and #2.3 (Table 2.2) to evaluate the influence of the noble metals with a sum content of up to 300 ppm on

[6] Two batches: 250-630 µm and 560-900 µm

the formation and accumulation of RD and RP. The advanced Li_4SiO_4 pebbles with a highest content of the noble metals (Sample #2.1) were thermally treated up to 1220 K for 3 weeks in air atmosphere to reduce the number of intrinsic defects, which may have formed during the fabrication process. The thermally treated pebbles are marked as Sample #2.1a.

Table 2.2 Specification of the investigated advanced Li_4SiO_4 pebbles with various contents of the noble metals.

	Sample #2.1	Sample #2.1a	Sample #2.2	Sample #2.3
Chemical composition:				
Li, wt%	21.9±0.2	21.9±0.2	21.20±0.06	21.40±0.08
Si wt%	18.30±0.04	18.30±0.04	20.0±0.2	20.2±0.1
Ti, wt%	8.03±0.05	8.03±0.05	7.04±0.01	6.96±0.04
Pt, ppm	289±2	289±2	102±2	22±1
Au, ppm	156±1	156±1	33±1	<6
Rh, ppm	<5	<5	<6	<6
Phase composition	80 mol% Li_4SiO_4 20 mol% Li_2TiO_3	80 mol% Li_4SiO_4 20 mol% Li_2TiO_3	83 mol% Li_4SiO_4 17 mol% Li_2TiO_3	83 mol% Li_4SiO_4 17 mol% Li_2TiO_3
Pebble colour	Off-white	Pale-yellow	Off-white	Off-white
Pebble size	250-1250 µm	650-900 µm	>1250 µm	>1250 µm
Thermal treatment	-	1220 K, 3 weeks, air	-	-

Influence of the pebble diameter and the grain size on the radiolysis. Two types of the reference Li_4SiO_4 pebbles (0 mol% Li_2TiO_3) with diameter bellow 50 µm and around 500 µm (further entitled as small and large pebbles) were selected (Table 2.3) to analyse the influence of the pebble diameter and the grain size on the formation and accumulation of RD and RP. The small pebbles and the large pebbles were produced in the same fabrication campaign by a melt-spraying process at the Schott AG and thus have identical chemical composition. To achieve crystallization and a microstructure with various grain sizes, the small pebbles and the large pebbles were thermally treated at various conditions in air atmosphere.

Table 2.3 Specification of the investigated reference Li_4SiO_4 pebbles (0 mol% Li_2TiO_3) with various pebble diameters and grain sizes.

Sample	Pebbles	Pebble diameter, µm	Thermal treatment		Grain size (aver.), µm
			Temperature, K	Time, h	
#3.1	Small	<50	1070	1	1
#3.2	Small	<50	1170	128	5
#3.3	Large	~500	1240	168	10

Influence of the chemisorption products on the radiolysis. The Li_4SiO_4 powders with three different chemical compositions were selected (Table 2.4) to analyse the influence of the chemisorption products of H_2O vapour and CO_2 (LiOH and Li_2CO_3) on the formation and accumulation of RD and RP. The powders were used instead of the pebbles, due to their high

surface area (approx. 20 m^2 g^{-1}) and smaller grain size (below 600 nm), to increase the amount of the accumulated chemisorption products. Li_2TiO_3 practically does not react with H_2O vapour and CO_2 [115], and therefore the influence of the additions of Li_2TiO_3 as a secondary phase on the formation and radiolysis of the chemisorption products on the surface of the advanced Li_4SiO_4 pebbles was not evaluated.

Table 2.4 Specification of the investigated Li_4SiO_4 powders with various chemical composition.

	Powders		
	"Pure"	**with 3 mol% SiO_2**	**with 6 mol% Li_2SiO_3**
Sample	#4.1	#4.2	#4.3
Phase composition	98 mol% Li_4SiO_4 2 mol% Li_2SiO_3	95 mol% Li_4SiO_4 2 mol% Li_2SiO_3 3 mol% SiO_2	92 mol% Li_4SiO_4 8 mol% Li_2SiO_3
Grain size	200-300 nm	200-400 nm	300-600 nm
Specific surface area	23±2 m^2 g^{-1}	22±2 m^2 g^{-1}	17±2 m^2 g^{-1}
Thermal treatment	890 K, 1 h, air	-	920 K, 3.5 h, air

The "pure" Li_4SiO_4 powder was produced by a plasma synthesis [116] at the Institute of Inorganic Chemistry (Riga Technical University). For the synthesis, Li_2CO_3 and SiO_2 were used as raw materials. To eliminate residues of raw materials, the produced powder was thermally treated up to 890 K for 1 h in air atmosphere. The formation of Li_2SiO_3 as a secondary phase during the fabrication process can be explained by un-stoichiometry of raw materials.

The 2 wt% (3 mol%) excess of SiO_2 was added to the fabricated "pure" Li_4SiO_4 powder to obtain similar chemical composition as in the reference Li_4SiO_4 pebbles (90 mol% Li_4SiO_4 and 10 mol% Li_2SiO_3). The mixture of both powders, L_4SiO_4 and SiO_2, was homogenized by milling for 3 h in ball mill and was thermally treated up to 920 K for 3.5 h in air atmosphere. The slight specific surface decrease of the Li_4SiO_4 powder with excess of SiO_2 during thermal treatment can be attributed to the particle agglomerations and to the formation of Li_2SiO_3 phase. The formation of Li_2SiO_3 was represented by the following simplified reaction:

$$Li_4SiO_4 + SiO_2 \rightarrow 2\ Li_2SiO_3 \qquad (2.1)$$

2.2 Preparation and irradiation of samples

In this doctoral thesis, the linear electron accelerator ELU-4 (Salaspils) producing the 5 MeV accelerated electron beam was used as a high energy radiation source. The thermally treated Li_4SiO_4 pebbles with various contents of Li_2TiO_3 (Table 2.1) were encapsulated in quartz tubes with a dry argon and were irradiated with 5 MeV accelerated electrons, up to 4 h per day. The irradiation was performed up to 24 MGy absorbed dose at 300-350 K and up to 5000 MGy absorbed dose at 380-1285 K. The irradiation conditions (absorbed dose, dose rate and

irradiation temperature) of each irradiation campaign are specified in Table 2.5. Several quartz tubes with the encapsulated pebbles were broken during irradiation at elevated temperature, most likely due to the high temperature differences during one of the irradiation cycles, and therefore were omitted from characterization.

Table 2.5 Specification of the irradiation conditions of the Li_4SiO_4 pebbles with various contents of Li_2TiO_3 with 5 MeV accelerated electrons up to 24 MGy absorbed dose at 300-350 K and up to 5000 MGy absorbed dose at 380-1285 K (n/a - not analysed).

Irradiation campaign	Absorbed dose, MGy	Irradiation temperature, K			Dose rate (aver.), kGy s^{-1}
		Average	Min	Max	
#1	0.01	300	n/a	n/a	0.67
#2	0.05	300	n/a	n/a	0.67
#3	0.15	300	n/a	n/a	0.67
#4	0.5	300	n/a	n/a	0.83
#5	1.5	300	n/a	n/a	0.64
#6	2	300	n/a	n/a	0.64
#7	3	305	300	310	0.85
#8	6	305	300	310	0.85
#9	6	n/a	n/a	1285	33
#10	12	310	300	315	0.85
#11	24	320	300	345	0.85
#12	42	520	460	580	11.7
#13	42	670	630	730	11.7
#14	84	630	533	720	11.7
#15	100	710	580	840	2.6
#16	100	730	500	950	2.6
#17	193	710	690	730	13.4
#18	249	940	875	990	21.3
#19	1000	460	380	560	11.7
#20	3700	520	440	670	13.4
#21	5000	520	380	650	11.6

The accelerated electron beam diameter is limited (depends on the distance from the linear electron accelerator), and therefore up to four quartz tubes with the encapsulated Li_4SiO_4 pebbles with various contents of Li_2TiO_3 were irradiated simultaneously. The location of each quartz tube was changed after each irradiation cycle (up to 4 h per day) in order to avoid differences in the absorbed dose depending on quartz tube location in the irradiation area. Due to the collisions of the accelerated electrons with the solid-state matter, most of the kinetic energy of the accelerated electrons is transferred into heat within the specimen, causing a local temperature rise. The irradiation temperature was controlled by the distance of quartz tubes from the linear electron accelerator and by the cooling with dry air flow and was continuously measured by a chromel-alumel thermocouple, that was located in the central part of irradiated area, with an Agilent 34970A multichannel digital voltmeter and an Agilent 34902A multiplexer and recorded

with an PC using the Agilent BenchLink Data Logger 3 software. The measured irradiation temperature range during one irradiation campaign can be associated with electron beam centre displacement, un-even cooling with dry air flow, slight current or voltage changes of the linear electron accelerator etc.

The thermal stability and annihilation of the accumulated RD and RP. The irradiated Li_4SiO_4 pebbles with various contents of Li_2TiO_3 were stepwise isochronally annealed in inert atmosphere (vacuum, nitrogen or dry argon) to investigate the thermal stability and annihilation of the accumulated RD and RP. The annealing temperature was increased stepwise from room temperature up to 1070 K. The temperature interval between two annealing steps was up to 50 K, while the duration time of each annealing step was up to 30 min. After each annealing step, the pebbles were cooled down to room temperature and were analysed by ESR spectrometry.

Influence of the noble metals on the radiolysis. The un-treated and thermally treated advanced Li_4SiO_4 pebbles with various contents of the noble metals (Table 2.2) were encapsulated in quartz tubes with a dry argon and were irradiated with 5 MeV accelerated electrons, up to 12 MGy absorbed dose (average dose rate: 0.85 kGy s^{-1}) at 300-350 K, to study the influence of the noble metals on the formation and accumulation of RD and RP. The irradiation parameters (absorbed dose and irradiation temperature) were selected to mainly accumulate primary and secondary RD and to avoid the formation of RP, for example small and large Li_n particles, molecular O_2, Li_2SiO_3 etc.

Influence of the pebble diameter and the grain size on the radiolysis. The thermally treated small pebbles and large pebbles (Table 2.3) were encapsulated in quartz tubes with a dry argon or air and were irradiated with 5 MeV accelerated electrons, up to 11000 MGy absorbed dose (dose rate: up to 25 kGy s^{-1}) at around 550-590 K, to study the influence of the pebble diameter and the grain size on the formation and accumulation of RD and RP. The irradiation conditions (absorbed dose and irradiation temperature) were selected in order to reach conditions comparable to the irradiated Li_4SiO_4 pebbles with various contents of Li_2TiO_3 (Table 2.5). To investigate the thermal stability and annihilation of the accumulated RD and RP, the irradiated small pebbles and large pebbles were stepwise isochronally annealed up to 620 K for 30 min in air atmosphere. After each annealing step, the pebbles were cooled down to room temperature and were analysed by the MCS and ESR spectrometry.

Influence of the chemisorption products on the radiolysis. To understand the processes, which may occur during one of the irradiation cycles (up to 4 h), on the surface of the small pebbles and the large pebbles in air atmosphere, the Li_4SiO_4 powders with three different chemical compositions were used (Table 2.4). The type of radiation practically does not affect

the qualitative composition of the accumulated RD and RP, and therefore X-rays instead of 5 MeV accelerated electrons were used, due to the smaller dose rate and lower irradiation temperature. The 5 MeV accelerated electron beam of the linear electron accelerator ELU-4 was converted into X-rays by a water-cooled W plate.

The Li_4SiO_4 powders with three different chemical compositions were irradiated by X-rays, up to 56 kGy absorbed dose (average dose rate: 0.23 kGy s^{-1}) at around 300 K, in air atmosphere to study the influence of the chemisorption products on the formation and accumulation of RD and RP. The dose rate and absorbed dose was reduced to mainly accumulate primary and secondary RD and to avoid the formation of RP, for example small and large Li_n particles, molecular O_2, Li_2SiO_3 etc. To investigate the thermal stability and annihilation of the accumulated RD, the irradiated powders were stepwise isochronally annealed up to 620 K for 30 min in air atmosphere. After each annealing step, the powders were cooled down to room temperature and were analysed by ESR spectrometry.

To simulate the processes, which may occur on the surface of the small pebbles and the large pebbles during one of the irradiation cycles (up to 4 h) at around 550-590 K in air atmosphere, the Li_4SiO_4 powder with additions of Li_2SiO_3 as a secondary phase was thermally treated up to 570 K for 4 h in air atmosphere and was irradiated with X-rays up to 56 kGy absorbed dose at around 300 K in air atmosphere.

2.3 Methods of characterisation

Electron spin resonance (ESR) spectrometry. The accumulated paramagnetic RD and RP in the Li_4SiO_4 pebbles with various contents of Li_2TiO_3 and in the Li_4SiO_4 powders after irradiation were analysed by ESR spectrometry (also called as electron paramagnetic resonance or shortly EPR) [117] at the Latvian Institute of Organic Synthesis. The ESR spectra were recorded using a Bruker BioSpin X-band EPR spectrometer (microwave frequency: 9.8 GHz, microwave power: 0.2 mW, modulation amplitude: 0.5 mT, field sweep: 20, 100 and 400 mT) operating at room temperature. The pebbles and powders before and after irradiation were analysed in Bruker ER 221TUB/3 clear fused quartz (CFQ) quality sample tubes with an inner diameter of 3 mm or in Bruker ER 221TUB/2 CFQ quality sample tubes with an inner diameter of 2 mm. The reference marker Bruker ER 4119HS-2100 with a g-factor 1.9800±0.0005 (the concentration of un-paired electrons: $1.15 \cdot 10^{-3}$ %) was used for the quantitative measurements.

The g-factor of the ESR signals was calculated using the following equation:

$$g = \frac{h \cdot v}{\mu_B \cdot B_o}, \text{ with} \qquad (2.2)$$

h – Plank constant, v – microwave frequency, μ_B – Bohr magneton and B_o – magnetic field.

The total concentration of the accumulated paramagnetic RD and RP in the irradiated pebbles and powders was calculated by a double integration method of the first derivative ESR signals and by comparison with the ESR signal of the reference marker (Eq. 2.3).

$$C_x = \frac{S_x \cdot N_{ref}}{S_{ref} \cdot m}, \text{ with} \quad (2.3)$$

S_x – area under an absorption curve of the analysed ESR signal, S_{ref} – area under an absorption curve of the reference marker, N_{ref} – the concentration of un-paired electrons in the reference marker and m – sample mass.

Thermally stimulated luminescence (TSL) technique. The thermally stimulated recombination processes of the accumulated RD and RP in the Li_4SiO_4 pebbles with various contents of Li_2TiO_3 after irradiation were studied by TSL technique (also called as thermo-luminescence or shortly TL) [118].

At the Institute of Chemical Physics (University of Latvia) the TSL glow curves of the irradiated pebbles were measured with a photomultiplier tube. The TSL glow curves of the pebbles and crushed powders (approx. 5-10 mg) were measured from room temperature up to 770 K with five heating rates (0.1, 0.2, 0.5, 1 and 2 K s^{-1}) in air atmosphere.

The activation energy (E_a) values for the thermally stimulated recombination processes of the accumulated RD and RP in the irradiated pebbles were calculated by Hoogenstraaten method [119]. In this method, the plot of $\ln(T_m^2/\beta)$ versus $(1/T_m)$ at different heating rates of a first-order TSL glow peak gives rise to a straight line with a slope equal to (E_a/k), from which the E_a values can be determined. The symbol β stands for the heating rate, T_m for the maximum temperature of the TSL peak and k for the Boltzmann's constant.

At the Institute of Solid State Physics (University of Latvia) the TSL spectra of the irradiated pebbles were measured up to 570 K (heating rate: 1 K s^{-1}) in air atmosphere and were recorded with a monochromator Andor Shamrock SR-303i-B equipped with a CCD camera (spectral range: 250-800 nm). The pebbles before measurements were crushed into fine powder, and approx. 0.1 g of the crushed powder was pressed into pellet (diameter: 5 mm).

The obtained results of TSL glow curves and spectra were compared with data recorded with another experimental setup at the Institute of Solid State Physics (University of Latvia). The TSL glow curves of the irradiated pebbles were measured up to 770 K (heating rate: 2 K s^{-1}, high vacuum) with a photomultiplier tube (HAMAMATSU H8259) with a 300-500 nm bandpass filter. To acquire information about spectral distribution of the TSL glow curves, an Andor Shamrock B-303i spectrograph equipped with a CCD camera (Andor DU-401A-BV) was used.

The pebbles before measurements were crushed into fine powder, and approx. 0.2 g of the crushed powder was pressed into pellet (diameter: 10 mm).

Method of chemical scavengers (MCS). The accumulated electron type RD and RP in the reference Li_4SiO_4 pebbles (0 mol% Li_2TiO_3) after irradiation were analysed by the MCS [120] at the Institute of Chemical Physics (University of Latvia). In this method, the irradiated pebbles are dissolved in acid containing scavenger solutions, and consequently various electron type RD and RP are transformed into gaseous H_2, which then can be detected by GC.

To evaluate the content of simple and complex electron type centres, the irradiated pebbles before measurements were crushed into fine powder, and approx. 10 mg of the crushed powder was dissolved in two scavenger solutions: (1) 0.1 M H_2SO_4 solution with 1 M C_2H_5OH, and (2) 0.1 M H_2SO_4 solution with 1 M $NaNO_3$. In the first solution, the electrons from simple and complex electron type centres are scavenged and transformed into gaseous H_2. While in the second solution, the generation of gaseous H_2 occurs only from complex electron type centres, but the electrons from simple electron type centres are scavenged. The chemical processes in these two scavenger solutions can be represented by the following reactions:

$$e^-_{aq} + H_3O^+ \rightarrow H^o + H_2O \quad (2.4)$$

$$2\,H^o \rightarrow H_2 \quad (2.5)$$

$$H^o + C_2H_5OH \rightarrow H_2 + \cdot C_2H_4OH \quad (2.6)$$

$$e^-_{aq} + NO_3^- \rightarrow NO_3^{2-} \quad (2.7)$$

The concentration of the generated gaseous H_2 from the obtained data of GC and the concentration of simple and complex electron type centres in the dissolved pebbles was calculated using the following equations:

$$n_{H_2(H^+/EtOH)\,or(H^+/NO_3^-)} = \frac{I \cdot 2.20 \cdot 10^{12}}{m} \quad (2.8)$$

$$n_{simple\ e^- centres} = n_{H_2(H^+/EtOH)} - n_{H_2(H^+/NO_3^-)} \quad (2.9)$$

$$n_{complex\ e^- centres} = 2\,n_{H_2(H^+/NO_3^-)}, \text{ with} \quad (2.10)$$

I – the detected number of pulses by GC, m – sample mass, $n_{H_2(H^+/EtOH)}$– the concertation of the generated gaseous molecular H_2, which was detected from the acid solvent with 1 M C_2H_5OH by GC, and $n_{H_2(H^+/NO_3^-)}$ – the concentration of the generated gaseous molecular H_2, which was detected from the acid solvent with 1M $NaNO_3$ by GC.

Diffuse reflectance spectrometry. The accumulated optically active RD and RP (colour centres) in the Li_4SiO_4 pebbles with various contents of Li_2TiO_3 after irradiation were analysed by diffuse reflectance spectrometry [121].

At the Institute of Solid State Physics (University of Latvia) the diffuse reflectance spectra of the pebbles before and after irradiation were measured by a SPECORD-210 spectrometer (spectral range: 380-1100 nm). The pebbles before measurements were crushed into fine powder, and approx. 0.1 g of the crushed powder was pressed into pellet (diameter: 5 mm).

At the Institute of Chemical Physics (University of Latvia) the diffuse reflectance spectra of the irradiated pebbles were measured by a SPECORD-M40 spectrometer (spectral range: 340-840 nm). The pebbles before measurements were crushed into fine powder. The linear coefficient of absorption (k) was calculated against the crushed powder of the un-irradiated pebbles according to equation 2.11.

$$k = \frac{s(1-r)^2}{2r}, \text{ with} \qquad (2.11)$$

s – scattering constant, r – ratio of light intensity of the diffuse reflection from the irradiated sample and the un-irradiated sample.

Powder X-ray diffractometry (p-XRD). The phase composition of the Li_4SiO_4 pebbles with various contents of Li_2TiO_3 and the Li_4SiO_4 powders before and after irradiation were analysed by p-XRD [122] at the Faculty of Chemistry (University of Latvia) and at the Karlsruhe Institute of Technology. The pebbles before measurement were crushed into fine powder. The p-XRD patterns were obtained by a Bruker D8 diffractometer (range: 10-70° 2theta, scan speed: 0.02-0.05° 2theta, step time: 5 s, source: CuKα, wavelength: 0.15418 nm). The following datasets were used from the JCPDS PDF-2 (Release 2010) database: Li_4SiO_4 (074-0307), Li_2SiO_3 (029-0828) and Li_2TiO_3 (033-0831).

Fourier transformation infrared (FTIR) spectrometry. The bond vibrations in the Li_4SiO_4 pebbles with various contents of Li_2TiO_3 and in the Li_4SiO_4 powders before and after irradiation were analysed by FTIR spectrometry [123]. The pebbles before measurement were crushed into fine powder. The absorption FTIR spectra were obtained by a Perkin Elmer Spectrum Two spectrometer (range: 450-4000 cm^{-1}, pressed in potassium bromide pellets, air) at the Faculty of Chemistry (University of Latvia). The attenuated total reflectance (ATR) FTIR spectra of the crushed powder were recorded by a Bruker Vertex 70 v FTIR spectrometer with a Platinum diamond ATR accessory (range: 400-4000 cm^{-1}, resolution: 4 cm^{-1}, vacuum pressure: <3 hPa) at the Institute of Chemical Physics (University of Latvia).

Scanning electron microscopy (SEM) coupled with energy dispersive X-ray (EDX) spectrometry. The microstructure, grain size and surface chemical composition of the Li_4SiO_4 pebbles with various contents of Li_2TiO_3 and the Li_4SiO_4 powders before and after irradiation was studied by SEM coupled with EDX spectrometry [124]. The SEM-EDX images were obtained by a field emission SEM Hitachi S-4800 using an EDX system Bruker XFlash Quad

5040 123 eV at the Institute of Chemical Physics (University of Latvia). The microstructure at the cross-sections of the pebbles was examined with a field emission SEM (SUPRA 55, Zeiss) at the Karlsruhe Institute of Technology. The pebbles before SEM measurements were impregnated in epoxy resin and were polished and grinded to about half of their size. The cross-section of the pebbles was chemically etched to enhance the distinction between the occurring phases.

X-ray fluorescence (XRF) spectrometry. The chemical composition of the Li_4SiO_4 pebbles with various contents of Li_2TiO_3 and the Li_4SiO_4 powders before and after irradiation was analysed by XRF spectrometry [125] at the Faculty of Chemistry (University of Latvia). The XRF spectra of the pebbles, crushed powders and pressed pellets were recorded by a Bruker S8-TIGER spectrometer (pebbles and crushed powders were measured on 5 μm polypropylene film, helium atmosphere).

Thermogravimetry-differential thermal analysis (TG-DTA). The absorbed gases, phase transitions and melting of the Li_4SiO_4 pebbles with various contents of Li_2TiO_3 and the Li_4SiO_4 powders before and after irradiation were studied by TG-DTA [126] at the Institute of Chemical Physics (University of Latvia). The TG-DTA curves were obtained by a Seiko EXTAR 6300 (sample holder: Pt or corundum crucible, sample holder diameter/height: 5/5 mm or 5/2.5 mm, sample mass: approx. 10 mg, temperature range: up to 1470 K, heating rate: 2-10 K min^{-1}, atmosphere: argon, nitrogen or air, gas flow: up to 150 ml min^{-1}).

X-ray photoelectron spectrometry (XPS). The top-surface chemical composition of the un-treated and thermally treated advanced Li_4SiO_4 pebbles with various contents of the noble metals before irradiation was analysed by XPS [127] at the Kaunas University of Technology (Lithuania). The XPS spectra were recorded by a Thermo Scientific ESCALAB 250Xi spectrometer (vacuum pressure: $2 \cdot 10^{-9}$ Torr, source: Al Kα, energy: 1486.6 eV, analysed area: approx. 0.3 mm). The energy scale of the system was calibrated according to Au $4f_{7/2}$, Ag $3d_{5/2}$ and Cu $2p_{3/2}$ peaks position.

3. RESULTS AND DISCUSSION

In this chapter, for the first time the formation and accumulation of RD and RP in the Li_4SiO_4 pebbles with various contents of Li_2TiO_3 are analysed and described under action of 5 MeV accelerated electrons to estimate and compare the parameters, which characterises the radiation stability. The thermal stability and annihilation of the accumulated RD and RP in the irradiated Li_4SiO_4 pebbles are studied to predict the possible tritium release temperature range. The behaviour of the Li_4SiO_4 pebbles is investigated under the simultaneous action of 5 MeV accelerated electrons and high temperature to evaluate the high-temperature radiolysis processes. In addition, to exclude effects from technological factors on the formation and accumulation of RD and RP in the Li_4SiO_4 pebbles during irradiation, the influence of the noble metals, the pebble diameter, the grain size and the chemisorption products on the radiolysis is studied and evaluated separately.

3.1 Formation, accumulation and annihilation of radiation-induced defects and radiolysis products in Li_4SiO_4 pebbles with various contents of Li_2TiO_3

The un-treated and thermally treated advanced Li_4SiO_4 pebbles with additions of Li_2TiO_3 as a secondary phase show an off-white colour (pale yellow, pink, purple or brown) before irradiation, while the reference Li_4SiO_4 pebbles (0 mol% Li_2TiO_3) are “pearl” white. During thermal treatment, up to 1220 K for 3 weeks in air atmosphere, slight colour changes for the advanced Li_4SiO_4 pebbles with additions of Li_2TiO_3 were also observed. The photos of the thermally treated Li_4SiO_4 pebbles with various contents of Li_2TiO_3 before and after irradiation with 5 MeV accelerated electrons, up to 6 MGy absorbed dose at around 305 K and up to 1285 K in a dry argon atmosphere, are shown in Fig. 3.1. The content of Li_2TiO_3 is given in the upper row, while the irradiation conditions are shown on the left side.

The absorption edges of Li_4SiO_4 and Li_2TiO_3 are located at around 210 nm [128] and 320 nm [129], respectively. Therefore, it is assumed that the off-white colour of the advanced Li_4SiO_4 pebbles with additions of Li_2TiO_3 as a secondary phase before irradiation (Fig. 3.1, upper row) might be caused by the raw materials, for example due to the reduction of tetravalent titanium (Ti^{4+}) ions, by the presence of metallic trace-impurities, which can be added to the advanced Li_4SiO_4 pebbles during the fabrication process, or by the formation of oxygen vacancies during the fabrication process. Using diffuse reflectance spectrometry, at least three broad absorption bands with wavelengths between 350 nm and 700 nm were detected in the spectra of the advanced Li_4SiO_4 pebbles with additions of Li_2TiO_3 before irradiation. According

to K. Morinaga et al. [130], the absorption bands with maxima close to 500 nm can be attributed to trivalent titanium (Ti^{3+}) ions. While the absorption band with a maximum <350 nm can be linked to Ti^{4+} ions [131].

Fig. 3.1 Photos of the Li_4SiO_4 pebbles with various contents of Li_2TiO_3 before and after irradiation with 5 MeV accelerated electrons up to 6 MGy absorbed dose at around 305 K and up to 1285 K in a dry argon atmosphere.

The Li_4SiO_4 pebbles with various contents of Li_2TiO_3 are spherically shaped, and the surface and the microstructure at the chemically etched cross-section of the Li_4SiO_4 pebbles before irradiation is shown in Fig. 3.2 and 3.3, respectively. The content of Li_2TiO_3 is given above the SEM images. The advanced Li_4SiO_4 pebbles with additions of Li_2TiO_3 as a secondary phase have a "peach-like" form, and on the surface of the advanced Li_4SiO_4 pebbles various two- and three-dimensional defects, such as open pores, joints, cavities and cracks, can be seen (Fig. 3.2). While on the surface of the reference Li_4SiO_4 pebbles (0 mol% Li_2TiO_3) such defects were not detected. It is assumed that the cracks on the surface of the advanced pebbles are caused during the fabrication process, due to the rapid quenching of the obtained pebbles in liquid nitrogen and the collisions of the obtained pebbles with liquid nitrogen receptacle. The cavities and open porosity, on the other hand, may result from the density differences between the liquid state and the solid state during the rapid quenching process. The surface of the pebbles shrinks prior to the volume during the fabrication process, due to the rapid quenching in liquid nitrogen, and therefore tension will form, which can produce various intrinsic defects.

In the reference Li_4SiO_4 pebbles (0 mol% Li_2TiO_3) at the chemically etched cross-section before irradiation, the Li_4SiO_4 phase is displayed in dark grey colour with inclusions of smaller,

light grey grains of Li_2SiO_3 as a secondary phase (Fig. 3.3). While in the advanced Li_4SiO_4 pebbles, light grey grains of Li_2TiO_3 as a secondary phase are very small and homogeneously distributed as inclusions in the Li_4SiO_4 phase, which appears dark-grey. The advanced Li_4SiO_4 pebbles with 20 mol% Li_2TiO_3 have a slightly different microstructure in comparison to the two other advanced pebbles, which is formed during the fabrication process, probably due to the insufficient homogenization of the Li_4SiO_4-Li_2TiO_3 melt or the rapid quenching of the obtained pebbles in liquid nitrogen.

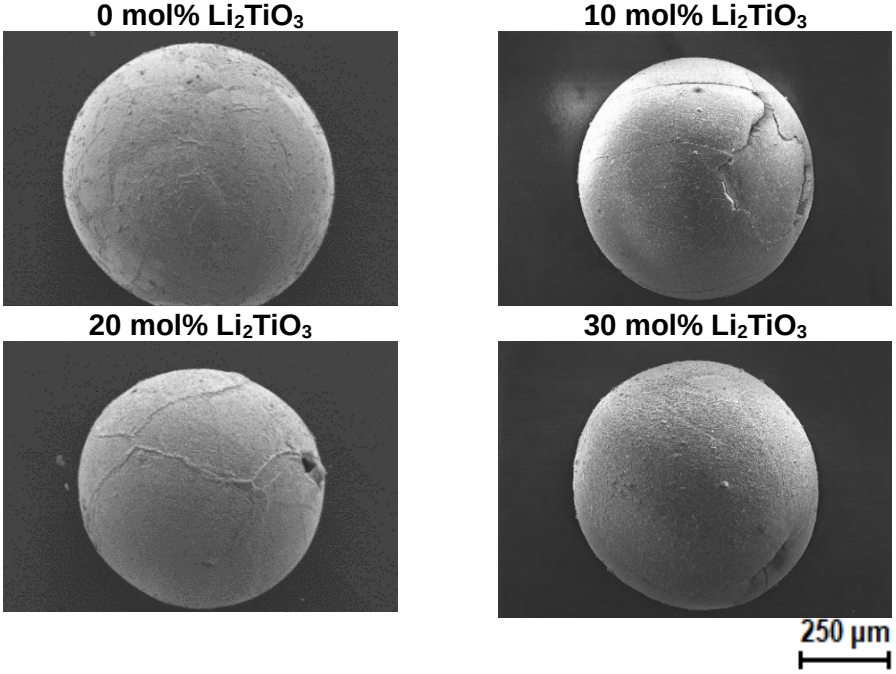

Fig. 3.2 Surface microstructure of the Li_4SiO_4 pebbles with various contents of Li_2TiO_3 before irradiation.

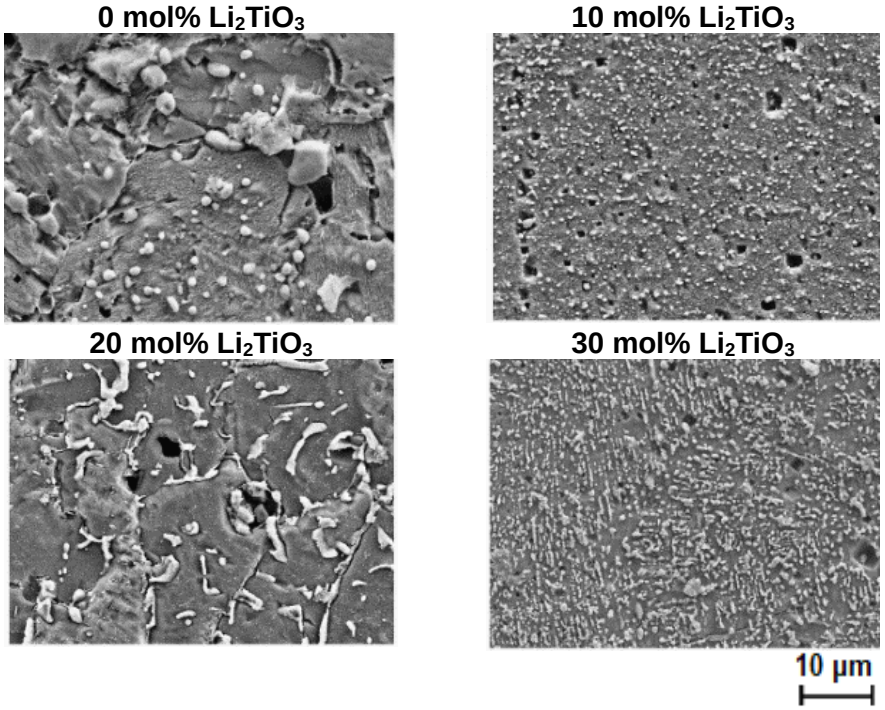

Fig. 3.3 Microstructure at the chemically etched cross-section of the Li_4SiO_4 pebbles with various contents of Li_2TiO_3 before irradiation.

Using p-XRD it was detected that the advanced pebbles before irradiation feature two crystalline phases, monoclinic Li_4SiO_4 as the primary phase and monoclinic Li_2TiO_3 (β-form) as a secondary phase. While in the p-XRD patterns of the reference Li_4SiO_4 pebbles (0 mol% Li_2TiO_3), the diffraction reflexes of orthorhombic Li_2SiO_3 as a secondary phase were detected, due to the excess of SiO_2, which was added during the fabrication process [84]. The obtained p-XRD patterns are shown in Fig. 3.4. No traces of the ternary compounds (Li_2TiSiO_5 [12]), the noble metals (Pt, Au and Rh) or the chemisorption products of H_2O vapour and CO_2 (LiOH or Li_2CO_3) were detected. As expected from the obtained results of SEM (Fig. 3.3), the p-XRD patterns of the advanced Li_4SiO_4 pebbles with 20 mol% Li_2TiO_3 slightly differs from the two other advanced pebbles.

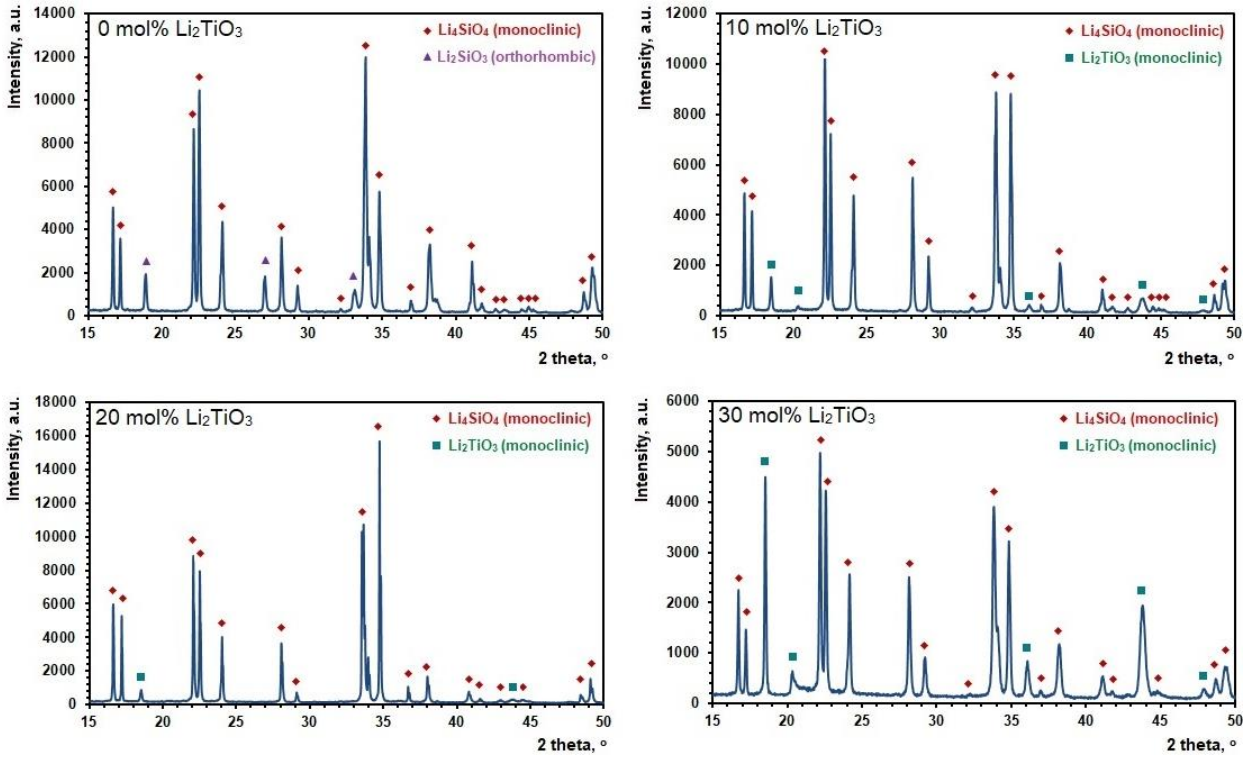

Fig. 3.4 p-XRD patterns of the Li_4SiO_4 pebbles with various contents of Li_2TiO_3 before irradiation.

Using ATR-FTIR spectrometry, in the Li_4SiO_4 pebbles with various contents of Li_2TiO_3 before irradiation, multiple vibrational bands located between 400 cm^{-1} and 1100 cm^{-1} were detected and are attributed to the stretching and bending bond vibrations of the primary and a secondary phase. The obtained ATR-FTIR spectra are shown in Fig. 3.5. In the ATR-FTIR spectra of the advanced Li_4SiO_4 pebbles with additions of Li_2TiO_3 as a secondary phase, the vibrations between 400 cm^{-1} and 1100 cm^{-1} are related to Li-O, Si-O, O-Si-O and Ti-O bonds, but the vibrations at about 1400-1500 cm^{-1} to C-O bonds [95, 96]. While in the ATR-FTIR spectra of the reference Li_4SiO_4 pebbles (0 mol% Li_2TiO_3) additional vibrations at around 740 cm^{-1} and 1070 cm^{-1} are attributed to the stretching and bending vibrations of Si-O-Si bonds, which are characteristic to the Li_2SiO_3 phase. The detected C-O bond vibrations are related to

Li_2CO_3, which may form on the surface of the Li_4SiO_4 pebbles during handling, thermal treatment or storage stage in contact with air atmosphere (Eq. 1.15). Previously, the formation of Li_2CO_3 layer with thickness less than 1 μm on the surface of the reference Li_4SiO_4 pebbles was detected and reported by M. H.H. Kolb et al. [94].

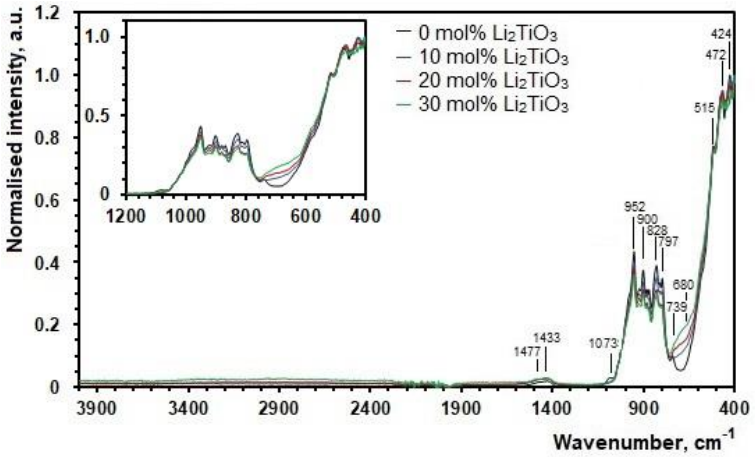

Fig. 3.5 ATR-FTIR spectra of the Li_4SiO_4 pebbles with various contents of Li_2TiO_3 before irradiation.

As expected from the obtained results of ATR-FTIR spectrometry (Fig. 3.5), using TG-DTA, no major weight loss for the Li_4SiO_4 pebbles with various contents of Li_2TiO_3 was detected, due to the desorption of absorbed and chemisorbed H_2O or CO_2, in contrast to the observations of R. Knitter et al. [84]. H. Kashimura et al. [132] detected the lithium vaporization from the Li_2TiO_3 pebbles and the Li_4SiO_4 pebbles at temperatures >1170 K, however it is assumed that the lithium vaporization is negligible in this case. The obtained DTA curves are shown in Fig. 3.6. The three endothermic peaks between 820 K and 1020 K (Peaks 1-3) in the Li_4SiO_4 pebbles with various contents of Li_2TiO_3 are caused by the polymorphic transitions of the primary Li_4SiO_4 phase [133]. The two endothermic peaks at around 1280 K (Peaks 4 and 5) in the reference Li_4SiO_4 pebbles (0 mol% Li_2TiO_3) refer to the eutectic melting of the Li_4SiO_4-Li_2SiO_3 system [134]. While the broad endothermic peak at temperatures >1390 K (Peak 6) can be attributed to the melting of the primary Li_4SiO_4 phase [12].

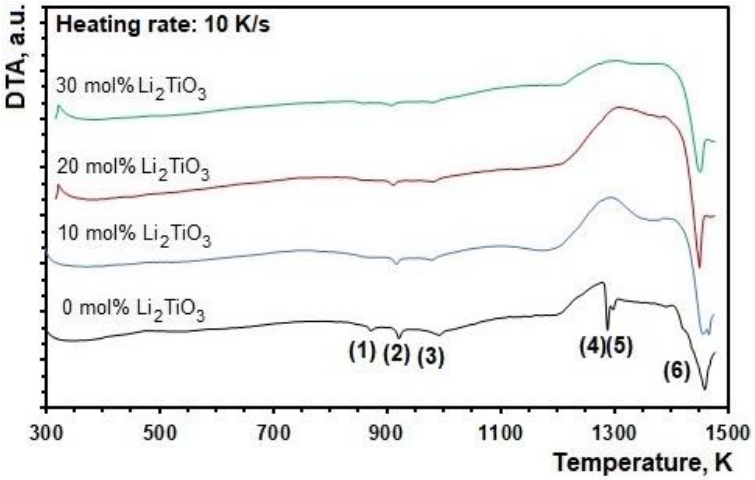

Fig. 3.6. DTA curves of the Li_4SiO_4 pebbles with various contents of Li_2TiO_3 before irradiation.

The elevated content of Pt in the advanced Li_4SiO_4 pebbles with additions of Li_2TiO_3 as a secondary phase before irradiation was detected by SEM-EDX and XRF spectrometry. The obtained XRF spectra of the Li_4SiO_4 pebbles with various contents of Li_2TiO_3 are shown in Fig. 3.7. The presence of Pt in the reference Li_4SiO_4 pebbles (0 mol% Li_2TiO_3) was not detected, due to the detections limits of SEM-EDX and XRF spectrometry. Previously, M. H.H. Kolb et al. [93], using ICP-OES, determined that the content of Pt in the reference Li_4SiO_4 pebbles is approx. 50 ppm. The Pt trace-impurities in the Li_4SiO_4 pebbles are derived from the fabrication process, due to the surface corrosion of the Pt alloy crucible components during the melting process of the raw materials.

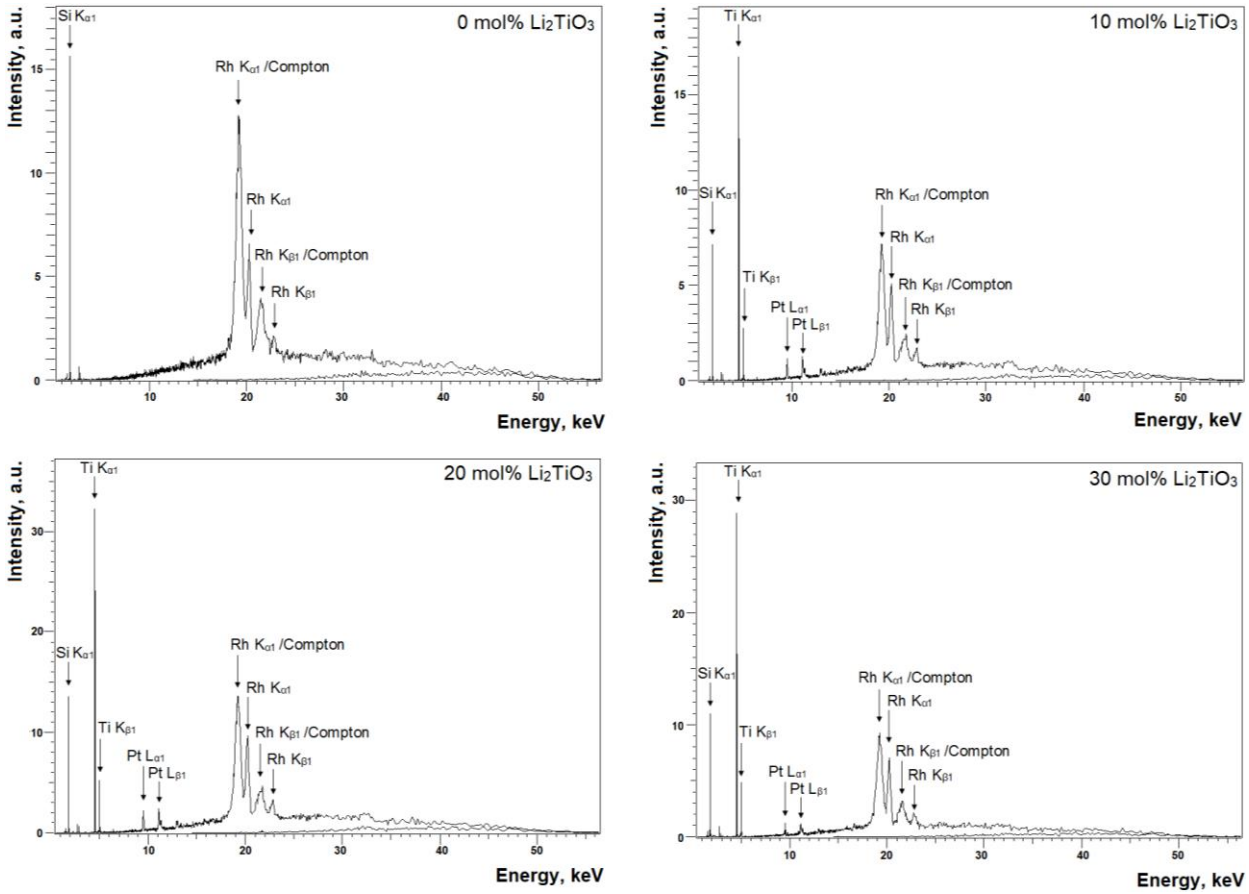

Fig. 3.7 XRF spectra of the Li_4SiO_4 pebbles with various contents of Li_2TiO_3 before irradiation. The pebbles were milled into powder before measurements; Rh lines in the XRF spectra are from the excitation source.

The obtained results of SEM-EDX and XRF spectrometry indirectly suggest that the pale-yellow colour of the advanced Li_4SiO_4 pebbles with additions of Li_2TiO_3 as a secondary phase before irradiation could be caused by the corrosion products of the Pt alloy crucible, such as yellow-green lithium platinate (Li_2PtO_3) [135, 136]. Yet, it is not excluded that this observation can be attributed to some other effect, for example the chemical reduction of Ti^{4+} ions during the fabrication process, which was described by T. Hoshino et al. [137, 138]. T. Sekiya et al. [139] reported that single crystals of TiO_2 (anatase) may have blue colour, due to the crystalline lattice

imperfections (vacancies, interstitials, impurity atoms etc.), but after thermal treatment in oxygen atmosphere the colour change (from blue through yellow to colourless) was detected.

3.1.1 Formation and accumulation of RD and RP

As described above, the advanced Li_4SiO_4 pebbles with additions of Li_2TiO_3 are biphasic without solid solutions, and therefore it is anticipated that the formation and accumulation of RD and RP under actions of 5 MeV accelerated electrons will be similar to single-phase ceramics. The formation mechanism and the structure of the formed RD and RP in the reference Li_4SiO_4 pebbles (0 mol% Li_2TiO_3) and in the Li_2TiO_3 pebbles was described above in the literature review (Chapters 1.3.1 and 1.3.2, respectively). In addition, the thermal treatment decreases the number of intrinsic defects, which may remain in the Li_4SiO_4 pebbles with various contents of Li_2TiO_3 after the fabrication process, and therefore it is expected that the thermally treated pebbles will have a higher radiation stability in comparison to the un-treated pebbles.

After irradiation with 5 MeV accelerated electrons, up to 24 MGy absorbed dose at 300-350 K in a dry argon atmosphere, a slight colour change for the Li_4SiO_4 pebbles with various contents of Li_2TiO_3 was observed and the Li_4SiO_4 pebbles turned light-grey (Fig. 3.1, middle row). A. Bishay [140] and E.J. Friebele et al. [141] summarized absorption bands of various hole and electron type centres, which may form in alkaline silicate glasses under action of ionizing radiation and cause glass coloration. Therefore, the observed colour changes for the Li_4SiO_4 pebbles during irradiation are related to the formation and accumulation of optically active RD and RP (colour centres), for example F^+ and F^o centres (localised electrons in oxygen vacancy), E' centres ($\equiv Si\cdot$ or SiO_3^{3-}), HC_2 centres ($\equiv Si\text{-}O\cdot$ or SiO_4^{3-}), peroxide radicals ($\equiv Si\text{-}O\text{-}O\cdot$), small and large Li_n particles etc. The differences between the obtained diffuse reflectance spectra of the un-irradiated and irradiated pebbles were negligible, and thus these spectra are not presented.

Major changes in the microstructure, chemical and phase composition of the irradiated Li_4SiO_4 pebbles with various contents of Li_2TiO_3 were not detected by SEM, p-XRD, TG-DTA and ATR-FTIR spectrometry in comparison to the un-irradiated pebbles, and thus these results will not be further discussed. Yet, due to the relatively small absorbed dose and low irradiation temperature, significant changes were not expected.

The chemical methods (the MCS and LL technique) cannot be used for the analysis of the accumulated RD and RP in the irradiated advanced Li_4SiO_4 pebbles with additions of Li_2TiO_3 as a secondary phase, due to the low solubility of the Li_2TiO_3 phase [28]. Therefore, the formation and accumulation of RD and RP in the Li_4SiO_4 pebbles with various contents of Li_2TiO_3 under action of 5 MeV accelerated electrons were investigated by ESR spectrometry. The ESR

spectrometry is a powerful technique for the analysis of the accumulated paramagnetic RD and RP (contains un-paired electrons), and it is based upon the resonant absorption of microwaves by un-paired electrons tuned by an externally applied magnetic field. The obtained ESR spectra of the reference Li_4SiO_4 pebbles (0 mol% Li_2TiO_3) and the advanced Li_4SiO_4 pebbles with 10 mol% Li_2TiO_3 before and after irradiation with various absorbed doses are shown in Fig. 3.8. The ESR spectra of the advanced Li_4SiO_4 pebbles with 20 and 30 mol% Li_2TiO_3 before and after irradiation are similar to the shown ESR spectra of the advanced pebbles with 10 mol% Li_2TiO_3, and thus these spectra were not included in Fig. 3.8.

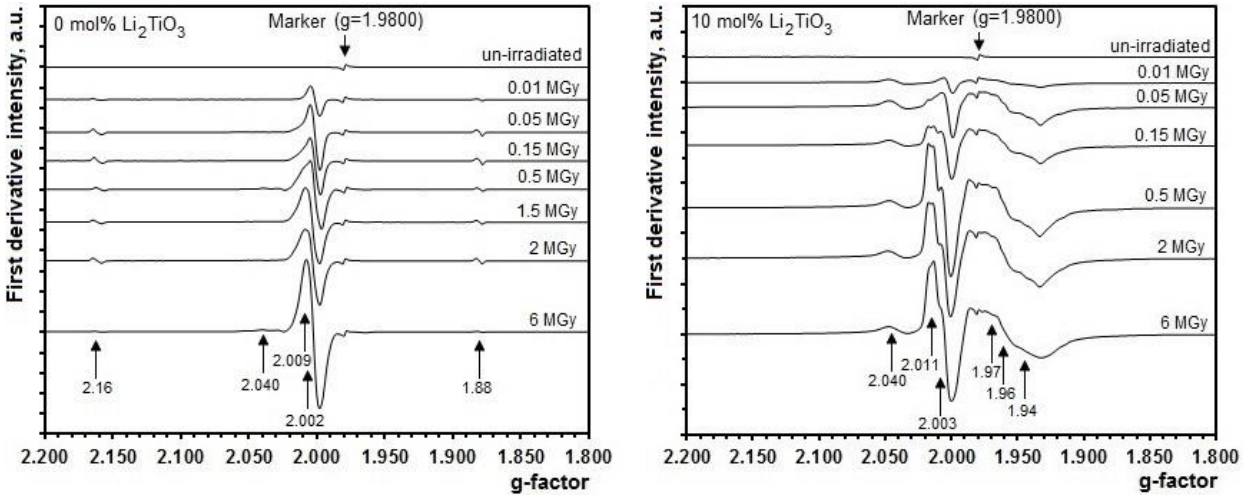

Fig. 3.8 ESR spectra of the reference Li_4SiO_4 pebbles (0 mol% Li_2TiO_3) and the advanced Li_4SiO_4 pebbles with 10 mol% Li_2TiO_3 as a secondary phase before and after irradiation with 5 MeV accelerated electrons up to 6 MGy absorbed dose at 300-350 K in a dry argon atmosphere.

In the ESR spectra of the Li_4SiO_4 pebbles with various contents of Li_2TiO_3 before irradiation, no first derivative ESR signals were detected, except for the ESR signal of the reference marker with a g-factor 1.9800±0.0005. While the line-shape of the ESR spectra of the Li_4SiO_4 pebbles after irradiation indicate the existence of several groups of paramagnetic centres. The numerical analysis of the line-shape of the ESR spectra indicated only a poor approximation by the fitting of single or several Gauss and Lorentz signals (lines), due to different g-factors, line-widths and line-shapes of the ESR signals (arising from different symmetry of un-paired electron orbital). Therefore, the identification of individual ESR signals in this doctoral thesis was based on previous investigations and literature study. The g-factor, line-shape and peak-to-peak line-width (ΔB_{pp}) of the ESR signals were selected as main comparative parameters.

In the ESR spectra of the reference Li_4SiO_4 pebbles (0 mol% Li_2TiO_3) after irradiation, up to 24 MGy absorbed dose at 300-350 K in a dry argon atmosphere, at least five first derivative ESR signals were detected (Fig. 3.8, left). The ESR signal with a g-factor 2.002±0.001 (singlet, ΔB_{pp}=0.8±0.1 mT) was assigned to E' centres ($\equiv Si\cdot$ or SiO_3^{3-}), which have been previously studied and described by several authors [20, 22, 40, 112]. The E' centre is described as an

un-paired electron in a dangling tetrahedral (sp^3) orbital of a single silicon atom, which is bonded to three oxygens in crystalline structure. The overlapping ESR signal with a g-factor at around 2.009 most likely consists of at least two signals with g-factors 2.010±0.001 (ΔB_{pp}=0.4±0.1 mT) and 2.015±0.001 (ΔB_{pp}=0.7±0.1 mT), which were attributed to HC_2 centres (≡Si-O· or SiO_4^{3-}). The HC_2 centre is described as a hole trapped on two or three non-bridging oxygen atoms of a SiO_4 tetrahedra. The two symmetric ESR signals with g-factors at around 2.16 and 1.88 (splitting around 50 mT) were attributed to atomic hydrogen (H·) [142], which may form due to the radiolysis of absorbed and chemisorbed H_2O (Eqs. 1.36, 1.38 and 1.40). While the interpretation of the ESR signal with a g-factor 2.040±0.003 (ΔB_{pp}=2.0±0.1 mT) is more complicated. In irradiated alkaline silicates, an ESR signal with similar characteristics was often attributed to peroxide radicals (≡Si-O-O·) [20, 112], however it is not excluded that this ESR signal can also be attributed to HC_2 centres, oxygen related defects (for example O^- or O_2^- ions [120]) or paramagnetic RD of Li_2CO_3 [143]. The peroxide radical (also called as peroxy radical or shortly POR) is described as a hole delocalized over antibonding π type orbitals of the O-O bond.

The characteristic ESR signals of small Li_n particles (narrow singlet, g=2.0025, $\Delta B<10^{-2}$ mT) and F^+ centres (broad multiplet, g=2.003), which have been previously detected in irradiated Li_2O [114, 144], were not detected in the ESR spectra of the reference Li_4SiO_4 pebbles (0 mol% Li_2TiO_3) after irradiation. It is assumed that the relatively narrow ESR signal of small Li_n particles cannot be observed due to the particle aggregation or overlapping with other ESR signals, while the ESR signal of F^+ centres is too broad to be analysed.

In the ESR spectra of the advanced Li_4SiO_4 pebbles with additions of Li_2TiO_3 as a secondary phase after irradiation, up to 24 MGy absorbed dose at 300-350 K in a dry argon atmosphere, two main groups of the first derivative ESR signals were detected (Fig. 3.8, right). The first group consists of four ESR signals with g-factors from 2.040 to 2.003, while the second group of at least three ESR signals is observed from 1.98 to 1.93.

The ESR signals of the first group with g-factors from 2.040 to 2.003 in the ESR spectra of the irradiated advanced Li_4SiO_4 pebbles with additions of Li_2TiO_3 as a secondary phase have similar characteristics (g-factor, line-shape and line-width) to the ESR signals, which are detected in the irradiated reference Li_4SiO_4 pebbles (Fig. 3.8, left), Li_2SiO_3 ceramic [20] and Li_2TiO_3 pellets (Fig. 1.15, a) [41]. Therefore, the ESR signal with a g-factor 2.003±0.003 (ΔB_{pp}=0.9±0.1 mT) was attributed to E' centres (SiO_3^{3-} and TiO_3^{3-}). The two overlapped ESR signals with g-factors 2.011±0.003 (ΔB_{pp}=0.8±0.2 mT) and 2.016±0.003 (ΔB_{pp}=0.4±0.1 mT) were assigned to HC_2 centres (SiO_4^{3-} and TiO_3^{-}). While the ESR signal with a g-factor 2.040±0.003 (ΔB_{pp}=2.2±0.2 mT) can be attributed to peroxide radicals (≡Si-O-O·).

The second group of the ESR signals with g-factors 1.97±0.01 (ΔB_{pp}≈1 mT), 1.96±0.01 (ΔB_{pp}≈3 mT) and 1.94±0.01 (ΔB_{pp}≈3 mT) in the ESR spectra of the irradiated advanced Li_4SiO_4 pebbles with additions of Li_2TiO_3 as a secondary phase is broad, complex and un-characteristic for the irradiated reference Li_4SiO_4 pebbles (0 mol% Li_2TiO_3). Previously, S. Arafa and F. Assabghy [145] detected ESR signals with similar characteristics in X-ray irradiated sodium silicate glasses and attributed them to titanium impurity centres. H. Bohm and G. Bayer [146], Y.M. Kim and P.J. Bray [147], V. Grismanovs et al. [41] and P. Lombard et al. [148] reported about similar ESR signals in the irradiated Li_2TiO_3 and other alkali titanates containing ceramics and related them to, so called "Ti^{3+} ion trapped-electron centres" (in the following text entitled as Ti^{3+} centres). In this doctoral thesis, the formation of Ti^{3+} centres during irradiation was described by simplified reaction (Eq. 3.1). The existence of different ESR signals, which can be attributed to Ti^{3+} centres, might be related to various environments around the titanium ions in the crystalline structure [148].

$$Ti^{4+} + e^- \rightarrow Ti^{3+} \quad (3.1)$$

The total concentration of the accumulated paramagnetic RD and RP in the irradiated Li_4SiO_4 pebbles with various contents of Li_2TiO_3 was calculated by using the double integration method of the first derivative ESR signals and by comparison with the ESR signal of the reference marker. The calculated total concentration of the accumulated paramagnetic RD and RP in the irradiated Li_4SiO_4 pebbles as a function of the absorbed dose is shown in Fig. 3.9.

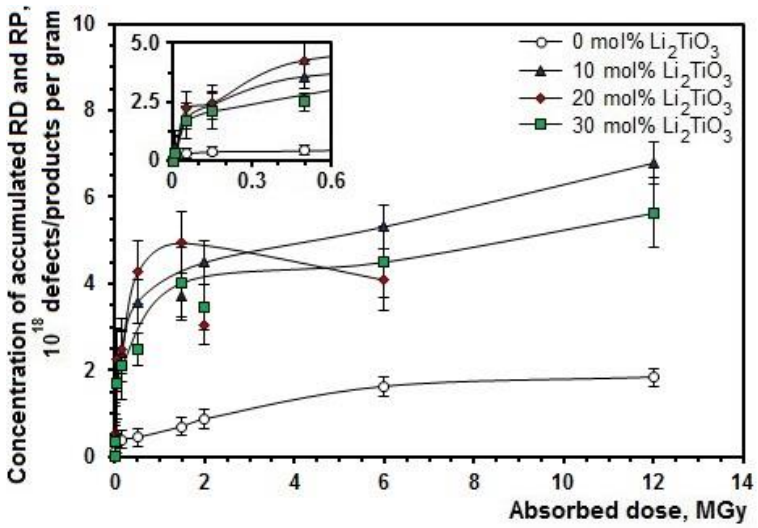

Fig. 3.9 Total concentration of the accumulated paramagnetic RD and RP in the irradiated Li_4SiO_4 pebbles with various contents of Li_2TiO_3 as a function of the absorbed dose. The pebbles were irradiated with 5 MeV accelerated electrons up to 12 MGy absorbed dose at 300-350 K in a dry argon atmosphere.

The formation and accumulation of paramagnetic RD and RP in the Li_4SiO_4 pebbles with various contents of Li_2TiO_3 under action of 5 MeV accelerated electrons takes place through two stages: (1) the fast generation of primary RD and RP on intrinsic and extrinsic defects, and

(2) the slow generation due to the radiolysis of the basic matrix. As soon as intrinsic and extrinsic defects in the Li_4SiO_4 pebbles are consumed during irradiation (in this research below 6 MGy absorbed dose), it is expected that the formation of RD and RP further occurs only in the crystalline lattice of the primary and a secondary phase.

Previous studies [36, 37, 41] already showed that the Li_2TiO_3 pebbles have a smaller radiolysis degree (α) and radiation chemical yield (G) of RD and RP than the reference Li_4SiO_4 pebbles (0 mol% Li_2TiO_3), and thus the additions of Li_2TiO_3 as a secondary phase could increase the radiation stability of the advanced Li_4SiO_4 pebbles. However, the obtained results of ESR spectrometry do not confirm this suggestion, and by adding Li_2TiO_3 in the advanced Li_4SiO_4 pebbles, the total concentration of the accumulated paramagnetic RD and RP slightly increases in comparison to the reference Li_4SiO_4 pebbles. Nevertheless, the advanced Li_4SiO_4 pebbles with additions of Li_2TiO_3 have a good radiation stability and the radiation chemical yield of paramagnetic RD and RP is below 0.8 defects/products per 100 eV. As expected from previous studies, the radiation chemical yield of paramagnetic RD ad RP in the reference Li_4SiO_4 pebbles is approx. 0.15 defects/products per 100 eV.

The slight increase of the total concentration of the accumulated paramagnetic RD and RP in the advanced Li_4SiO_4 pebbles with additions of Li_2TiO_3 as a secondary phase in comparison to the reference Li_4SiO_4 pebbles (0 mol% Li_2TiO_3) can be linked both to intrinsic defects and to extrinsic defects, which might be formed or introduced in the advanced Li_4SiO_4 pebbles during the fabrication process. By using SEM, various surface and bulk defects (cracks, joints, cavities, pores etc.) were detected on the surface and in the microstructure at the chemically etched cross-section of the advanced Li_4SiO_4 pebbles before irradiation (Fig. 3.2 and 3.3, respectively). Nevertheless, it is also not excluded that diamagnetic Ti^{4+} ions (extrinsic defects), which might be incorporated into the crystalline structure of the primary Li_4SiO_4 phase during the fabrication process, due to the melting of the Li_4SiO_4-Li_2TiO_3 system, can act as potential trapping centres for secondary electrons during irradiation and therebay forming paramagnetic Ti^{3+} centres, which were detected in the advanced pebbles after irradiation by ESR spectrometry (Fig. 3.8, right).

3.1.2 Thermal stability and annihilation of accumulated RD and RP

The thermal stability and annihilation of the accumulated RD and RP in the irradiated Li_4SiO_4 pebbles with various contents of Li_2TiO_3 were analysed by ESR spectrometry (using stepwise isochronal annealing method) and TSL technique. The obtained ESR spectra of the irradiated reference Li_4SiO_4 pebbles (0 mol% Li_2TiO_3) and advanced Li_4SiO_4 pebbles with 10 mol% Li_2TiO_3 as a secondary phase before and after stepwise isochronal annealing up to

920 K in a dry argon atmosphere are shown in Fig. 3.10. The ESR spectra of the irradiated advanced Li_4SiO_4 pebbles with 20 and 30 mol% Li_2TiO_3 before and after annealing are similar to the shown ESR spectra of the advanced pebbles with 10 mol% Li_2TiO_3, and thus these spectra were not included in Fig. 3.10.

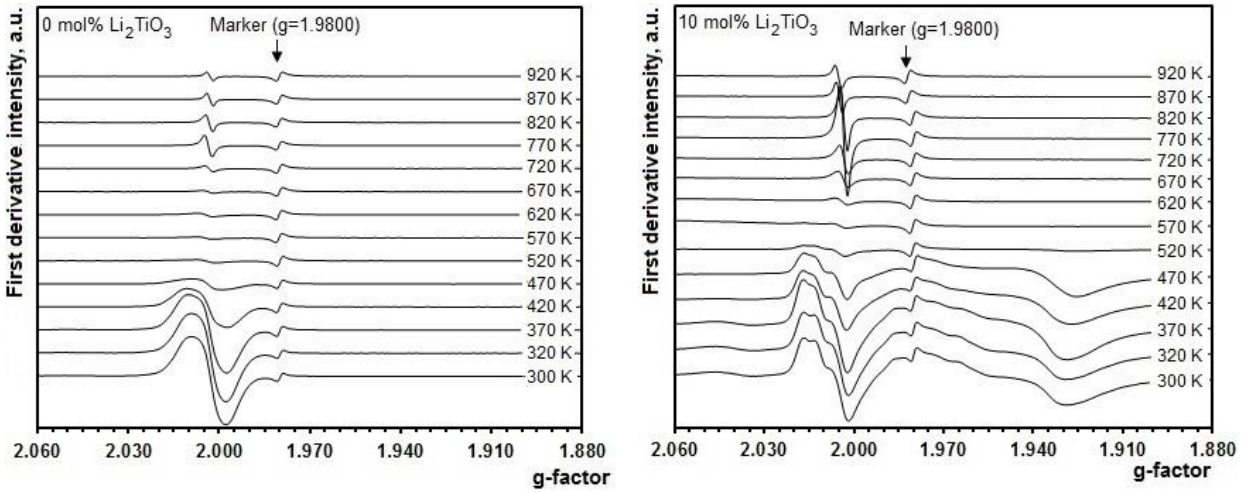

Fig. 3.10 ESR spectra of the irradiated reference Li_4SiO_4 pebbles (0 mol% Li_2TiO_3) and advanced Li_4SiO_4 pebbles with additions of 10 mol% Li_2TiO_3 as a secondary phase before and after stepwise isochronal annealing up to 920 K for 25 min in a dry argon atmosphere. The pebbles were irradiated with 5 MeV accelerated electrons up to 12 MGy absorbed dose at 300-350 K in a dry argon atmosphere.

The accumulated paramagnetic RD, namely E' centres, HC_2 centres and peroxide radicals (ESR signals with g-factors from 2.040 to 2.002), in the irradiated Li_4SiO_4 pebbles with various contents of Li_2TiO_3 annihilate between 370 and 570 K. The intensity of the ESR signal with a g-factor close to 2.002, which was attributed to E' centres, decreases rapidly after annealing up to 570 K, due to the E' centre recombination with the mobile O^- ions. The intensity of the ESR signals with g-factors at around 2.010 and 2.015, which were related to HC_2 centres, decreases between 420 K and 520 K, due to the HC_2 centre recombination with the localised electron centres or other transformation processes, for example disproportion. The annihilation of the ESR signal with a g-factor at around 2.040, which can be related to peroxide radicals, practically ends at around 420 K, and it was noted that the recombination process of peroxide radicals can be linked to the E' centres annihilation. It was also observed that the intensity and line-shape of the broad and complex ESR signals with g-factors from 1.93 to 1.98, which were attributed to Ti^{3+} centres, in the advanced Li_4SiO_4 pebbles with additions of Li_2TiO_3 as a secondary phase slightly change at about 370 K, and these ESR signals practically disappear at around 520 K.

After stepwise isochronal annealing at temperatures >570 K in a dry argon atmosphere, only one, relatively small and narrow ESR signal with a g-factor close to 2.0030 (ΔB_{pp}<0.2 mT) was detected in the ESR spectra of the irradiated Li_4SiO_4 pebbles with various contents of Li_2TiO_3. This relatively narrow ESR signal only disappears after annealing at temperatures

>920 K and therefore can be attributed to Li_n particles. While the slight increase of the intensity of this ESR signal during annealing up to 770 K can be explained by the decomposition of large Li_n particles into small Li_n particles or by the disproportion of another diamagnetic RP.

The total concentration of the accumulated paramagnetic RD and RP in the irradiated Li_4SiO_4 pebbles with various contents of Li_2TiO_3 as a function of the annealing temperature is shown in Fig. 3.11. The obtained results indicate that during annealing between 370 K and 570 K, up to 99 % of the accumulated paramagnetic RD and RP in the irradiated Li_4SiO_4 pebbles were annihilated, due to the thermally stimulated recombination processes. The annihilation behaviour of the accumulated paramagnetic RD and RP in the irradiated advanced Li_4SiO_4 pebbles with additions of Li_2TiO_3 as a secondary phase is similar to the irradiated reference Li_4SiO_4 pebbles (0 mol% Li_2TiO_3). Nevertheless, it was also observed that the additions of Li_2TiO_3 slightly increase the annihilation temperature of the accumulated paramagnetic RD and RP in the advanced Li_4SiO_4 pebbles in comparison to the reference Li_4SiO_4 pebbles. It is assumed that this phenomenon can be related to the formation of Ti^{3+} centres in the advanced pebbles during irradiation and their recombination mechanism during annealing.

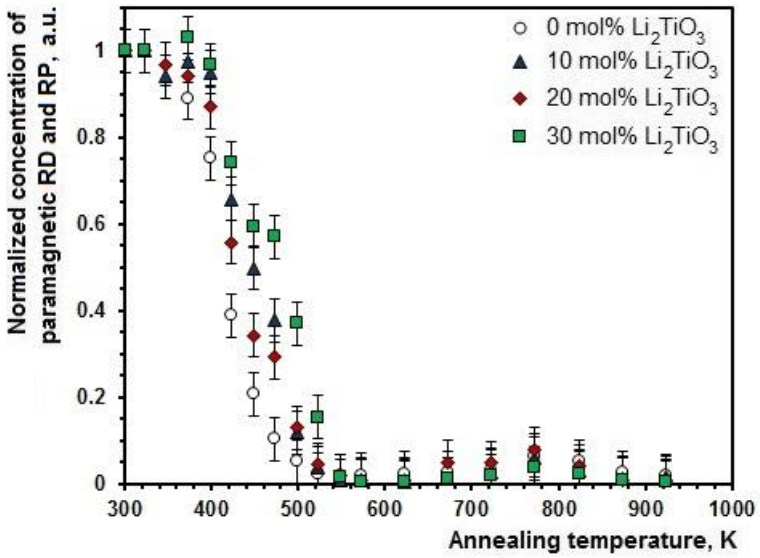

Fig. 3.11 Normalised total concentration of the accumulated paramagnetic RD and RP in the irradiated Li_4SiO_4 pebbles with various contents of Li_2TiO_3 as a function of stepwise isochronal annealing temperature. The pebbles were irradiated with 5 MeV accelerated electrons up to 12 MGy absorbed dose at 300-350 K in a dry argon atmosphere.

To supplement the obtained results of ESR spectrometry, the TSL glow curves and spectra of the irradiated Li_4SiO_4 pebbles with various contents of Li_2TiO_3 were measured. The obtained TSL glow curves are shown in Fig. 3.12. During annealing, the luminescence emission occurs due to the thermally stimulated recombination reactions between various hole and electron type RD and RP. In the simplest case, increasing annealing temperature the localised electrons are liberated from their traps and recombine with various hole type centres, which may result in the

luminescence emission with specific energy and wavelength. Another possibility is that the localised holes are released from their traps and recombine with electron type centres. The maximum temperature (T_m), half-width and shape of the TSL peaks characterises the depth and structure of the electron or hole traps, while the intensity and integrated area (sometimes also called as light sum) of the TSL peaks is proportional to the concentration of recombination centres (also known as luminescence centres).

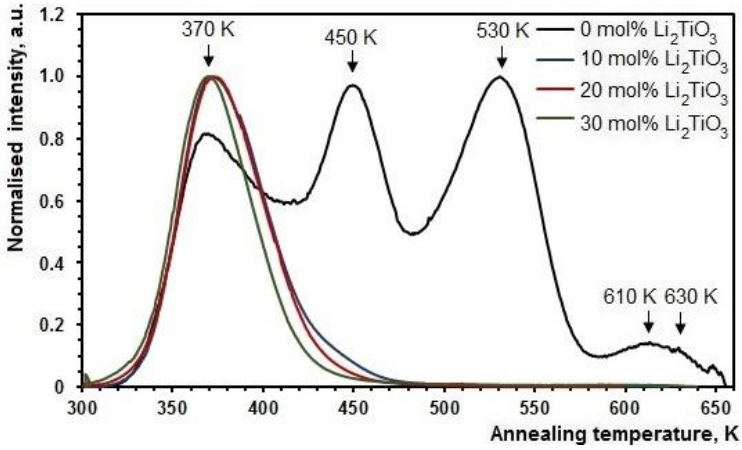

Fig. 3.12 Normalized TSL glow curves of the irradiated Li_4SiO_4 pebbles with various contents of Li_2TiO_3. The heating rate is 2 K s^{-1}. The pebbles were irradiated with 5 MeV accelerated electrons up to 6 MGy absorbed dose at 300-350 K in a dry argon atmosphere.

The TSL glow curve of the irradiated reference Li_4SiO_4 pebbles (0 mol% Li_2TiO_3) is complex and consists of several overlapped peaks with maxima between 300 K and 650 K. While in the TSL glow curves of the irradiated advanced Li_4SiO_4 pebbles with additions of Li_2TiO_3 as a secondary phase overlapped peaks with maxima between 300 K and 450 K were detected. The Gaussian functions were applied to separate these TSL peaks. According to N. Chandrasekhar and R.K. Gartia [149], this may be acceptable to find the number of TSL peaks and their peak maxima (T_m). The deconvoluted TSL glow curves of the reference Li_4SiO_4 pebbles and the advanced Li_4SiO_4 pebbles with 10 mol% Li_2TiO_3 are shown in Fig. 3.13.

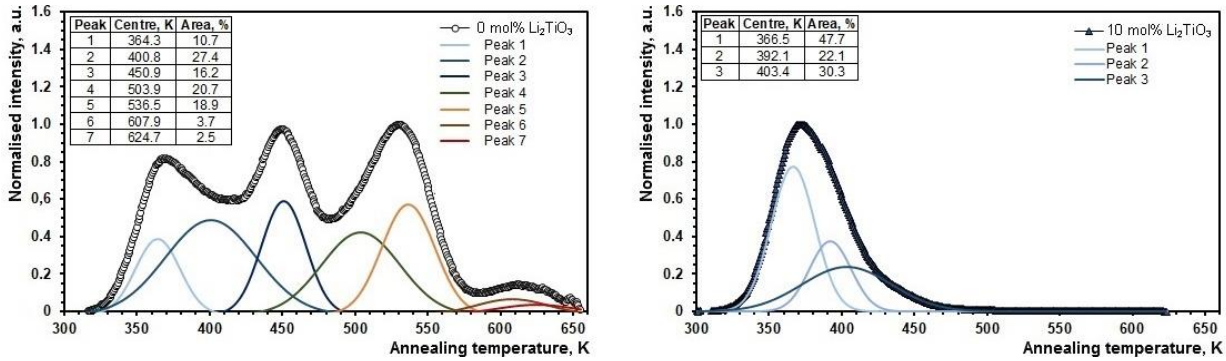

Fig. 3.13 Deconvoluted TSL glow curves of the irradiated reference Li_4SiO_4 pebbles (0 mol% Li_2TiO_3) and advanced Li_4SiO_4 pebbles with 10 mol% Li_2TiO_3 as a secondary phase with the Gaussian-shaped peak functions. The heating rate is 2 K s^{-1}. The pebbles were irradiated with 5 MeV accelerated electrons up to 6 MGy absorbed dose at 300-350 K in a dry argon atmosphere.

The TSL glow curve of the irradiated reference Li_4SiO_4 pebbles (0 mol% Li_2TiO_3) consists of at least seven peaks with maxima at around 365 K, 400 K, 450 K, 500 K, 540 K, 610 K and 630 K. While in the TSL glow curve of the irradiated advanced Li_4SiO_4 pebbles with additions of Li_2TiO_3 as a secondary phase up to three peaks with maxima at about 365 K, 390 K and 400 K were separated. Previously, in the TSL glow curves of the irradiated Li_4SiO_4 ceramics similar peaks between 400 K and 700 K were detected by several authors [111, 150]. E. Feldbach et al. [150] suggested that these TSL peaks can be related to the recombination processes of electron type RD and RP, which could act as scavenger traps for the highly mobile tritium. Examples of such tritium scavenger traps are F^+ and F^o centres, which have been detected in the irradiated Li_2O crystals [151], or E' centres, small and large Li_n particles, which have been detected in the irradiated Li_4SiO_4 ceramics [19, 20, 23, 112]. While in the TSL glow curves of the irradiated Li_2TiO_3 ceramics at least two main peaks with maxima at around 400 K and 500 K were detected by M. Gonzalez and V. Correcher [42, 43].

The obtained results of TSL technique indicate that by increasing the absorbed dose (from 0.01 MGy to 0.5 MGy), a substantial TSL peak shifting to lower temperatures (below 400 K) occurs in the advanced Li_4SiO_4 pebbles with additions of Li_2TiO_3 as a secondary phase. The obtained TSL glow curves of the advanced Li_4SiO_4 pebbles with 10 mol% Li_2TiO_3 after irradiation with various absorbed doses are shown in Fig. 3.14. In the TSL glow curves of the advanced Li_4SiO_4 pebbles with additions of Li_2TiO_3, which were irradiated up to 0.01 MGy absorbed dose, at least four TSL peaks with maxima at around 400 K, 450 K, 520 K and 610 K were detected. These TSL peaks are practically identical to the peaks, which are detected in the TSL glow curves of the reference Li_4SiO_4 pebbles (0 mol% Li_2TiO_3) after irradiation up to 24 MGy absorbed dose at 300-350 K (Fig. 3.13, left).

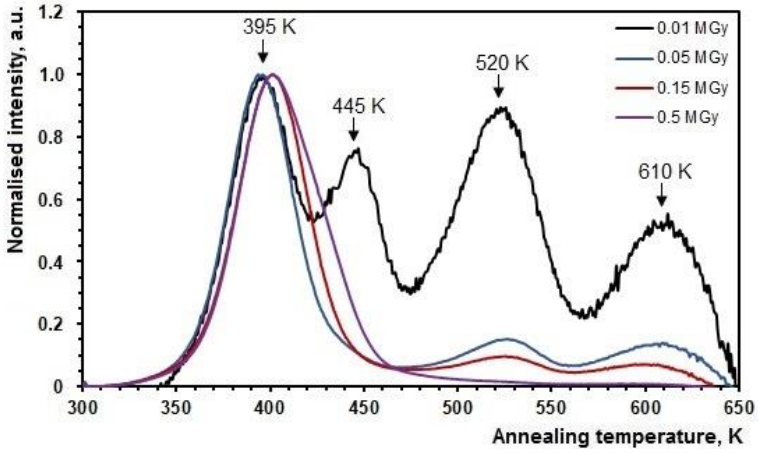

Fig. 3.14 Normalized TSL glow curves of the irradiated advanced Li_4SiO_4 pebbles with 10 mol% Li_2TiO_3 as a secondary phase. The heating rate is 2 K s^{-1}. The pebbles were irradiated with 5 MeV accelerated electrons up to 0.01 MGy, 0.05 MGy, 0.15 MGy and 0.5 MGy absorbed dose at around 300 K in a dry argon atmosphere.

Previously, similar effects have been observed and reported by A. Abramenkovs et al. [111] for the irradiated Li_4SiO_4 pellets with additions of polyvalent transition metal ions, such as Fe^{3+}, Cr^{3+} and Pb^{4+}. It was suggested that the additions of polyvalent transition metal ions can significantly increase the probability for the recombination processes of primary RD during irradiation and thereby reduce the formation of secondary RD and chemical stable RP, which have a more complicated structure and a higher thermal stablity. On the basis of these considerations, it is sugested that similar phenomena can also occure in the advanced Li_4SiO_4 pebbles with additions of Li_2TiO_3 as a secondary phase during irradiation, due to the trapping of secondary electrons on the incorporated Ti^{4+} ions (extrinsic defects) in the crystalline structure of the primary Li_4SiO_4 phase.

The TSL peaks with maxima below 400 K in the irradiated Li_4SiO_4 pebbles with various contents of Li_2TiO_3 are not stable at room temperature and the intensity of these TSL peaks decreases rapidly after irradiation. The obtained TSL glow curves and the integrated area (light sum) of the TSL glow curves of the advanced Li_4SiO_4 pebbles with 10 mol% Li_2TiO_3 as a secondary phase at different times after irradiation, up to 2400 h, are shown in Fig. 3.15. This behaviour of the low-temperature TSL peaks is associated with the release probability of the localised electrons or holes from the shallow traps that occurs very rapidly at room temperature. While other TSL peaks with maxima at temperatures >400 K seem to be stable at room temperature, and therefore it is assumed that the electrons or holes are localised in the deeper traps, which require additional energy to leave their position.

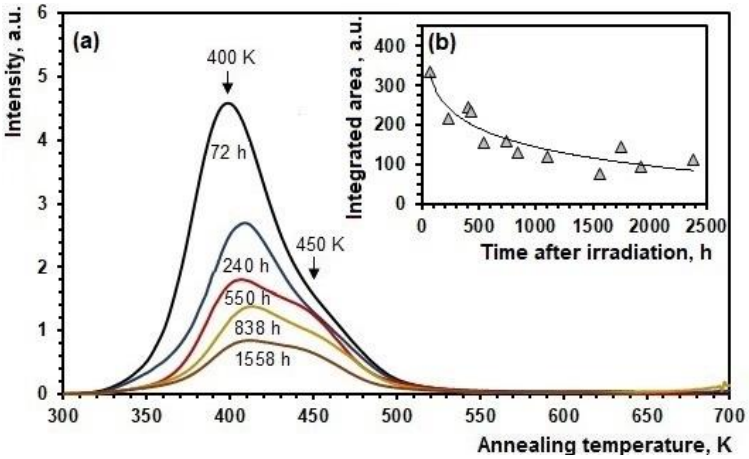

Fig. 3.15 (a) TSL glow curves and (b) the integrated area of the TSL glow curves of the irradiated advanced Li_4SiO_4 pebbles with 10 mol% Li_2TiO_3 as a secondary phase at different times, up to 2400 h, after irradiation. The heating rate is 2 K s^{-1}. The pebbles were irradiated with 5 MeV accelerated electrons up to 12 MGy absorbed dose at 300-350 K in a dry argon atmosphere.

The activation energy (E_a) values for the thermally stimulated recombination processes of the accumulated RD and RP (also called as electron or hole trap depth) in the irradiated Li_4SiO_4 pebbles with various contents of Li_2TiO_3 were calculated by the Hoogenstraaten method. This

method uses various heating rates to calculate E_a values for the first order recombination processes. The TSL glow curves of the irradiated reference Li_4SiO_4 pebbles (0 mol% Li_2TiO_3) with five heating rates are shown in Fig. 3.16. As the heating rate (β) is increased from 0.1 K s^{-1} to 2 K s^{-1}, the maximum temperature (T_m), intensity and integrated area (light sum) of the TSL peaks increases.

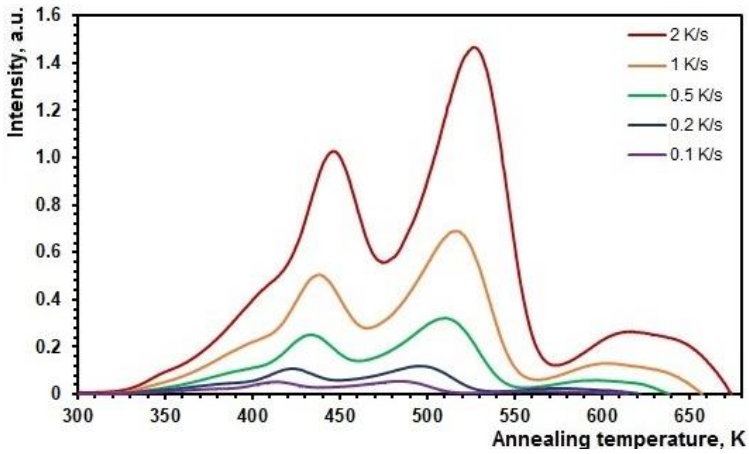

Fig. 3.16 TSL glow curves of the irradiated reference Li_4SiO_4 pebbles (0 mol% Li_2TiO_3) with five heating rates. The pebbles were irradiated with 5 MeV accelerated electrons up to 12 MGy absorbed dose at 300-350 K in a dry argon atmosphere.

The calculated E_a values for the thermally stimulated recombination processes of the accumulated RD and RP in the irradiated Li_4SiO_4 pebbles with various contents of Li_2TiO_3 are between 0.5 eV and 1.7 eV (depends on the localisation type of electrons or holes). The obtained Hoogenstraaten plot for the deconvoluted TSL peak with a maximum at around 530 K in the irradiated reference Li_4SiO_4 pebbles (0 mol% Li_2TiO_3) is shown in Fig. 3.17. However, due to the complex nature of the TSL glow curves of the Li_4SiO_4 pebbles, it is difficult to separate individual peaks and to determine the precise maximum temperature of these peaks, and consequently the calculated E_a values need to be regarded with caution.

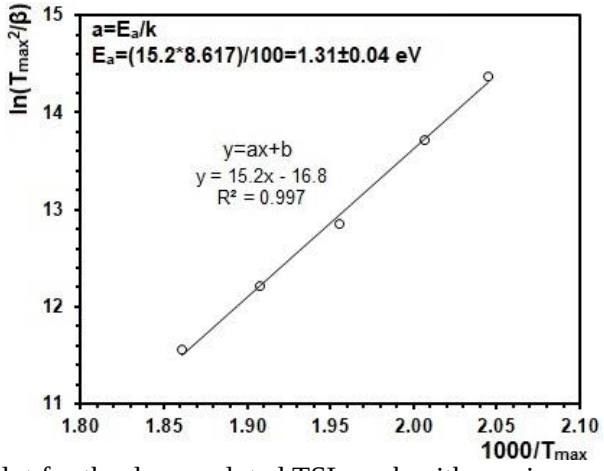

Fig. 3.17 Hoogenstraaten plot for the deconvoluted TSL peak with maximum at around 530 K in the TSL glow curves of the irradiated reference Li_4SiO_4 pebbles (0 mol% Li_2TiO_3). The pebbles were irradiated with 5 MeV accelerated electrons up to 12 MGy absorbed dose at 300-350 K in a dry argon atmosphere.

Previously, M. Oyaidzu et al. [21] and Y. Nishikawa et al. [20] calculated E_a values for the thermally stimulated recombination process of E' centres (occurs between 400 K and 700 K) in neutron-irradiated Li_2TiO_3 (E_a=0.41 eV), Li_2SiO_3 (E_a=0.63 eV) and Li_4SiO_4 (E_a=0.56 eV) on the basis of the results of ESR spectrometry. Slight differences between the calculated E_a values from TSL technique and ESR spectrometry can be caused by the method of calculation or by the type of used radiation, which was previously suggested by S. Suzuki et al. [152].

To acquire information about the spectral distribution of the TSL glow curves and the recombination centres (luminescence centres), the TSL spectra of the irradiated Li_4SiO_4 pebbles with various contents of Li_2TiO_3 were measured. The obtained TSL spectra of the reference Li_4SiO_4 pebbles (0 mol% Li_2TiO_3) and the advanced Li_4SiO_4 pebbles with 10 mol% Li_2TiO_3 as a secondary phase are shown in Fig. 3.18. The TSL spectra of the irradiated Li_4SiO_4 pebbles exhibit a similar behaviour, consisting of one main band with a maximum close to 450 nm (2.76 eV) regardless of the Li_2TiO_3 content.

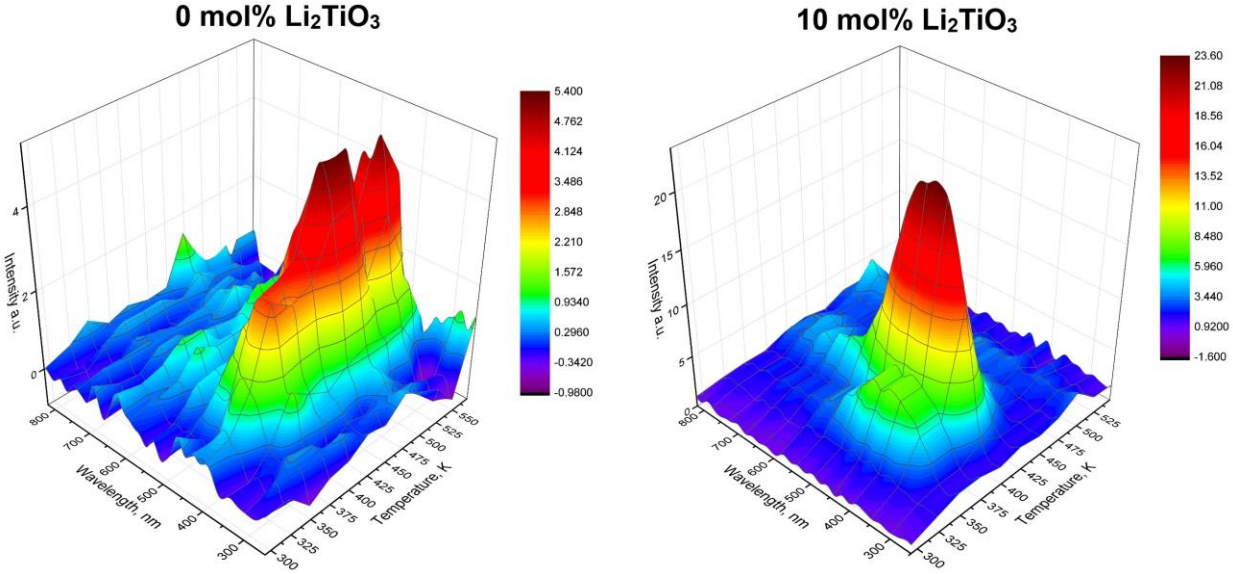

Fig. 3.18 TSL spectra of the irradiated reference Li_4SiO_4 pebbles (0 mol% Li_2TiO_3) and advanced Li_4SiO_4 pebbles with 10 mol% Li_2TiO_3 as a secondary phase. The heating rate is 1 K s^{-1}. The pebbles were irradiated with 5 MeV accelerated electrons up to 1.5 MGy absorbed dose at 300-350 K in a dry argon atmosphere.

The obtained TSL spectra results of the irradiated Li_4SiO_4 pebbles with various contents of Li_2TiO_3 correlates with results, which were previously reported by E. Feldbach et al. [150], K. Moritani et al. [39], M. Gonzalez and V. Correcher [42, 43]. In the CL spectra of Li_4SiO_4 two maxima at around 2.8 eV and 3.8 eV were detected, while for Li_2TiO_3 two maxima at around 1.8 eV and 2.9 eV were observed. G.H. Sigel Jr. [153] suggested that the blue emission (with a maximum at around 2.7 eV) may result from the radiative recombination of holes, which were thermally activated out of a continuous distribution of shallow traps, with E' centres. K. Moritani

et al. [39] reported that the band with a maximum at around 460 nm (2.7 eV) in the ion-induced luminescence spectra of the Li_4SiO_4 pellets can be associated with the radiative recombination of E' centres (≡Si· or SiO_3^{3-}) or some variants of oxygen deficiency centres (ODCs) with oxygen related defects, for example O^- ions. The ODC in the simplest case can be described as a neutral oxygen vacancy and is generally indicated as ≡Si···Si≡. However, the ODCs are diamagnetic and cannot be detected by ESR spectrometry.

On the basis of the obtained results of ESR spectrometry and TSL technique, it is proposed that in the irradiated advanced Li_4SiO_4 pebbles with additions of Li_2TiO_3 as a secondary phase similar recombination processes of hole and electron type RD and RP occur during annealing as in the irradiated reference Li_4SiO_4 pebbles (0 mol% Li_2TiO_3). However, it is not excluded that not all accumulated RD and RP have paramagnetic properties (contains un-paired electrons) or recombine with emission of luminescence and therefore may explain the differences between the obtained results of ESR spectrometry (Fig. 3.11) and TSL technique (Fig. 3.12).

3.1.3 Summary of results

In this section, for the first time the formation and accumulation of RD and RP in the advanced Li_4SiO_4 pebbles with additions of Li_2TiO_3 as a secondary phase were analysed and described under action of 5 MeV accelerated electrons, up to 24 MGy absorbed dose at 300-350 K in a dry argon atmosphere, to estimate and compare the parameters, which characterise the radiation stability. The thermal stability and annihilation of the accumulated RD and RP in the irradiated advanced Li_4SiO_4 pebbles with additions of Li_2TiO_3 were studied to predict the possible tritium release temperature range.

Summarising all the above-mentioned results, it is concluded that the combination of Li_4SiO_4 and Li_2TiO_3 does not significantly deteriorate the radiation stability of the ceramic breeder pebbles and, because of the improved mechanical properties, the advanced Li_4SiO_4 pebbles with additions of Li_2TiO_3 as a secondary phase should be used as an alternative candidate for the tritium breeding in future nuclear fusion reactors. The advanced Li_4SiO_4 pebbles with additions of Li_2TiO_3 are biphasic without solid solutions, and therefore the formation mechanism and the structure of the formed RD and RP (except Ti^{3+} centres) during irradiation is similar to the single-phase ceramics. By using ESR spectrometry, it was determined that in the advanced Li_4SiO_4 pebbles, several species of electron and hole type RD and RP are formed and accumulated, such as E' centres (SiO_3^{3-} and TiO_3^{3-}), HC_2 centres (SiO_4^{3-} and TiO_3^-) etc. The additions of Li_2TiO_3 in the advanced Li_4SiO_4 pebbles slightly increase the total concentration of the accumulated paramagnetic RD and RP in comparison to the reference

Li_4SiO_4 pebbles (0 mol% Li_2TiO_3). Nevertheless, the advanced Li_4SiO_4 pebbles with additions of Li_2TiO_3 have a good radiation stability and the radiation chemical yield (G) of paramagnetic RD and RP is below 0.8 defects/products per 100 eV. The slight increase of the total concentration of the accumulated paramagnetic RD and RP in the advanced Li_4SiO_4 pebbles in comparison to the reference Li_4SiO_4 pebbles can be attributed to intrinsic defects (crystalline lattice imperfections) and to extrinsic defects (incorporated Ti^{4+} ions), which can be formed or introduced in the advanced pebbles during the fabrication process.

The additions of Li_2TiO_3 as a secondary phase in the advanced Li_4SiO_4 pebbles does not provide new or different RD and RP (except Ti^{3+} centres), which could act as possible tritium scavenger centres, and therefore it is expected that the tritium release behaviour will be similar to single-phase ceramics. The obtained results of TSL technique indicate that the formation of Ti^{3+} centres in the advanced Li_4SiO_4 pebbles with additions of Li_2TiO_3 during irradiation can reduce the formation of thermally stable RD and RP, which have a more complicated structure, for example small and large Li_n particles etc. The accumulated RD and RP in the advanced Li_4SiO_4 pebbles annihilates between 300 K and 650 K (except large Li_n particles), and it is expected that the tritium release will start in this temperature range. The preliminary deuterium and tritium release studies by M. Gonzalez et al. [13] and M. Yang et al. [14] confirm this suggestion, nevertheless additional short and long-term neutron-irradiation experiments, in-pile and out-of-pile tritium release studies are required in order to confirm the applicability of the advanced pebbles as an alternative candidate for the tritium breeding.

3.2 Behaviour of Li_4SiO_4 pebbles with various contents of Li_2TiO_3 under simultaneous action of accelerated electrons and high temperature

As discussed above, the formation mechanism and the structure of the formed RD and RP (except Ti^{3+} centres) in the advanced Li_4SiO_4 pebbles with additions of Li_2TiO_3 as a secondary phase under action of 5 MeV accelerated electrons is similar to single-phase ceramics. The accumulated paramagnetic RD, namely E' centres (SiO_3^{3-} and TiO_3^{3-}), HC_2 centres (SiO_4^{3-} and TiO_3^{-}), peroxide radicals (≡Si-O-O·) and Ti^{3+} centres, in the irradiated advanced Li_4SiO_4 pebbles with additions of Li_2TiO_3 annihilate between 300 K and 650 K, and therefore it is expected, that during irradiation at temperatures >380 K, the thermally stimulated recombination processes of primary and secondary RD will dominate. During irradiation, up to 5000 MGy absorbed dose at 380-1285 K in a dry argon atmosphere, the formation and accumulation of thermally stable RP, such as small and large Li_n particles, Si_n particles, molecular O_2 and various compounds with silanol (≡Si-Si≡), disilicate (≡Si-O-Si≡) and peroxide (≡Si-O-O-Si≡) bonds, is mainly expected.

3.2.1 Microstructural changes and phase transitions after irradiation

Under action of 5 MeV accelerated electrons up to 5000 MGy absorbed dose at 380-1285 K in a dry argon atmosphere, a rapid colour change and melting of the Li_4SiO_4 pebbles with various contents of Li_2TiO_3 was observed. During irradiation, up to 1120 K, the reference Li_4SiO_4 pebbles (0 mol% Li_2TiO_3) became "black" or light-brown, while the advanced Li_4SiO_4 pebbles with additions of Li_2TiO_3 as a secondary phase turned blue-grey. The photos of the Li_4SiO_4 pebbles before and after irradiation are shown in Fig. 3.19. The content of Li_2TiO_3 is given in the upper row, while the irradiation conditions are shown on the left side.

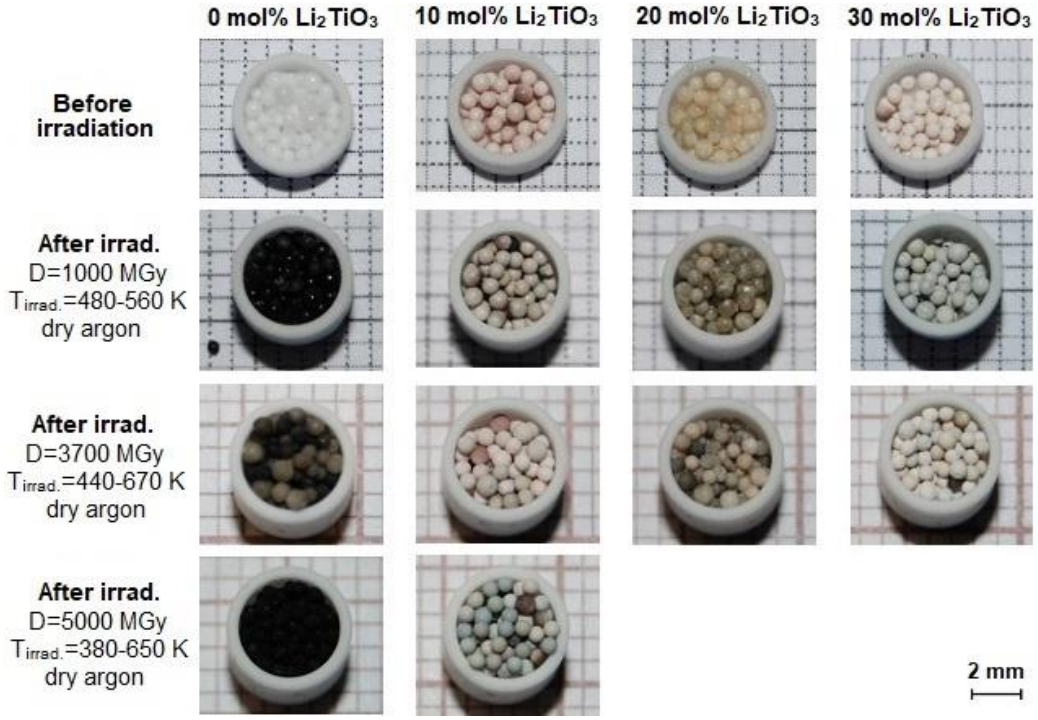

Fig. 3.19 Photos of the Li_4SiO_4 pebbles with various contents of Li_2TiO_3 before and after irradiation with 5 MeV accelerated electrons up to 1000 MGy, 3700 MGy and 5000 MGy absorbed dose at 380-670 K in a dry argon atmosphere.

Previously, similar effects have also been observed and described for irradiated Li_2O (dirty yellow/black) [114], Li_2TiO_3 (dark grey) [153], Li_4SiO_4 (dark brown), Li_2SiO_3 (grey/blue) and SiO_2 (brown). Therefore, the observed colour changes for the Li_4SiO_4 pebbles with various contents of Li_2TiO_3 during irradiation are attributed to the formation and accumulation of optically active RD or RP (colour centres), for example F^+ and F^o centres, E' centres (SiO_3^{3-} and TiO_3^{3-}), HC_2 centres (SiO_4^{3-} and TiO_3^{-}), peroxide radicals (≡Si-O-O·), Ti^{3+} centres, small and large Li_n particles etc. The absorption band of Ti^{3+} centres is located at around 500 nm (green colour) [130] and therefore can explain the blue-grey colour of the irradiated advanced Li_4SiO_4 pebbles with additions of Li_2TiO_3 as a secondary phase.

During irradiation, up to 1285 K, the melting of the reference Li_4SiO_4 pebbles (0 mol% Li_2TiO_3) and the advanced Li_4SiO_4 pebbles with 10 mol% Li_2TiO_3 as a secondary

phase was observed, while the advanced Li_4SiO_4 pebbles with 20 and 30 mol% Li_2TiO_3 practically do not lose their shape (Fig. 3.1, lower row). The melting of the reference Li_4SiO_4 pebbles is attributed to the eutectic melting of the Li_4SiO_4-Li_2SiO_3 system, which was detected to occur at around 1280 K in the reference pebbles before irradiation (Fig. 3.6). While the melting of the advanced Li_4SiO_4 pebbles with 10 mol% Li_2TiO_3 during irradiation is not fully explained, yet this process could be attributed to the minor variation in the chemical composition of the advanced Li_4SiO_4 pebbles, which might be formed during the fabrication process. The melting of the advanced pebbles before irradiation was detected to start at temperatures >1390 K (Fig. 3.6).

During irradiation, up to 5000 MGy absorbed dose at 380-1285 K, the radiolysis of the primary and a secondary phase can be expected to cause recrystallization and grain growth in the Li_4SiO_4 pebbles with various contents of Li_2TiO_3. However, no major changes in the p-XRD patterns and in the ATR-FTIR spectra of the irradiated Li_4SiO_4 pebbles were detected in comparison to the un-irradiated pebbles. The p-XRD patterns of the reference Li_4SiO_4 pebbles (0 mol% Li_2TiO_3) and the advanced Li_4SiO_4 pebbles with 10 mol% Li_2TiO_3 as a secondary phase before and after irradiation are shown Fig. 3.20.

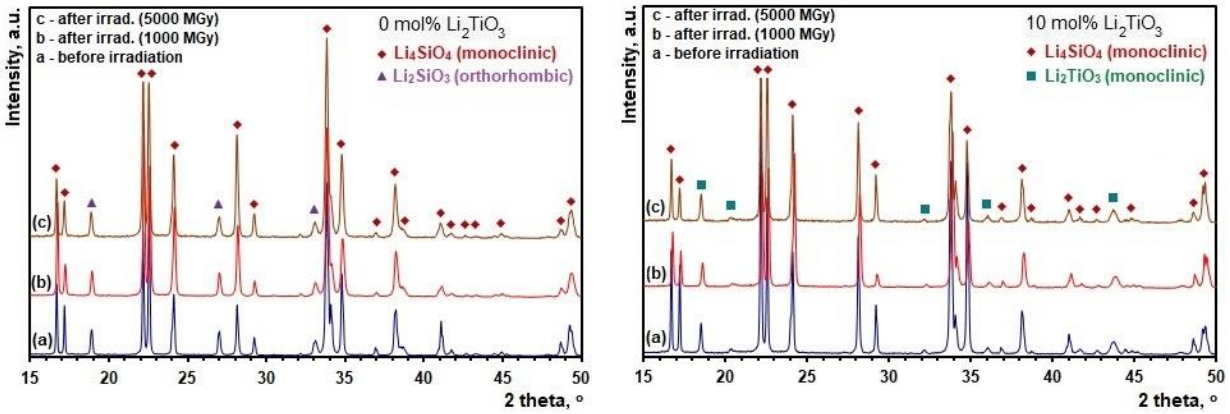

Fig. 3.20 p-XRD patterns of the reference Li_4SiO_4 pebbles (0 mol% Li_2TiO_3) and the advanced Li_4SiO_4 pebbles with 10 mol% Li_2TiO_3 as a secondary phase before and after irradiation with 5 MeV accelerated electrons up to 1000 MGy and 5000 MGy absorbed dose at 380-650 K in a dry argon atmosphere.

Due to the high absorbed dose, the formation and accumulation of RP, such as Li_2SiO_3 or SiO_2, which feature disilicate (≡Si-O-Si≡) bonds, were expected in the Li_4SiO_4 pebbles with various contents of Li_2TiO_3. This effect is related to the detection limits of both methods and to the small radiolysis degree of the Li_4SiO_4 phase ($\alpha_{1000\ MGy}$=0.1-1 mol% [37]) and the Li_2TiO_3 phase ($\alpha_{500\ MGy}=10^{-3}$ mol% [37]). The detection limit of p-XRD depends on several factors (preferred orientation, texturing, particle size etc.), nevertheless it is below 1 wt%. While the detection limit of ATR-FTIR spectrometry is around 0.1 wt%. On the basis of these assumptions, it is suggested that the radiolysis degree (α) of the advanced Li_4SiO_4 pebbles with additions of Li_2TiO_3 as a secondary phase is under 1 mol% after irradiation up to 5000 MGy absorbed dose.

The high-temperature radiolysis may cause changes in the microstructure of the Li_4SiO_4 pebbles with various contents of Li_2TiO_3 during irradiation, due to the evolution of molecular O_2 and the formation of cracks, dislocations and micro-pores. The microstructure at the chemically etched cross-sections of the Li_4SiO_4 pebbles before and after irradiation is shown in Fig. 3.21. The content of Li_2TiO_3 is given in the upper row, while the irradiation conditions are shown on the left side. As expected from the obtained results of p-XRD (Fig. 3.20) and ATR-FTIR spectrometry, the microstructure of the irradiated Li_4SiO_4 pebbles is only slightly changed in comparison to the un-irradiated pebbles, due to small radiolysis degree. Nevertheless, after irradiation at high temperature, the agglomeration of pores and cracking can be seen.

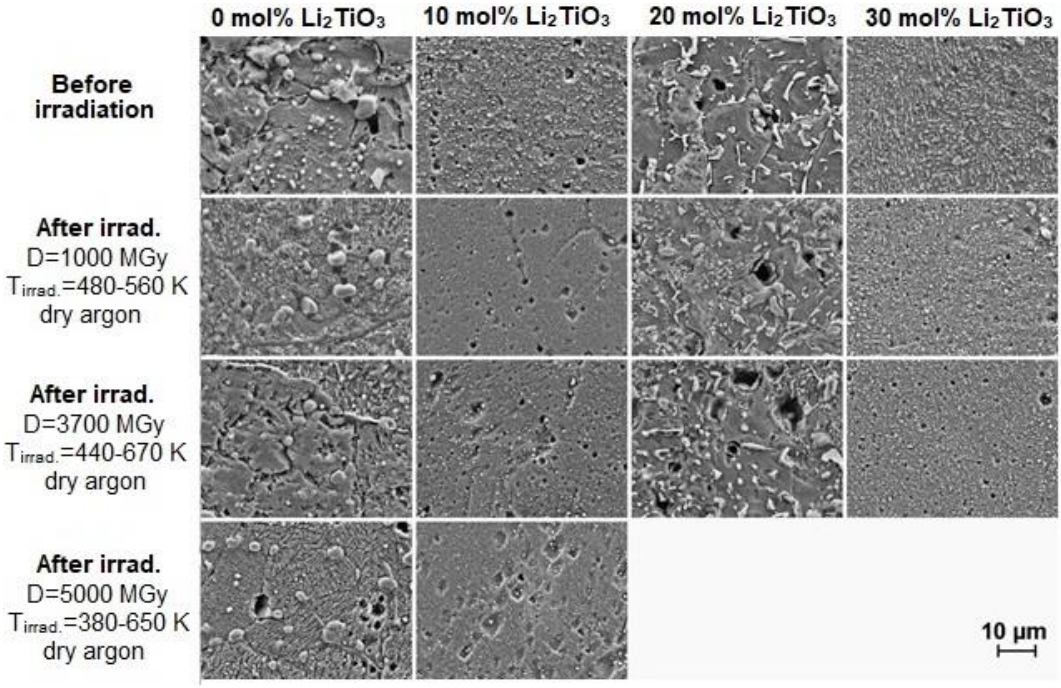

Fig. 3.21 Microstructure at the chemically etched cross-section of the Li_4SiO_4 pebbles with various contents of Li_2TiO_3 before and after irradiation with 5 MeV accelerated electrons up to 1000 MGy, 3700 MGy and 5000 MGy absorbed dose at 380-670 K in a dry argon atmosphere.

3.2.2 Formation and accumulation of RD and RP

After irradiation with 5 MeV accelerated electrons up to 5000 MGy absorbed dose at 380-730 K in a dry argon atmosphere, in the Li_4SiO_4 pebbles with various contents of Li_2TiO_3 similar paramagnetic RD and RP were observed as in the Li_4SiO_4 pebbles, which were irradiated up to 24 MGy absorbed dose at 300-350 K (Fig. 3.22, a and b). The obtained ESR spectra of the Li_4SiO_4 pebbles, which were irradiated up to 1000 MGy absorbed dose at 380-560 K, are shown in Fig. 3.22, c and d.

In the ESR spectra of the reference Li_4SiO_4 pebbles (0 mol% Li_2TiO_3), which were irradiated up to 5000 MGy absorbed dose at 380-730 K (Fig. 3.22, c), one main ESR signal with

a g-factor 2.002±0.001 was detected and related to E' centres (≡Si· or SiO_3^{3-}). The intensity reduction of the ESR signals with g-factors at around 2.008, 2.017 and 2.040, which were related to HC_2 centres (≡Si-O· or SiO_4^{3-}) and peroxide radicals (≡Si-O-O·), can be attributed to the secondary and third stage reactions of the radiolysis, due to the high absorbed dose, or to the thermally stimulated recombination processes, due to the elevated irradiation temperature.

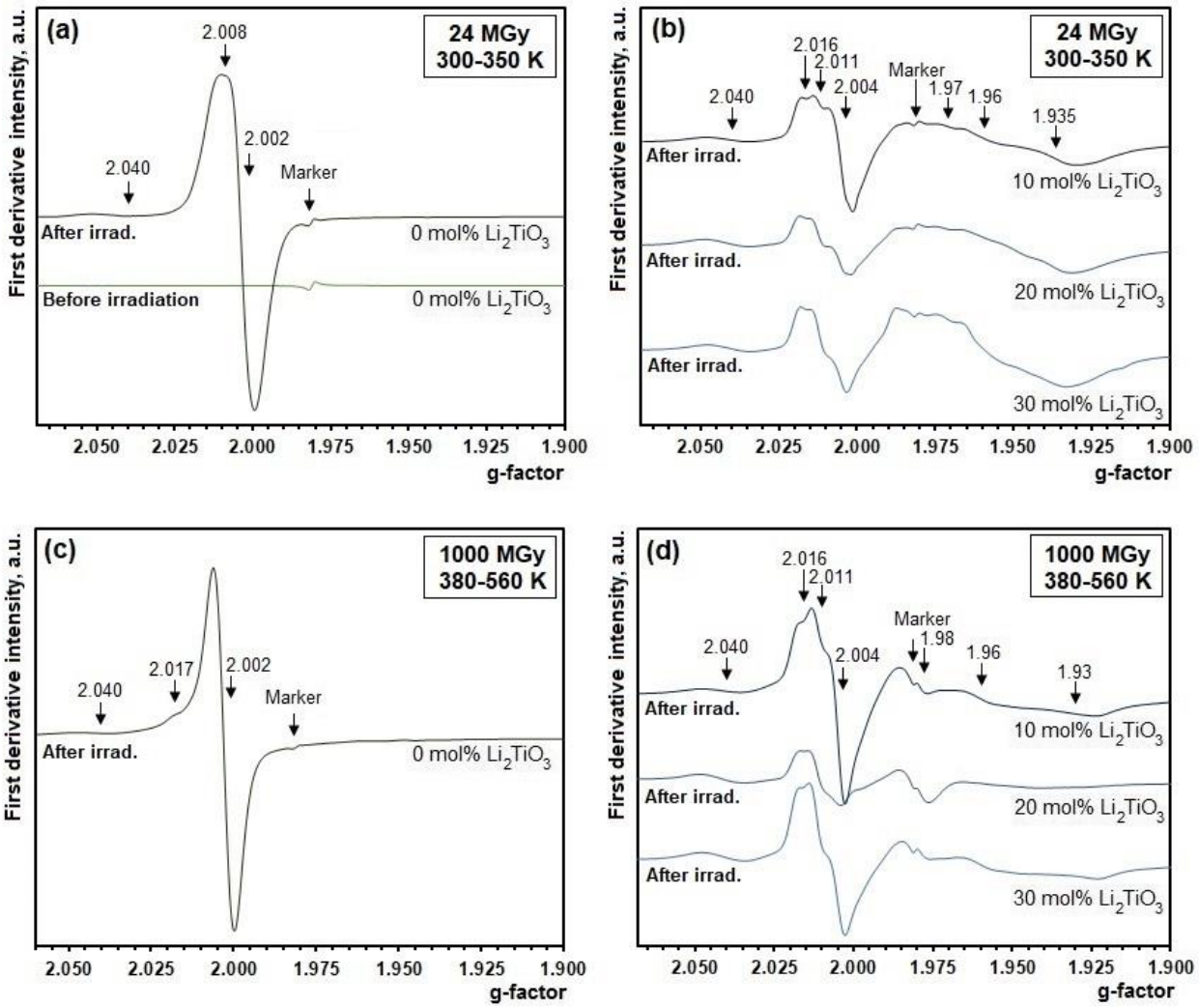

Fig. 3.22 ESR spectra of the reference Li_4SiO_4 pebbles without additions of Li_2TiO_3 (a and c) and the advanced Li_4SiO_4 pebbles with additions of Li_2TiO_3 as a secondary phase (b and d) before and after irradiation with 5 MeV accelerated electrons up to 24 MGy absorbed dose at 300-350 K (a and b) and up to 1000 MGy absorbed dose at 380-560 K (c and d) in a dry argon atmosphere.

In the ESR spectra of the advanced Li_4SiO_4 pebbles with additions of Li_2TiO_3 as a secondary phase, which were irradiated up to 5000 MGy absorbed dose at 380-730 K (Fig. 3.22, d), the ESR signals of both groups were detected. The ESR signals of the first group with g-factors from 2.004 to 2.040 were attributed to E' centres (SiO_3^{3-} and TiO_3^{3-}), HC_2 centres (SiO_4^{3-} and TiO_3^{-}) and peroxide radicals (≡Si-O-O·), respectively. The intensity of the second group of the ESR signals with g-factors from 1.93 to 1.98, which were attributed to Ti^{3+} centres, significantly decrease in comparison to the advanced Li_4SiO_4 pebbles with additions of Li_2TiO_3,

which were irradiated at 300-350 K (Fig. 3.22, b). It is assumed that the Ti^{3+} centres are thermally un-stable at temperatures >380 K and therefore can influence the thermally stimulated recombination processes in the advanced Li_4SiO_4 pebbles during irradiation at high temperature.

In the ESR spectra of the Li_4SiO_4 pebbles with various contents of Li_2TiO_3, which were irradiated between 630 K and 770 K, only one, relatively small and narrow signal with a g-factor close to 2.0030 (ΔB_{pp}<0.5 mT) was detected. It is suggested that this narrow ESR signal can be associated with electron type RD and RP, for example Li_n particles, E' centres etc. In contrast to these measurements, the accumulation of paramagnetic RD and RP in the Li_4SiO_4 pebbles practically ends during irradiation at temperatures >800 K, and in the obtained ESR spectra no characteristic ESR signals of paramagnetic RD or RP were detected besides very small ESR signals, which are most likely related to metallic trace-impurities, such as Mn^{2+}, Cu^{2+}, Fe^{3+} etc.

The total concentration of the accumulated paramagnetic RD and RP in the irradiated Li_4SiO_4 pebbles with various contents of Li_2TiO_3 as a function of the absorbed dose and the average irradiation temperature is shown in Fig. 3.23. The obtained results clearly show that during irradiation up to 5000 MGy absorbed dose at 380-770 K, the total concentration of the accumulated paramagnetic RD and RP significantly decreases in comparison to the Li_4SiO_4 pebbles, which were irradiated up to 24 MGy absorbed dose at 300-350 K (Fig. 3.23, a). Also, by adding Li_2TiO_3 as a secondary phase in the advanced Li_4SiO_4 pebbles, the total concentration of the accumulated paramagnetic RD and RP slightly decreases in comparison to the reference Li_4SiO_4 pebbles (0 mol% Li_2TiO_3). A dependence of the absorbed dose for the Li_4SiO_4 pebbles, which were irradiated between 380 K and 770 K, was not observed, due to the influence of the different irradiation temperatures (Fig. 3.23, b). The total concentration of the accumulated paramagnetic RD and RP in the pebbles decreases with increasing the irradiation temperature.

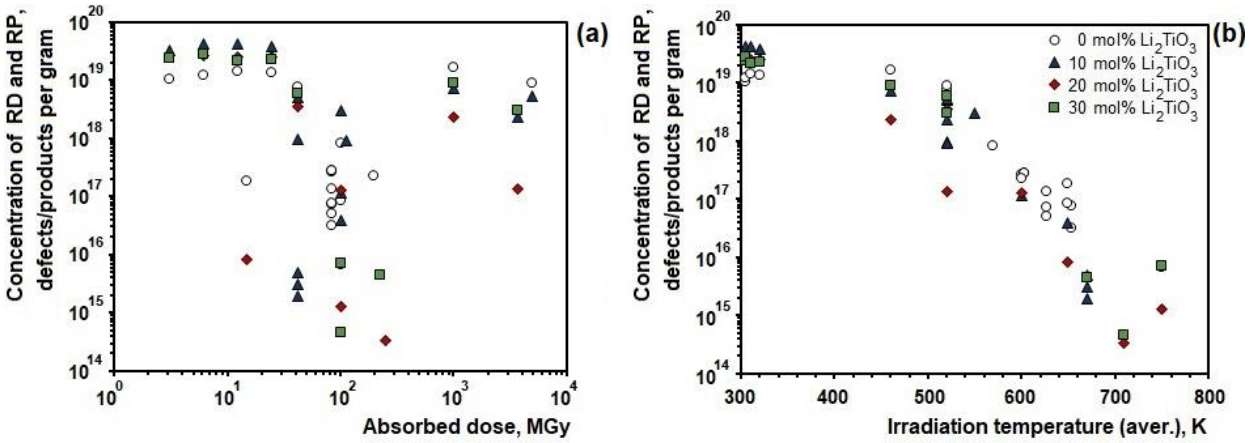

Fig. 3.23 Total concentration of the accumulated paramagnetic RD and RP in the irradiated Li_4SiO_4 pebbles with various contents of Li_2TiO_3 as a function of (a) the absorbed dose and (b) the average irradiation temperature. The pebbles were irradiated with 5 MeV accelerated electrons up to 5000 MGy absorbed dose at 300-770 K in a dry argon atmosphere.

3.2.3 Thermal stability and annihilation of accumulated RD and RP

The "black" colour of the irradiated reference Li_4SiO_4 pebbles (0 mol% Li_2TiO_3) and the blue-grey colour of the irradiated advanced Li_4SiO_4 pebbles with additions of Li_2TiO_3 as a secondary phase practically disappears after stepwise isochronal annealing up to 1070 K in vacuum, due to the thermally stimulated recombination processes of optically active RD and RP (colour centres) or other transformation of them. The photos of the un-irradiated and irradiated Li_4SiO_4 pebbles with various contents of Li_2TiO_3 before and after annealing are shown in Fig. 3.24. The content of Li_2TiO_3 is given in the upper row, while the irradiation and annealing conditions are shown on the left side.

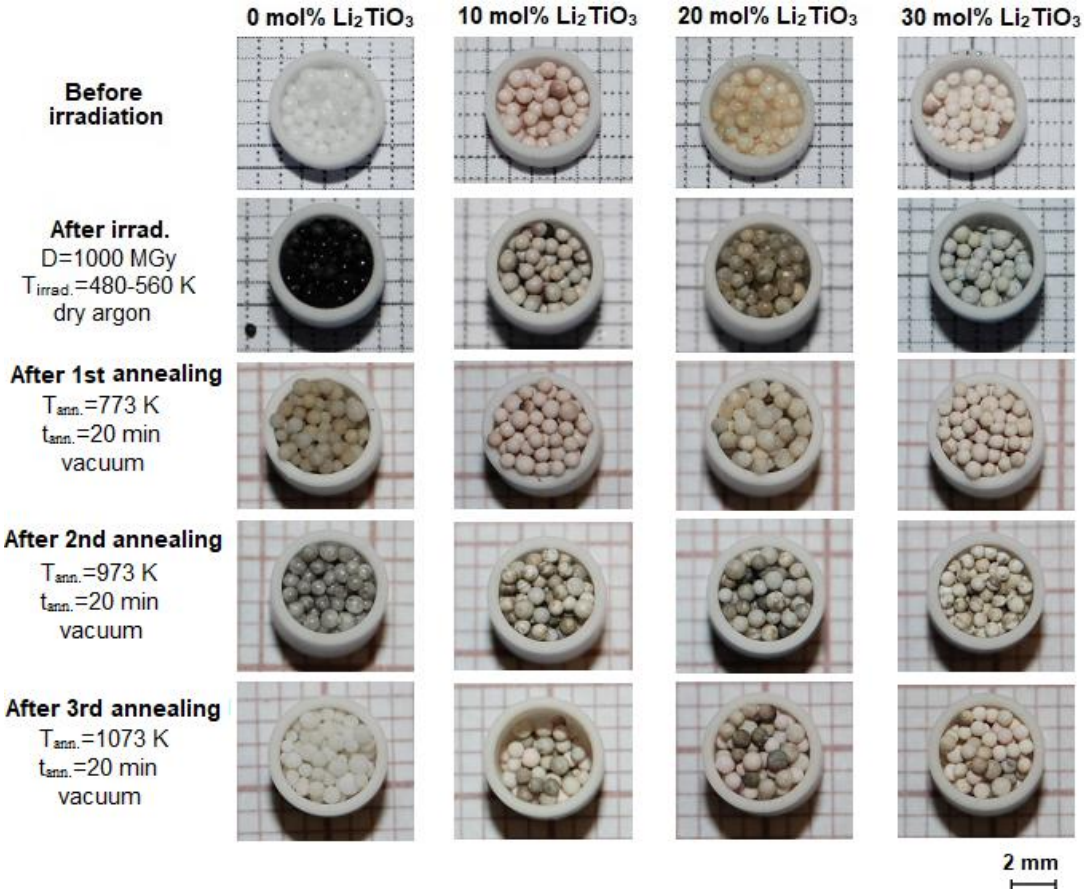

Fig. 3.24 Photo of the un-irradiated and irradiated Li_4SiO_4 pebbles with various contents of Li_2TiO_3 before and after stepwise isochronal annealing up to 770 K, 970 K and 1070 K for 20 min in vacuum. The pebbles were irradiated with 5 MeV accelerated electrons up to 1000 MGy absorbed dose at 480-560 K in a dry argon atmosphere.

After stepwise isochronal annealing up to 1070 K in vacuum, for the irradiated reference Li_4SiO_4 pebbles (0 mol% Li_2TiO_3) a colour change from "black" (through brown and metallic grey) to practically white was detected, while the irradiated advanced Li_4SiO_4 pebbles with additions of Li_2TiO_3 as a secondary phase changed to practically white or dark-grey/black. The observed colour changes for the irradiated reference Li_4SiO_4 pebbles during annealing are related to the selective recombination of optically active RD and RP (colour centres). While the dark-

grey/black colour of the irradiated advanced Li_4SiO_4 pebbles, which was observed after annealing, can be attributed to the formation of the metallic Pt particles on the surface of the advanced pebbles. The elevated content of Pt in the advanced pebbles before irradiation was detected by SEM-EDX and XRF spectrometry (Fig. 3.7).

The surface microstructure and chemical composition of the dark-grey/black irradiated advanced Li_4SiO_4 pebbles with additions of Li_2TiO_3 as secondary phase after stepwise isochronal annealing up to 970 K in vacuum is shown in Fig. 3.25. The excitation area of SEM-EDX spectrometry (blue cross in Fig. 3.25, right) is larger than the grains of the metallic Pt particles (size below 500 nm), and therefore oxygen, silicon and titanium was detected as well.

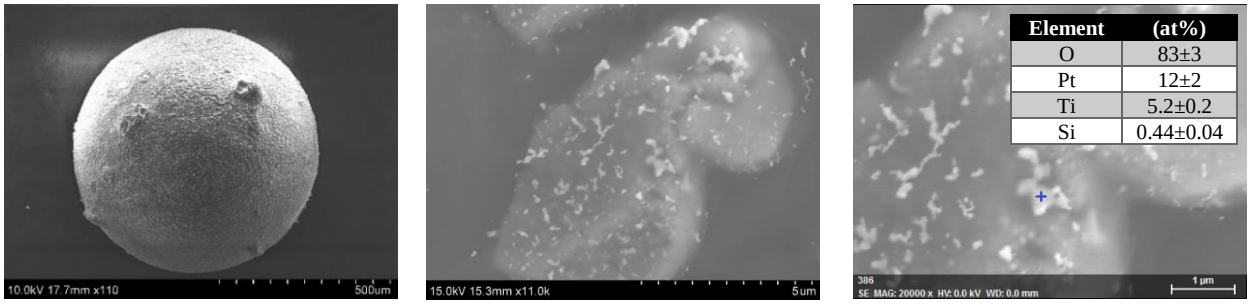

Fig. 3.25 Surface microstructure (with three amplifications) of the dark-grey/black irradiated advanced Li_4SiO_4 pebble with 10 mol% Li_2TiO_3 as a secondary phase after isochronal annealing up to 970 K for 20 min in vacuum. The blue cross indicates the place where the surface chemical composition was measured by SEM-EDX spectrometry.

To analyse the thermal stability and annihilation of the accumulated paramagnetic RD and RP, the reference Li_4SiO_4 pebbles (0 mol% Li_2TiO_3) and the advanced Li_4SiO_4 pebbles with 10 mol% Li_2TiO_3 as a secondary phase, which were irradiated with 5 MeV accelerated electrons up to 5000 MGy absorbed dose at 380-650 K, were stepwise isochronally annealed up to 970 K in a nitrogen atmosphere. The obtained ESR spectra of the irradiated advanced Li_4SiO_4 pebbles with 10 mol% Li_2TiO_3 before and after annealing are shown in Fig. 3.26, a. The total concentration of the accumulated paramagnetic RD and RP in the irradiated reference Li_4SiO_4 pebbles and advanced Li_4SiO_4 pebbles with 10 mol% Li_2TiO_3 as a function of the annealing temperature is shown in Fig. 3.26, b.

The obtained results indicate that during stepwise isochronal annealing between 450 K and 630 K, up to 98% of the accumulated paramagnetic RD and RP in the irradiated Li_4SiO_4 pebbles with various contents of Li_2TiO_3 were annihilated, due to the thermally stimulated recombination processes. As expected, during irradiation at temperatures >380 K, thermally stable RD and RP were mainly accumulated, and therefore the annealing temperature of the accumulated paramagnetic RD and RP in the Li_4SiO_4 pebbles slightly increases in comparison to the pebbles, which were irradiated at 300-350 K (Fig. 3.11). In the ESR spectra of the irradiated Li_4SiO_4

pebbles after annealing at temperatures >750 K, only one, relatively narrow ESR signal with a g-factor 2.0032±0.0005 (ΔB_{pp}<0.08 mT) was detected and can be attributed to Li_n particles. As expected from previous results of stepwise isochronal annealing of the irradiated pebbles (Fig. 3.10), this relatively narrow ESR signal practically disappears at temperatures >970 K.

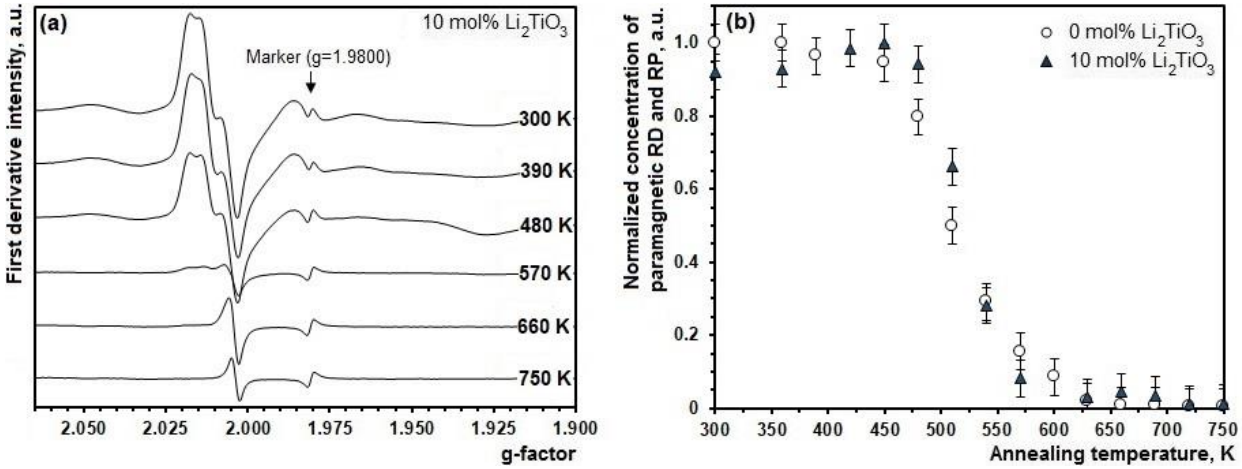

Fig. 3.26 (a) ESR spectra of the irradiated advanced Li_4SiO_4 pebbles with 10 mol% Li_2TiO_3 as a secondary phase before and after stepwise isochronal annealing up to 750 K for 25 min in nitrogen atmosphere. (b) Annihilation behaviour of the accumulated paramagnetic RD and RP in the irradiated reference Li_4SiO_4 pebbles (0 mol% Li_2TiO_3) and advanced Li_4SiO_4 pebbles with 10 mol% Li_2TiO_3 as a secondary phase. The pebbles were irradiated with 5 MeV accelerated electrons up to 5000 MGy absorbed dose at 380-650 K in a dry argon atmosphere.

To supplement the obtained results of ESR spectrometry, the TSL glow curves and spectra of the irradiated reference Li_4SiO_4 pebbles (0 mol% Li_2TiO_3) and advanced Li_4SiO_4 pebbles with 10 mol% Li_2TiO_3 as a secondary phase were measured. The obtained TSL glow curves with deconvoluted gaussian peaks are shown in Fig. 3.27.

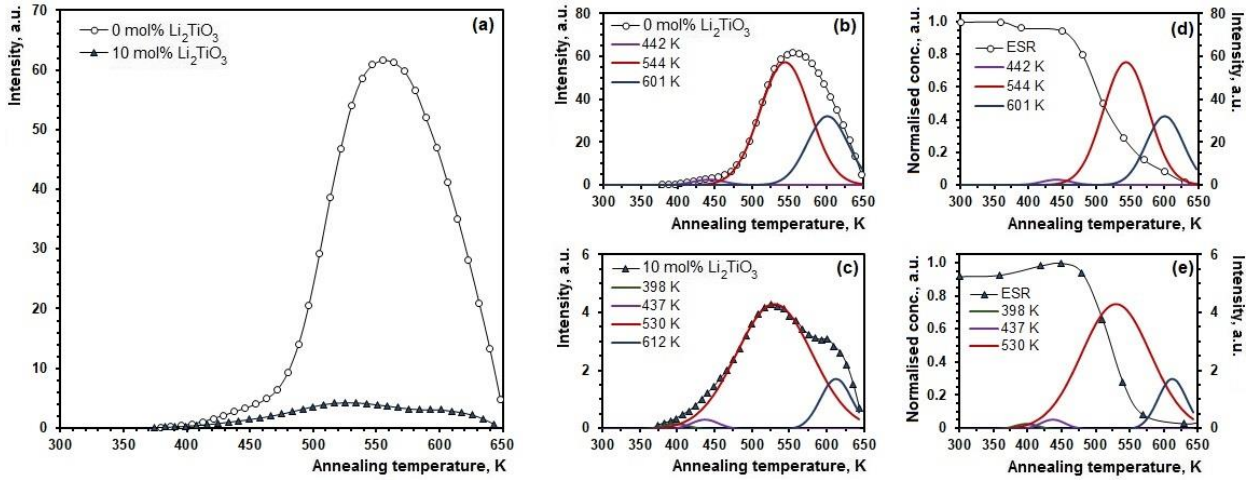

Fig. 3.27 TSL glow curves of the Li_4SiO_4 pebbles with various contents of Li_2TiO_3 after irradiation with 5 MeV accelerated electrons, up to 5000 MGy absorbed dose at 380-650 K in dry argon atmosphere. (a) The TSL glow curves, (b, c) the TSL glow curves with deconvoluted gaussian peaks and (d, e) the combined results of ESR spectrometry and TSL technique. The heating rate is 2 K s^{-1}.

The obtained data of TSL technique (Fig. 3.27, a) correlate with the results of ESR spectrometry (Fig. 3.23), and the intensity of the TSL glow curves decreases, due to the additions of Li_2TiO_3 as a secondary phase in the advanced Li_4SiO_4 pebbles in comparison to the reference Li_4SiO_4 pebbles (0 mol% Li_2TiO_3). The TSL glow curves of the irradiated Li_4SiO_4 pebbles consist of two main peaks with maxima at around 540 K and 610 K regardless of the Li_2TiO_3 content (Fig. 3.27, b and c). The TSL peaks with maxima below 500 K were practically not detected, due to the high irradiation temperature. The obtained results of TSL technique also show a good correlation with the obtained data of ESR spectrometry (Fig. 3.27, d and e). However, no signal was detected, when measuring the TSL spectra with a CCD camera and a spectrometer as the intensity of emission was below the sensitivity limit of the detection system.

3.2.4 Summary of results

In this section, the advanced Li_4SiO_4 pebbles with additions of Li_2TiO_3 as a secondary phase were investigated before and after the simultaneous action of 5 MeV accelerated electrons (up to 5000 MGy absorbed dose) and high temperature (up to 1285 K) to understand the high-temperature radiolysis processes. The irradiation temperature was chosen in order to reach conditions comparable to the operation conditions of the nuclear fusion reactors.

Summarising all the above-mentioned results, it is concluded that the radiolysis degree (α) of the advanced Li_4SiO_4 pebbles with additions of Li_2TiO_3 as a secondary phase is under 1 mol% after irradiation up to 5000 MGy absorbed dose. In addition, due to the relatively small radiolysis degree, no major changes in the microstructure, chemical and phase composition of the advanced Li_4SiO_4 pebbles with additions of Li_2TiO_3 after irradiation were detected. The melting of the advanced Li_4SiO_4 pebbles is expected to start at temperatures >1390 K.

The irradiation temperature has a significant impact on the formation and accumulation of RD and RP in the advanced Li_4SiO_4 pebbles with additions of Li_2TiO_3 as a secondary phase. The obtained results of TSL technique and ESR spectrometry corroborates that the additions of Li_2TiO_3 in the advanced Li_4SiO_4 pebbles decrease the concentration of the accumulated RD and RP in comparison to the reference Li_4SiO_4 pebbles (0 mol% Li_2TiO_3). It is suggested that the Ti^{3+} centres are thermally un-stable at temperatures >380 K and therefore can influence the thermally stimulated recombination processes in the advanced Li_4SiO_4 pebbles during irradiation at elevated temperature. The obtained results of ESR spectrometry clearly show that during irradiation up to 770 K, the concentration of the accumulated paramagnetic RD and RP in the advanced pebbles decreases with increasing the irradiation temperature. The accumulation of paramagnetic RD and RP practically ends during irradiation at temperature >800 K.

During irradiation at temperatures >380 K, the thermally stimulated recombination processes of primary and secondary RD dominate in the advanced Li_4SiO_4 pebbles with additions of Li_2TiO_3 as a secondary phase and therefore thermally stable RP mainly accumulates, such as small and large Li_n particles. In addition, due to the high irradiation temperature, the annihilation temperature of the accumulated RD and RP in the advanced Li_4SiO_4 pebbles with additions of Li_2TiO_3 slightly increases (from 300-650 K to 400-650 K) in comparison to the advanced pebbles, which were irradiated at 300-350 K.

3.3 Influence of noble metals on radiolysis

Although the concentration of the noble metals (Pt, Au and Rh) in the advanced Li_4SiO_4 pebbles with additions of Li_2TiO_3 as a secondary phase was previously studied by O. Leys et al. [18], the oxidation states and distribution of the noble metals and their influence on the formation and accumulation of RD and RP in the advanced pebbles during irradiation were not analysed. Therefore, to remedy this situation, the advanced pebbles with similar chemical and phase composition (approx. 80 mol% Li_4SiO_4 and 20 mol% Li_2TiO_3), but with different contents of the noble metals (up to 300 ppm) were analysed.

In an *enhanced* melt-based process, which was described above in the literature review (Chapter 1.2.1), the molten raw materials and synthesis products can react with the surface of Pt-Rh and Pt-Au alloy crucible components (Eqs. 3.2 and 3.3), and thereby the noble metals can be introduced into the Li_4SiO_4-Li_2TiO_3 melt.

$$Pt + 2\ LiOH + O_2 \rightarrow Li_2PtO_3 + H_2O\uparrow \quad (3.2)$$

$$Pt + Li_4SiO_4 + O_2 \rightarrow Li_2PtO_3 + Li_2SiO_3 \quad (3.3)$$

Bright yellow-green Li_2PtO_3 is thermally stable up to 1375 K [135], and therefore it can accumulate in the advanced Li_4SiO_4 pebbles with additions of Li_2TiO_3 as a secondary phase during the fabrication process. Au is one of the least reactive chemical elements and usually its compounds are thermally un-stable, and it is assumed that Au in the advanced Li_4SiO_4 pebbles with additions of Li_2TiO_3 will accumulate in a metallic form. The common oxidation state of Rh is +3, and it is supposed that black lithium rhodate ($LiRhO_2$) can also form in the advanced pebbles during the fabrication process [155].

To estimate the presence and distribution of the noble metals (Pt, Au and Rh) and their corrosion products (Li_2PtO_3 and $LiRhO_2$), the surface microstructure, chemical and phase composition of the un-treated and thermally treated advanced Li_4SiO_4 pebbles with various contents of the noble metals was analysed before irradiation.

3.3.1 Surface microstructure and chemical composition before irradiation

The un-treated advanced Li_4SiO_4 pebbles with different contents of the noble metals show an off-white colour (Sample #2.1, #2.2 and #2.3) before irradiation, while the thermally treated advanced Li_4SiO_4 pebbles with highest content of the noble metals have a pale-yellow colour (Sample #2.1a). The advanced Li_4SiO_4 pebbles are spherically shaped, and the grains of a secondary phase, Li_2TiO_3, are very small (grain size: <4 μm) and homogeneously distributed on the surface of the advanced pebbles. The surface of the three randomly selected thermally treated advanced pebbles with highest content of the noble metals (Sample #2.1a) is shown in Fig. 3.28.

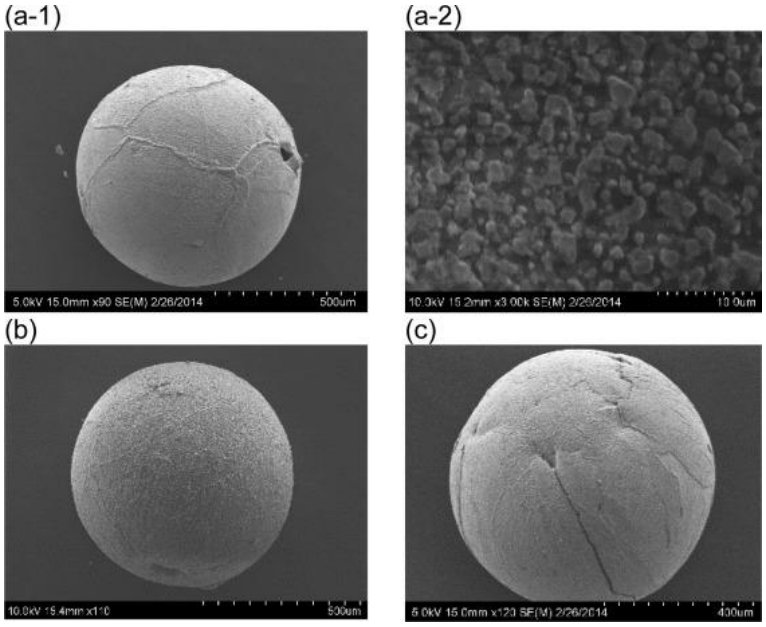

Fig. 3.28 Surface of the three randomly selected thermally treated advanced Li_4SiO_4 pebbles with highest content of the noble metals (Sample #2.1a) before irradiation.

Using SEM-EDX spectrometry, mainly oxygen, silicon, titanium and Pt trace-impurities were detected on the surface of the thermally treated advanced Li_4SiO_4 pebbles with highest content of the noble metals (Sample #2.1a), and the element mapping is shown in Fig. 3.29. The origins of oxygen, silicon and titanium are the primary phase, Li_4SiO_4, and a secondary phase, Li_2TiO_3. The presence of Au and Rh on the surface of the advanced Li_4SiO_4 pebbles was not detected, due to small amount and the detection limit of SEM-EDX spectrometry.

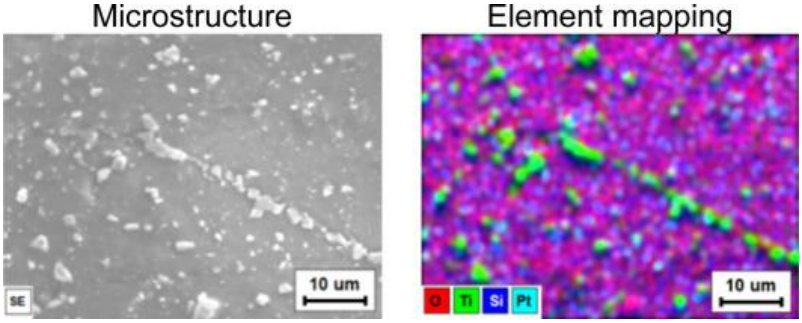

Fig. 3.29 Surface microstructure (left) and chemical composition (right) of the thermally treated advanced Li_4SiO_4 pebble with highest content of the noble metals (Sample #2.1a) before irradiation.

The Pt trace-impurities are heterogeneously distributed on the surface of the advanced Li_4SiO_4 pebbles and are mainly localised as a separate phase at the grain boundaries of the primary and a secondary phase or as the inclusions within the primary phase. The distribution of Pt and titanium on the surface of the thermally treated advanced pebbles with the highest content of the noble metals (Sample #2.1a) is shown in Fig. 3.30.

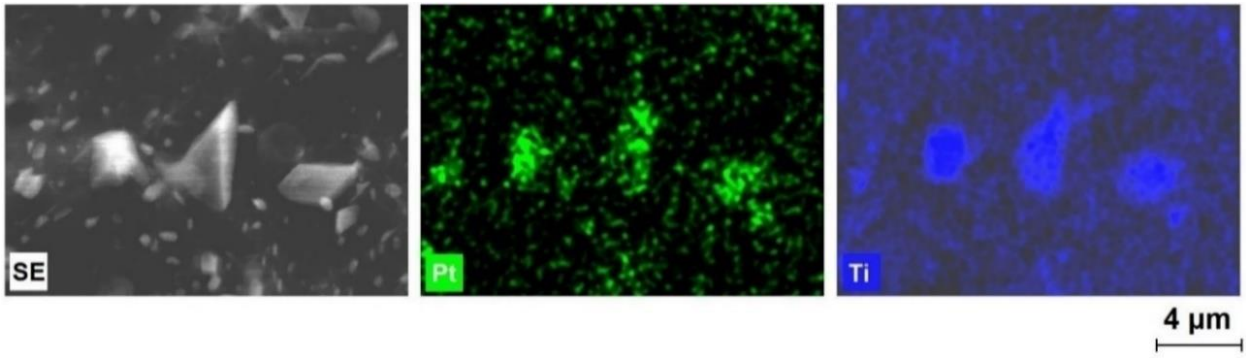

Fig. 3.30 Surface microstructure (left), Pt distribution (middle) and titanium (Ti) distribution (right) on the thermally treated advanced Li_4SiO_4 pebbles with highest content of the noble metals (Sample #2.1a) before irradiation.

3.3.2 Chemical and phase composition before irradiation

In the p-XRD patterns of the un-treated advanced Li_4SiO_4 pebbles with various contents of the noble metals (Fig. 3.31, Sample #2.1, #2.2 and #2.3) before irradiation, the diffraction reflexes of two crystalline phases were detected, monoclinic Li_4SiO_4 as the primary phase and cubic, disordered Li_2TiO_3 (α-form) as a secondary phase. After thermal treatment, up to 1220 K for 3 weeks in air atmosphere, the cubic, disordered Li_2TiO_3 phase was transformed into the monoclinic Li_2TiO_3 (β-form) phase (Fig. 3.31, Sample #2.1a). No reflexes of the noble metals (Pt, Au and Rh) or their corrosions products (Li_2PtO_3 and $LiRhO_2$) were detected by p-XRD, due to small amounts and overlapping of the reflexes with the primary or a secondary phase.

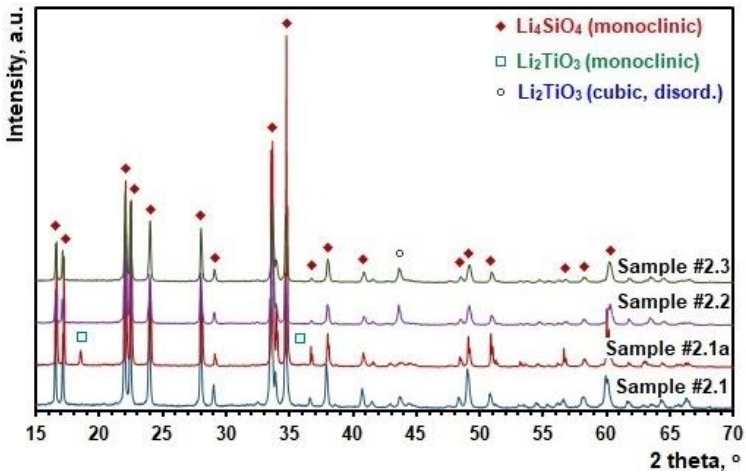

Fig. 3.31 p-XRD patterns of the advanced Li_4SiO_4 pebbles with different contents of the noble metals before irradiation. The Sample #2.1a is thermally treated, while other pebbles are un-treated.

Using ATR-FTIR spectrometry, the stretching and bending bond vibrations of the primary and a secondary phase were mainly detected in the un-treated and thermally treated advanced Li_4SiO_4 pebbles with various contents of the noble metals (Fig. 3.32). The detected vibrations at around 400-1050 cm^{-1} are related to Li-O, Si-O, O-Si-O and Ti-O bonds, but at about 1400-1500 cm^{-1} to C-O bonds. While the Pt-O bond vibrations of Li_2PtO_3, which are expected to be between 400 cm^{-1} and 700 cm^{-1} [156], were not detected, due to small amounts and overlapping with bond vibrations of the primary or a secondary phase.

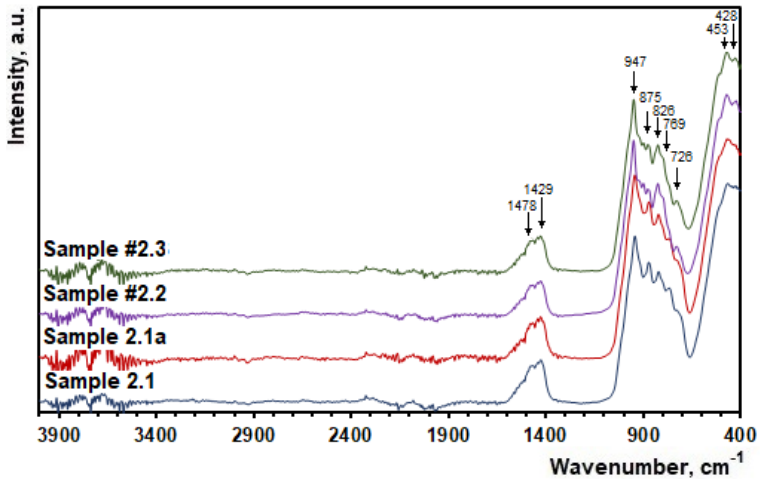

Fig. 3.32 ATR-FTIR spectra of the advanced Li_4SiO_4 pebbles with different contents of the noble metals before irradiation. The Sample #2.1a is thermally treated, while other pebbles are un-treated.

To explain the formation of C-O bonds, which were detected by ATR-FTIR spectrometry, the top-surface chemical composition (depths: ~5-10 nm [157]) of the un-treated and thermally treated advanced Li_4SiO_4 pebbles with various contents of the noble metals was examined by XPS (Fig. 3.33). In the XPS, mainly the core level spectra of carbon, oxygen, lithium, titanium and silicon were observed. All core level spectra showed one peak for the corresponding elements except carbon. The position of the carbon main peak at 289.8 eV is in good agreement with the known peak position at 289.8 eV for $LiCO_3$ [158]. Other peaks of carbon at 284.5 eV, 286.2 eV and 288.4 eV can be assigned to C-C, C-O and O=C-O bonds [159, 160].

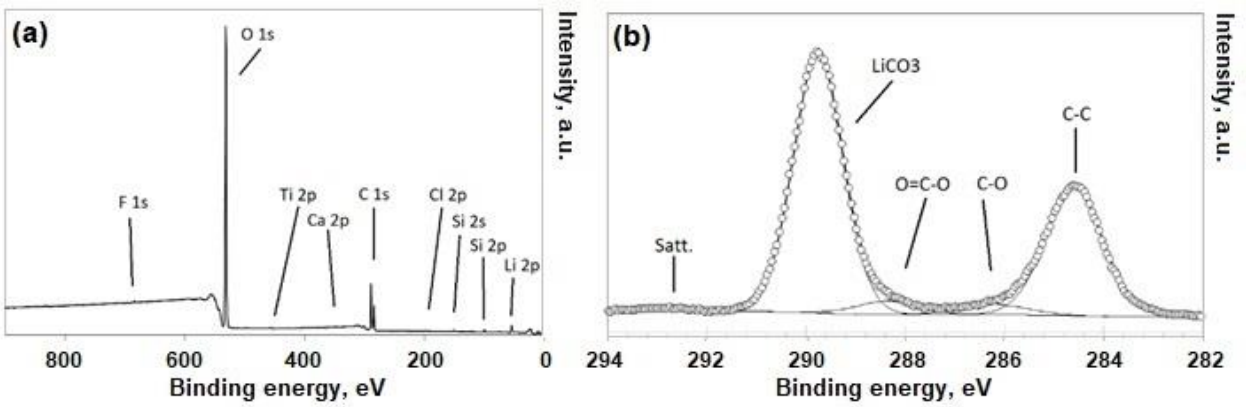

Fig. 3.33 XPS of the thermally treated advanced Li_4SiO_4 pebble with highest content of the noble metals (Sample #2.1a) before irradiation. (a) Survey spectrum; (b) detailed spectrum of carbon peaks.

As expected from the obtained results of ATR-FTIR spectrometry (Fig. 3.32) and XPS (Fig. 3.33), using TG-DTA, a weight loss (up to 1.5 wt%) during heating up to 1100 K was detected for the un-treated and thermally treated advanced Li_4SiO_4 pebbles with various contents of the noble metals, due to the release of absorbed and chemisorbed H_2O and CO_2 (Fig. 3.34). The DTA curves reveals four endothermic peaks between 670 K and 1020 K. On the basis of the obtained results of p-XRD (Fig. 3.31), the irreversible peaks (1) and (2) are related to the phase transition of the secondary Li_2TiO_3 phase (α form → β form) [12]. While the reversible peaks (3) and (4) are caused by polymorphic transitions of the primary Li_4SiO_4 phase [84].

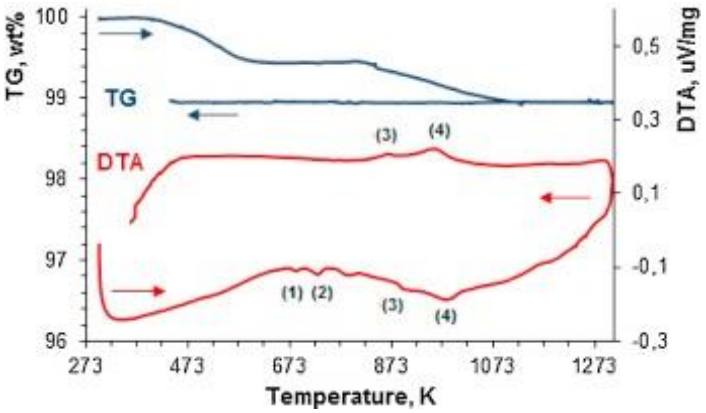

Fig. 3.34 TG-DTA curves of the un-treated advanced Li_4SiO_4 pebbles with highest content of the noble metals (Sample #2.1) before irradiation.

Other processes, such as the melting of the noble metals (Pt, Au and Rh) or the decomposition of the corrosion products of the noble metals (Li_2PtO_3 and $LiRhO_2$), occur at temperature >1300 K or the mass of the noble metals and their corrosion products is too small to detect a reaction enthalpy by TG-DTA. The Li_2PtO_3 decomposes at around 1375 K (Eq. 3.4), while the metallic Au melts at 1307 K, Pt at 2041 K and Rh at 2236 K.

$$Li_2PtO_3 \rightarrow Li_2O + Pt + O_2\uparrow \qquad (3.4)$$

3.3.3 Formation and accumulation of RD and RP

To evaluate the influence of the noble metals on the formation and accumulation of RD and RP, the un-treated and thermally treated advanced Li_4SiO_4 pebbles with various contents of the noble metals were irradiated with 5 MeV accelerated electrons, up to 12 MGy absorbed dose at 300-350 K in a dry argon atmosphere and were investigated by ESR spectrometry (Fig. 3.35). In the ESR spectra of the advanced Li_4SiO_4 pebbles before irradiation, no ESR signals were detected, except the ESR signal of the reference marker with a g-factor 1.9800±0.0005, and thus these spectra were not included in Fig. 3.35. After irradiation, the complex ESR spectra were observed for the advanced Li_4SiO_4 pebbles, however significant changes in the ESR spectra depending on the content of the noble metals were not detected. Therefore, the detected ESR

signals are attributed to peroxide radicals (≡Si-O-O·), HC_2 centres (SiO_4^{3-} and TiO_3^{-}), E' centres (SiO_3^{3-} and TiO_3^{3-}) and Ti^{3+} centres, respectively. Presumably, the narrow ESR signal of small Li_n particles cannot be observed, due to overlapping with other ESR signals. Nevertheless, it is not excluded that the ESR signals of the paramagnetic metallic trace-impurities can overlap with other ESR signals.

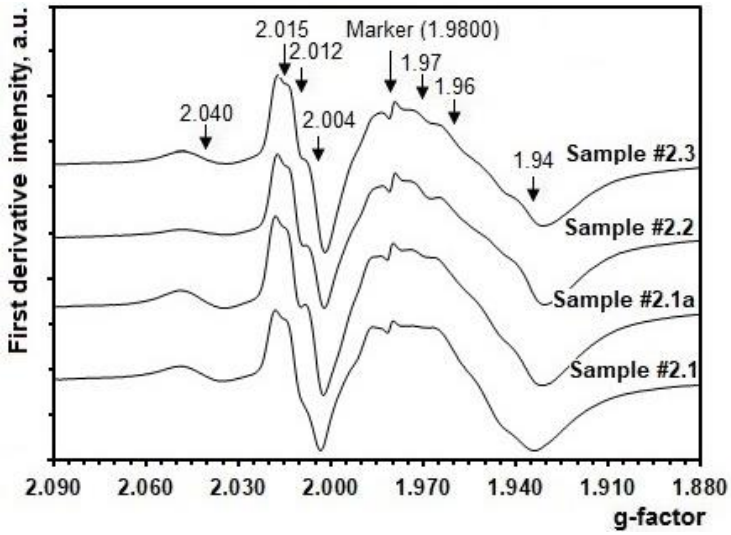

Fig. 3.35 ESR spectra of the irradiated advanced Li_4SiO_4 pebbles with various contents of the noble metals. The Sample #2.1a is thermally treated, while other pebbles are un-treated. The pebbles were irradiated with 5 MeV accelerated electrons up to 12 MGy absorbed dose at 300-350 K in a dry argon atmosphere.

The obtained results of ESR spectrometry indicate that the formation and accumulation of paramagnetic RD and RP under action of 5 MeV accelerated electrons, up to 12 MGy absorbed dose at 300-350 K, is analogous for the un-treated and thermally treated advanced Li_4SiO_4 pebbles with various contents of the noble metals (Fig. 3.36).

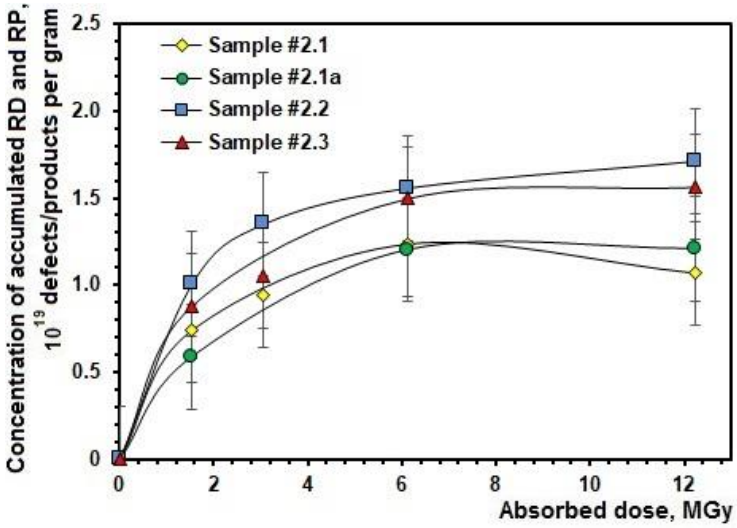

Fig. 3.36 Total concentration of the accumulated paramagnetic RD and RP in the irradiated advanced Li_4SiO_4 pebbles with different contents of the noble metals as a function of the absorbed dose. The Sample #2.1a is thermally treated, while other pebbles are un-treated.

As suggested above, the noble metals in the advanced Li_4SiO_4 pebbles with additions of Li_2TiO_3 localises as a separate phase at the grain boundaries of the primary and a secondary phase or as inclusions within the primary phase and therefore do not affect the formation and accumulation of RD and RP in the crystalline structure of the Li_4SiO_4 phase and the Li_2TiO_3 phase during irradiation. The slight differences in the total concentration of the accumulated paramagnetic RD and RP in the advanced pebbles with various contents of the noble metals can be explained by slight differences in the chemical and phase composition, various amounts of the chemisorption products or small differences in the microstructure.

On the basis of the obtained results, it is concluded that the influence of the noble metals with a sum content of up to 300 ppm is negligible on the formation and accumulation of RD and RP in the Li_4SiO_4 pebbles with various contents of Li_2TiO_3 during irradiation, and it is also expected that the noble metals do not have a negative effect on the functional properties of the ceramic breeder pebbles. The generated tritium from the surface of the ceramic breeder pebbles is released via the exchange reaction with sweep gases containing hydrogen, and therefore the noble metals can substantially promote the isotope exchange reactions at lower temperatures [161]. The formation and accumulation of the corrosion products of the noble metals (Li_2PtO_3 and $LiRhO_2$) in the advanced Li_4SiO_4 pebbles were not confirmed by p-XRD, TG-DTA and ATR-FTIR spectrometry, due to small amounts and the detection limits of these methods.

3.3.4 Summary of results

In this section, the influence of the noble metals on the formation and accumulation in the advanced Li_4SiO_4 pebbles with additions of Li_2TiO_3 as a secondary phase was analysed and evaluated. The noble metals (Pt, Au and Rh) with a sum content of up to 300 ppm into the advanced Li_4SiO_4 pebbles with additions of Li_2TiO_3 can be introduced during the fabrication process, due to the surface corrosion of the Pt-Rh and Pt-Au alloy crucible components.

Summarising all the above-mentioned results, it is concluded that the influence of the noble metals on the radiolysis of the advanced Li_4SiO_4 pebbles with additions of Li_2TiO_3 as a secondary phase is negligible, and it is also expected that the noble metals do not have a negative effect on the functional properties of the ceramic breeder pebbles. The noble metals have heterogeneous distribution on the surface and most likely in the volume of the advanced Li_4SiO_4 pebbles, and they localise as a separate phase at the grain boundaries of the primary and a secondary phase or as inclusions within the primary phase. The formation and accumulation of the corrosion products of the noble metals (Li_2PtO_3 and $LiRhO_2$) were not confirmed, due to small amounts of the noble metals and the detection limits of used methods.

3.4 Influence of pebble diameter and grain size on radiolysis

The fabricated Li_4SiO_4 pebbles with various contents of Li_2TiO_3 have a very broad diameter distribution (from 10 μm to 1500 μm), various microstructures (granular, dendritic and amorphous) and different grain sizes (from 1 μm to 10 μm). To evaluate the influence of the pebble diameter and the grain size on the formation and accumulation of RD and RP, the reference Li_4SiO_4 pebbles (0 mol% Li_2TiO_3) with two diameters, small pebbles (<50 μm) and large pebbles (~500 μm), were used. The microstructure at the chemically etched cross-sections of the un-treated and thermally treated small pebbles and large pebbles before and after irradiation with 5 MeV accelerated electrons, up to 11000 MGy (11 GGy) absorbed dose at 550-590 K in a dry argon and air atmosphere, is shown in Fig. 3.37. The pebble diameter can be seen in the upper row, while the preparation/irradiation conditions are shown on the left side.

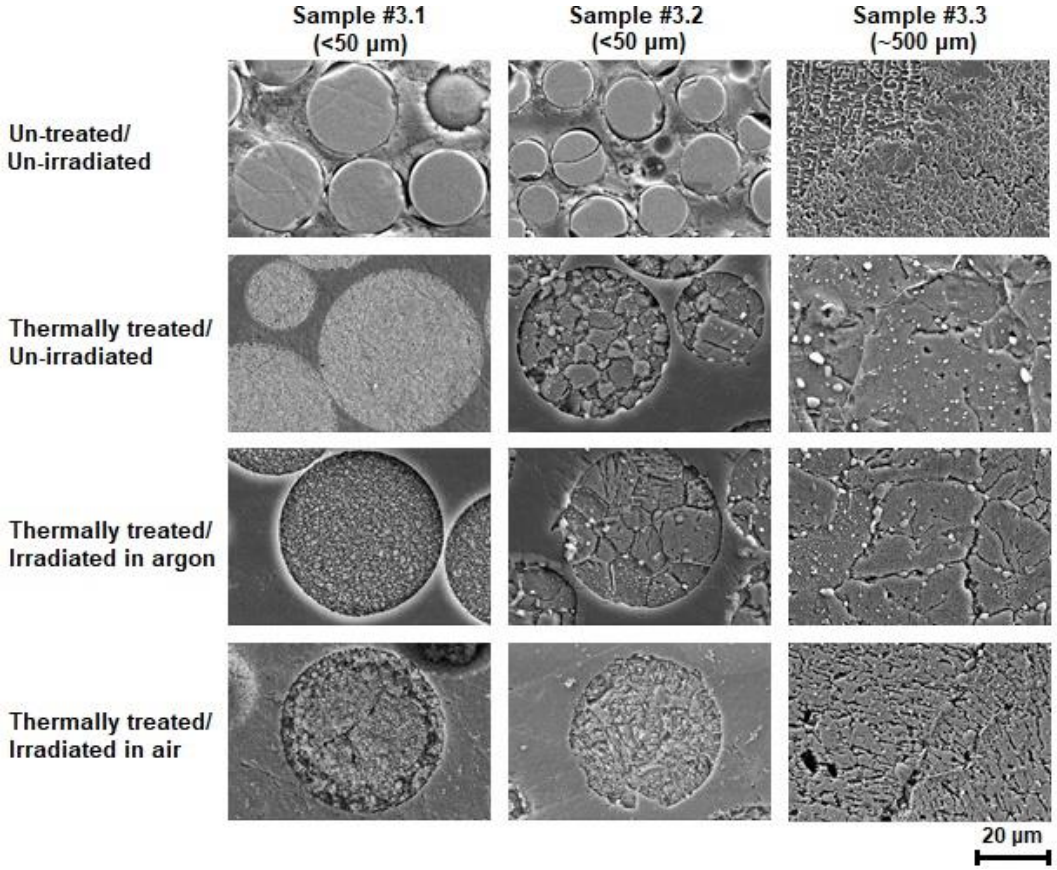

Fig. 3.37 Microstructure at the chemically etched cross-section of the un-treated and thermally treated small pebbles and the large pebbles before and after irradiation with 5 MeV accelerated electrons up to 11000 MGy absorbed dose at 550-590 K in a dry argon or air atmosphere.

The small pebbles and the large pebbles were produced in the same fabrication campaign and thus have identical chemical composition (approx. 88 mol% Li_4SiO_4 and 12 mol% $Li_6Si_2O_7$ [84]). The high-temperature phase, $Li_6Si_2O_7$, forms due to the rapid quenching of the obtained pebbles during the fabrication process (Eq. 1.12). The small pebbles (Samples #3.1 and #3.2) have an amorphous microstructure, due to the rapid cooling during the fabrication process, while

the large pebbles (Sample #3.3) have a dendrite microstructure, due to the heterogeneous nucleation at pores and cracks or the pebble collision (Fig. 3.37, first row from the top).

To achieve various microstructures and grain sizes, the small pebbles were thermally treated up to 1070 K for 1 h (Sample #3.1) and up to 1170 K for 128 h (Sample #3.2), while the large pebbles were treated up to 1240 K for 168 h in air atmosphere (Sample #3.3). In the small pebbles and in the large pebbles at the chemically etched cross-section after thermal treatment, the Li_4SiO_4 phase is displayed in dark-grey colour with smaller, light-grey grains of Li_2SiO_3 phase as inter- or intra-crystalline inclusions (Fig. 3.37, second row from the top). In the small pebbles (Sample #3.2) grains of the primary and a secondary phase seems to be only loosely connected, and therefore some of the small pebbles were destroyed during the preparation process for the SEM measurements (polishing, grinding and etching). The average grain size for the large pebbles is around 10 μm (Sample #3.3) and for the small pebbles is approx. 5 μm (Sample #3.2). While in the small pebbles, which were thermally treated up to 1070 K for 1 h, the average grain size is below 1 μm (Sample #3.1).

3.4.1 Microstructure and phase composition after irradiation

During irradiation with 5 MeV accelerated electrons up to 11000 MGy absorbed dose at 550-590 K in a dry argon atmosphere, the microstructure at the chemically etched cross-section of the small pebbles (Sample #3.2) and the large pebbles (Sample #3.3) practically do not changes (Fig. 3.37, third row from the top). While the small pebbles, which were thermally treated up to 1070 K for 1 h (Sample #3.1), after irradiation seems to exhibit a slightly more porous microstructure with more gaping grain boundaries. Nevertheless, the preparation process of the small pebbles and the large pebbles for the SEM measurements is subject to fluctuations, and therefore the appearance of the microstructure at the etched cross-sections may display a corrosion effect and must be regarded with suspicion.

After irradiation in air atmosphere, the large pebbles (Sample #3.3) at the chemically etched cross-section exhibit a fissured microstructure, while the small pebbles (Samples #3.1 and #3.2) nearly appear to be disintegrated (Fig. 3.37, fourth row from the top). This effect is related with the formation and radiolysis of the chemisorption products of H_2O vapour and CO_2 (LiOH and Li_2CO_3) on the surface of the small pebbles and the large pebbles during irradiation in air atmosphere. Especially for the reference pebbles with small diameter and large surface area, the formation of Li_2CO_3 and LiOH may significantly be increased by the surface reactions.

Using p-XRD it was confirmed that the thermally treated small pebbles and large pebbles before irradiation consists from two crystalline phases, 90 mol% monoclinic Li_4SiO_4 as the

primary phase and 10 mol% orthorhombic Li_2SiO_3 as a secondary phase. The high-temperature phase, $Li_6Si_2O_7$, is metastable at room temperature and decomposes during thermal treatment into Li_4SiO_4 and Li_2SiO_3 (Eq. 1.13). The obtained p-XRD patterns of the thermally treated small pebbles (Sample #3.1) and large pebbles (Sample #3.3) before and after irradiation with 5 MeV accelerated electrons in a dry argon and air atmosphere are shown in Fig. 3.38.

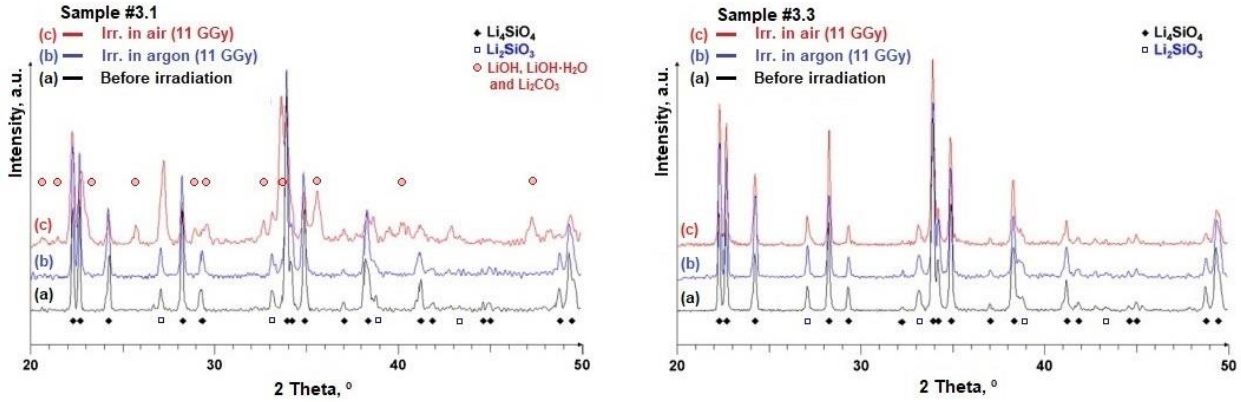

Fig. 3.38 p-XRD patterns of the large pebbles (Sample #3.3) and the small pebbles (Sample #3.1) before and after irradiation with 5 MeV accelerated electrons up to 11000 MGy absorbed dose at 550-590 K in a dry argon or air atmosphere.

After irradiation in a dry argon atmosphere, no major phase composition changes for the small pebbles and the large pebbles were detected. While after irradiation in air atmosphere, in the p-XRD patterns of the small pebbles significant number of additional diffraction reflexes were detected, which can be attributed to the chemisorption products of H_2O vapour and CO_2. Due to the large number of diffraction reflexes, only LiOH, $LiOH \cdot H_2O$ and traces of Li_2CO_3 can be verified. In addition, an increase of the initial concentration of the Li_2SiO_3 phase in the small pebbles and in the large pebbles was detected after irradiation in air atmosphere.

3.4.2 Formation, accumulation and annihilation of RD and RP

A rapid colour change (from “pearl” white to “black” or light-brown) was observed for the small pebbles and the large pebbles, which were irradiated with 5 MeV accelerated electrons, up to 11000 MGy absorbed dose at 550-590 K in a dry argon and air atmosphere. To identify the accumulated optically active RD or RP (colour centres) in the irradiated small pebbles and large pebbles, diffuse reflectance spectrometry was used. The obtained spectra of the small pebbles (Sample #3.1) after irradiation up to 5300 MGy absorbed dose in air atmosphere are shown in Fig. 3.39.

In the diffuse reflectance spectra of the small pebbles and the large pebbles after irradiation with 5 MeV accelerated electrons in a dry argon and air atmosphere, at least three overlapped absorption bands with maxima at around 360 nm, 410 nm and 560 nm were detected regardless

from the absorbed dose. According to X. Fu et al. [162] and H.-S. Tsai et al. [163], the absorption band with a maximum at around 410 nm can be attributed to HC_1 centres, while the absorption band at about 560 nm to HC_2 centres (SiO_4^{3-} or ≡Si-O·). The HC_1 centre is described as a hole trapped on non-bridging oxygen of a SiO_4 tetrahedra, which is affected by the closely located lithium cation (≡Si-O·…Li^+). A. K. Sandhu et al. [164] and K. Kadono et al. [165] suggested that the absorption band with a maximum at around 360 nm can be linked to the localised electron centres. L. I. Bryukvina and E. F. Martynovich [166] suggested that an absorption band of Li_n particles is located at around 420-520 nm. While the E' centres (≡Si· or SiO_3^{3-}) have an absorption band with a maximum at around 215 nm [167], and consequently this band was not detected.

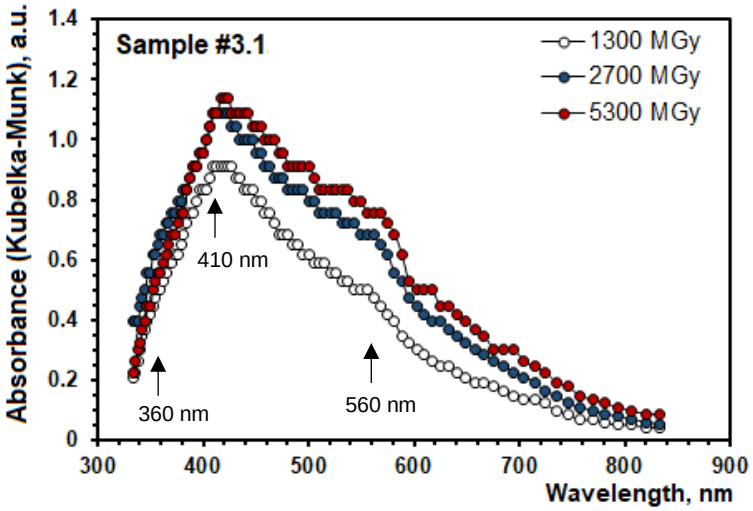

Fig. 3.39 Diffuse reflectance spectra of the irradiated small pebbles (Sample #3.1). The pebbles were irradiated with 5 MeV accelerated electrons up to 1300 MGy, 2700 MGy and 5300 MGy absorbed dose at 550-590 K in air atmosphere.

The electron and hole type RD and RP in the small pebbles and in the large pebbles during irradiation with 5 MeV accelerated electrons forms in equal amounts [37], and therefore it is sufficient to analyse only one type of RD and RP in order to determine the radiolysis efficiency. The accumulated electron type RD and RP in the small pebbles and in the large pebbles after irradiation in a dry argon atmosphere were analysed by the MCS. The MCS is based on the dissolution of the irradiated pebbles in two acid containing scavenger solutions: (1) 0.4 M H_2SO_4 with 1 M C_2H_5OH, and (2) 0.4 M H_2SO_4 with 1 M $NaNO_3$. In the first system, all localized electrons (from simple and complex electron type centres) are scavenged and transformed into the H_2, which can be then detected by GC. While in the second system, the generation of H_2 occurs only from complex electron type centres. The simple electron type centres comprise E' centres (≡Si· or SiO_3^{3-}), F^+ and F° centres, while the complex electron type centres consist of the aggregates of simple electron type centres, small and large Li_n particles. The obtained results of the MCS as a function of the absorbed dose are shown in Fig. 3.40. Up to 95 % of the

accumulated electron type RD and RP in the irradiated small pebbles and large pebbles are complex electron type centres. The obtained results of the MCS indicate that the formation and accumulation of electron type RD and RP up to 5300 MGy absorbed dose is analogous for the small pebbles and the large pebbles. The slight differences in the total concentration of the accumulated electron type RD and RP in the small pebbles and in the large pebbles after irradiation up to 11000 MGy absorbed dose are attributed to the fluctuation of the irradiation conditions (absorbed dose or irradiation temperature), yet it cannot be ruled out that this effect may also be related to the slight microstructure changes, which occurs during irradiation at high temperature (Fig. 3.37, third row from the top).

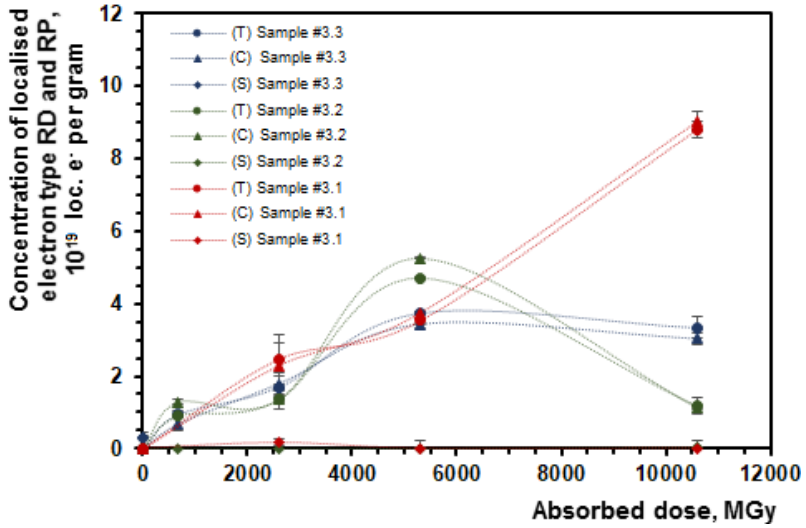

Fig. 3.40 Total (T), complex (C) and simple (S) electron type centre concentration in the irradiated small and large pebbles as a function of the absorbed dose. The pebbles were irradiated with 5 MeV accelerated electrons up to 11000 MGy absorbed dose at 550-590 K in a dry argon atmosphere.

The radiolysis degree (α) values for the small pebbles and the large pebbles, which were irradiated up to 11000 MGy absorbed dose at 550-590 K in a dry argon atmosphere, were calculated from the determined concentration of complex electron type centres (small and large Li_n particles). In this doctoral thesis, the radiolysis of the Li_4SiO_4 phase was described by the simplified summary reaction (Eq. 3.5). The calculated radiolysis degree values for the small pebbles and the large pebbles are between 0.1 mol% and 0.9 mol% (average value: 0.5 mol%) after irradiation up to 11000 MGy absorbed dose.

$$Li_4SiO_4 \rightsquigarrow 2\ Li + Li_2SiO_3 + ½\ O_2 \qquad (3.5)$$

The obtained values of the radiolysis degree for the small pebbles and the large pebbles after irradiation up to 11000 MGy absorbed dose at 550-590 K in a dry argon atmosphere are in a good agreement with the radiolysis degree ($\alpha_{11000\ MGy} \approx 0.5$ mol%), which was calculated on the basis of empiric equation (Eq. 3.6), which was proposed by J. Tiliks et al. [36].

$$\alpha\ (mol\%) = 5 \times 10^{-3} \times D^{0.5}, \text{ where D is absorbed dose, MGy.} \qquad (3.6)$$

The thermal stability of the accumulated electron type RD and RP in the small pebbles and large pebbles, which were irradiated up to 11000 MGy absorbed dose at 550-590 K in a dry argon atmosphere, were analysed by the MCS and ESR spectrometry (using stepwise isochronal annealing method). The obtained results indicate that simple electron type centres (F^+ and F° centres and E' centres) annihilates between 300 K and 520 K. While complex electron type centres (small and large Li_n particles) annihilates in two stages: at around 520-570 K and above 620 K.

By using the MCS, it was not possible to determine the concentration of complex electron type centres (small and large Li_n particles) in the small pebbles and in the large pebbles, which were irradiated up to 11000 MGy absorbed dose at 550-590 K in air atmosphere. Therefore, the radiolysis degree values for these irradiated pebbles were calculated from the obtained results of p-XRD and FTIR spectrometry and the content of the Li_2SiO_3 phase. The estimated radiolysis degree values for the small pebbles and the large pebbles, which were irradiated in air atmosphere, are higher than 2 mol% at 11000 MGy absorbed dose.

In addition, to supplement the obtained results of the MCS, the small pebbles and the large pebbles after irradiation were investigated both by ESR spectrometry and by TSL technique. The obtained ESR spectra of the large pebbles (Sample #3.3) before and after irradiation with 5 MeV accelerated electrons, up to 11000 MGy absorbed dose at 550-590 K in a dry argon and air atmosphere, are shown in Fig. 3.41.

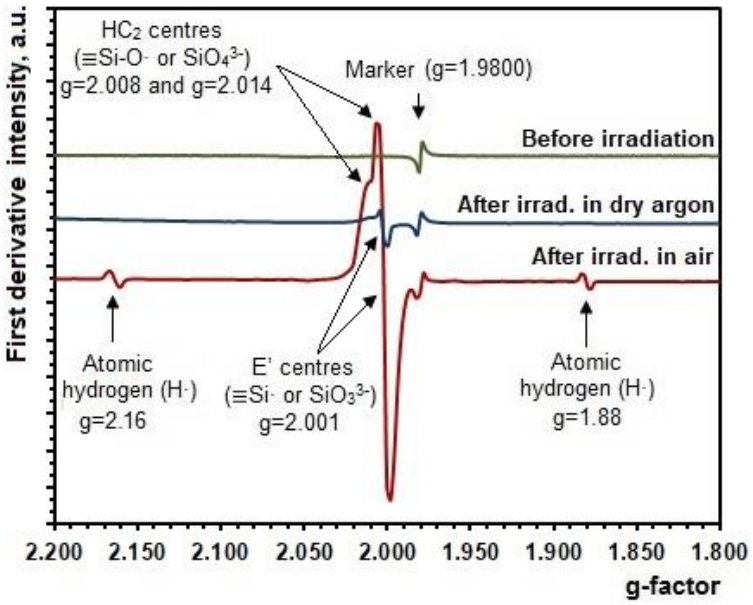

Fig. 3.41 ESR spectra of the large pebbles (Sample #3.3) before and after irradiation with 5 MeV accelerated electrons up to 11000 MGy absorbed dose at 550-590 K in a dry argon and air atmosphere.

After irradiation in a dry argon atmosphere, in the ESR spectra of the small pebbles and the large pebbles one main ESR signal with a g-factor 2.001±0.001 (singlet, $\Delta B_{pp} \approx 1$ mT) was detected and attributed to E' centres (≡Si· or SiO_3^{3-}). As expected from previous results, the ESR

signals of HC_2 centres (≡Si-O· or SiO_4^{3-}) and peroxide radicals (≡Si-O-O·) were not detected, due to the secondary and third stage reactions of the radiolysis or the thermally stimulated recombination processes. A very weak and board multiplex ESR signal with a g-factor approx. 2.0022 was detected in the small pebbles (Sample #3.1) after irradiation and can be attributed to F^+ centres. Presumably, the relatively narrow ESR signal of small Li_n particles was not observed, due to the particle aggregation.

Using air instead of a dry argon as the irradiation atmosphere of the small pebbles and the large pebbles, not only the ESR signal of E' centres was observed in the ESR spectra, but also two symmetric ESR signals (g-factors: 2.16 and 1.88) with splitting around 50 mT and two ESR signals with g-factors 2.008±0.001 and 2.014±0.001. The ESR signals with g-factors 2.008 and 2.014 were attributed to HC_2 centres, while the two ESR symmetric signals to atomic hydrogen (H·). Previously, the formation of atomic hydrogen was detected in the reference Li_4SiO_4 pebbles during irradiation in a dry argon atmosphere (Fig. 3.8) and was explained with the radiolysis of absorbed and chemisorbed H_2O on the pebble surface. However, in the same time, the increase of the paramagnetic RD concentration (from 10^{15}-10^{18} to 10^{17}-10^{20} defects per gram) and the formation of HC_2 centres during irradiation at elevated temperature in air atmosphere was not completely understood.

In the TSL glow curves of the irradiated small pebbles and large pebbles, the high-temperature peaks with maxima between 550 K and 700 K were mainly detected regardless of the irradiation atmosphere, due to the high irradiation temperature. The obtained TSL glow curves are shown in Fig. 3.42. In the same time, using air instead of a dry argon as the irradiation atmosphere, in the TSL glow curves of the irradiated small pebbles and large pebbles relatively high intensities of the low-temperature peaks were observed (with maxima below 550 K).

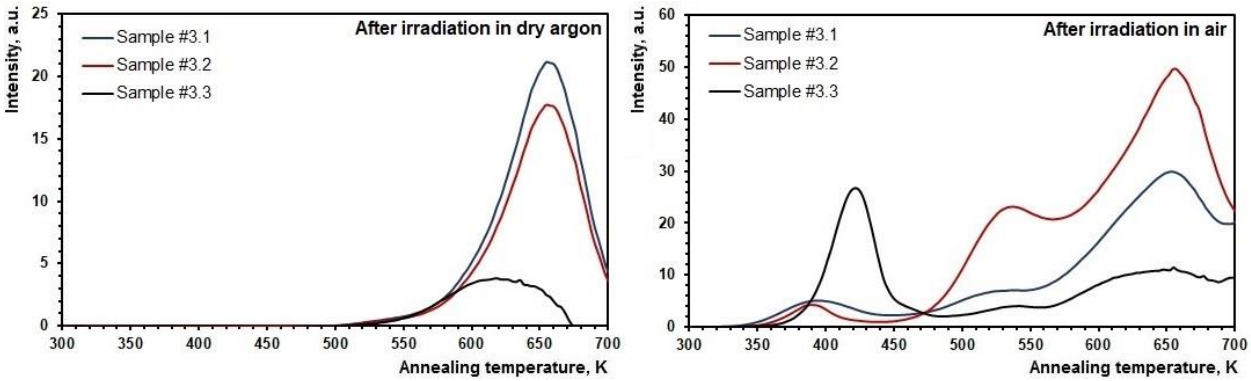

Fig. 3.42 TSL glow curves of the irradiated small pebbles and large pebbles. The heating rate is 2 K s^{-1}. The pebbles were irradiated with 5 MeV accelerated electrons up to 11000 MGy absorbed dose at 550-590 K in a dry argon and air atmosphere.

Previously, G. Kizane et al. [19] reported that up to 70 % of the accumulated RD and RP localize in a 50 μm subsurface layer of the reference Li_4SiO_4 pebbles (0 mol% Li_2TiO_3), due to

the surface defects (open pores, cracks, cavities etc.), which may form during the fabrication process. On the basis of these results, it is suggested that the radiolysis of the chemisorption products of H_2O vapour and CO_2 (LiOH and Li_2CO_3) on the surface of the small pebbles and the large pebbles could influence the formation of RD and RP, and so a rapid increase of the RD and RP concentration and the radiolysis degree can be detected after irradiation in air atmosphere. The radiolysis of the chemisorption products, which were detected in the irradiated small pebbles by p-XRD (Fig. 3.38, right) and FTIR spectrometry, in this doctoral thesis was described by simplified summary reactions (Eqs. 3.7 and 3.8).

$$2\ LiOH \rightsquigarrow 2\ Li + H_2O + ½\ O_2 \quad (3.7)$$

$$Li_2CO_3 \rightsquigarrow 2\ Li + CO_2 + ½\ O_2 \quad (3.8)$$

3.4.3 Summary of results

In this section, the influence of the pebble diameter and the grain size on the formation and accumulation of RD and RP in the reference Li_4SiO_4 pebbles (0 mol% Li_2TiO_3) was studied and evaluated under the simultaneous action of 5 MeV accelerated electrons (up to 11000 MGy absorbed dose) and high temperature (550-590 K) in a dry argon and air atmosphere. The fabricated Li_4SiO_4 pebbles with various contents of Li_2TiO_3 have a very broad size distribution (from 10 μm to 1500 μm), various microstructures (granular, dendritic and amorphous) and different grain sizes (from 1 μm to 10 μm).

Summarising all the above-mentioned results, it is concluded that the influence of the pebble diameter and the grain size on the high-temperature radiolysis of the reference Li_4SiO_4 pebbles (0 mol% Li_2TiO_3) is negligible. Due to the high absorbed dose and elevated irradiation temperature, the formation of thermally stable RP (small and large Li_n particles, molecular O_2, Li_2SiO_3 etc.) in the reference Li_4SiO_4 pebbles mainly occurs, and consequently the efficiency of the radiolysis is determined by the chemical and phase composition of the reference pebbles. The radiolysis degree (α) of the reference pebbles is between 0.1 mol% and 0.9 mol% (average value: 0.5 mol%) after irradiation up to 11000 MGy absorbed dose.

In the same time, it was confirmed that the irradiation atmosphere has a significant impact on the high-temperature radiolysis of the reference Li_4SiO_4 pebbles (0 mol% Li_2TiO_3). A major increase of the radiolysis degree (>2 mol%) for the reference Li_4SiO_4 pebbles was detected during irradiation in air in comparison to the reference pebbles, which were irradiated in a dry argon atmosphere. In additions, essential changes in the microstructure, chemical and phase composition of the reference pebbles were detected after irradiation up to 11000 MGy absorbed dose in air atmosphere, due to the formation and radiolysis of the chemisorption products of H_2O

vapour and CO_2 (LiOH and Li_2CO_3) on the pebble surface. Especially for the pebbles with small diameter and large surface area, the formation of LiOH and Li_2CO_3 may significantly be increased by the surface reactions.

The reference Li_4SiO_4 pebbles (0 mol% Li_2TiO_3) exhibit a broad diameter distribution, due to the spraying with dry air flow during the fabrication process. Only 50 wt% of the fabricated reference Li_4SiO_4 pebbles have the required diameter (between 250 μm and 630 μm), while up to 40 wt% of all produced pebbles have diameters <250 μm. Therefore, from an economical point of view, it would be reasonable to consider the possibility to use the small pebbles with diameters <250 μm as a filler material in order to reduce space between the pebbles with the required diameter and to increase the tritium production. However, the use of such pebbles could be difficult, due to the purge gas (helium with 0.1 vol% hydrogen) flow and the construction of the HCPB TBM concept.

3.5 Influence of chemisorption products on high-temperature radiolysis

The formation and radiolysis of the chemisorption products of H_2O vapour and CO_2 (LiOH and Li_2CO_3) on the surface of the reference Li_4SiO_4 pebbles (0 mol% Li_2TiO_3) during irradiation with 5 MeV accelerated electrons, up to 11000 MGy absorbed dose at 570-590 K, in air atmosphere can be influenced by several factors, for example irradiation temperature and time, absorbed dose and dose rate, chemical composition and surface area of the pebbles. Therefore, to understand the processes, which may occur during one of the irradiation cycles (up to 350 MGy absorbed dose at around 550-590 K) on the surface of the reference Li_4SiO_4 pebbles in air atmosphere, the influence of (1) the irradiation atmosphere, (2) the chemical composition, and (3) the irradiation temperature on the radiolysis was investigated separately. Li_2TiO_3 practically does not react with H_2O vapour and CO_2 [115], and therefore the influence of the additions of Li_2TiO_3 as a secondary phase on the formation and radiolysis of the chemisorption products on the surface of the advanced Li_4SiO_4 pebbles was not evaluated.

To increase the surface area and thus the amount of accumulated chemisorption products, the "pure" Li_4SiO_4 powder with high specific surface area (approx. 20 $m^2\ g^{-1}$) and small grain size (below 600 nm) was selected instead of the reference Li_4SiO_4 pebbles (0 mol% Li_2TiO_3). The powder before irradiation contains small amounts of Li_2CO_3 and LiOH, which may form on the grain surface during the fabrication, thermal treatment, handling or storage stage in contact with air atmosphere. In the p-XRD pattern, the traces of additional diffraction reflexes were observed and attributed to Li_2CO_3 and LiOH (Fig. 3.43, a). While in the FTIR spectrum, the bond additional vibrations of C-O (at around 1400-1500 cm^{-1}) and O-H (at around 2800-

3500 cm^{-1}) were detected (Fig. 3.43, b). By using TG-DTA, a mass loss up to 2 wt% was observed for the powder during heating up to 1070 K and was un-ambiguously assigned to the desorption of chemisorbed H_2O (at around 420-570 K) and CO_2 (at around 670-870 K).

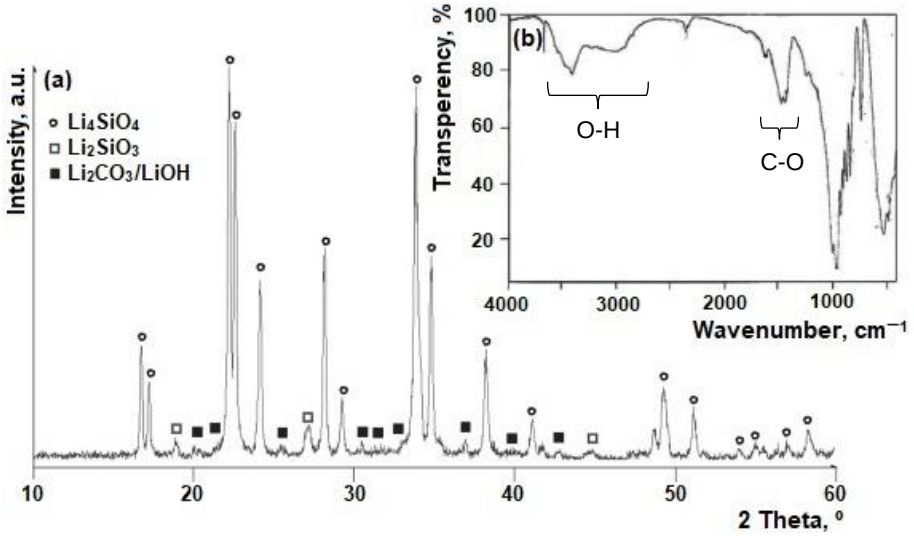

Fig. 3.43 (a) p-XRD pattern and (b) FTIR spectrum of the "pure" Li_4SiO_4 powder before irradiation.

3.5.1 Influence of air atmosphere on radiolysis

The irradiation type practically does not affect the qualitative composition of the accumulated RD and RP, and therefore X-rays instead of 5 MeV accelerated electrons were used, due to smaller dose rate and lower irradiation temperature. The absorbed dose was reduced (from 350 MGy to 56 kGy) to accumulate mainly primary and secondary RD, which have paramagnetic properties (contains un-paired electrons), and to avoid the formation of RP, for example small and large Li_n particles, molecular O_2, Li_2SiO_3 etc.

After irradiation with X-rays up to 56 kGy absorbed dose at around 300 K in air atmosphere, in the ESR spectrum of the "pure" Li_4SiO_4 powder, at least seven ESR signals with g-factors close to 2.000 were detected (Fig. 3.44). The detected ESR signals were related to atomic hydrogen (H·), HC_2 centres (≡Si-O· and SiO_4^{3-}), E' centres (≡Si· and SiO_3^{3-}) and peroxide radicals (≡Si-O-O·), respectively. Yet, in previous investigations in the ESR spectra of the irradiated LiOH and Li_2CO_3 powders signals with similar characteristics (g-factor, line-shape and line-width) were observed. This suggests that the origins of the ESR signals with g-factors at around 2.036 and 2.026 could not be only peroxide radicals, HC_2 centres or oxygen related defects, but also paramagnetic RD of the chemisorption products of H_2O vapour and CO_2 (LiOH and Li_2CO_3). Due to that, both of them were marked as un-identified. Other ESR signals, which could be related to the paramagnetic RD of Li_2CO_3, for example CO_2^- (g-factor: 2.0006), CO_3^- (g-factor: 2.0036) and CO_3^{3-} (g-factor: 2.00415) [143], in the ESR spectrum of the powder were not observed, probably due to overlapping with the ESR signals of E' centres and HC_2 centres.

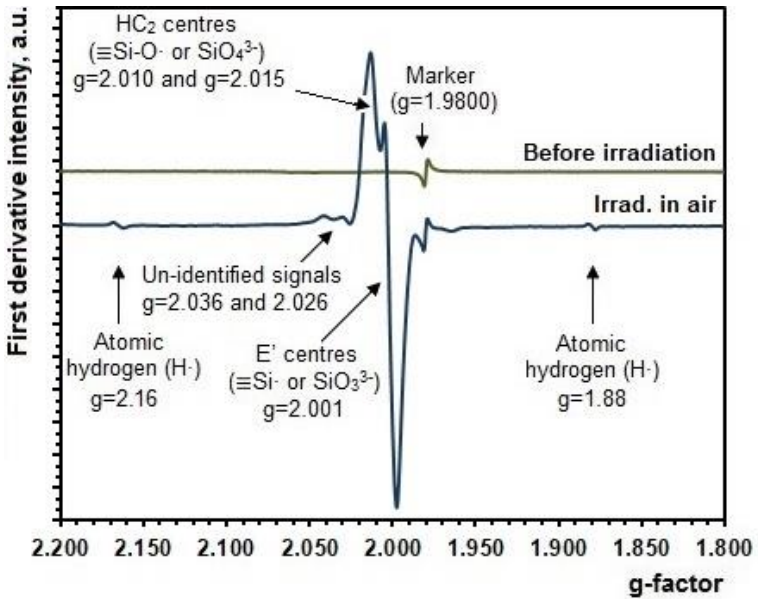

Fig. 3.44 ESR spectra of the "pure" Li_4SiO_4 powder before and after irradiation with X-rays up to 56 kGy absorbed dose at around 300 K in air atmosphere.

3.5.2 Influence of chemical composition on radiolysis in air

After adding 2 wt% (3 mol%) excess of SiO_2 and subsequent homogenization by milling, the resulting Li_4SiO_4 powder after irradiation with X-rays, up to 56 kGy absorbed dose at around 300 K, in air atmosphere shows a rapid decrease of the total concentration of the accumulated paramagnetic RD (up to 40 %). The obtained ESR spectra of the Li_4SiO_4 powders with three various chemical compositions after irradiation in air atmosphere are shown in Fig. 3.45, a. The additions of SiO_2 practically does not influence the surface area and the grain size (Table 2.4), and therefore the decrease the total concentration of the accumulated paramagnetic RD in the powder can be related to the chemical properties of SiO_2.

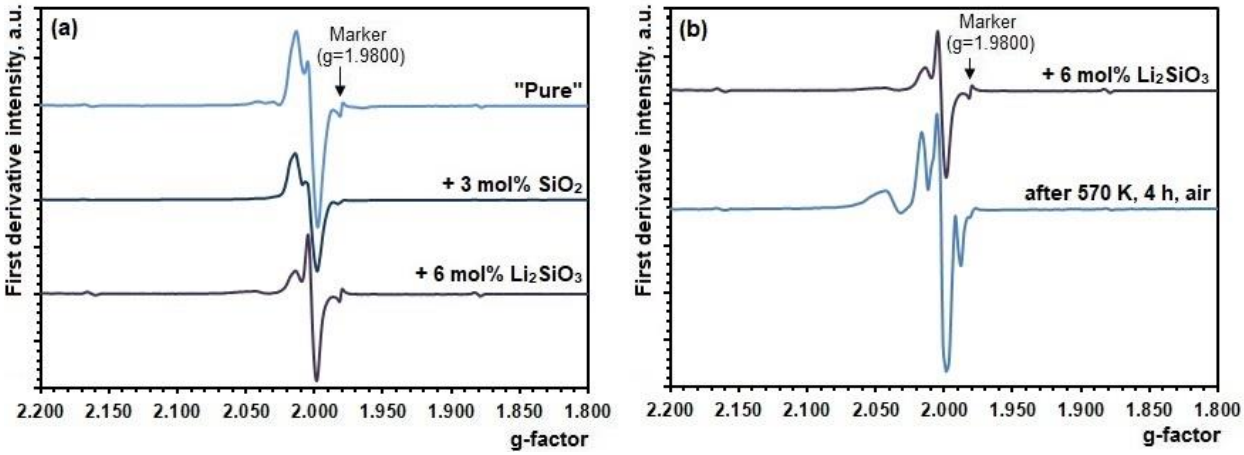

Fig. 3.45 (a) ESR spectra of the irradiated "pure" Li_4SiO_4 powder, with 3 mol% SiO_2 and with 6 mol% Li_2SiO_3. (b) ESR spectra of the irradiated Li_4SiO_4 powder with 6 mol% Li_2SiO_3 before and after isochronal thermal treatment at around 570 K for 4 h in air atmosphere. The powders were irradiated with X-rays up to 56 kGy absorbed dose at around 300 K in air atmosphere.

During thermal treatment, up to 920 K for 3.5 h in air atmosphere, SiO_2 reacts with the Li_4SiO_4 phase, and the surface area of the Li_4SiO_4 powder decreases from 22 $m^2\ g^{-1}$ to 17 $m^2\ g^{-1}$ (Table 2.4), due to the particle agglomeration. The formation of 6 mol% Li_2SiO_3 phase in the powder also decreases the total concentration of the accumulated paramagnetic RD (up to 25%). The decrease of the total concentration of the accumulated paramagnetic RD can be attributed both to a change of the contact surface area with air atmosphere and to the chemical properties of the Li_2SiO_3 phase.

3.5.3 Influence of irradiation temperature on radiolysis in air

To simulate the processes, which may occur on the surface of the reference Li_4SiO_4 pebbles (0 mol% Li_2TiO_3) during one of the irradiation cycles, up to 4 h per day, at high temperature in air atmosphere, the Li_4SiO_4 powder with additions of Li_2SiO_3 as a secondary phase was used. The obtained results of ESR spectrometry suggest that atomic hydrogen recombines at around 320 K, HC_2 centres at about 400-550 K, un-identified RD (probably peroxide radicals) at around 420-520 K and E' centres at about 450-550 K. Besides that, investigations by TG-DTA in air atmosphere, suggest that simultaneously with the thermally stimulated recombination reactions of the accumulated paramagnetic RD the formation of the chemisorption products of H_2O vapour and CO_2 (LiOH and Li_2CO_3) may occur at temperatures <420 K. At higher temperatures both gases are released in two steps: first occurs the desorption of chemisorbed H_2O (at around 420-570 K) and then of CO_2 (at around 670-920 K). On the basis of these results it is supposed that during irradiation at 550-590 K in air atmosphere, besides the thermally stimulated recombination processes of primary and secondary RD, on the surface of the reference Li_4SiO_4 pebbles mainly the formation and radiolysis of the chemisorption products of CO_2 (Li_2CO_3) occur.

After thermal treatment, up to 570 K for 4 h in air atmosphere, using TG-DTA, it was determined that the Li_4SiO_4 powder with Li_2SiO_3 as a secondary phase contained up to 12 wt% of H_2O vapour and CO_2. Due to the radiolysis of the chemisorption products of H_2O vapour and CO_2, an increase of the total concentration of the accumulated paramagnetic RD (up to 50 %) was detected after irradiation. The obtained ESR spectra of the un-treated and isochronally thermally treated powder after irradiation with X-rays up to 56 kGy absorbed dose at 300 K in air atmosphere are shown in Fig. 3.45, b. The results of ESR spectrometry confirm that the chemisorption products increase not only the concentration of E' centres, but also the amount of HC_2 centres and un-identified RD. The obtained results clearly correlate with the data of the small pebbles and the large pebbles, which were irradiated up to 11000 MGy at 550-590 K in air

atmosphere (Fig. 3.41). These results also confirm the suggestion that the chemisorption products, due to the formation at temperatures <420 K and radiolysis, can increase the total concentration of hole and electron type RD and RP in the ceramic breeder pebbles.

3.5.4 Summary of results

In this section, the influence of the chemisorption products of H_2O vapour and CO_2 (LiOH and Li_2CO_3) on the formation and accumulation of RD and RP in the reference Li_4SiO_4 pebbles (0 mol% Li_2TiO_3) was analysed and evaluated. The ceramic breeder pebbles under exploitation conditions of the HCPB TBM will be exposed to purge gas (helium with 0.1 vol% hydrogen), and thereby the detected chemical reactions with H_2O vapour and CO_2 on the surface of the reference Li_4SiO_4 pebbles can only occur during the fabrication process, thermal treatment, handling or storage stage in contact with air atmosphere. Li_2TiO_3 practically does not react with H_2O vapour and CO_2 [115], and therefore the influence of the additions of Li_2TiO_3 as a secondary phase on the formation and radiolysis of the chemisorption products on the surface of the advanced Li_4SiO_4 pebbles was not evaluated.

Summarising all the above-mentioned results, it is concluded that the chemisorption products of H_2O vapour and CO_2 can increase the total concentration of RD and RP (up to 50%) in the reference Li_4SiO_4 pebbles (0 mol% Li_2TiO_3) and may hereby affect the tritium diffusion, retention and the released species. It was determined that the formation and radiolysis of the chemisorption products on the surface of the reference Li_4SiO_4 pebbles depend on the chemical composition and the irradiation temperature. Because of the different chemical properties, the additions of secondary phases, such as SiO_2 and Li_2SiO_3, can disturb the formation of the chemisorption products on the surface of the reference pebbles and thereby decrease the total concentration of the accumulated RD and RP (up to 40%). While at high irradiation temperatures, the total concentration of the accumulated RD and RP in the reference pebbles significantly increases (up to 50%), due to the formation and radiolysis of the chemisorption products from air atmosphere.

RECOMMENDATIONS

On the basis of the scientific findings of this doctoral thesis, the recommendations for the producers of the ceramic tritium breeder pebbles and the manufactures of the solid breeder test blanket concepts are developed in order to improve the fabrication process and properties of the ceramic breeder pebbles.

1. The combination of Li_4SiO_4 and Li_2TiO_3 does not significantly deteriorate the radiation stability of the ceramic breeder pebbles and, because of the improved mechanical properties, the advanced Li_4SiO_4 pebbles with additions of Li_2TiO_3 as a secondary phase should be used as an alternative candidate for the tritium breeding in the solid breeder test blanket modules.
2. The noble metals (Pt, Au and Rh) with a sum content of up to 300 ppm do not have a negative effect on the functional properties of the advanced Li_4SiO_4 pebbles with additions of Li_2TiO_3 as a secondary phase.
3. From an economical point of view, it would be reasonable to consider the possibility to use the small Li_4SiO_4 pebbles with diameters <250 μm as a filler material in order to reduce space between the reference pebbles with diameters between 250 μm and 630 μm and to increase the tritium production. However, the use of such pebbles could be difficult, due to the purge gas flow and the construction of the solid breeder test blanket module.
4. The formation of the chemisorption products of CO_2 and H_2O vapour (Li_2CO_3 and LiOH) on the surface of the Li_4SiO_4 pebbles in contact with air atmosphere need to be avoided, because they can significantly affect the radiolysis and can increase the concentration of the accumulated radiation-induced defects and radiolysis products and hereby reduce the tritium release and affect the released species.

CONCLUSIONS

In this doctoral thesis, for the first time the formation, accumulation and annihilation of radiation-induced defects and radiolysis products in the advanced Li_4SiO_4 pebbles with additions of Li_2TiO_3 as a secondary phase are analysed and described under the simultaneous action of radiation and high temperature in order to evaluate a new two-phase chemical composition for the advanced ceramic breeder pebbles, which could be used an alternative candidate for the tritium breeding in future nuclear fusion reactors.

1. The advanced Li_4SiO_4 pebbles with additions of Li_2TiO_3 are biphasic without solid solutions, and the formation mechanism and the structure of the formed radiation-induced defects and radiolysis products (except Ti^{3+} centres) during irradiation is similar to the single-phase ceramics.
2. The advanced Li_4SiO_4 pebbles with additions of Li_2TiO_3 as a secondary phase have a good radiation stability in comparison to the reference Li_4SiO_4 pebbles (without additions of Li_2TiO_3), the radiation chemical yield (G) of paramagnetic radiation-induced defects and radiolysis products is below 0.8 defects/products per 100 eV and the radiolysis degree (α) is under 1 mol% after irradiation up to 5000 MGy absorbed dose.
3. The accumulated radiation-induced defects and radiolysis products in the advanced Li_4SiO_4 pebbles with additions of Li_2TiO_3 as a secondary phase annihilate between 300 K and 650 K (except large colloidal lithium particles), and it is suggested that the tritium release can be expected to start in this temperature range.
4. The irradiation temperature has a significant impact on the formation and accumulation of radiation-induced defects and radiolysis products in the advanced Li_4SiO_4 pebbles with additions of Li_2TiO_3 as a secondary phase, and the concentration of the accumulated radiation-induced defects and radiolysis products decreases with increasing the irradiation temperature.
5. The influence of the noble metals (Pt, Au and Rh) with a sum content of up to 300 ppm is insignificant for the radiolysis of the advanced Li_4SiO_4 pebbles with additions of Li_2TiO_3 as a secondary phase.
6. The formation and accumulation of radiation-induced defects and radiolysis products in the reference Li_4SiO_4 pebbles (without additions of Li_2TiO_3) during irradiation at high temperature does practically not depend on the pebble diameter (from 10 μm to 1500 μm) and on the grain size (from 1 μm to 10 μm).

7. The chemisorption products of CO_2 and H_2O vapour (Li_2CO_3 and LiOH) can significantly affect the formation and accumulation of radiation-induced defects and radiolysis products on the surface of the reference Li_4SiO_4 pebbles (without additions of Li_2TiO_3) and can increase the total concentration of the accumulated radiation-induced defects and radiolysis products up to 50%.

REFERENCES

1. R. Knitter, P. Chaudhuri, Y.J. Feng, T. Hoshino and I.-K. Yu. Recent developments of solid breeder fabrication. Journal of Nuclear Materials, 442 (2013) s420-s424.
2. Y. Poitevin et al. Tritium breeder blankets design and technologies in Europe: Development status of ITER Test Blanket Modules, test & qualification strategy and roadmap towards DEMO. Fusion Engineering and Design, 85 (2010) 2340-2347.
3. L.M. Giancarli et al. Overview of the ITER TBM Program. Fusion Engineering and Design, 87 (2012) 395-402.
4. A. Vītiņš, G. Ķizāne, J. Tīliks, J. Tīliks and E. Kolodinska. Tritium release from breeding blanket materials in high magnetic field. Fusion Engineering and Design, 82 (2007) 2341-2346.
5. S. Yamamoto et al. Impact of irradiation effects on design solutions for ITER diagnostics. Journal of Nuclear Materials, 283-287 (2000) 60-69.
6. S. van Til, A.V. Fedorov and A.J. Magielsen. Study of ceramic pebble beds in Post Irradiation Examination of the Pebble Bed Assemblies irradiation experiment. Fusion Engineering and Design, 87 (2012) 885-889.
7. G. Piazza, F. Scaffidi-Argentina and H. Werle. Post-irradiation examinations of Li_4SiO_4 pebbles irradiated in the EXOTIC-7 experiment. Journal of Nuclear Materials, 283-287 (2000) 1396-1400.
8. G. Piazza, A. Erbe, R. Rolli and O. Romer. Post-irradiation examinations of Li_4SiO_4 pebbles irradiated in the EXOTIC-8 experiment. Journal of Nuclear Materials, 329-333 (2004) 1260-1265.
9. M.M.W. Peeters, A.J. Magielsen, M.P. Stijkel and J.G. van der Laan. In-pile tritium release behaviour of lithium metatitanate produced by extrusion–spheroidisation–sintering process in EXOTIC-9/1 in the high flux reactor, Petten. Fusion Engineering and Design, 82 (2007) 2318-2325.
10. M.E. Sawan and M.A. Abdou. Physics and technology conditions for attaining tritium self-sufficiency for the DT fuel cycle. Fusion Engineering and Design, 81 (2006) 1131-1144.
11. R. Knitter, M.H.H. Kolb, U. Kaufmann and A.A. Goraieb. Fabrication of modified lithium orthosilicate pebbles by addition of titania. Journal of Nuclear Materials, 442 (2013) s433-s436.

12. D. A.H. Hanaor, M. H.H. Kolb, Y. Gan, M. Kamlah and R. Knitter. Solution based synthesis of mixed-phase materials in the Li_2TiO_3-Li_4SiO_4 system. Journal of Nuclear Materials, 456 (2015) 151-161.

13. M. Yang, G. Ran, H. Wang, C. Dang, Z. Huang, X. Chen, T. Lu and C. Xiao. Fabrication and tritium release property of Li_2TiO_3-Li_4SiO_4 biphasic ceramics. Journal of Nuclear Materials, 503 (2018) 151-156.

14. M. González, E. Carella, A. Moroño, M. H.H. Kolb and R. Knitter. Thermally induced outdiffusion studies of deuterium in ceramic breeder blanket materials after irradiation. Fusion Engineering and Design, 98-99 (2015) 1771-1774.

15. M. H.H. Kolb, R. Rolli and R. Knitter. Tritium adsorption/release behaviour of advanced EU breeder pebbles. Journal of Nuclear Materials, 489 (2017) 229-235.

16. K. Mukai, P. Pereslavtsev, U. Fischer and R. Knitter. Activation calculations for multiple recycling of breeder ceramics by melt processing. Fusion Engineering and Design, 100 (2015) 565-570.

17. K. Mukai, F. Sanchez and R. Knitter. Chemical compatibility study between ceramic breeder and EUROFER97 steel for HCPB-DEMO blanket. Journal of Nuclear Materials, 488 (2017) 196-203.

18. O. Leys, T. Bergfeldt, M. H.H. Kolb, R. Knitter and A. A. Goraieb. The reprocessing of advanced mixed lithium orthosilicate/metatitanate tritium breeder pebbles. Fusion Engineering and Design, 107 (2016) 70-74.

19. G. Kizane, J. Tiliks, A. Vitins and J. Rudzitis. Tritium localisation and release from the ceramic pebbles of breeder. Journal of Nuclear Materials, 329-333 (2004) 1287-1290.

20. Y. Nishikawa, M. Oyaidzu, A. Yoshikawa, K. Munakata, M. Okada, M. Nishikawa and K. Okuno. Correlation between tritium release and thermal annealing of irradiation damage in neutron-irradiated Li_2SiO_3. Journal of Nuclear Materials, 367-370 (2007) 1371-1376.

21. M. Oyaidzu, Y. Morimoto, H. Kodama, M. Sasaki, H. Kimura, K. Munakata, M. Okada, K. Kawamoto, H. Moriyama and M. Nishikawa. Correlation between annihilation of radiation defects and tritium release in Li_2TiO_3. Journal of Nuclear Materials, 329-333 (2004) 1313-1317.

22. S. Akahori, E. Tega, Y. Morimoto, K. Okuno, M. Nishikawa, K. Munkata, H. Moriyama, K. Kawamoto and M. Okada. Hot atom chemical behavior of tritium produced by $^6Li(n,a)^3H$ in Li_4SiO_4. Journal of Radioanalytical and Nuclear Chemistry, 255 (2003) 257-260.

23. A. Abramenkovs, J. Tiliks, G. Kizane, V. Grishmanovs and A. Supe. Basic study of influence of radiation defects on tritium release processes from lithium silicates. Journal of Nuclear Materials, 248 (1997) 116-120

24. M. Oyaidzu, Y. Nishikawa, T. Suda, T. Shinozaki, A. Yoshikawa, Y. Oya, K. Munakata and K. Okuno. Detrapping behavior of tritium trapped via hot atom chemical process in neutron-irradiated ternary lithium oxides. Journal of Nuclear Materials, 375 (2008) 1-7.

25. T. Tanifuji, D. Yamaki and S. Jitsukawa. Tritium release from neutron-irradiated Li_2O sintered pellets: isothermal annealing of tritium traps. Journal of Nuclear Materials, 329-333 (2004) 1266-1269.

26. M. Oyaidzu, H. Kimura, A. Yoshikawa, Y. Nishikawa K. Munakata. M. Okada, M. Nishikawa and K. Okuno. Correlation between annihilation of irradiation defects and tritium release in neutron-irradiated lithium zirconate. Fusion Engineering and Design, 81 (2006) 583-588.

27. J. Tiliks, S. Tanaka, G. Kizane, A. Supe, A. Abramenkovs and V. Grischmanovs. The influence of magnetic field on the radiolysis of the lithium orthosilicate ceramics. Fusion Technology, 1 (1996) 1507-1510.

28. T. Hoshino, K. Tsuchiya, K. Hayashi, M. Nakamura, H. Terunuma and K. Tatenuma. Preliminary test for reprocessing technology development of tritium breeders. Journal of Nuclear Materials, 386-388 (2009) 1107-1110.

29. F. Dobran. Fusion energy conversion in magnetically confined plasma reactors. Progress in Nuclear Energy, 60 (2012) 89-116.

30. Y. Poitevin, L.V. Boccaccini, G. Dell'Orco, E. Diegele, R. Lasser, J.-F. Salavy, J. Sundstrom and M. Zmitko. The test blanket modules project in Europe: From the strategy to the technical plan over next 10 years. Fusion Engineering and Design, 82 (2007) 2164-2170.

31. M. Zmitko, Y. Poitevin, L.V. Boccaccini, J.-F. Salavy, R. Knitter, A. Moslang, A.J. Magielsen, J.B.J. Hegeman and R. Lasser. Development and qualification of functional materials for the EU Test Blanket Modules: Strategy and R&D activities Journal of Nuclear Materials, 417 (2011) 678-683.

32. L.V. Boccaccini et al. Objectives and status of EUROfusion DEMO blanket studies. Fusion Engineering and Design, 109-111 (2016) 1199-1206.

33. R. Knitter and B. Lobbecke. Reprocessing of lithium orthosilicate breeder material by remelting. Journal of Nuclear Materials, 361 (2007) 104-111.

34. J.D. Lulewicz and N. Roux. Fabrication of Li_2TiO_3 pebbles by the extrusion-spheronisation-sintering process. Journal of Nuclear Materials, 307-311 (2002) 803-806.

35. J.B.J. Hegeman, E.D.L. van Essen, M. Jong, J.G. van der Laan and J. Reimann. Thermomechanical behaviour of ceramic breeder pebble stacks for HICU. Fusion Engineering and Design, 69 (2003) 425-429.

36. J.E. Tiliks, G.K. Kizane, A.A. Supe, A.A. Abramenkovs, J.J. Tiliks and V.G. Vasiljev. Formation and properties of radiation-induced defects and radiolysis products in lithium orthosilicate. Fusion Engineering and Design, 17 (1991) 17-20.

37. J. Tiliks, G. Kizane, A. Vitins, G. Vitins and J. Meisters. Physicochemical processes in blanket ceramic materials. Fusion Engineering and Design, 69 (2003) 519-522.

38. E. Carella and T. Hernández. Ceramics for fusion reactors: The role of the lithium orthosilicate as breeder. Physica B: Condensed Matter, 407 (2012) 4431-4435.

39. K. Moritani, S. Tanaka and H. Moriyama. Production behaviour of irradiation defects in lithium silicates and silica under ion beam irradiation. Journal of Nuclear Materials, 281 (2000) 106-111.

40. J. Tiliks, G. Kizane, A. Abramenkovs, A. Supe, J. Tiliks Jr., V. Vasiljev and H. Werle. Radiolysis of solid blanket materials. Fusion technology, 1992 (1993) 1523-1527.

41. V. Grismanovs, T. Kumada, T. Tanifuji and T. Nakazawa. ESR spectroscopy of γ-irradiated Li_2TiO_3 ceramics. Radiation Physics and Chemistry, 58 (2000) 113-117.

42. M. González and V. Correcher. On the cathodoluminescence and thermoluminescence emission of lithium titanate ceramics. Journal of Nuclear Materials, 445 (2014) 149-153.

43. V. Correcher and M. Gonzalez. Preliminary results on the relationship between luminescence and crystalline structure of lithium metatitanate. Nuclear Instruments and Methods in Physics Research B, 326 (2014) 86-89

44. E. Carella, M. Leon, T. Sauvage and M. Gonzalez. On ion implantation and damage effect in Li_2TiO_3 as a fusion breeder blanket: A technological approach for degradation testing. Fusion Engineering and Design, 89 (2014) 1529-1533.

45. K. Moritani and H. Moriyama. In situ luminescence measurement of irradiation defects in ternary lithium ceramics under ion beam irradiation. Journal of Nuclear Materials, 248 (1997) 132-139.

46. J. Pejchal, V. Babin, A. Beitlerova, S. Kurosawa, Y. Yokota, A. Yoshikawa and M. Nikl. Improvement of the growth of Li_4SiO_4 single crystals for neutron detection and their scintillation and luminescence properties. Journal of Crystal Growth, 457 (2017) 143-150.

47. O. Motojima. The ITER project construction status. Nuclear Fusion, 55 (2015) 104023.

48. G. Federici et al. Overview of the design approach and prioritization of R&D activities towards an EU DEMO. Fusion Engineering and Design, 109-111 (2016) 1464-1474.

49. O.C. Onar and A. Khaligh. Energy Sources. Alternative Energy in Power Electronics (2015) 81-154.

50. J. Ongena and Y. Ogawa. Nuclear fusion: Status report and future prospects. Energy Policy, 96 (2016) 770-778.

51. J. Ongena, R. Koch, R. Wolf and H. Zohm. Magnetic-confinement fusion. Nature Physics, 12 (2016) 398-410.

52. E. I. Moses and W. R. Meier. Preparing for ignition experiments on the National Ignition Facility. Fusion Engineering and Design, 83 (2008) 997-1000.

53. M.S. Hutton, S. Azevedo, R. Beeler, R. Bettenhausen, E. Bond. A. Casey, J. Liebman, A. Marsh, T. Pannell and A. Warrick. Experiment archive, analysis, and visualization at the National Ignition Facility. Fusion Engineering and Design, 87 (2012) 2087-2091.

54. Y. Xu. A general comparison between tokamak and stellarator plasmas. Matter and Radiation at Extremes. 1 (2016) 192-200.

55. A.E. Costley. On the fusion triple product and fusion power gain of tokamak pilot plants and reactors. Nuclear Fusion, 56 (2016) 066003.

56. M. Gasparotto, C. Baylard, H.S. Bosch, D. Hartmann, T. Klinger, R. Vilbrandt, L. Wegener and W7-X Team. Wendelstein 7-X – Status of the project and commissioning planning. Fusion Engineering and Design, 89 (2014) 2121-2127.

57. C. Wndell Horton Jr. and S. Benkadda. ITER Physics, 2015, pp. 233.

58. ITER Organization home page. https://www.iter.org.

59. E. Pajuste, G. Kizane, A. Vitins, I. Igaune, L. Avotina, R. Zarins and JET contributors. Structure, tritium depth profile and desorption from ‘plasma-facing’ beryllium materials of ITER-Like-Wall at JET. Nuclear Materials and Energy, 12 (2017) 642-647.

60. E. Pajuste, G. Kizane, J.P. Coad, A. Vitins, A. Kirillova, M. Halitovs and JET-EFDA Contributors. Structural changes and distribution of accumulated tritium in the carbon based JET tiles. Journal of Nuclear Materials, 415 (2011) S765-S768.

61. B. G. Hong. Overview of ITER TBM program objectives and management. International Journal of Energy Research. (2017) Published online in Wiley Online Library (wileyonlinelibrary.com). DOI: 10.1002/er.3759

62. L. Giancarli, V. Chuyanov, M. Abdou, M. Akiba, B.G. Hong, R. Lässer, C. Pan, Y. Strebkov and TBWG Team. Test blanket modules in ITER: An overview on proposed designs and required DEMO-relevant materials. Journal of Nuclear Materials, 367-370 (2007) 1271-1280.

63. L.M. Giancarli et al. Overview of the ITER TBM Program. Fusion Engineering and Design, 87 (2012) 395-402.

64. L.M. Giancarli et al. Progress and challenges of the ITER TBM Program from the IO perspective. Fusion Engineering and Design, 109-111 (2016) 1491-1497.

65. B. Bornschein, C. Day, D. Demange and T. Pinna. Tritium management and safety issues in ITER and DEMO breeding blankets. Fusion Engineering and Design, 88 (2013) 466-471.

66. M. Glugla, D.K. Murdoch, A. Antipenkov, S. Beloglazov, I. Cristescu, I.-R. Cristescu, C. Day, R. Laesser and A. Mack. ITER fuel cycle R&D: Consequences for the design. Fusion Engineering and Design, 81 (2006) 733-744.

67. K.C. Jordan, W.A. Dudley. Half-life of tritium. Journal of Inorganic and Nuclear Chemistry, 29 (1967) 2129-2131.

68. T. Tanabe. Tritium fuel cycle in ITER and DEMO: Issues in handling large amount of fuel. Journal of Nuclear Materials, 438 (2013) S19-S26.

69. L. Morgan and J. Pasley. Tritium breeding control within liquid metal blankets. Fusion Engineering and Design, 88 (2013) 107-112.

70. T. B. Coplen et al. Isotope-abundance variations of selected elements. Pure Appl. Chem., 74 (2002), 1987-2017.

71. M. Zmitko, Y. Poitevin, L. Boccaccini, J.-F. Salavy, R. Knitter, A. Möslang, A.J. Magielsen, J.B.J. Hegeman and R. Lässer. Development and qualification of functional materials for the EU Test Blanket Modules: Strategy and R&D activities Journal of Nuclear Materials, 417 (2011) 678-683.

72. M. Zmitko et al. The European ITER Test Blanket Modules: EUROFER97 material and TBM's fabrication technologies development and qualification. Fusion Engineering and Design (2017) in press. DOI: 10.1016/j.fusengdes.2017.04.051.

73. H. Neuberger, A. von der Weth and J. Rey. KIT induced activities to support fabrication, assembly and qualification of technology for the HCPB-TBM. Fusion Engineering and Design, 86 (2011) 2039-2042.

74. J.-F. Salavy et al. Overview of the last progresses for the European Test Blanket Modules projects. Fusion Engineering and Design, 82 (2007) 2105-2112.

75. E. Alves, L.C. Alves, N. Franco, M.R. da Silva, A. Paúl, J.B. Hegeman and F. Druyts. Characterization and stability studies of titanium beryllides. Fusion Engineering and Design, 75-79 (2005) 759-763.

76. M. Nakamichi and J.-H. Kim. Development of beryllide pebbles with low-hydrogen generation as advanced neutron multipliers. Fusion Engineering and Design (2017) In Press. DOI: 10.1016/j.fusengdes.2017.04.039

77. M. Nakamichi, J.-H. Kim and K. Ochiai. Beryllide pebble fabrication of Be-Zr compositions as advanced neutron multipliers. Fusion Engineering and Design, 109-111 (2016) 1719-1723.

78. C.E. Johnson, K. Noda and N. Roux. Ceramic breeder materials: Status and needs. Journal of Nuclear Materials, 258-263 (1998) 140-148.

79. J.G. van der Laan, H. Kawamura, N. Roux and D. Yamaki. Ceramic breeder research and development: progress and focus. Journal of Nuclear Materials, 283-287 (2000) 99-109.

80. S. Claus, H. Kleykamp and W. Smykatz-Kloss. Phase equilibria in the Li_4SiO_4-Li_2SiO_3 region of the pseudobinary Li_2O-SiO_2 system. Journal of Nuclear Materials, 230 (1996) 8-11.

81. K. Munakata, T. Shinozaki, K. Inoue, S. Kajii, Y. Shinozaki, R. Knitter, N. Bekris, T. Fujii, H. Yamana and K. Okuno. Tritium release from lithium silicate pebbles produced from lithium hydroxide. Fusion Engineering and Design, 83 (2008) 1317-1320.

82. A. Abou-Sena, B. Löbbecke, A. von der Weth and R. Knitter. Effect of post welding heat treatment of the HCPB TBM on Eurofer and lithium orthosilicate pebbles. Fusion Engineering and Design, 86 (2011) 2254-2257.

83. R. Knitter, U. Fischer, S. Herber and C. Adelhelm. Reduction of impurities and activation of lithium orthosilicate breeder materials. Journal of Nuclear Materials, 386-388 (2009) 1071-1073.

84. R. Knitter, B. Alm and G. Roth. Crystallisation and microstructure of lithium orthosilicate pebbles. Journal of Nuclear Materials, 367-370 (2007) 1387-1392.

85. G. Schumacher, M. Dalle-Donne, V. Geiler, R. Huber and I. Schub. Improvement of the mechanical stability of lithium-orthosilicate pebbles. Fusion Engineering and Design, 17 (1991) 31-36.

86. M. Xiang, Y. Zhang, C. Wang, Y. Zhang, W. Liu and G. Li. Preparation of Li_4SiO_4-xLi_2O powders and pebbles for advanced tritium breeders. Ceramics International, 43 (2017) 2314-2319.

87. X.W. Wu, Z.Y. Wen, X.G. Xu and Y. Liu. Fabrication of Li_4SiO_4 pebbles by a sol-gel technique. Fusion Engineering and Design, 85 (2010) 222-226.

88. X.L. Gao, X.J. Chen and M. Gu. Fabrication and characterization of Li_4SiO_4 ceramic pebbles by wet method. Journal of Nuclear Materials, 424 (2012) 210-215.

89. E. Carella and M.T. Hernandez. High lithium content silicates: A comparative study between four routes of synthesis. Ceramics International, 40 (2014) 9499-9508.

90. J. Tīliks, G. Ķizāne, A. Vītiņš and B. Leščinskis. Nanostructured ceramic blanket materials. In the book: CBBI-13. Proceedings of the 13th International Workshop on Ceramic Breeder Blanket Interactions. Santa Barbara, CA, USA. November 30 - December 2, 2005.

91. R. Knitter, G. Piazza, J. Reimann, P. Risthaus and L.V. Boccaccini. Fabrication and characterization of lithium orthosilicate pebbles using LiOH as a new raw material. CBBI-11, Kyoto, Japan, December (2003)

92. Y.J. Feng, K.M. Feng, Q.X. Cao, J. Hu and H. Tang. Fabrication and characterization of Li_4SiO_4 pebbles by melt spraying method. Fusion Engineering and Design, 87 (2012) 753-756.

93. M.H.H. Kolb, R. Knitter, U. Kaufmann and D. Mundt. Enhanced fabrication process for lithium orthosilicate pebbles as breeding material. Fusion Engineering and Design, 86 (2011) 2148-2151.

94. M.H.H. Kolb, M. Bruns, R. Knitter and S. van Til. Lithium orthosilicate surfaces: Characterization and effect on tritium release. Journal of Nuclear Materials, 427 (2012) 126-132.

95. A. López Ortiz, M.A. Escobedo Bretado, V. Guzmán Velderrain, M. Meléndez Zaragoza, J. Salinas Gutiérrez, D. Lardizábal Gutiérrez and V. Collins-Martínez. Experimental and modeling kinetic study of the CO_2 absorption by Li_4SiO_4. International Journal of Hydrogen Energy, 39 (2014) 16656-16666.

96. J. Ortiz-Landeros, L. Martinez-dlCruz, C. Gomez-Yanez and H. Pfeiffer. Towards understanding the thermoanalysis of water sorption on lithium orthosilicate (Li_4SiO_4). Thermochimica Acta, 515 (2011) 73-78.

97. G.M. Ran, C.J. Xiao, X.J. Chen, Y. Gong, C.M. Kang and X.L. Wang. Correlation between the processes of water desorption and tritium release from Li_4SiO_4 ceramic pebbles. Journal of Nuclear Materials, 466 (2015) 316-321.

98. Q. Zhou, Y. Mou, X. Ma, L. Xue and Y. Yan. Effect of fuel-to-oxidizer ratios on combustion mode and microstructure of Li_2TiO_3 nanoscale powders. Journal of the European Ceramic Society, 34 (2014) 801-807.

99. H. Kleykamp. Enthalpy, heat capacity and enthalpy of transformation of Li_2TiO_3. Journal of Nuclear Materials, 295 (2001) 244-248.

100. T. Hoshino, M. Dokiya, T. Terai, Y. Takahashi and M. Yamawaki. Non-stoichiometry and its effect on thermal properties of Li_2TiO_3. Fusion Engineering and Design, 61–62 (2002) 353-360.

101. T. Hoshino. Pebble fabrication of super advanced tritium breeders using a solid solution of $Li_{2+x}TiO_{3+y}$ with Li_2ZrO_3. Nuclear Materials and Energy, 9 (2016) 221-226.

102. A. Ying, M. Akiba, L.V. Boccaccini, S. Casadio, G. Dell'Orco, M. Enoeda, K. Hayashi, J.B. Hegeman, R. Knitter, J. van der Laan, J.D. Lulewicz and Z.Y. Wen. Status and perspective of the R&D on ceramic breeder materials for testing in ITER. Journal of Nuclear Materials, 367-370 (2007) 1281-1286.

103. K. Tsuchiya, H. Kawamura, M. Uchida, S. Casadio, C. Alvani and Y. Ito. Improvement of sintered density of Li_2TiO_3 pebbles fabricated by direct-wet process. Fusion Engineering and Design, 69 (2003) 449-453.

104. K. Tsuchiya, H. Kawamura, K. Fuchinoue, H. Sawada and K. Watarumi. Fabrication development and preliminary characterization of Li_2TiO_3 pebbles by wet process. Journal of Nuclear Materials, 258-263 (1998) 1985-1990.

105. K. Tsuchiya, H. Kawamura, S. Casadio and C. Alvani. Effects of gelation and sintering conditions on granulation of Li_2TiO_3 pebbles from Li–Ti complex solution. Fusion Engineering and Design, 75-79 (2005) 877-880.

106. O. Leys, C. Odemer, U. Maciejewski, M.H.H. Kolb and R. Knitter. Microstructural analysis of melt-based lithium orthosilicate/metatitanate pebbles. Practical Metallography, 50 (2013) 196-204.

107. M. H.H. Kolb, K. Mukai, R. Knitter and T. Hoshino. Li_4SiO_4 based breeder ceramics with Li_2TiO_3, $LiAlO_2$ and $Li_XLa_YTiO_3$ additions, part I: Fabrication. Fusion Engineering and Design, 115 (2017) 39-48.

108. R.K. Annabattula, M. Kolb, Y. Gan, R. Rolli and M. Kamlah. Size-Dependent Crush Analysis of Lithium Orthosilicate Pebbles. Fusion Science and Technology 66 (2014) 136-141.

109. S. Zhao, Y. Gan, M. Kamlah, T. Kennerknecht and R. Rolli. Influence of plate material on the contact strength of Li_4SiO_4 pebbles in crush tests and evaluation of the contact strength in pebble-pebble contact. Engineering Fracture Mechanics, 100 (2013) 28-37.

110. E. Carella and T. Hernández. The effect of γ-radiation in Li_4SiO_4 ceramic breeder blankets. Fusion Engineering and Design, 90 (2015) 73-78.

111. A. Abramenkovs, E. Kaschejva, V. Grishmanovs and S. Tanaka. Thermoluminescence study of irradiated lithium orthosilicate. Fusion Engineering and Design, 39-40 (1998) 693-697.

112. G. Ran, C. Xiao, X. Chen, Y. Gong, L. Zhao, H. Wang and X. Wang. Annihilation behavior of irradiation defects in Li_4SiO_4 irradiated with high thermal neutron fluence. Journal of Nuclear Materials, 491 (2017) 43-47.

113. T. Tang, P. Chen, W. Luo, D. Luo and Y. Wang. Crystalline and electronic structures of lithium silicates: A density functional theory study. Journal of Nuclear Materials, 420 (2012) 31-38.

114. F. Beuneu, P. Vajda and G. Jashierowicz. Formation of two kinds of nonspherical lithium colloids in electron-irradiated Li_2O single crystals. Physic Review, 55 (1997) 11263-11269.

115. S. Ueda, R. Inoue, K. Sasaki, K. Wakuta and T. Ariyama. CO_2 absorption and desorption abilities of Li_2O–TiO_2 compounds. ISIJ International, 51 (2011) 530-537.

116. A.A. Kaukis, J.E. Tiliks, V.V. Tamuzhs, A.A. Abramenkovs, G.K. Kizane, J.A. Ubele and V.G. Vasiljev. Preparation and properties of lithium silicates and zirconates ceramic blanket materials. Fusion Engineering and Design, 17 (1991) 13-16.

117. J.E. Wertz and J. R. Bolton. Electron Spin Resonance: Elementary Theory and Practical Applications. Chpman and Hall New Ork. London. Springer Science & Business Media, 2012, p. 500.

118. R. Chen and V. Pagonis. Thermally and Optically Stimulated Luminescence: A Simulation Approach. John Wiley & Sons, 2011, p. 434.

119. M. S. Rasheedy. Method of Hoogenstraaten as a tool for obtaining the trap parameters of general-order thermoluminescence glow peaks. Radiation Effects & Defects in Solids, 160 (2005) 383-390.

120. J. Tiliks, A. Supe, G. Kizane, J. Tiliks Jr., V. Grishmanov and S. Tanaka. The radiolysis of lithium oxide ceramics. Proceedings of the sixth international workshop on ceramic breeder blanket interactions, October 22-24,1997, Mito city, Japan. 215-219.

121. F. M. Mirabella. Modern Techniques in Applied Molecular Spectroscopy. John Wiley & Sons, 1998, p. 410.

122. R. Jenkins and R. Snyder. Introduction to X-Ray Powder Diffractometry. Wiley, 2012, p. 432.

123. B.C. Smith. Fundamentals of Fourier Transform Infrared Spectroscopy, Second Edition. CRC Press, 2011, p. 207.

124. F. Adams and C. Barbante. Chemical Imaging Analysis. Elsevier, 2015, p. 480.

125. E. Margui and R. Van Grieken. X-Ray Fluorescence Spectrometry and Related Techniques: An Introduction. Momentum Press, 2013, p. 142.

126. M.E. Brown. Introduction to Thermal Analysis: Techniques and Applications. Springer Science & Business Media, 2006, p. 264.

127. P. van der Heide. X-ray Photoelectron Spectroscopy: An introduction to Principles and Practices. John Wiley & Sons, 2011, p. 264.

128. X. Xiang, W. Zhu, T. Lu, T. Gao, Y. Shi, M. Yang, Y. Gong, X. Yu, L. Feng, Y. Wei, and Z. Lu. Density functional theory calculations of point defects and hydrogen isotopes in Li_4SiO_4. AIP Advances, 5 (2015) 107136

129. Y. Hosogi, H. Kato and A. Kudo. Visible light response of $AgLi_{1/3}M_{2/3}O_2$ (M=Ti and Sn) synthesized from layered Li_2MO_3 using molten $AgNO_3$. Journal of Materials Chemistry, 18 (2008) 647-653.

130. K. Morinaga, H. Yoshida and H. Takebe. Compositional Dependence of Absorption Spectra of Ti^{3+} in Silicate, Borate, and Phosphate Glasses. Journal of the American Ceramic Society, 77 (1994) 3113-3118.

131. F.H. ElBatal, M.A. Marzouk and H.A. ElBatal. Optical and crystallization studies of titanium oxide doped sodium and potassium silicate glasses. Journal of Molecular Structure, 1121 (2016) 54-59.

132. H. Kashimura, M. Nishikawa, K. Katayama, S. Matsuda, M. Shimozori, S. Fukada and T. Hoshino. Mass loss of Li_2TiO_3 pebbles and Li_4SiO_4 pebbles. Mass loss of Li_2TiO_3 pebbles and Li_4SiO_4 pebbles, Fusion Engineering and Design, 88 (2013) 2202-2205.

133. C. Masquelier, H. Kageyama, T. Takeuchi, Y. Saito and O. Nakamura. Chemistry and structure analysis in the $Li_{4+x}B_xSi_{1-x}O_4$ solid solution. Journal of Power Sources, 54 (1995) 448-451.

134. S. Claus, H. Kleykamp and W. Smykatz-Kloss. Phase equilibria in the Li_4SiO_4-Li_2SiO_3 region of the pseudobinary Li_2O-SiO_2 system. Journal of Nuclear Materials 230 (1996) 8-11.

135. M.J. O'Malley, H. Verweij and P.M. Woodward. Structure and properties of ordered Li_2IrO_3 and Li_2PtO_3. Journal of Solid State Chemistry, 181 (2008) 1803-1809.

136. R. Kasuya, T. Miki and Y. Tai. Preparation of Li_2PtO_3 and its dissolution properties in hydrochloric acid. Journal of the Ceramic Society of Japan 121 (2013) 261-264.

137. T. Hoshino, K. Sasaki, K. Tsuchiya, K. Hayashi, A. Suzuki, T. Hashimoto and T. Terai. Crystal structure of advanced lithium titanate with lithium oxide additives. Journal of Nuclear Materials, 386–388 (2009) 1098-1011.

138. T. Hoshino, H. Kawamura, M. Dokiya, Y. Takahashi, T. Terai and M. Yamawaki. Non-stoichiometry of Li_2TiO_3 under hydrogen atmosphere conditions. Journal of Nuclear Materials, 329-333 (2004) 1300-1304.

139. T. Sekiya, K. Ichimura, M. Igarashi and S. Kurita. Absorption spectra of anatase TiO_2 single crystals heat-treated under oxygen atmosphere. Journal of Physics and Chemistry of Solids, 61 (2000) 1237-1242.

140. A. Bishay. Radiation induced color centers in multicomponent glasses. Journal of Non-Crystalline Solids, 3 (1970) 54-114.

141. E.J. Friebele. D.R. Uhlmann, N.J. Kreidl (Eds.), Optical Properties of Glass, American Ceramic Society, Westerville, OH (1991) 205-262.

142. S. Stoll, A. Ozarowski, R.D. Britt and A. Angerhofer. Atomic hydrogen as high-precision field standard for high-field EPR. Journal of Magnetic Resonance, 207 (2010) 158-163.

143. E. Herrera, F. Urena-Nunez and A. Delfin Loya. Lithium carbonate (Li_2CO_3) as a material for thermal neutron fluence measurements. Applied Radiation and Isotopes, 63 (2005) 241-246.

144. P. Vajda and F. Beuneu. Electron radiation damage and Li-colloid creation in Li_2O. Physical review B, 53 (1991) 5335-5340.

145. S. Arata and F. Assabghy. Titanium impurity center induced in irradiated silicate glasses. Journal of Applied Physics 45 (1974) 5269-5271.

146. H. Bohm and G. Bayer. ESR-spectra of sodium-titanium-silicate glasses and of titanium-containing oxide compounds. Journal of Physics and Chemistry of Solids, 31 (1970) 2125-2137.

147. Y.M. Kim and P.J. Bray. Electron Spin Resonance Studies of Gamma-Irradiated Alkali Titanate Glasses. Journal of Chemical Physics, 53 (1970) 716-723.

148. P. Lombard, N. Ollier and B. Boizot. EPR study of Ti^{3+} ions formed under beta irradiation in silicate glasses. Journal of Non-Crystalline Solids, 357 (2011) 1685-1689.

149. N. Chandrasekhar and R.K. Gartia. Gaussian approximation of thermoluminescence (TL) peaks: A common misconception for analysis of TL of persistent luminescent materials. Journal of Alloys and Compounds, 745 (2018) 773-778.

150. E. Feldbach, A. Kotlov, I. Kudryavtseva, P. Liblik, A. Maaroos, I. Martinson, V. Nagrnyi and E. Vasilchenko. Low-temperature irradiation effects in lithium orthosilicates. Nuclear Instruments and Methods in Physics Research Section B: Beam Interactions with Materials and Atoms, 250 (2006) 159-163

151. K. Uchida, K. Noda, T. Tanifuji, Sh. Nasu, T. Kirihara and A. Kukuchi. Optical absorption spectra of neutron-irradiated Li_2O. Physics Status Solidi A, 58 (1980) 557-566.

152. S. Suzuki, M. Kobayashi, R. Kurata, W. Wang, T. Fujii, H. Yamana, K. Feng, Y. Oya and K. Okuno. Elucidation of annihilation processes of defects induced by γ-irradiation in Li_2TiO_3. Fusion Engineering and Design, 85 (2010) 2331-2333.

153. G.H. Sigel Jr. Ultraviolet spectra of silicate glasses: a review of some experimental evidence. Journal of Non-Crystalline Solids, 13 (1973) 372-398.

154. Y. Chikhray, V. Shestakov, O. Maksimkin, L. Turubarova, I. Osipov, T. Kulsartov, A. Kuykabayeba, I. Tazhibayeva, H. Kawamura and K. Tsuchiya. Study of Li_2TiO_3 + 5 mol% TiO_2 lithium ceramics after long-term neutron irradiation. Journal of Nuclear Materials, 386-388 (2009) 286-289.

155. S. Madhavi, G. V. Subba Rao, B. V. R. Chowdari and S. F. Y. Li. Synthesis and Cathodic Properties of $LiCo_{1-y}Rh_yO_2$ ($0 \leqslant y \leqslant 0.2$) and $LiRhO_2$. Journal of Electrochemical Society, 148 (2001) A1279-A1286.

156. Y. Gong and M. Zhou. Water Adsorption on Platinum Dioxide and Dioxygen Complex: Matrix Isolation Infrared Spectroscopic and Theoretical Study of Three PtO_2–H_2O Complexes. A European Journal of Chemical Physics and Physical Chemistry, 11 (2010) 1888-1894.

157. S. Alexandrova, E. Halova, S. Bakalova, A. Szekeres, A. Marin, P. Osiceanu, M. Gartner and N. Koujuharova. XPS study of nanoscale SiO_xN_y layers synthezised by plasma immersion implantation of nitrogen. Journal of Physics: Conference Series, 514 (2014) 012035.

158. J. P. Contour, A. Salesse, M. Froment, M. Garreau, J. Thevenin and D. Warin. Analysis by electron microscopy and photoelectron spectroscopy of lithium surfaces polarized in anhydrous organic electrolytes. Journal de Microscopie et de Spectroscopie Electroniques, 4 (1979) 483-491.

159. P.-Y. Jouan, M.-C. Peignon, Ch. Cardinaud and G. Lempérière. Characterisation of TiN coatings and of the TiN/Si interface by X-ray photoelectron spectroscopy and Auger electron spectroscopy. Applied Surface Science, 68 (1993) 595-603.

160. B. Gupta, C. Plummer, I. Bisson, P. Frey and J. Hilborn. Plasma-induced graft polymerization of acrylic acid onto poly(ethylene terephthalate) films: characterization and human smooth muscle cell growth on grafted films. Biomaterials, 23 (2002) 863-871.

161. K. Mochizuki, K. Munakata, T. Wajima, K. Hara, K. Wada, T. Shinozaki, T. Takeishi, R. Knitter, N. Bekris and K. Okuno. Study of isotope exchange reactions on ceramic breeder materials deposited with noble metal. Fusion Engineering and Design, 85 (2010) 1185-1189.

162. X. Fu, L. Song and J. Li. Radiation induced color centers in cerium-doped and cerium-free multicomponent silicate glasses. Journal of Rare Earths, 32 (2014) 1037-1042.

163. H.-S. Tsai, D.-S. Chao, Y.-H. Wu, Y.-T. He, Y.-L. Chueh and J.-H. Liang. Spectroscopic investigation of gamma radiation-induced coloration in silicate glass for nuclear applications. Journal of Nuclear Materials, 453 (2014) 233-238.

164. A. K. Sandhu, S. Singh and O. P. Pandey. Effect of neutron-irradiation on optical properties of SiO_2-Na_2O-MgO-Al_2O_3 glasses. Indian Journal of Physics, 83 (2009) 985-991.

165. K. Kadono, N. Itakura, T. Akai, M. Yamashita and T. Yazawa. Formation of color centers in a soda-lime silicate glass by excimer laser irradiation. Journal of Physics: Condensed Matter, 22 (2010) 045901.

166. L. I. Bryukvina and E. F. Martynovich. Formation and Properties of Metallic Nanoparticles in Lithium and Sodium Fluorides with Radiation-Induced Color Centers. Physics of the Solid State, 54 (2012) 2248-2253.

167. S. Agnello, M. Cannas, F. Messina, L. Nuccio and B. Boizot. In situ observation of β-ray induced UV optical absorption in a-SiO_2: Radiation darkening and room temperature recovery. Journal of Non-Crystalline Solids, 355 (2009) 1042-1045.

168. A. Zariņš. Silīcija dioksīda un termiskās apstrādes ietekme uz litiju saturošas keramikas fizikāli ķīmiskajiem procesiem inertā un gaisa atmosfērā. Maģistra darbs. LU Ķīmijas fakultāte, Rīga, 2012.

169. A. Zariņš. Litija ortosilikāta minilodīšu un nanopulveru radiolīze. Bakalaura darbs. LU Ķīmijas fakultāte, Rīga, 2010.

APPENDIX

Appendix 1. Publications

Appendix 1.1 Publications in international journals

1) A. Zariņš, O. Valtenbergs, G. Ķizāne, A. Supe, S. Tamulevičius, M. Andrulevičius, E. Pajuste, L. Baumane, O. Leys, M. H.H. Kolb and R. Knitter. Characterisation and radiolysis of modified lithium orthosilicate pebbles with noble metal impurities. Fusion Engineering and Design, 124 (2017) 934-939.
2) A. Zarins, O. Leys, G. Kizane, A. Supe, L. Baumane, M. Gonzalez, A. Zolotarjovs and R. Knitter. Behaviour of advanced tritium breeder pebbles under simultaneous action of accelerated electrons and high temperature. Fusion Engineering and Design, 121C (2017) 167-173.
3) A. Zarins, O. Valtenbergs, G. Kizane, A. Supe, R. Knitter, M. H.H. Kolb, O. Leys, L. Baumane and D. Conka. Formation and accumulation of radiation-induced defects and radiolysis products in modified lithium orthosilicate pebbles with additions of titanium dioxide. Journal of Nuclear Materials, 470 (2016) 187-196.
4) A. Zarins, G. Kizane, A. Supe, R. Knitter, M. H.H. Kolb, J. Tiliks Jr. and L. Baumane. Influence of chemisorption products of carbon dioxide and water vapour on radiolysis of tritium breeding ceramic. Fusion Engineering and Design, 89 (2014) 1426-1430.
5) A. Zarins, A. Supe, G. Kizane, R. Knitter and L. Baumane. Accumulation of radiation defects and products of radiolysis in lithium orthosilicate pebbles with silicon dioxide additions under action of high absorbed doses and high temperature in air and inert atmosphere. Journal of Nuclear Materials, 429 (2012) 34-39.

Appendix 1.2 Attended international conferences

1) A. Zarins, G. Kizane, O. Valtenbergs, J. Cipa, A. Supe, L. Baumane, A. Zolotarjovs, O. Leys and R. Knitter. Radiolysis of advanced lithium orthosilicate pebbles with additions of lithium metatitanate. The 18th International Conference on Fusion Reactor Materials (ICFRM-18), November 5 to 10, 2017, Aomori, Japan. *Book of abstracts.* Aomori, Japan, 2017, 9PT66.
2) A. Zariņš, G. Ķizāne, A. Supe, O. Valtenbergs, S. Tamulevičius, M. Andrulevičius, E. Pajuste, V. Rudoviča, L. Baumane, M. H.H. Kolb, O. Leys and R. Knitter. Characterisation and radiolysis of modified lithium orthosilicate pebbles with addition of

noble metals. 29th Symposium on Fusion Technology (SOFT 2016), 5th-9th September 2016, Prague, Czech Republic. *Book of abstracts.* Prague, Czech Republic, 2016, P3.170, p. 612.

3) A. Zarins, O. Valtenbergs, G. Kizane, A. Supe, R. Knitter and L. Baumane. Physicochemical processes in modified Li_4SiO_4 pebbles under action of accelerated electron irradiation, Functional Materials and Nanotechnologies (FM&NT-2015), October 5th-8th, 2015, Vilnius, Lithuania. Book of Abstracts, Vilnius, Lithuania, 2015, p. 88.

4) A. Zarins, G. Kizane, A. Supe, L. Baumane and O. Valtenbergs. Physico-chemical properties and application possibility of nano-sized lithium orthosilicate powders, EuroNanoForum 2015, June 10-12, 2015, Riga, Latvia.

5) A. Zarins, G. Kizane, A. Supe, R. Knitter, M. H.H. Kolb, O. Leys, L. Baumane, D. Conka and O. Valtenbergs. High-temperature radiolysis of modified lithium orthosilicate pebbles with additions of titania. 25th Fusion Energy Conference, October 13-18, 2014, Saint Petersburg, Russia. *Programme and Book of Abstracts,* St. Petersburg, Russian Federation, 2014, p. 709.

6) A. Zarins, G. Kizane, A. Supe, R. Knitter, M. Kolb, L. Baumane and O. Valtenbergs. Formation and annihilation of radiation defects and radiolysis products in modified lithium orthosilicate pebbles with addition of titania. 28th Symposium on Fusion Technology, September 29th - October 3rd, 2014, San Sebastian, Spain. *Book of Abstracts,* San Sebastian, Spain, 2014, poster No. P4.141, p. 758.

7) A. Zarins, G. Kizane, R. Knitter and A. Supe. Influence of chemisorption products of carbon dioxide on radiolysis of tritium breeding ceramic. 11th International Symposium on Fusion Nuclear Technology (ISFNT-11), September 16-20, 2013, Barcelona, Spain. Abstract book, Barcelona, Spain, P3-036, p. 436.

8) A. Zarins, G. Kizane, R. Knitter, M. Kolb, A. Supe, J. Kalnacs and O. Valtenbergs. Characterization of Li_4SiO_4 pebbles with TiO_2 additions, using methods of thermal analysis. 2nd International Central and Eastern European Conference for Thermal Analysis and Calorimetry, August 27-30, 2013, Vilnius, Lithuania. Book of abstracts, Vilnius, Lithuania, PS.2.48, p.302.

9) A. Zarins, G. Kizane, A. Supe, R. Knitter, M. Kolb, L. Baumane and O. Valtenbergs. Radiation stability of differently synthesized and pre-treated tritium breeding ceramic. 3rd PhD Event in Fusion Science and Engineering, June 22-26, 2013, York, United Kingdom. *Book of abstracts, 2*013, p. 71.

10) A. Zarins, G. Kizane, A. Supe, R. Knitter, M. Kolb and O. Leys. Influence of Li_2TiO_3 on chemical reactivity of Li_4SiO_4 pebbles. International conference "Functional Materials and Nanotechnologies 2013" (FM&NT 2013), April 21-24, 2013, Tartu, Estonia. *Book of abstracts, 2*013, PO-154.

11) A. Zarins, G. Kizane, A. Supe, L. Baumane, A. Berzins, Dz. Rasmane and I. Steins. Influence of SiO_2 admixes on radiolysis of powders of Li_4SiO_4. International conference "Functional materials and nanotechnologies 2012" (FM&NT 2012), April 17-20, 2012, Institute of solid state physics, University of Latvia, Riga, Latvia. *Book of abstracts, 2*012, p. 307.

12) A. Zarins, G. Kizane, B. Lescinskis, L. Avotina, A. Berzins and I. Steins. Changes of stehiometric and nonstehiometric nanopowders of lithium orthosilicate under thermal treatment and action of moisture. The 8th annual conference of Young Scientists on Energy Issues (CYSENI), May 26-27, 2011, Kaunas, Lithuania. *Conference proceedings*, 2011, on-line: www.cyseni.com.

13) A. Zarins, A. Supe, G. Kizane, Br. Lescinskis, L. Baumene, I. Steins and A. Berzins. Accumulation of radiolysis products and defects in nanopowders of lithium orthosilicate. International conference Functional materials and nanotechnologies 2011 (FM&NT 2011), April 5-8, 2011, Riga, Latvia. *Book of abstracts,* 2011, p. 131.

14) A. Zarins, A. Supe, G. Kizane, J. Tiliks, L. Baumane, I. Steins and R. Knitter. Influence of silicon dioxide on the radiation defects formation and accumulation in lithium orthosilicate nanopowders. The 12th International Conference Advanced Materials and Technologies, August 27-31, 2010, Lithuania, Palanga. *Abstracts,* Palanga, Lithiuania, 2010, p. 74.

15) A. Zariņš, A. Supe, G. Ķizāne, J. Tīliks, L. Baumane and I. Šteins. Radiācijas defektu un radiolīzes produktu pētījumi plazmā sintezētos litija ortosilikāta pulveros. Daugavpils universitātes 52. starptautiskā zinātniska konference, 14.-17. aprīlis, 2010, Daugavpils, Latvija. *Tēzes,* Daugavpils, 2010, 24 lpp.

16) A. Zarins, A. Supe, G. Kizane, J. Tiliks Jun., L. Baumane, J. Grabis and I. Steins. Accumulation of radiolysis and defects in nanopowders of lithium ortosilicate. International conference Functional materials and nanotechnologies 2010 (FM&NT 2010), March 16-19, 2010, Riga, Latvia. *Abstracts,* Riga, 2010, p. 131.

17) A. Zariņš, G. Ķizāne, A. Supe, A. Vitiņš, V. Tīlika un L. Baumane. Litija ortosilikata minilodīšu struktūras izmaiņas radiācijas ietekmē. Rīgas Tehniskas universitātes 50. starptautiska zinātniskā conference, Materiālzinātnes un lietišķās ķīmijas sekcija, 16. oktobris, 2009, Rīga, Latvija.

Appendix 1.3 Attended local conferences

1) A. Zariņš, J. Čipa, O. Valtenbergs, A. Supe, G. Kizāne, A. Zolotarjovs un L. Baumane. Radiācijas defektu un radiolīzes produktu uzkrāšanās modificētā tritiju ģenerējošā keramikā/ Accumulation of radiation-induced defects and radiolysis products in modified tritium breeding ceramic. Latvijas Universitātes Cietvielu fizikas institūta 33. zinātniskā konference, 22.-24. februāris, 2017, Riga, Latvija. Tēzes, LU Cietvielu fizikas institūts, Rīga, 2017, 26. lpp.

2) A. Zarins, O. Valtenbergs, G. Kizane, A. Supe, R. Knitter, M.H.H. Kolb, O. Leys, L. Baumane un D. Conka. Radiācijas defektu un radiolīzes produktu veidošanās un uzkrāšanās modificētās Li_4SiO_4 minilodītēs ar titāna dioksīda piedevām. 1st conference "Nano-materials and radiation effects", February 16, 2016, Riga, Latvia.

3) A. Zariņš, G. Ķizāne, A. Supe, L. Baumane, O. Valtenbergs un R. Knitter. Cēlmetālu piemaisījumu ietekme uz modificēto litija ortosilikāta minilodīšu radiolīzi/ Influence of noble metal impureties on radiolysis of modified lithium orthosilicate pebbles. Latvijas Universitātes Cietvielu fizikas institūta 32. zinātniskā konference, 17.-19. februāris, 2016, Rīga, Latvija. Tēzes, LU Cietvielu fizikas institūts, Rīga, 2016, 73. lpp.

4) A. Zarins, G. Kizane, A. Supe, L. Baumane, D. Conka and O. Valtenbergs. Influence of accelerated electrons radiation on physico-chemical properties of tritium breeding ceramic. Workshop "Investigation of changes of physico-chemical properties of fusion reactor functional materials under influence of high-energy radiation", June 17, 2015, Riga, Latvia.

5) A. Zariņš, G. Ķizāne, A. Supe L. Baumane, R. Knitter, M. Kolb un O. Valtenbergs. Litija ortosilikāta minilodīšu augsttemperatūras radiolīze paātrināto elektronu ietekmē, Latvijas Universitātes Cietvielu fizikas institūta 31. zinātniskā konference, 24. - 26. februāris, 2015, Rīga, Latvija.

6) A. Zariņš, O. Valtenbergs, G. Ķizāne, A. Supe, L. Baumane un R. Knitter**.** Fizikālķīmiskie procesi litija ortosilikāta keramikā jonizējošā starojuma ietekmē. Latvijas Universitātes 73. konference, Fizikālās un analītiskās ķīmijas sekcija, 13. februāris, 2015, Rīga, Latvija.

7) A. Zariņš, G. Ķizāne, A. Supe, R. Knitter, M. Kolb, L. Baumane un O. Valtenbergs. Radiācijas defektu un radiolīzes produktu veidošanās modificētajās litija ortosilikāta minilodītēs. Latvijas Universitātes Cietvielu fizikas institūta 30. zinātniskā konference, 19. - 21. februāris, 2014, Rīga, Latvija. *Tēzes*, LU Cietvielu fizikas institūts, Rīga, 2014, 105. lpp.

8) A. Zariņš, G. Ķizāne, A. Supe, R. Knitter, M. H.H. Kolb, O. Leys, L. Baumane, O. Valtenbergs un D. Čonka. Dažādi sinetezētu un sagatavotu tritiju ģenerējošo keramiku radiācijas stabilitāte. Latvijas Universitātes 72. konference, Fizikālās un analītiskās ķīmijas sekcija, 14. februāris, 2014, Rīga, Latvija.

9) A. Zariņš, G. Ķizāne, A. Supe, R. Knitter un L. Ansone. Termiskās apstrādes procesu gaisa atmosfērā modelēšana izvēlētai tritiju ģenerējošai keramikai. Latvijas Universitātes 71. konference, Analītiskās ķīmijas sekcija, 22. februāris, 2013, Rīga, Latvija.

10) A. Zariņš, G. Ķizāne, A. Supe, R. Knitter un L. Ansone. Tritiju ģenerējošās keramikas Li_2CO_3 pievirsmas slāņa veidošanās cēloņi: termiskās apstrādes procesā gaisa atmosfērā. Latvijas Universitātes Cietvielu fizikas institūta 29. zinātniskā konference, 20. - 22. februāris, 2013, Rīga, Latvija. *Tēzes*, LU Cietvielu fizikas institūts, Rīga, 2013, 56. lpp.

11) A. Zariņš, G. Ķizāne, A. Supe, L. Baumane, A. Bērziņš, Dz. Rašmane un I. Šteins. Termiskās apstrādes ietekme uz litija ortosilikāta radiācijas stabilitāti un radiolīzi gaisa atmosfērā. LU Cietvielu fizikas institūta 28. zinātniskā konference, 8. - 10. februāris, 2012, Rīga, Latvija. *Tēzes*, LU Cietvielu fizikas institūts, Rīga, 43. lpp.

12) A. Zariņš, G. Ķizāne, A. Supe, L. Baumane, A. Bērziņš, Dz. Rašmane un I. Šteins. Gaisa atmosfēras ietekme uz litija ortosilikāta nanopulvera sastāvu un radiolīzi paaugstinātā temperatūrā. Latvijas Universitātes 70. konference, Analītiskās un fizikālās ķīmijas sekcija, 9. februāris, 2012, Rīga, Latvija.

13) A. Zariņš, G. Ķizāne, B. Leščinskis, L. Avotiņa, A. Bērziņš un I. Šteins. Litija ortosilikāta nanopulveru izmaiņas mitruma ietekmē. Latvijas Universitātes Cietvielu fizikas institūta 27. zinātniskā konference, 14. - 16. februāris, 2011, Rīga, Latvija. *Tēzes*, LU Cietvielu fizikas institūts, Rīga, 2011, 76. lpp.

14) A. Zariņš, G. Ķizāne, A. Supe, L. Baumane un A. Bērziņš. Brīvo radikāļu veidošanās litija ortosilikāta nanopulveros mitruma ietekmē. Latvijas Universitātes 69. konferences Analītiskās un fizikālās ķīmijas sekcija, 18. februāris, 2011, Rīga, Latvija.

15) A. Zariņš, G. Ķizāne, A. Supe, L. Baumane, V. Tīlika, E. Pajuste un R. Knitter. Litija ortosilikāta minilodīšu priekšapstrādes ietekme uz to radiācijas stabilitāti. Latvijas Universitātes Cietvielu fizikas institūta 26. zinātniskā konference, 17. - 19. februāris, 2010, Rīga, Latvija. *Tēzes*, Rīga, 2010, 71. lpp.

16) A. Zariņš, G. Ķizāne, A. Supe, L. Baumane, J. Tīliks un E. Pajuste. Litija ortosilikāta radiācijas stabilitāte. Latvijas Universitātes 68. konference, Ķīmijas sekcija, 12. februāris 2010, Rīga, Latvija.

17) A. Zariņš, I. Reinholds, G. Ķizāne, A. Supe un L. Baumane. Radiācijas defektu veidošanās tritiju atražojošajos blanketa zonas materiālos. Latvijas Universitātes 67. konference, Ķīmijas sekcija, 13. februāris, 2009, Rīga, Latvija.

I hereby declare and confirm with my signature that the doctoral thesis "**Formation, accumulation and annihilation of radiation-induced defects and radiolysis products in advanced two-phase ceramic tritium breeder pebbles**" is exclusively the result of my own autonomous work based on my research and literature published, which is seen in the notes and bibliography used. I also declare that no part of the submitted doctoral thesis has been made in an inappropriate way, whether by plagiarizing or infringing on any third person's copyright. Finally, I declare that no part of the submitted doctoral thesis has been used for any other thesis in another higher education institution, research institution or educational institution.

Author: Artūrs Zariņš
Signature _____

Supervisor: Leading researcher, Dr. chem. Gunta Ķizāne
Signature _____

Thesis submitted in the Promotion Council in Chemistry of University of Latvia for the commencement of the degree of Doctor of Chemistry on _____.

Secretary of the Promotion Council: Jāzeps Logins _____

Thesis defended at the session of Promotion Council in Chemistry of University of Latvia for the commencement of the degree of Doctor of Chemistry on September 13, 2018, protocol No. _____

Secretary of the Promotion Council: Jāzeps Logins _____

Fusion Engineering and Design 124 (2017) 934–939

Contents lists available at ScienceDirect

Fusion Engineering and Design

journal homepage: www.elsevier.com/locate/fusengdes

Characterisation and radiolysis of modified lithium orthosilicate pebbles with noble metal impurities

A. Zariņš[a,b,*], O. Valtenbergs[a,c], G. Ķizāne[a], A. Supe[a], S. Tamulevičius[d,e], M. Andrulevičius[d,e], E. Pajuste[a], L. Baumane[a,f], O. Leys[g], M.H.H. Kolb[g], R. Knitter[g]

[a] University of Latvia, Institute of Chemical Physics, Jelgavas street 1, LV-1004, Riga, Latvia
[b] Daugavpils University, Faculty of Natural Science and Mathematics, Department of Chemistry and Geography, Parades street 1a, LV-5401, Daugavpils, Latvia
[c] University of Latvia, Faculty of Chemistry, Jelgavas street 1, LV-1004, Riga, Latvia
[d] Kaunas University of Technology, Institute of Materials Science,Barsausko street 59, LT-50131, Kaunas, Lithuania
[e] Kaunas University of Technology, Department of Physics,Studentu street 50, LT-51368, Kaunas, Lithuania
[f] Latvian Institute of Organic Synthesis,Aizkraukles street 21, LV-1006, Riga, Latvia
[g] Karlsruhe Institute of Technology, Institute for Applied Materials (IAM-KWT), 76021, Karlsruhe, Germany

HIGHLIGHTS

- Noble metals can be introduced into tritium breeder pebbles during fabrication process.
- Trace-impurities of noble metals have heterogeneous distribution on pebble surface.
- Influence of noble metals (up to 300 ppm) on radiolysis of tritium breeder pebbles is negligible.

ARTICLE INFO

Article history:
Received 25 August 2016
Received in revised form 4 January 2017
Accepted 9 January 2017
Available online 18 January 2017

Keywords:
Lithium orthosilicate
Tritium breeding ceramic
Radiolysis
Noble metals

ABSTRACT

Modified lithium orthosilicate (Li_4SiO_4) pebbles with additions of titanium dioxide (TiO_2) are suggested as an alternative tritium breeding ceramic for the European solid breeder test blanket module. The noble metals – platinum (Pt), gold (Au) and rhodium (Rh), can be introduced into the modified Li_4SiO_4 pebbles during the melt-based process, due to the corrosion of Pt-Rh and Pt-Au alloy crucible components. In this study, the surface microstructure, chemical and phase composition of the modified Li_4SiO_4 pebbles with different contents of the noble metals was analysed. The influence of the noble metals on the radiolysis was evaluated after irradiation with accelerated electrons (E = 5 MeV), up to 12 MGy absorbed dose at 300–345 K in a dry argon atmosphere. Using electron spin resonance (ESR) spectroscopy, it was determined that the noble metals (up to 300 ppm) do not significantly influence the formation and accumulation of radiation-induced defects (RD) in the modified Li_4SiO_4 pebbles.

1. Introduction

Lithium based ceramics are considered as solid breeder materials for the tritium breeding in deuterium-tritium (D-T) nuclear fusion reactors. Modified lithium orthosilicate (Li_4SiO_4) pebbles with additions of titanium dioxide (TiO_2) are suggested as an alternative tritium breeding ceramic for the European Union's proposed Helium Cooled Pebble Bed (HCPB) Test Blanket Module (TBM) [1]. Due to the additions of TiO_2, the modified pebbles have two main phases – Li_4SiO_4 as the primary and lithium metatitanate (Li_2TiO_3) as the secondary phase.

The tritium breeding ceramic in the HCPB TBM will be under the action of harsh operation conditions – neutron radiation, high temperatures and a magnetic field [2]. The nuclear reactions, atomic displacements and radiolysis can take place as a result of neutron radiation, and unstable radiation-induced defects (RD) and chemically active radiolysis products (RP) can form and accumulate. The formed RD and RP can interact with the generated tritium and may thus disturb tritium diffusion and hinder its release. Therefore, it is a critical issue to determine and evaluate the factors, which can influence the formation and accumulation of RD and RP.

* Corresponding author at: University of Latvia, Institute of Chemical Physics, Jelgavas street 1, LV-1004, Riga, Latvia.
E-mail addresses: arturs.zarins@lu.lv, arturs.zarins.lukf@gmail.com (A. Zariņš).

http://dx.doi.org/10.1016/j.fusengdes.2017.01.008
0920-3796/

The fabrication process of ceramic materials represents a determining step as it governs their properties and hence their performance. The most promising fabrication method of the modified Li_4SiO_4 pebbles is an *enhanced* melt-based process [3]. For the synthesis, lithium hydroxide monohydrate ($LiOH{\cdot}H_2O$), silicon dioxide (SiO_2) and TiO_2 are used as raw materials. The mixture of the raw materials is heated to about 1573 K for 30 min in a platinum (Pt)-rhodium (Rh) alloy crucible and a melt of Li_4SiO_4 and Li_2TiO_3 is obtained (Eqs. (1)–(3)). The formed liquid is then released through a Pt-gold (Au) alloy nozzle (diameter: 300 μm) to form droplets that are quenched into liquid nitrogen to obtain pebbles.

$$LiOH{\cdot}H_2O \rightarrow LiOH + H_2O \uparrow \quad (1)$$

$$4LiOH + SiO_2 \rightarrow Li_4SiO_4 + 2H_2O \uparrow \quad (2)$$

$$2LiOH + TiO_2 \rightarrow Li_2TiO_3 + H_2O \uparrow \quad (3)$$

Kolb et al. [4] found that Pt particles can be released from the crucible, due to the exposure to molten raw materials or synthesis products at high temperatures. Leys et al. [5], using inductively coupled plasma optical emission spectrometry (ICP-OES), detected elevated contents (up to 300 ppm) of the noble metals – Pt, Au and Rh, in the modified Li_4SiO_4 pebbles, due to the surface corrosion of Pt-Rh alloy crucible and Pt-Au alloy nozzle. Tiliks et al. [6] determined that the additions of transition metal ions, such as iron, chromium and lead, can hinder the formation of RD and RP. However, until now, the influence of the noble metals on the radiolysis was not taken into account and analysed.

The aim of this study is to characterise the modified Li_4SiO_4 pebbles with different contents of the noble metals and to evaluate the influence of the noble metals on the formation of RD and RP. However, to estimate and to exclude the influence of other factors on the radiolysis of the pebbles, it is crucial to analyse the pebble surface microstructure, phase composition, oxidation state and distribution of the noble metals.

2. Experimental

During a fabrication campaign, several batches of the modified Li_4SiO_4 pebbles with additions of TiO_2 were produced by an *enhanced* melt-based process at the KALOS facility (KArlsruhe Lithium OrthoSilicate) and the chemical composition was analysed by ICP-OES. Three types of the pebbles with similar chemical compositions, but with different contents of the noble metals – Pt, Au and Rh, were selected and were marked as Samples #1, #2 and #3 (Table 1).

The fabricated Li_4SiO_4 pebbles with the same chemical composition as in the Sample #1 were annealed at 1223 K for 3 weeks in air to reduce possible structural defects, which may have formed during the fabrication process. The annealed pebbles were marked as Sample #1a.

High energy accelerated electrons (E = 5 MeV) were used instead of neutron irradiation to introduce radiolysis effects in order to avoid nuclear reactions and thereby the formation of radioactive isotopes. The samples were encapsulated in quartz tubes with dry argon and were irradiated by a linear electron accelerator ELU-4 (Salaspils, Latvia). The irradiation was performed up to 12 MGy absorbed dose (P = 0.85 kGy s^{-1}) at 300–345 K. The irradiation parameters were selected to accumulate primary and secondary RD and to avoid the formation of RP, such as colloidal lithium (Li_n) particles, molecular oxygen (O_2) etc.

The phase composition of the modified Li_4SiO_4 pebbles was analysed by powder X-ray diffractometry (p-XRD). The p-XRD patterns were obtained by a Bruker D8 diffractometer (range: 10–70° 2θ, scan step: 0.02° 2θ, Source: Cu Kα, wavelength: 0.15418 nm).

The bond vibrations were studied by attenuated total reflectance Fourier transform infrared (ATR-FTIR) spectroscopy. The ATR-FTIR spectra were recorded by a using the Bruker Vertex 70 v FT-IR spectrometer and Platinum diamond ATR accessory (range: 400–4000 cm^{-1}, resolution: 4 cm^{-1}, vacuum pressure: <3 hPa).

The absorbed gases and phase transitions were investigated by thermogravimetry-differential thermal analysis (TG-DTA). The TG-DTA curves were measured by a Seiko EXTAR 6200 (sample pan: alumina, temperature range: 290–1273 K, heating rate: 10 K min^{-1}, air).

The surface microstructure and chemical composition were studied by scanning electron microscopy (SEM) coupled with energy dispersive X-ray (EDX) spectroscopy. The SEM-EDX images were obtained by a field emission SEM Hitachi S-4800 using an EDX system Bruker XFlash Quad 5040 123 eV.

The top-surface chemical composition was analysed by X-ray photoelectron spectroscopy (XPS). The XPS spectra were recorded by a Thermo Scientific ESCALAB 250Xi spectrometer (pressure: 2×10^{-9} Torr, Source: Al Kα, energy: 1486.6 eV, analysed area: 0.3 mm). The energy scale of the system was calibrated acording to Au $4f_{7/2}$, Ag $3d_{5/2}$ and Cu $2p_{3/2}$ peaks position.

The formation and accumulation of paramagnetic RD were investigated by electron spin resonance (ESR) spectroscopy. The ESR spectra were recorded by a Bruker BioSpin X-band ESR spectrometer (microwave frequency: 9.8 GHz, microwave power: 0.2 mW, modulation amplitude: 0.5 mT, field sweep: 20 and 100 mT) operating at room temperature.

3. Results and discussion

Although the concentration of the noble metals – Pt, Au and Rh, in the modified Li_4SiO_4 pebble have been previously studied [5], little attention has been given to evaluate the oxidation state and the distribution of the noble metals and their influence on the formation and accumulation of RD and RP. Therefore, to remedy this situation an investigation of the modified pebbles with different contents of the noble metals was started. During the *enhanced* melt based-process, which is described above in the introduction, the molten raw materials and synthesis products can react with Pt-Rh alloy crucible and Pt-Au alloy nozzle (Eqs. (4) and (5)) and thus the noble metals impurities could be introduced into the melt of Li_4SiO_4 and Li_2TiO_3. Bright yellow lithium platinate (Li_2PtO_3) is thermally stable up to 1375 K [7] and thus can accumulate in the pebbles during the fabrication process.

$$Pt + 2LiOH + O_2 \rightarrow Li_2PtO_3 + H_2O \uparrow \quad (4)$$

$$Pt + Li_4SiO_4 + O_2 \rightarrow Li_2PtO_3 + Li_2SiO_3 \quad (5)$$

Au is one of the least reactive chemical elements, and it has been assumed that micro-impurities of Au in the modified Li_4SiO_4 pebbles most likely will accumulate in a metallic form. The common oxidation state of Rh is +3, and it has been supposed that black lithium rhodate ($LiRhO_2$) could form during the melt-based process [8]. To estimate the presence of the noble metals or their compounds, the surface microstructure, chemical and phase composition on the pebbles was analysed before irradiation.

3.1. Surface microstructure and chemical composition of modified Li_4SiO_4 pebbles

The modified Li_4SiO_4 pebbles with different contents of the noble metals (Sample #1, #2 and #3), show an off-white colour, while the annealed pebbles (Sample #1a) have a yellow colour. The pebbles are spherically shaped and the grains of the secondary phase – Li_2TiO_3, are very small (diameter: <4 μm) and homogeneously distributed on the surface of the pebbles (Fig. 1). The structural defects, such as open pores, cracks, cavities and joints,

Table 1
Specification of the investigated modified Li_4SiO_4 pebbles.

	Sample #1	Sample #1a	Sample #2	Sample #3
Chemical composition				
Li, wt%	21.9 ± 0.2	21.9 ± 0.2	21.20 ± 0.06	21.40 ± 0.08
Si, wt%	18.30 ± 0.04	18.30 ± 0.04	20.0 ± 0.2	20.2 ± 0.1
Ti, wt%	8.03 ± 0.05	8.03 ± 0.05	7.04 ± 0.01	6.96 ± 0.04
Pt, ppm	289 ± 2	289 ± 2	102 ± 2	22 ± 1
Au, ppm	156 ± 1	156 ± 1	33 ± 1	<6
Rh, ppm	<5	<5	<6	<6
Phase composition	80 mol% Li_4SiO_4 20 mol% Li_2TiO_3	80 mol% Li_4SiO_4 20 mol% Li_2TiO_3	83 mol% Li_4SiO_4 17 mol% Li_2TiO_3	83 mol% Li_4SiO_4 17 mol% Li_2TiO_3
Pebble diameter	250–1250 μm	650–900 μm	>1250 μm	>1250 μm
Thermal treatment	–	1220 K, 3 weeks, air	–	–

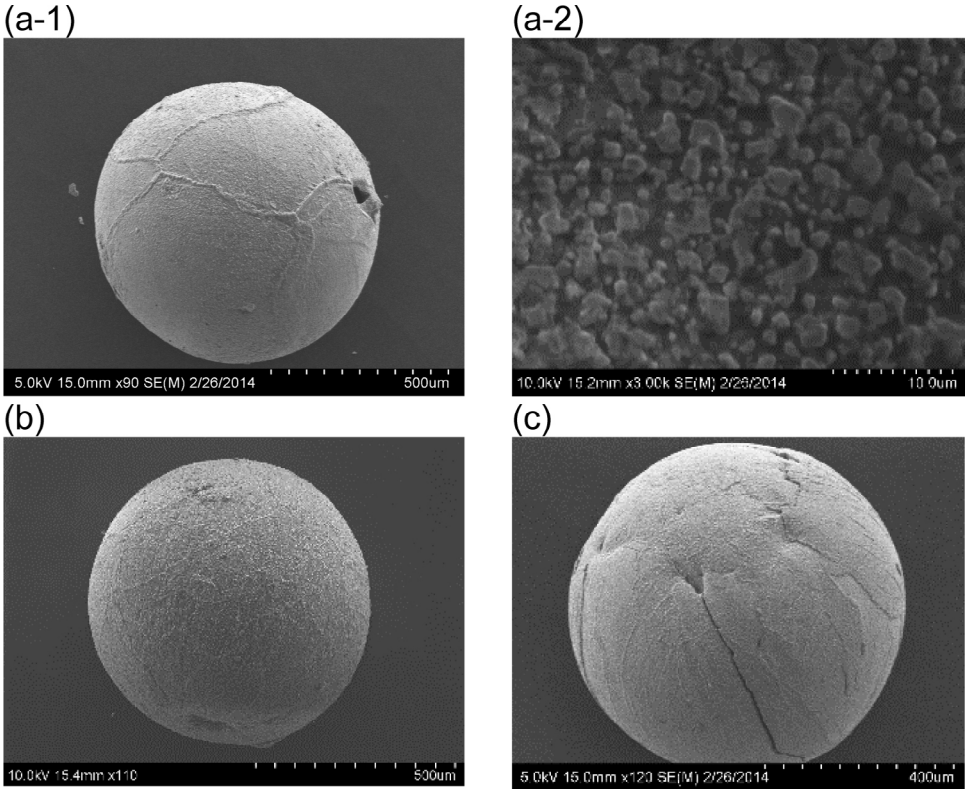

Fig. 1. SEM images of the surface microstructure of three randomly selected modified Li_4SiO_4 pebbles (Sample #1a).

are also detected. It is assumed that the cracks are caused during the melt-based process, due to the rapid quenching of the obtained pebbles in liquid nitrogen. The cavities and open porosity, on the other hand, may result from the density differences between the liquid and the crystallised state.

Using SEM-EDX spectroscopy, mainly oxygen, silicon, titanium and Pt trace-impurities were detected on the surface of the modified Li_4SiO_4 pebbles and the element mapping is shown in Fig. 2. The presence of Au, Rh could not be detected, due to the detection limits of EDX spectroscopy or the heterogonous distribution of these elements. The origins of oxygen, silicon and titanium are the primary phase – colourless Li_4SiO_4, and the secondary phase – off-white Li_2TiO_3, while the Pt trace-impurities are heterogeneously distributed on the pebble surface and localise mainly on grain boundaries or as inclusions. Obtained SEM-EDX results indirectly confirm that the light yellow colour of the pebbles most likely could be caused by the corrosion products of the Pt, for example, Li_2PtO_3.

3.2. Chemical and phase composition of modified Li_4SiO_4 pebbles

In the p-XRD patterns of the modified Li_4SiO_4 pebbles before annealing (Fig. 3), the peaks of two crystallised phases have been detected – monoclinic Li_4SiO_4 as the primary and cubic, disordered Li_2TiO_3 as a secondary phase. After annealing up to 1223 K for 3 weeks in air, the cubic, disordered Li_2TiO_3 phase was transformed to the monoclinic phase. The peaks of Pt or Li_2PtO_3 were not detected, most likely due to very small amounts or the overlapping of the peaks with the primary and secondary phases.

Using ATR-FTIR spectroscopy, the bond vibrations mainly of the primary and secondary phases were detected (Fig. 4). The vibrations at 400–650 and 700–1050 cm^{-1} are related to Li—O, Si—O, O—Si—O and Ti—O bonds, but at 1400–1500 cm^{-1} to C—O bonds [9,10]. The Pt—O bond vibrations (around 400–700 cm^{-1} [11]) of Li_2PtO_3 most likely overlap with bond vibrations of the primary or the secondary phase (Fig. 5).

To explain the formation of C—O bonds, which were detected by ATR-FTIR spectroscopy, the top-surface chemical composition of

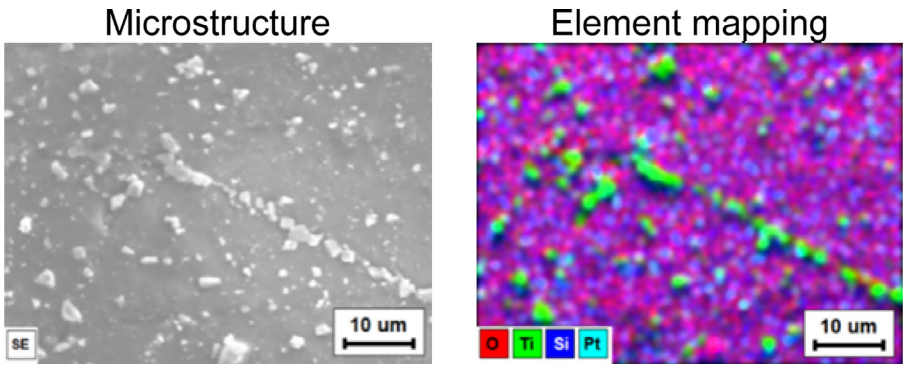

Fig. 2. SEM-EDX images showing the surface microstructure (left) and chemical composition (right) of the modified Li_4SiO_4 pebbles (Sample #1a).

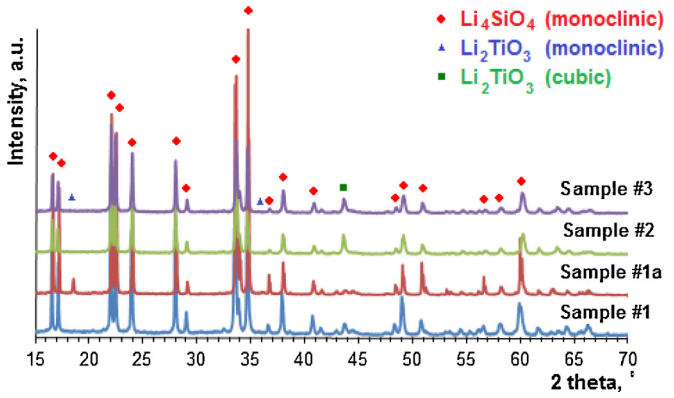

Fig. 3. p-XRD patterns of the modified Li_4SiO_4 pebbles with different contents of the noble metals.

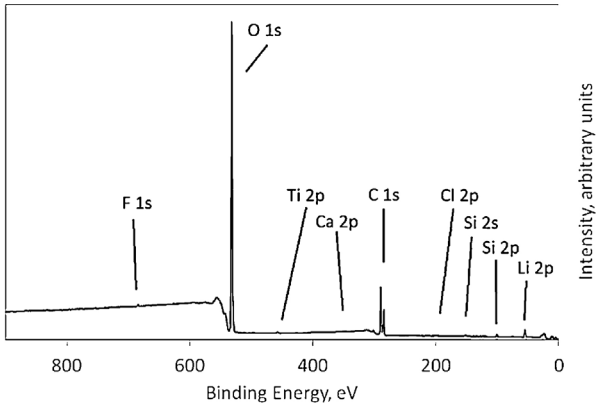

Fig. 5. Survey XPS spectrum on the surface of the modified Li_4SiO_4 pebbles (Sample #1a).

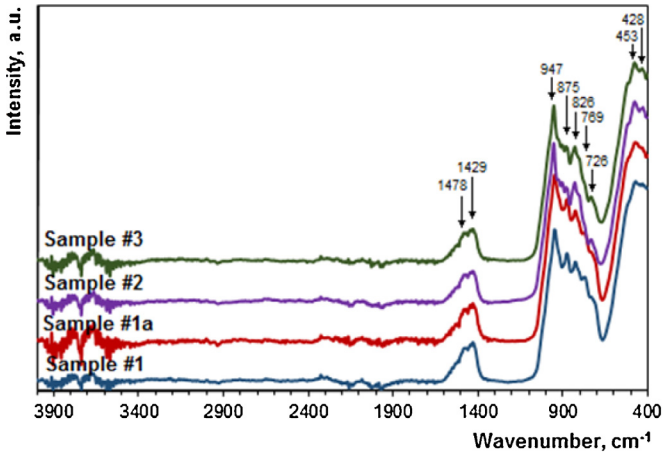

Fig. 4. ATR-FTIR spectra of the modified Li_4SiO_4 pebbles with different contents of the noble metals.

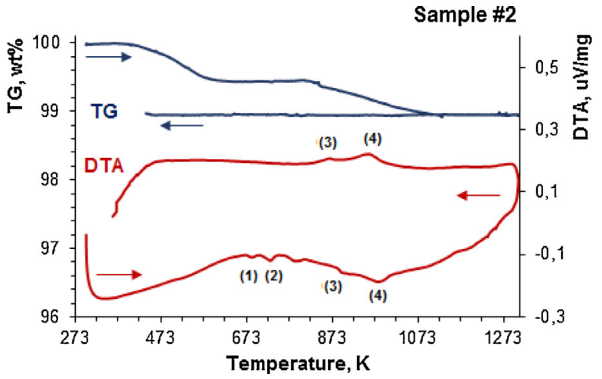

Fig. 6. TG-DTA curves of the modified Li_4SiO_4 pebbles with the noble metal impurities (Sample #2, heating and cooling rate 10 K min^{-1}, air).

the modified Li_4SiO_4 pebbles (depths: ~5–10 nm [12]) was examined by XPS (Fig. 6). In the XPS, mainly the core level spectra of carbon, oxygen, lithium, titanium and silicon were observed. All core level spectra showed one peak for the corresponding elements except carbon. The position of the carbon main peak at 289.8 eV is in good agreement with the known peak position at 289.8 eV for $LiCO_3$ [13]. Other peaks of carbon at 284.5 eV, 286.2 eV and 288.4 eV can be assigned to C—C, C—O and O=C—O bonds [14,15].

The formation of chemisorption products of carbon dioxide (CO_2) and water (H_2O) vapour – lithium carbonate (Li_2CO_3) and LiOH, on the surface of the Li_4SiO_4 pebbles was described previously [9,16] and most likely occurs during handling, thermal treatment or storage (Eqs. (6)–(8)).

$$Li_4SiO_4 + CO_2 \rightarrow Li_2SiO_3 + Li_2CO_3 \quad (6)$$

$$Li_4SiO_4 + H_2O \rightarrow Li_2SiO_3 + 2\,LiOH \quad (7)$$

$$2\,LiOH + CO_2 \rightarrow Li_2CO_3 + H_2O \quad (8)$$

Using TG-DTA (Fig. 6), a weight loss (0.3–1.4 wt%) during heating up to 1100 K was confirmed in the modified Li_4SiO_4 pebbles, due to the release of chemisorbed H_2O and CO_2 [16]. DTA curves reveals four endothermic peaks between 673 and 1023 K. The peaks (1) and (2) could be related to the phase transition of cubic, disordered Li_2TiO_3, while peaks (3) and (4) are caused by polymorphic

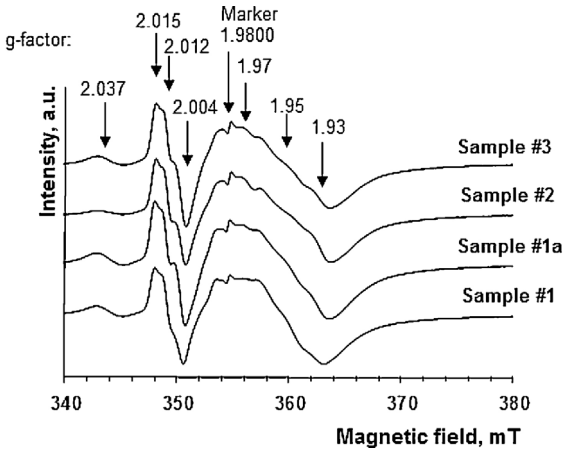

Fig. 7. ESR spectra of the modified Li_4SiO_4 pebbles after irradiation up to 12 MGy absorbed dose at 300–345 K in a dry argon atmosphere.

transitions of Li_4SiO_4. Other processes, such as the melting of Pt and the decomposition of Li_2PtO_3 (Eq. (9)) occur at higher temperatures than 1300 K, or the mass of the compounds is too small to detect a reaction enthalpy by TG-DTA. The melting of the modified pebbles takes place around 1470 K.

$$Li_2PtO_3 \rightarrow Li_2O + Pt + O_2\uparrow \quad (9)$$

3.3. *Influence of noble metals on the radiolysis of modified Li_4SiO_4 pebbles*

A previous study [17] already showed that the modified Li_4SiO_4 pebbles have good radiation stability (radiation chemical yield: <0.5 defects per 100 eV) and after irradiation up to 5000 MGy absorbed dose, major changes in the microstructure and phase composition do not occur. Therefore, after irradiation with accelerated electrons (E = 5 MeV) up to 12 MGy absorbed dose, the pebbles with different noble metals contents were analysed by ESR spectroscopy only (Fig. 7).

In the ESR spectra of the modified Li_4SiO_4 pebbles before irradiation, ESR signals were not detected, except the signal of the marker with a g-factor 1.9800 ± 0.0005 and thus were not included. After irradiation, complex ESR spectra were observed and the shape of the spectra indicates the existence of several groups of paramagnetic RD. It has been assumed that the ESR signal with a g-factor 2.004 ± 0.001, could be attributed to E' centres (SiO_3^{3-} and TiO_3^{3-}), 2.012 ± 0.001 and 2.015 ± 0.001 to HC_2 centres (SiO_4^{3-} and TiO_3^{-}), 2.040 ± 0.001 probably to peroxide radicals (≡Si—O—O•), while signals with g-factor around 1.97, 1.95 and 1.93 could be related to *so called* "Ti^{3+} ion trapped-electron centres" [17]. Significant changes in the ESR spectra of the pebbles depending on the content of the noble metals were not detected. However, it is not excluded that the signals of the paramagnetic metallic trace-impurities can overlap with the ESR signals of peroxide radicals, E', HC_2 or Ti^{3+} centres.

The total concentration of the accumulated RD in the modified Li_4SiO_4 pebbles was calculated from the ESR results using a double integration method, and the results versus the absorbed dose are shown in Fig. 8.

The accumulation of paramagnetic RD up to 12 MGy absorbed dose is analogous for the modified Li_4SiO_4 pebbles with different contents of the noble metals. The slight concentration differences can be explained by a different phase composition, microstructure or the irradiation temperature. Previously, using the lyo-luminescence (LL) technique, it has been shown that the RD and RP mainly localise close to the surface of the Li_4SiO_4 pebbles, due to the structural defects or different chemical composition

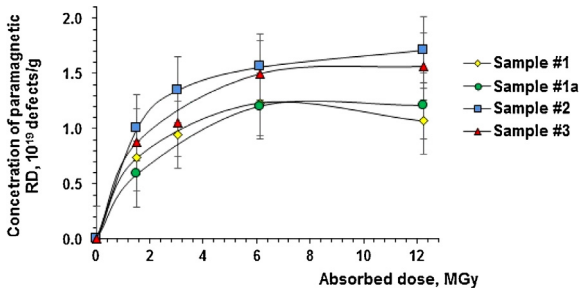

Fig. 8. Dependence of the total concentration of the accumulated paramagnetic RD in the modified Li_4SiO_4 pebbles with different contents of the noble metals on the absorbed dose.

[18]. Therefore, it has been assumed that the radiolysis of the modified pebbles could be also affected by the surface structural defects (open pores and cavities) and chemisorption products (LiOH and Li_2CO_3).

On the basis of the obtained results, it can be concluded that the influence of the noble metals, with a sum content of up to 300 ppm, on the radiolysis of the modified Li_4SiO_4 pebbles is negligible in comparison with other factors, which are mentioned above. It is also expected that the noble metals don't have a negative effect on the functional properties of tritium breeder.

4. Conclusions

In this research, the modified Li_4SiO_4 pebbles with different contents of the noble metals – Pt, Au and Rh, were characterised and the influence of the noble metals on the formation and accumulation of RD was evaluated. The pebbles mainly consist of two crystallised phases – monoclinic Li_4SiO_4 as the main and cubic/monoclinic Li_2TiO_3 as the secondary phase. The presence of Pt trace-impurities was detected on the pebble surface and thus it has been suggested that the light yellow colour of the pebbles could be caused by the corrosion products of the Pt alloy, for example, Li_2PtO_3. Using ESR spectroscopy, it was shown that the trace-impurities of the noble metals (up to 300 ppm) do not significantly influence the formation of RD in the pebbles. It has been suggested that the influence of the noble metals on the radiolysis of the modified Li_4SiO_4 pebbles is negligible in comparison with other factors, for example, a different phase composition, microstructure, structural defects or the irradiation temperature.

Acknowledgments

The authors greatly acknowledge the technical and experimental support of Agris Berzins and Artis Kons (Faculty of Chemistry, University of Latvia). This research of the Baltic-German University Liaison Office was supported by the German Academic Exchange Service (DAAD) with funds from the Foreign Office of the Federal Republic Germany. The views and opinions expressed herein do not reflect those of the Baltic-German University Liaison Office.

References

[1] R. Knitter, et al., J. Nucl. Mater. 442 (2013) S420–S424.
[2] D. Carloni, et al., Fusion Eng. Des. 89 (2014) 1341–1345.
[3] R. Knitter, et al., J. Nucl. Mater. 442 (2013) S433–S436.
[4] M.H.H. Kolb, et al., Fusion Eng. Des. 86 (2011) 2148–2151.
[5] O. Leys, et al., J. Nucl. Mater. 107 (2016) 70–74.
[6] J. Tiliks, et al., Fusion Eng. Des. 17 (1991) 17–20.
[7] M.J. O'Malley, et al., J. Solid State Chem. 181 (2008) 1803–1809.
[8] S. Madhavi, et al., J. Electrochem. Soc. 148 (2001) A1279–A1286.
[9] J. Ortiz-Landeros, et al., Thermochim. Acta 15 (2011) 73–78.
[10] Q. Zhou, et al., J. Eur. Ceram. Soc. 34 (2014) 801–807.

[11] Y. Gong, M. Zhou, ChemPhysChem 11 (2010) 1888–1894.
[12] S. Alexandrova, et al., J. Phys.: Conf. Ser. 514 (2014) 012035.
[13] J.P. Contour, et al., J. Microsc. Spectrosc. Electron. 4 (1979) 483.
[14] P.-Y. Jouan, et al., Appl. Surf. Sci. 68 (1993) 595–603.
[15] B. Guptaa, et al., Biomaterials 23 (2002) 863–871.
[16] R. Knitter, et al., J. Nucl. Mater. 367–370 (2007) 1387–1392.
[17] A. Zarins, et al., J. Nucl. Mater. 470 (2016) 187–196.
[18] G. Kizane, et al., J. Nucl. Mater. 329–333 (2004) 1287–1290.

Fusion Engineering and Design 121 (2017) 167–173

Contents lists available at ScienceDirect

Fusion Engineering and Design

journal homepage: www.elsevier.com/locate/fusengdes

Behaviour of advanced tritium breeder pebbles under simultaneous action of accelerated electrons and high temperature

A. Zarins[a,b,*], O. Leys[c], G. Kizane[a], A. Supe[a], L. Baumane[a,d], M. Gonzalez[e], V. Correcher[e], C. Boronat[e], A. Zolotarjovs[f], R. Knitter[c]

[a] University of Latvia, Institute of Chemical Physics, Jelgavas street 1, LV-1004, Riga, Latvia
[b] Daugavpils University, Faculty of Natural Science and Mathematics, Department of Chemistry and Geography, Parades street 1a, Daugavpils, LV-5401, Latvia
[c] Karlsruhe Institute of Technology, Institute for Applied Materials (IAM-KWT), 76021, Karlsruhe, Germany
[d] Latvian Institute of Organic Synthesis, Aizkraukles street 21, LV-1006, Riga, Latvia
[e] LNF-CIEMAT, Materials for Fusion Group, Av. Complutense 40, 28040, Madrid, Spain
[f] University of Latvia, Institute of Solid State Physics, Kengaraga street 8, LV-1063, Riga, Latvia

HIGHLIGHTS

- Irradiation temperature affects accumulation of radiation-induced defects (RD) and radiolysis products (RP).
- With an increasing content of Li_2TO_3 in the advanced pebbles, the concentration of accumulated RD and RP decreases.
- The accumulated RD and RP annihilates around 423–773 K.
- Mechanical properties of the advanced pebbles practically do not change after irradiation.

ARTICLE INFO

Article history:
Received 9 February 2017
Received in revised form 16 June 2017
Accepted 25 June 2017
Available online 11 July 2017

Keywords:
Lithium orthosilicate
Lithium metatitanate
Tritium breeding ceramic
Radiolysis

ABSTRACT

Advanced lithium orthosilicate (Li_4SiO_4) pebbles with additions of lithium metatitanate (Li_2TiO_3) as a secondary phase are suggested as a potential source for tritium breeding in future nuclear fusion reactors. The advanced Li_4SiO_4 pebbles with different contents of Li_2TiO_3 were examined before and after simultaneous action of 5 MeV accelerated electron beam (dose rate: up to 10 MGy h^{-1}) and high temperature (up to 1120 K) in a dry argon atmosphere. The accumulated radiation-induced defects (RD) and radiolysis products (RP) were studied by electron spin resonance (ESR) spectrometry and thermally stimulated luminescence (TSL) technique. The phase transitions were studied with powder X-ray diffraction (*p*-XRD). The microstructure and mechanical strength of the pebbles, before and after irradiation, were investigated by scanning electron microscopy (SEM) and comprehensive crush load tests. The obtained results revealed that the irradiation temperature has a significant impact on the accumulation of RD and RP in the advanced Li_4SiO_4 pebbles, and with an increasing content of Li_2TiO_3, the concentration of accumulated paramagnetic RD and RP decreases. Major changes in the mechanical strength, microstructure and phase composition of the advanced pebbles were not detected after irradiation.

1. Introduction

Lithium orthosilicate (Li_4SiO_4) and lithium metatitanate (Li_2TiO_3) in the form of ceramic pebbles have been developed as two of the most promising tritium breeder candidates for future nuclear fusion reactors [1]. Under the operation conditions of the fusion reactors, the tritium breeder pebbles will be exposed to an intense neutron fluence (up to 10^{18} n m^{-2} s^{-1}), a high temperature (up to 1193 K) and a magnetic field (up to 7–10 T) [2]. The latest results of the post-irradiation examination [3] confirmed that both tritium breeder pebbles will perform sufficiently well under the expected operation conditions. However, it has also been reported that the mechanical properties of pure Li_4SiO_4 pebbles need to be improved, while Li_2TiO_3 pebbles require a higher enrichment with lithium-6, to increase tritium production.

* Corresponding author at: University of Latvia, Institute of Chemical Physics, Jelgavas street 1, LV-1004, Riga, Latvia.
E-mail address: arturs.zarins@lu.lv (A. Zarins).

http://dx.doi.org/10.1016/j.fusengdes.2017.06.033
0920-3796/

Table 1
Specification of the investigated advanced Li_4SiO_4 pebbles with different contents of Li_2TiO_3 and the reference pebbles.

Sample	Pebbles	Phase compositions			Pebble size (μm)	Description
		Li_4SiO_4, mol%	Li_2TiO_3, mol%	Li_2SiO_3, mol%		
#0	Reference	90	0	10	500	Un-treated
					650–900	Thermally pre-treated
#1	Advanced	90	10	0	1000	Un-treated
					650–900	Thermally pre-treated
#2	Advanced	80	20	0	500	Un-treated
					650–900	Thermally pre-treated
#3	Advanced	75	25	0	500	Un-treated
#4	Advanced	70	30	0	500	Un-treated
					650–900	Thermally pre-treated
#5	Advanced	60	40	0	1000	Thermally pre-treated

The advanced Li_4SiO_4 pebbles with additions of Li_2TiO_3 as a secondary phase have been proposed as an alternative candidate for the tritium breeding [4]. The optimum content of Li_2TiO_3 has yet to be evaluated; nonetheless the advanced pebbles have enhanced mechanical properties, without losing the benefit of a high lithium density and melting temperature [5]. The preliminary studies indicate that the change in the chemical composition of the pebbles does not significantly affect the radiation stability [6], release characteristics [7] and activation behaviour [8]. The re-melting and lithium re-enrichment studies [9] also revealed that the recycling of the advanced breeder pebbles, without a deterioration of the material properties, is possible using an *enhanced* melt-based process.

However, to develop a new two-phase composition for the tritium breeder pebbles, it is a critical issue to study the behaviour of the advanced Li_4SiO_4 pebbles under the simultaneous action of radiation, temperature and magnetic field. From previous long-term irradiation studies [10,11], it is known that under such conditions various physicochemical processes (lithium burn-up, atomic displacements, radiation-induced chemical processes and phase transitions) can take place and thus affect the phase composition and microstructure, as well as the thermal and mechanical properties of the breeder pebbles. The accumulated radiation-induced defects (RD) and radiolysis products (RP) may interact with generated tritium and strongly influence the tritium transport and release processes [12–14]. Previously, the correlation between the tritium release processes and the thermal annealing of RD and RP have been detected [15] and it has been assumed that the recombination of RD and RP could trigger the tritium detrapping.

We herein report on the behaviour of the advanced Li_4SiO_4 pebbles with various contents of Li_2TiO_3 considering simultaneous action of 5 MeV accelerated electron beam (dose rate: up to 10 MGy h^{-1}) and high temperature (up to 1120 K) in dry argon atmosphere, to predict the tritium diffusion and release mechanisms. Such study was performed by means of electron spin resonance (ESR), powder X-ray diffraction (*p*-XRD), thermally stimulated luminescence (TSL) and scanning electron microscopy (SEM) techniques and, as a preliminary approach, only the flux of accelerated electrons was used instead of neutron irradiation, to introduce RD and RP while avoiding nuclear reactions and thereby the formation of radioactive isotopes. The irradiation temperature was chosen in order to reach conditions comparable to the operation conditions of the fusion nuclear reactor.

2. Experimental

The advanced Li_4SiO_4 pebbles with five different contents of Li_2TiO_3 were selected for this research together with the reference pebbles (Table 1). The reference pebbles (0 mol% Li_2TiO_3) consist of two main phases – Li_4SiO_4 as the primary and lithium metasilicate (Li_2SiO_3) as a secondary phase, and they are the present reference material for tritium breeding in the EU developed concept [1]. The advanced pebbles were produced by an *enhanced* melt-based process at the Karlsruhe Institute of Technology (Karlsruhe, Germany) [4], while the reference pebbles were fabricated by a melt-spraying method at Schott AG (Mainz, Germany) [16]. To achieve an operation relevant microstructure, the fabricated advanced and reference pebbles were thermally pre-treated at 1223 K for 504 h in air.

Both, the un-treated and thermally pre-treated Li_4SiO_4 pebbles with different contents of Li_2TiO_3 were encapsulated in quartz tubes with a dry argon and were irradiated with the linear electron accelerator ELU-4 (Salaspils, Latvia), up to 4 h per day (Table 2). During one irradiation campaign (three irradiation cycles) with 5 MeV accelerated electrons, up to 100 MGy absorbed dose (dose rate: <10 MGy h^{-1}), up to four quartz tubes were irradiated simultaneously. The electron beam diameter is around 40 mm and to avoid differences in the absorbed dose depending on tube location in the irradiation area, the location of each tube was changed after each irradiation cycle. Due to the collision of accelerated electrons with quartz tubes and pebbles, most of the kinetic energy of the accelerated electrons is transferred into heat within the specimen, causing a local temperature rise (up to 1120 K). Therefore, the irradiation temperature was continuously measured by a chromel-alumel thermocouple, that was located in central part of irradiated area, with an Agilent 34970 A multichannel digital voltmeter and an Agilent 34902 A multiplexer and recorded with a PC using the Agilent BenchLink Data Logger 3 software. The measured temperature differences between separate irradiation cycles could be associated with beam center displacement, linear electron accelerator current or voltage changes etc.

The accumulated paramagnetic RD and RP were investigated by ESR spectrometry. The ESR spectra were recorded using Bruker BioSpin X-band ESR spectrometer (microwave frequency: 9.8 GHz, microwave power: 0.2 mW, modulation amplitude: 5 G, field sweep: 200 and 1000 G) operating at room temperature. The pebbles were analysed in ER 221TUB/3 CFQ quality tubes with a diameter of 3 mm, both before and after irradiation. The reference marker ER 4119HS-2100 (g-factor: 1.9800 ± 0.0005, radical concentration: $1.15 \cdot 10^{-3}$ %) was used for quantitative measurements.

The thermal stability and recombination of accumulated RD and RP were studied by TSL technique. The TSL glow emission, observed through a blue filter (a FIB002 of the Melles-Griot Company), was carried out using an automated Risø TL reader model TL DA-12 with an EMI 9635 QA photomultiplier. The reader is provided with a $^{90}Sr/^{90}Y$ beta source with a dose rate of 0.011 Gy s^{-1} calibrated against a ^{137}Cs gamma source in a secondary standard laboratory. The samples were measured using a linear heating rate of 5 K s^{-1} from room temperature up to 773 K in a nitrogen atmosphere. To acquire information about spectral distribution of TSL, another experimental setup was used: Andor Shamrock B-303i spectrograph equipped with a CCD camera Andor DU-401A-BV with different cryostats: from nitrogen cryostat to high-power

Table 2
Specification of irradiation conditions of the advanced and the reference Li_4SiO_4 pebbles with 5 MeV accelerated electrons (D – absorbed dose, P – dose rate, T – irradiation temperature).

Sample	Description	D, MGy	P, MGy h^{-1}	$T_{(cycle)}$, K	$T_{(aver.)}$, K	$T_{(min)}$, K	$T_{(max)}$, K
#0; #1; #2; #4	Un-treated	100	<10	(1) 850–930 (2) 1010–1120 (3) 770–900	920	770	1120
#0; #1; #2; #4	Thermally pre-treated	100	<10	(1) 580–640 (2) 700–770 (3) 820–840	710	580	840
#3 #5	Un-treated Thermally pre-treated	100	<10	(1) 790–950 (2) 780–860 (3) 500–540	730	500	950

heating element providing temperature range 8–700 K with variable heating rate (2 K s^{-1} used).

The phase transitions and microstructural changes after irradiation were studied by *p*-XRD and SEM respectively. The *p*-XRD patterns were obtained by a Bruker D8 (range: 15–70° 2theta, scan speed: 0.02° 2theta, step time: 5 s, source: CuKα). The following datasets were used from the JCPDS PDF-2 (Release 2010) database: Li_4SiO_4 – 074-0307, Li_2SiO_3–029-0828 and Li_2TiO_3–033-0831. The microstructure of the pebbles was examined at etched cross-sections with a field emission SEM (SUPRA 55, Zeiss).

The mechanical properties of the pebbles were analysed by performing compressive crush load tests before and after irradiation. 40 single mono-sized pebbles (diameter: 500 or 1000 μm) were measured individually by a Zwick-Roell UTS electro-mechanical testing system. This method involves a continuously increasing load imposed onto single pebbles between sapphire plates until they break, after which the mean crush load was determined. Before the crush load test measurements, the pebbles were dried at 573 K for one hour in a nitrogen atmosphere to remove any moisture present.

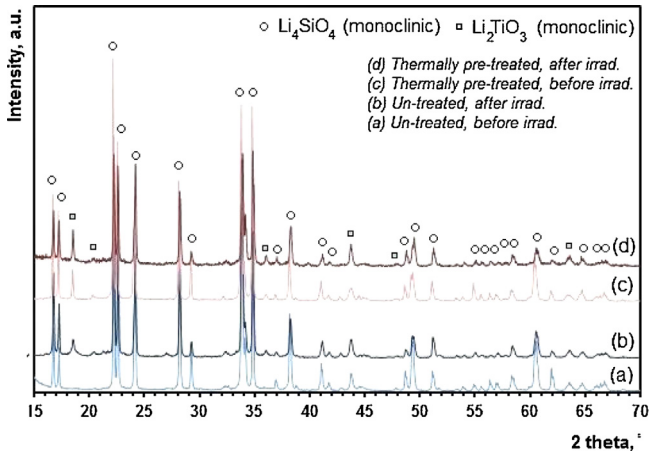

Fig. 1. *p*-XRD pattern of the un-treated and thermally pre-treated advanced Li_4SiO_4 pebbles with 10 mol% Li_2TiO_3 before and after irradiation with 5 MeV accelerated electrons up to 100 MGy absorbed dose at 500–1120 K in a dry argon atmosphere.

3. Results and discussion

The un-treated and thermally pre-treated advanced Li_4SiO_4 pebbles with additions of Li_2TiO_3 as a secondary phase show an off-white colour – pale yellow, pink, purple or brown, before irradiation. During thermal pre-treatment slight changes from initial colour of the pebbles have been observed. It has been assumed that the colour might be caused by a redox reaction due to the presence of metallic impurities, added in the pebbles during the fabrication process or by the raw materials [9] associated, for example, with the reduction of Ti^{4+} ions or formation of oxygen vacancies during the fabrication process. Using *p*-XRD, it has been determined that the un-treated advanced pebbles have two main crystalline phases – monoclinic Li_4SiO_4 as the primary phase and monoclinic Li_2TiO_3 as the secondary phase (Fig. 1). No traces of ternary compounds, such as, Li_2TiSiO_5 [17], or chemisorption products, such as, lithium hydroxide (LiOH) or carbonate (Li_2CO_3), were detected. After thermal pre-treatment, the diffraction peaks of Li_4SiO_4 and Li_2TiO_3 becomes higher and narrower, due to the increase in crystallinity.

In the advanced pebbles, both phases (Li_4SiO_4 and Li_2TiO_3) are fully separated [5] and it is anticipated that the mechanisms and the structure of the formed RD and RP during irradiation with 5 MeV accelerated electrons will be similar to single phase ceramics. Previously, the formation and accumulation of RD and RP in Li_4SiO_4 and Li_2TiO_3 ceramics under the action of neutron fluence, accelerated electrons and gamma rays have been investigated and described separately by several authors [18–25]. The formation and accumulation of RD and RP takes place through two stages: (1) fast generation of primary RD and RP on structural defects and impurities, and (2) slow generation due to the radiolysis of the basic matrix. As soon as the structural defects have been consumed, the formation of RD and RP occurs only at the crystalline lattice. The thermal pre-treatment decreases the amount of structural defects, which may remain in the pebbles after the fabrication process, and thus it is anticipated that the thermally pre-treated pebbles will have higher radiation stability. Previously, the accumulated RD, such as, E' centres (SiO_3^{3-} and TiO_3^{3-}), HC_2 centres (SiO_4^{3-} and TiO_3^{-}), peroxide radicals (≡Si—O—O•) and Ti^{3+} centres, in the advanced pebbles were annihilated up to 650 K [6] and it has been expected, that during irradiation with temperatures higher than 500 K, the recombination processes of RD will dominate. Therefore, the formation of thermally stable RP is mainly expected, such as, colloidal lithium (Li_n) particles, elementary silicon (Si_n), molecular oxygen (O_2), silanol (≡Si—Si≡), disilicate (≡Si—O—Si≡) and peroxide (≡Si—O—O—Si≡) bonds.

After irradiation with 5 MeV accelerated electrons up to 100 MGy absorbed dose at 500–1120 K, a colour change of the advanced Li_4SiO_4 pebbles was observed and the pebbles turned grey or black. Most likely, this effect is related to the formation and accumulation of optically active RD and RP, such as, F^+ and F^{00} centres (localised electrons in oxygen vacancies), Li_n particles etc. During irradiation at elevated temperatures, the radiolysis of the primary phase and the secondary phase can be expected to cause recrystallization and grain growth. However, major changes in the *p*-XRD patterns were not observed after irradiation (Fig. 1) and this effect could be related to the small radiolysis degree (α) of Li_4SiO_4 ($\alpha_{1000MGy}$ = 0.1–1 mol% [18]) and Li_2TiO_3 ($\alpha_{500MGy} = 10^{-3}$ mol% [18]) and the detection limits of this method. The radiolysis degree is the percentage proportion of the decomposed molecules/ions versus the initial number of molecules/ions before irradiation. The detection limit of the *p*-XRD analysis depends on several factors (preferred orientation, texturing and particle size etc.), nevertheless, the detection

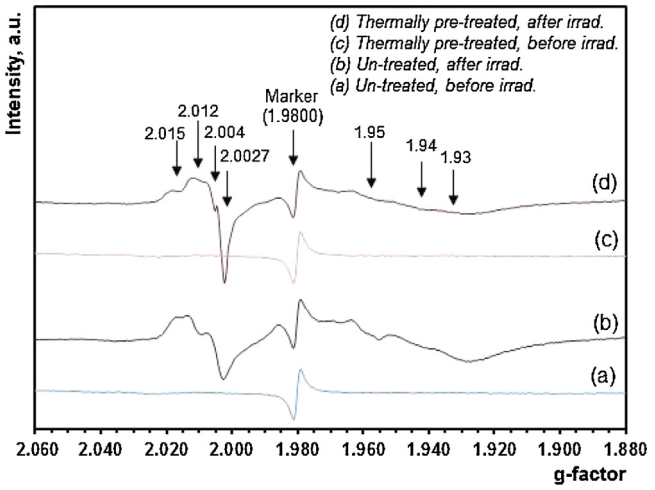

Fig. 2. ESR spectra of the un-treated and thermally pre-treated advanced Li_4SiO_4 pebbles with 10 mol% Li_2TiO_3 before and after irradiation with 5 MeV accelerated electrons up to 100 MGy absorbed dose at 500–1120 K in a dry argon atmosphere.

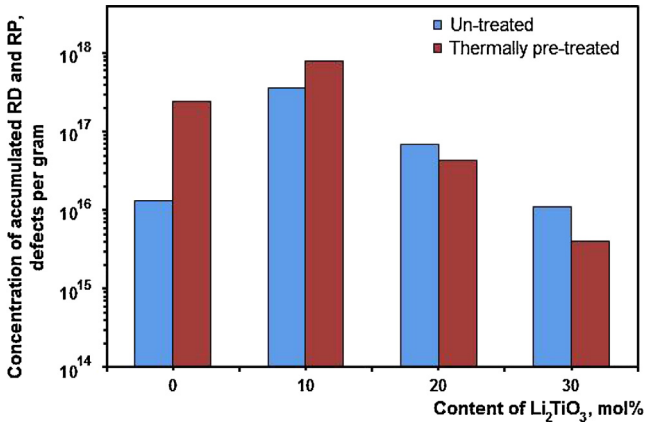

Fig. 3. The total concentration of accumulated paramagnetic RD and RP in the un-treated and thermally pre-treated Li_4SiO_4 pebbles with different contents of Li_2TiO_3 after irradiation with 5 MeV accelerated electrons up to 100 MGy absorbed dose at 500–1120 K in a dry argon atmosphere.

limit is typically around 0.1–1 wt.% for the samples with a mixed composition.

The ESR spectra of both the un-treated and thermally pre-treated advanced Li_4SiO_4 pebbles with 10 mol% Li_2TiO_3 before and after irradiation are shown in Fig. 2. In the ESR spectra, at least two groups of the first derivative signals were detected. The first group consists of four signals with g-factors from 2.015 to 2.002, while the second group of three signals is observed from 1.95 to 1.93. The signals of both groups have a similar shape, g-factor and linewidth to the signals, which were investigated and described in the single phase materials. Therefore, the ESR signals with a g-factor 2.012 ± 0.001 and 2.015 ± 0.001 were assigned to HC_2 centres (SiO_4^{3-} and TiO_3^{-}), while the signal with a g-factor of 2.004 ± 0.001 was attributed to E' centres (SiO_3^{3-} and TiO_3^{3-}). Presumably, the narrow ESR signal (singlet, $g = 2.0027$, $\Delta H < 0.2$ mT) could be associated with Li_n particles. The overlapping and wide signals with a g-factor from 1.95 to 1.93 might be associated to Ti^{3+} centres [26].

The E′ centres together with HC_2 centres are the primary stage electron and hole type RD, while Li_n particles (electron type RP) form in the second and third stage reactions of the radiolysis [19]. The Li_n particles form due to the aggregation of electron centers (F_n centers) and the following two kinds of particles may form – the fine particles with size <1 μm (Lorentz ESR line, $g = 2.0025$ and $\Delta H < 10^{-2}$ mT [18]) and coarse particles with a size of 1–10 μm (ESR singlet, $g = 2.0035$ and $\Delta H = 10$ mT [18]). Presumably, the signal of broad Li_n particles in the ESR spectra of the advanced pebbles cannot be observed due to overlapping with other signals. The accumulated RD and RP in single phase materials, Li_4SiO_4 and Li_2TiO_3, are stable up to 700 K [12,13]. Therefore, due to the high irradiation temperature (500–1120 K), the concentration of the accumulated paramagnetic RD and RP in the advanced Li_4SiO_4 pebbles is quite small (around 10^{15}–10^{18} defects g^{-1}). The total concentration of the accumulated RD and RP was calculated from the ESR results using a double integration method, and the results versus the content of Li_2TiO_3 are shown in Fig. 3. The irradiation temperature of the un-treated and thermally pre-treated Li_4SiO_4 pebbles with 0, 10, 20 and 30 mol% Li_2TiO_3 during the third irradiation cycle is comparable (range: 770–900 K) and thus these pebbles can be compared with each other. While, the detected concentration of paramagnetic RD and RP in the advanced pebbles with 25 and 40 mol% Li_2TiO_3 is slightly higher in comparison with other pebbles, most likely due to the smaller irradiation temperature in the last irradiation cycle (500–540 K), and thus these results were not included in Fig. 3.

A previous irradiation study [6] already confirmed that the irradiation temperature has a significant impact on the formation and accumulation of paramagnetic RD and RP in the advanced Li_4SiO_4 pebbles. Therefore, the minor changes in the concentration of the accumulated RD and RP in the un-treated and thermally pre-treated pebbles could be attributed to the differences in the irradiation temperature. Nevertheless, Li_2TiO_3 has a smaller decomposition degree and radiation chemical yield of RD than Li_4SiO_4 [18], and thus with increasing content of Li_2TO_3 as a secondary phase, the concentration of accumulated RD and RP in the advanced pebbles decreases. It has been assumed that the slight increase of accumulated RD and RP in the advanced pebbles with 10 mol% Li_2TiO_3 in comparison with the reference pebbles (0 mol% Li_2TiO_3) could be related to the structural defects (cracks, open and closed pores), which may form during the fabrication process due to the density differences between the liquid and the crystallised state.

To supplement the results of ESR spectrometry, the TSL glow curves and spectra of the advanced and the reference Li_4SiO_4 pebbles were measured. The thermally stimulated recombination of paramagnetic RD and RP in the advanced pebbles have been analysed in the previous research [6] and the correlation between results of the ESR spectrometry and the TSL technique have been detected. During heating, the luminescence emission occurs, due to the recombination reactions between various hole type RD and electron type RD and RP. The TSL glow curves of the pebbles (heating rate: 5 K s^{-1}) exhibit similar behaviour consisting of four peaks, three intense peaks at 450, 510 and 550 K and one weak maximum peaked in the range of 600–773 K regardless of the Li_2TiO_3 content (Fig. 4). Additionally, one can appreciate how the presence of Li_2TiO_3 practically do not affect to the shape of the TSL glow curves, number and position of peaks and therefore it has been assumed that similar hole-electron recombination processes occur in the advanced pebbles similar to the reference pebbles (0 mol% Li_2TiO_3). No signal was detected when measuring luminescence spectra with CCD camera and spectrometer in TSL peaks (heating rate: 2 K s^{-1}) as the intensity of emission was below the sensitivity limit of the detection system (TSL signal was observed only with photomultiplier tube connected directly). Previously, in the spectra of the reference pebbles at least two main bands with the maximum around 2.6-2.9 and 3.5-3.7 eV have been detected [24,27]. The luminescence band with the maximum around 2.6-2.9 eV most likely could be associated with E' centres (SiO_3^{3-}) [28], while the band with the maximum around 3.5–3.7 eV could be related to HC_2 centres (SiO_4^{3-}) [27].

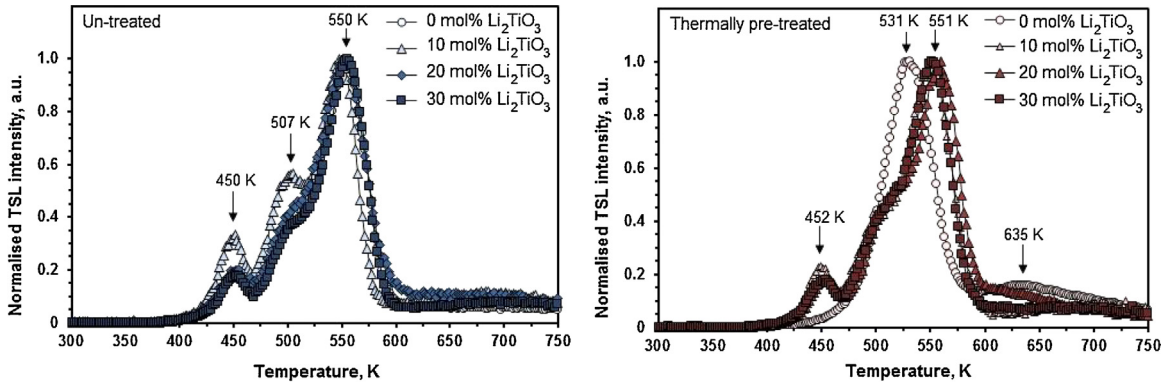

Fig. 4. Normalised TSL curves (heating rate: 5 K s^{-1}) of the un-treated and thermally treated Li_4SiO_4 pebbles with different contents of Li_2TiO_3 after irradiation with 5 MeV accelerated electrons up to 100 MGy absorbed dose at 500–1120 K in a dry argon atmosphere.

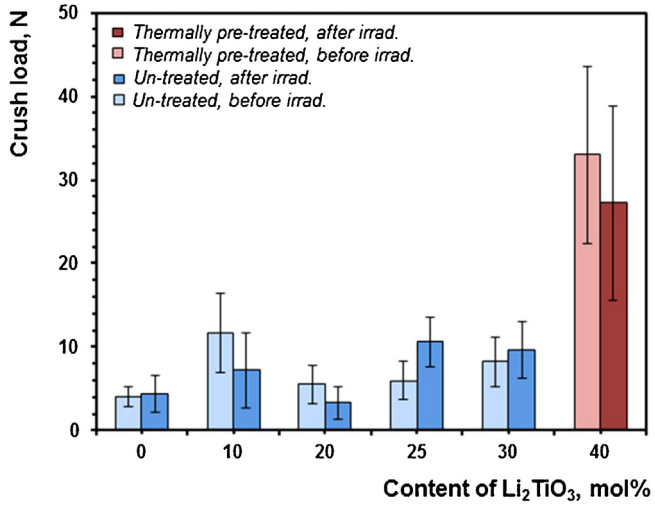

Fig. 5. Average crush load values of the Li_4SiO_4 pebbles with different contents of Li_2TiO_3 before and after irradiation with 5 MeV accelerated electrons up to 100 MGy absorbed dose at 500–1120 K in a dry argon atmosphere. The pebbles with 0, 20, 25 and 30 mol% of Li_2TiO_3 have a diameter of 500 μm and the pebbles with 10 and 40 mol% of Li_2TiO_3 have a diameter of 1000 μm.

The high-temperature radiolysis may cause changes to the microstructure of the advanced Li_4SiO_4 pebbles, due to the molecular oxygen evolution and the formation of micro-pores, cracks and dislocations. Therefore, to complement the results of *p*-XRD, ESR spectrometry and the TSL technique, the mechanical properties and the microstructure of the advanced Li_4SiO_4 pebbles before and after irradiation were studied by uniaxial compressive crush load tests and SEM, respectively. The crush load is dependent on the pebble size [29] and thus only mono-sized pebbles with diameters of 500 or 1000 μm were analysed. 40 individual pebbles were used to determine the average crush load for each sample and the results for the Li_4SiO_4 pebbles with different contents of Li_2TiO_3, both before and after irradiation, are shown in Fig. 5. The advanced pebbles with additions of 10 mol% and 40 mol% Li_2TiO_3 have a diameter 1000 μm and thus, the average crush load values are generally larger. The large standard deviation of the results is very common for ceramics and can be attributed to small differences in the pebble microstructure including structural defects, minor variations in the pebble size or the composition, as well as different orientations between the sapphire plates during the compression test. It can therefore be said, that the crush load of the pebbles practically does not change after irradiation and the minor differences are within the limits of the standard deviation, however, it is not excluded that these differences could partly also be attributed to the influence of various irradiation temperatures.

The microstructures of the Li_4SiO_4 pebbles with different contents of Li_2TiO_3, which were analysed by SEM at etched cross-sections before and after irradiation, are shown in Fig. 6. The chemical compositions of the pebbles are given in the upper row. In the reference pebbles (0 mol% Li_2TiO_3), the dendritic Li_4SiO_4 phase is displayed in a dark grey colour with inclusions of light grey grains of Li_2SiO_3. On the other hand, in the advanced pebbles with content up to 25 mol% Li_2TiO_3, light grey grains of the secondary phase are very small and homogeneously distributed as inclusions between the Li_4SiO_4 dendrites, which appear dark-grey. For the advanced pebbles with 30 and 40 mol% Li_2TiO_3, it can be seen that the lighter Li_2TiO_3 phase is the dominant crystal, taking a clear dendritic shape. In this case, the Li_4SiO_4 phase fills in the gaps between the Li_2TiO_3 dendrites, indicating a reverse in the crystallisation order. As expected from the results of the crush load test, the microstructure of the advanced pebbles after irradiation is only slightly changed. After irradiation, agglomeration of pores and cracking, due to the high irradiation temperature, can be seen. Nevertheless, it can be concluded that the advanced pebbles after irradiation maintain a microstructure comparable to the non-irradiated pebble.

On the basis of the obtained results, it can be concluded that the advanced Li_4SiO_4 pebbles with different contents of Li_2TiO_3 maintain a comparable radiation stability with the reference pebbles after the simultaneous action of 5 MeV accelerated electron beam (up to 10 MGy h^{-1}) and high temperature (up to 1120 K) in a dry argon atmosphere. The additions of Li_2TiO_3 as a secondary phase in the advanced Li_4SiO_4 pebbles does not provide new or different RD and RP, which could act as possible tritium scavenger centres, and thus it is expected that the tritium diffusion and release processes will be similar to single phase materials – Li_4SiO_4 pebbles and Li_2TiO_3 pebbles. The accumulated RD and RP annihilates around 423–773 K and thus it has been suggested that the main tritium release peaks could be expected in this temperature range. The preliminary deuterium and tritium release studies [7,30] confirm these assumptions, however additional research on the tritium release from the advanced pebbles is required to evaluate the applicability of the breeder pebbles.

4. Conclusion

The advanced Li_4SiO_4 pebbles with different contents of Li_2TiO_3 were examined before and after the simultaneous action of 5 MeV accelerated electron beam (dose rate: up to 10 MGy h^{-1}) and high

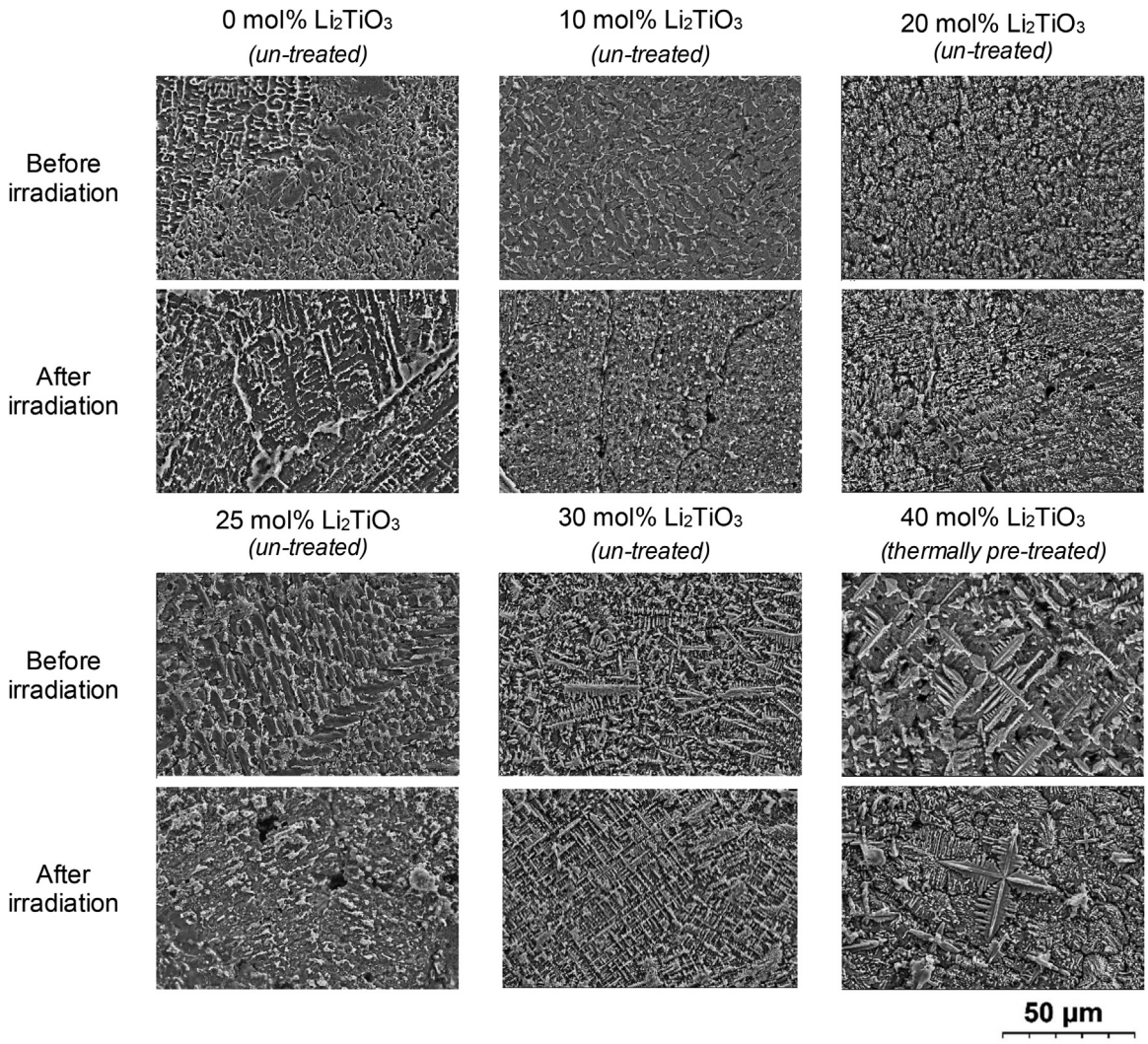

Fig. 6. SEM images of the Li_4SiO_4 pebbles with different contents of Li_2TiO_3 before and after irradiation with 5 MeV accelerated electrons up to 100 MGy absorbed dose at 500–1120 K in a dry argon atmosphere.

temperature (up to 1120 K) in a dry argon atmosphere. During the irradiation of the advanced Li_4SiO_4 pebbles, the recombination processes of RD dominated and the thermally stable RP were mainly accumulated. ESR spectrometry corroborates that in the advanced pebbles, several paramagnetic RD and RP, which are similar to single phase ceramics, are accumulated, namely, E' centres (SiO_3^{3-} and TiO_3^{3-}), HC_2 centres (SiO_4^{3-} and TiO_3^{-}), Li_n particles and Ti^{3+} centres. As well as the irradiation temperature that has a significant impact on the formation of RD and RP, and with an increasing content of Li_2TO_3, the concentration of accumulated paramagnetic RD and RP decreases. The TSL technique confirmed that the accumulated RD and RP recombine around 423–773 K. Major changes in the mechanical properties, microstructure and phase composition were not detected after irradiation.

Acknowledgements

The authors greatly acknowledge the technical and experimental support of O. Valtenbergs and L. Avotina (Institute of Chemical Physics, University of Latvia). The work is performed in the frames of the University of Latvia financed project No. Y9-B044-ZF-N-300, "Nano, Quantum Technologies, and Innovative Materials for Economics".

References

[1] R. Knitter, P. Chaudhuri, Y.J. Feng, T. Hoshino, I.-K. Yu, J. Nucl. Mater. 442 (2013) S420–S424.
[2] J. Tiliks, A. Vitins, G. Kizane, V. Tilika, E. Kolodinska, S. Kaleja, B. Lescinskis, Fusion Eng. Des. 84 (2009) 1842–1846.
[3] S. van Til, A.V. Fedorov, A.J. Magielsen, Fusion Eng. Des. 87 (2012) 885–889.
[4] L.V. Boccaccini, et al., Fusion Eng. Des. 109–111 (2016) 1199–1206.
[5] R. Knitter, M.H.H. Kolb, U. Kaufmann, A.A. Goraieb, J. Nucl. Mater. 442 (2013) S433–S436.
[6] A. Zarins, et al., J. Nucl. Mater. 470 (2016) 187–196.
[7] M. Gonzalez, E. Carella, A. Morono, M.H.H. Kolb, R. Knitter, Fusion Eng. Des. 98–99 (2015) 1771–1774.
[8] K. Mukai, P. Pereslavtsev, U. Fisher, R. Knitter, Fusion Eng. Des. 100 (2015) 565–570.
[9] O. Leys, T. Bergfeldt, M.H.H. Kolb, R. Knitter, A.A. Goraieb, Fusion Eng. Des. 107 (2016) 70–74.
[10] G. Piazza, A. Erbe, R. Rolli, O. Romer, J. Nucl. Mater. 329–333 (2004) 1260–1265.
[11] G. Piazza, F. Scaffidi-Argentina, H. Werle, J. Nucl. Mater. 283–287 (2000) 1396–1400.
[12] Y. Nishikawa, M. Oyaidzu, A. Yoshikawa, K. Munakata, M. Okada, M. Nishikawa, K. Okuno, J. Nucl. Mater. 367–370 (2007) 1371–1376.
[13] M. Oyaidzu, et al., J. Nucl. Mater. 329–333 (2004) 1313–1317.
[14] G. Kizane, J. Tiliks, A. Vitins, J. Rudzitis, J. Nucl. Mater. 329–333 (2004) 1287–1290.
[15] S. Akahori, et al., J. Radiochem. Nucl. Chem. 255 (2003) 257–260.
[16] R. Knitter, B. Alm, G. Roth, J. Nucl. Mater. 367–370 (2007) 1387–1392.
[17] D.A.H. Hanaor, M.H.H. Kolb, Y. Gan, M. Kamlah, R. Knitter, J. Nucl. Mater. 456 (2014) 151–161.

[18] J. Tiliks, G. Kizane, A. Vitins, G. Vitins, J. Meisters, Fusion Eng. Des. 69 (2003) 519–522.
[19] J.E. Tiliks, G.K. Kizane, A.A. Supe, A.A. Abramenkovs, J.J. Tiliks, V.G. Vasiljev, Fusion Eng. Des. 17 (1991) 17–20.
[20] V. Grismanovs, T. Kumada, T. Tanifuji, T. Nakazawa, Radiat. Phys. Chem. 58 (2000) 113–117.
[21] A. Zarins, G. Kizane, A. Supe, R. Knitter, M.H.H. Kolb, J. Tiliks Jr., Fusion Eng. Des. 89 (2014) 1426–1430.
[22] E. Carella, M. Leon, T. Sauvage, M. Gonzalez, Fusion Eng. Des. 89 (2014) 1529–1533.
[23] M. Gonzalez, V. Correcher, J. Nucl. Mater. 445 (2014) 149–153.
[24] E. Feldbach, et al., Nucl. Instr. Meth. B 250 (2006) 159–163.
[25] V. Correcher, M. Gonzalez, Nucl. Instr. Meth. B 326 (2014) 86–89.
[26] P. Lombard, N. Ollier, B. Boizot, J. Non-Cryst. Solids 357 (2011) 1685–1689.
[27] A. Zarins, A. Supe, G. Kizane, R. Knitter, L. Baumane, J. Nucl. Mater. 429 (2012) 34–39.
[28] K. Moritani, S. Tanaka, H. Moriyama, J. Nucl. Mater. 281 (2000) 106–111.
[29] R.K. Annabattula, M. Kolb, Y. Gan, R. Rolli, M. Kamlah, Fusion Sci. Technol. 66 (2014) 136–141.
[30] M.H.H. Kolb, R. Rolli, R. Knitter, J. Nucl. Mater. 489 (2017) 229–235.

Journal of Nuclear Materials 470 (2016) 187–196

Contents lists available at ScienceDirect

Journal of Nuclear Materials

journal homepage: www.elsevier.com/locate/jnucmat

Formation and accumulation of radiation-induced defects and radiolysis products in modified lithium orthosilicate pebbles with additions of titanium dioxide

Arturs Zarins [a, b, *], Oskars Valtenbergs [a, b], Gunta Kizane [a], Arnis Supe [a], Regina Knitter [c], Matthias H.H. Kolb [c], Oliver Leys [c], Larisa Baumane [a, d], Davis Conka [a, b]

[a] University of Latvia, Institute of Chemical Physics, Jelgavas Street 1, LV-1004, Riga, Latvia
[b] University of Latvia, Faculty of Chemistry, Jelgavas Street 1, LV-1004, Riga, Latvia
[c] Karlsruhe Institute of Technology, Institute for Applied Materials (IAM-KWT), 76021, Karlsruhe, Germany
[d] Latvian Institute of Organic Synthesis, Aizkraukles Street 21, LV-1006, Riga, Latvia

HIGHLIGHTS

- Formation of RD and RP in modified Li_4SiO_4 pebbles with additions of TiO_2 is analysed for the first time.
- Due to additions of TiO_2, concentration of paramagnetic RD slightly increased in modified Li_4SiO_4 pebbles.
- Modified Li_4SiO_4 pebbles have good radiation stability compared to reference pebbles.
- Irradiation temperature has significant impact on radiolysis of modified Li_4SiO_4 pebbles.

ARTICLE INFO

Article history:
Received 3 June 2015
Received in revised form
21 December 2015
Accepted 22 December 2015
Available online 24 December 2015

Keywords:
Tritium breeding ceramic
Lithium orthosilicate
Radiolysis
Accelerated electrons
Irradiation temperature

ABSTRACT

Lithium orthosilicate (Li_4SiO_4) pebbles with 2.5 wt.% excess of silicon dioxide (SiO_2) are the European Union's designated reference tritium breeding ceramics for the Helium Cooled Pebble Bed (HCPB) Test Blanket Module (TBM). However, the latest irradiation experiments showed that the reference Li_4SiO_4 pebbles may crack and form fragments under operation conditions as expected in the HCPB TBM. Therefore, it has been suggested to change the chemical composition of the reference Li_4SiO_4 pebbles and to add titanium dioxide (TiO_2), to obtain lithium metatitanate (Li_2TiO_3) as a second phase. The aim of this research was to investigate the formation and accumulation of radiation-induced defects (RD) and radiolysis products (RP) in the modified Li_4SiO_4 pebbles with different contents of TiO_2 for the first time, in order to estimate and compare radiation stability. The reference and the modified Li_4SiO_4 pebbles were irradiated with accelerated electrons (E = 5 MeV) up to 5000 MGy absorbed dose at 300–990 K in a dry argon atmosphere. By using electron spin resonance (ESR) spectroscopy it was determined that in the modified Li_4SiO_4 pebbles, several paramagnetic RD and RP are formed and accumulated, like, E' centres (SiO_3^{3-}/TiO_3^{3-}), HC_2 centres (SiO_4^{3-}/TiO_3^{-}) etc. On the basis of the obtained results, it is concluded that the modified Li_4SiO_4 pebbles with TiO_2 additions have comparable radiation stability with the reference pebbles.

1. Introduction

In the International Thermonuclear Experimental Reactor (ITER, Cadarache, France) several concepts of Test Blanket Modules (TBMs) will be tested and verified, because the tritium breeding is a key issue in future burning plasma machines, like, DEMO (Demonstration fusion power plant) [1–5]. The Helium Cooled Pebble Bed (HCPB) TBM, proposed by the European Union, will use lithium orthosilicate (Li_4SiO_4) pebbles with 2.5 wt% excess of silicon dioxide (SiO_2) as the reference tritium breeding ceramic [4–7]. Due to the excess of SiO_2, the reference pebbles have two phases – 90 mol% Li_4SiO_4 and 10 mol% lithium metasilicate (Li_2SiO_3) [8–10].

* Corresponding author. University of Latvia, Institute of Chemical Physics, Jelgavas Street 1, LV-1004, Riga, Latvia.
E-mail address: arturs.zarins@lu.lv (A. Zarins).

http://dx.doi.org/10.1016/j.jnucmat.2015.12.027
0022-3115/

The reference Li_4SiO_4 pebbles with 2.5 wt% excess of SiO_2 have appropriate properties for the tritium breeding, i.e. a high lithium density (up to 0.54 g cm^{-3}) and melting point (eutectic point at 1298 K), a good tritium release behaviour and chemical compatibility with structural materials, i.e. Eurofer steel [6,7]. However, beside the main task to produce and release tritium, the reference pebbles must also be able to withstand the harsh conditions as expected during exploitation.

The tritium breeding ceramic in the HCPB TBM will be simultaneously exposed to an intense neutron flux (up to 10^{18} neutrons m^{-2} s^{-1}), ionizing radiation dose rate (up to 1 kGy s^{-1}), a high magnetic field (7–10 T) and elevated temperatures (570–1190 K) [1,5,11,12].

The latest neutron irradiation experiments [13] showed that the reference Li_4SiO_4 pebbles will likely perform sufficiently well in the HCPB TBM. However, it has also been reported that the reference pebbles may crack and form fragments during irradiation. Therefore, it has been suggested to increase the mechanical stability of the reference pebbles, so that the pebbles withstand the operation conditions as expected in the HCPB TBM.

One possible option to increase the mechanical stability of the tritium breeding ceramic is to change the chemical composition of the reference Li_4SiO_4 pebbles by adding titanium dioxide (TiO_2) [6,7]. Due to the additions of TiO_2, lithium metatitanate (Li_2TiO_3) is obtained as a secondary phase in the modified Li_4SiO_4 pebbles. Li_2TiO_3 pebbles are also approved as a "back-up" solution for the tritium breeding in the HCPB TBM, due to the good tritium release behaviour and appropriate mechanical, thermal and chemical properties [4–7,13,14]. Therefore, in combining these two phases – Li_4SiO_4 and Li_2TiO_3 – it is anticipated to obtain a modified tritium breeding ceramic with improved mechanical properties, without losing the benefit of the high lithium density, melting temperature and good tritium release behaviour.

However, to develop a new chemical composition for the tritium breeding ceramic, it is a critical issue to understand the physico-chemical processes (e.g. radiolysis), phase transitions and micro-structural changes, which will occur during irradiation. From previous studies [15–17], it is known that the formation, accumulation and annihilation of radiation-induced defects (RD) and radiolysis products (RP) may occur in the ceramic during irradiation. Such RD and RP will induce changes of thermal and mechanical properties, swelling and degradation of mechanical integrity, and may also affect the tritium diffusion and release process [15–34].

The aim of this research was to investigate the formation and accumulation of RD and RP in the modified Li_4SiO_4 pebbles with different TiO_2 contents for the first time, in order to estimate and compare the radiation stability.

2. Literature review

For now, the modified Li_4SiO_4 pebbles with additions of TiO_2 have only been investigated by a few groups of researchers and thus there is a gap in the theoretical and practical knowledge about this ceramic. The first articles about the fabrication and development of the modified pebbles were published by R. Knitter et al. [7] and O. Leys et al. [35]. It was found that the additions of TiO_2 in the Li_4SiO_4 pebbles significantly increased the crush load, while the closed porosity slightly increased with increasing the content of TiO_2.

D. A.H. Hanaor et al. [36] made a behavioural phase transformation diagram of the quasi-binary Li_4SiO_4–Li_2TiO_3 system, to understand the phase stability and melting of the modified Li_4SiO_4 pebbles. It was reported that the mixed phase material shows liquid formation from the melting of the Li_4SiO_4 phase at temperatures >1373 K.

M. Gonzalez et al. [37] investigated the influence of the radiation-induced processes on the sorption and desorption of deuterium (D_2) in the modified Li_4SiO_4 pebbles. It was shown that the mechanisms of D_2 desorption in the modified pebbles highly depends on the radiation-induced effects.

However, until now, the radiolysis of the modified Li_4SiO_4 pebbles was not analysed, and thus additional research is required, to understand the formation, accumulation and annihilation of RD and RP during irradiation at elevated temperature. Previously, the radiolysis of the reference Li_4SiO_4 pebbles and the Li_2TiO_3 pebbles have been investigated separately.

2.1. Radiolysis of the reference Li_4SiO_4 pebbles with excess of SiO_2

The reference Li_4SiO_4 pebbles with excess of SiO_2 have two crystalline phases – Li_4SiO_4 as the primary phase and Li_2SiO_3 as a secondary phase. The radiolysis of the Li_4SiO_4 ceramic and the Li_2SiO_3 ceramic have been analysed and described by several authors [15–25]. Both, Li_4SiO_4 and Li_2SiO_3 have chemical bonds [≡Si–O^- Li^+] and thus the mechanisms of the radiolysis and the structure of the formed RD and RP will be similar in both cases. Therefore, the radiolysis of a secondary phase, Li_2SiO_3, in the reference pebbles will not be discussed separately in this research.

The mechanism of the radiolysis is the same for the Li_4SiO_4 powders, pebbles, pellets and other ceramics; only the quantitative parameters of the radiolysis are different [25]. The localisation of RD and RP takes place through two stages. In the first stage, primary RD and RP localise mainly on structural defects and impurities, while in the second stage, the radiolysis of the matrix occurs. At the second stage in bulk ceramics (pebbles, pellets etc.), the formation of RD and RP proceeds slowly in comparison with the powders. Therefore, dense ceramic materials usually have higher radiation stability in comparison with powders.

A. Abramenkovs et al. [16] and J. Tiliks et al. [15,17,25] reported that the radiolysis of the reference Li_4SiO_4 pebbles can be divided into three main stages. In the first stage, primary electron and hole type RD, like, E' centres (≡Si· or SiO_3^{3-}) and HC_2 centres (≡Si–O· or SiO_4^{3-}), are formed (Eqs. (1) and (2)). The symbol "≡" represents three bonds to three oxygen atoms in the crystal structure.

$$SiO_4^{4-} \rightsquigarrow SiO_4^{3-}\ (HC_2\ centre) + e^- \quad (1)$$

$$SiO_4^{4-} + e^- \rightarrow SiO_3^{3-}(E'centre) + O^{2-} \quad (2)$$

In the second stage of the radiolysis, secondary RD, like peroxide radicals (≡Si–O–O·) and chemically stable molecular compounds – RP, are generated (Eqs. (3)–(7)). The major RP are colloidal lithium (Li_n), elementary silicon (Si_n), molecular oxygen (O_2), silanol (≡Si–Si≡), disilicate (≡Si–O–Si≡) and peroxide (≡Si–O–O–Si≡) bonds.

$$n\ Li^+ + n\ e^- \rightarrow Li_n \quad (3)$$

$$\equiv Si - O\cdot\ (HC_2 centre) + \ \cdot O - Si\equiv \rightarrow \equiv Si - O - Si\equiv + {}^1\!/_2\, O_2 \quad (4)$$

$$\equiv Si\cdot\ (E'centre) + O_2 \rightarrow \equiv Si - O - O\cdot \quad (5)$$

$$\equiv Si\cdot + \cdot Si\equiv \rightarrow \equiv Si - Si\equiv \quad (6)$$

$$\equiv Si - O - O\cdot + \cdot Si\equiv \rightarrow \equiv Si - O - O - Si\equiv \quad (7)$$

In the third and final stage of the radiolysis, chemical reactions between RP proceed and chemical compounds, for example lithium oxide (Li_2O), are formed.

In previous studies, the radiolysis of the Li_4SiO_4 pebbles, pellets and powders were analysed by several physical and chemical methods [15–25]. The main physical methods, which can be used to analyse the accumulated RD and RP, are electron spin resonance (ESR) spectroscopy, thermally stimulated luminesce (TSL) and radio-luminesce (RL) techniques, powder X-ray diffraction (p-XRD), Raman and Fourier transform infrared (FT-IR) spectroscopy. The chemical methods, such as the method of chemical scavengers (MSC) or lyo-luminescence (LL) technique, are sample destructive methods and are based on the difference of redox properties of hole and electron type RD and RP in acid containing solvents. The gaseous RP, for example molecular O_2, can be detected and analysed by gas chromatography.

It was determined that the reference Li_4SiO_4 pebbles with 2 wt% excess of SiO_2 have a good radiation stability [17]. The initial chemical yield of RD and RP ($G_{RD\ and\ RP}$) and the radiolysis degree (α) were selected as the main comparable parameters of the radiation stability. The initial chemical yield is the number of a particular species, like, RD and RP, produced per 100 eV of energy loss of the charged particle or electromagnetic radiation. The radiolysis degree is the percentage proportion of the decomposed molecules/ions versus the initial number of molecules/ions before irradiation. In the reference pebbles, the radiation chemical yield of RD and RP is 0.1–0.4 localised electrons per 100 eV and the radiolysis degree is 0.1–1 mol% after irradiation up to 1000 MGy absorbed dose.

2.2. Radiolysis of Li_2TiO_3 pebbles

The radiolysis of the Li_2TiO_3 pellets and pebbles have been investigated and described by several authors [17,25–33]. However, extensive research with chemical methods, i.e. the MSC and LL technique, are limited in literature, due to the low solubility of Li_2TiO_3 [38]. Therefore, the formation of RD and RP in the Li_2TiO_3 ceramic were analysed only by physical methods, like, ESR spectroscopy, TSL and RL technique etc.

V. Grismanovs et al. [29] and J. Tiliks et al. [17] using ESR spectroscopy detected the formation of electron and hole type RD – E' centres (TiO_3^{3-}) and HC_2 centres (TiO_3^{-}), in the Li_2TiO_3 ceramic after irradiation (Eqs. (8) and (9)). At the same time, the formation of Li_n particles was not detected up to 500 MGy absorbed dose.

$$TiO_3^{2-} \rightsquigarrow TiO_3^{-}\ (HC_2\ centre) + e^{-} \quad (8)$$

$$TiO_3^{2-} + e^{-} \rightarrow TiO_3^{3-}\ (E'centre) \quad (9)$$

It was determined that the Li_2TiO_3 pebbles have very high radiation stability [17]. The initial radiation chemical yield of RD is approximately 10^{-2} defects per 100 eV and the radiolysis degree is around 10^{-3} mol% at 500 MGy absorbed dose.

3. Experimental

Three types of the modified Li_4SiO_4 pebbles with different contents of TiO_2 (screened to 650–900 μm) were selected for investigation together with the reference pebbles (Table 1). The reference and the modified pebbles were produced by an *enhanced* melting process at the Karlsruhe Institute of Technology (Karlsruhe, Germany) [7–9,39]. To achieve an operation relevant microstructure, the fabricated pebbles were annealed at 1220 K for 504 h in air.

3.1. Preparation and irradiation of samples

As mentioned above, the tritium breeding ceramic in the HCPB TBM will be subjected to an intense neutron and ionizing radiation at elevated temperatures. During irradiation, the formation of RD and RP, atomic displacements and nuclear reactions will occur in the tritium breeding ceramic [40]. However, in order to study the RD and RP while avoiding the formation of tritium and other nuclear reactions, an accelerated electron flux (E = 5 MeV) was used as a preliminary approach in this research.

The reference and the modified Li_4SiO_4 pebbles were encapsulated in quartz tubes with dry argon and were irradiated by a linear electron accelerator ELU-4 (Salaspils, Latvia), up to 5 h per day (Table 2). The irradiation was performed up to 24 MGy absorbed dose at 300–345 K and up to 5000 MGy absorbed dose at 380–990 K temperature.

Several quartz tubes with the reference and the modified Li_4SiO_4 pebbles during irradiation at 380–990 K were broken, most likely due to the high temperature difference during one of the irradiation cycles.

To investigate the thermal stability and annihilation of the paramagnetic RD and RP, the irradiated reference and modified Li_4SiO_4 pebbles were thermally treated up to 1023 K for 20 min in an inert atmosphere.

3.2. Methods of characterisation

The formation, accumulation and annihilation of RD and RP in the reference and the modified Li_4SiO_4 pebbles were analysed by ESR spectroscopy and TSL technique. The ESR spectra were recorded by a Bruker BioSpin X-band ESR spectrometer (microwave frequency: 9.8 GHz, microwave power: 0.2 mW, modulation amplitude: 5 G, field sweep: 200 and 1000 G) operating at room temperature. The TSL glow curves were measured up to 773 K (heating rate: 0.1, 0.5, 1 and 2 K s^{-1}). The TSL spectra were measured up to 650 K (heating rate: 0.1 K s^{-1}) with an Andor Shamrock B-303i spectrograph equipped with a CCD camera (Andor DU-401A-BV). The heating rate of 0.1 K s^{-1} was selected to prevent the possible overlapping of expected TSL signals.

The phase transitions in the reference and the modified Li_4SiO_4 pebbles were analysed by qualitative p-XRD and FT-IR spectroscopy. The p-XRD patterns were obtained by a Bruker D8 (range: 10–50° 2theta, scan speed: 0.05° 2theta, anode current: 40 mA, voltage: 40 kV, source: CuKα, wavelength: 0.15418 nm) and the FT-IR spectra by a Perkin Elmer Spectrum Two (range: 450–4000 cm^{-1}, resolution: 4 cm^{-1}, pressed in KBr tablets).

The microstructure of the reference and the modified Li_4SiO_4 pebbles was investigated at etched cross-sections by a Field Emission Scanning Electron Microscope (FE-SEM) Zeiss, Supra 55. The chemical composition of the pebble surface was analysed by a FE-SEM Hitachi S-4800 using an Energy-dispersive X-ray spectroscopy (EDS) system Bruker XFlash Quad 5040 123 eV.

The metallic trace-impurities in the reference and in the modified Li_4SiO_4 pebbles were detected by X-ray fluorescence (XRF) spectroscopy and the absorbed gases by thermogravimetry-differential thermal analysis (TG-DTA). The TG-DTA curves were obtained by a Seiko EXTAR 6300 (temperature range: 290–1273 K, heating rate: 10 K min^{-1}, atmosphere: argon, gas flow: 100–150 ml min^{-1}) and the XRF spectra by a Bruker S8-TIGER (pebbles and powder, on 5 μm polyethylene film, helium atmosphere).

4. Results and discussion

The modified Li_4SiO_4 pebbles with additions of TiO_2 show a light pink, brown or yellow colour before irradiation, while the reference pebbles are “pearl” white (Table 1). Using p-XRD and FT-IR spectroscopy it has been observed that the modified pebbles feature

Table 1
Specification of the investigated reference and modified Li_4SiO_4 pebbles (diameter: 650–900 μm).

Parameter	Reference pebbles	Modified pebbles		
		# 1	# 2	# 3
Chemical composition	90 mol% Li_4SiO_4 10 mol% Li_2SiO_3	90 mol% Li_4SiO_4 10 mol% Li_2TiO_3	80 mol% Li_4SiO_4 20 mol% Li_2TiO_3	70 mol% Li_4SiO_4 30 mol% Li_2TiO_3
Minor impurities[a]	*B.D.L.*[b]	Pt	Pt	Pt
Pebble colour	"Pearl" white	Pink-brown	Yellow	Light pink

[a] Detected by qualitative XRF spectroscopy and SEM-EDS.
[b] B.D.L. - below detection limit.

Table 2
Specification of irradiation conditions of the reference and modified Li_4SiO_4 pebbles with accelerated electrons (E = 5 MeV).

Parameter	Irradiation conditions											
	No. 1	No. 2	No. 3	No. 4	No. 5	No. 6	No. 7	No. 8	No. 9	No. 10	No. 11	No. 12
Absorbed dose, MGy	3	6	12	24	42	42	84	193	249	1000	3700	5000
Temperature (aver.), K	305	305	310	320	520	670	630	940	710	460	520	520
Temperature (min), K	300	300	300	300	460	630	533	875	690	380	440	380
Temperature (max), K	310	310	315	345	580	730	720	990	730	560	670	650
Dose rate, kGy s^{-1}	0.85	0.85	0.85	0.85	11.7	11.7	11.7	13.4	21.3	11.7	13.4	11.6

two crystallised phases – the main phase, Li_4SiO_4, and a secondary phase, Li_2TiO_3. The obtained p-XRD patterns of the reference Li_4SiO_4 pebbles with 10 mol% Li_2SiO_3 and the modified pebbles with 10 mol% Li_2TiO_3 are shown in Fig. 1.

By using TG-DTA, endothermic peaks between 823 K and 1023 K in the reference and the modified Li_4SiO_4 pebbles were detected. It has been assumed that these signals could be caused by polymorphic transitions of the Li_4SiO_4 phase. The major weight loss due to desorption of absorbed water or carbon dioxide however, was not detected in contrast to the observations of Knitter et al. [8]. H. Kashimura et al. [41] detected the vaporization of lithium (Li) from the Li_2TiO_3 pebbles and the Li_4SiO_4 pebbles at temperatures >1173 K, therefore it has been assumed that the vaporization of Li is negligible in this case.

The metallic trace-impurities, mostly platinum (Pt), in the modified Li_4SiO_4 pebbles were detected both by XRF and SEM-EDS. The obtained XRF spectra of the reference pebbles with 10 mol% Li_2SiO_3 and the modified pebbles with 10 mol% Li_2TiO_3 are shown in Fig. 2. The Pt trace-impurities in the reference pebbles were not detected, most likely due to the detections limits of both methods. Previously M.H.H. Kolb et al. [39], using Inductively Coupled Plasma Optical Emission Spectrometry (ICP-OES), determined that the Pt content in the reference pebbles is approximately 50 ppm. The metallic trace-impurities are most likely derived from the fabrication process, due to the melting in a Pt alloy crucible, or are introduced by the raw materials.

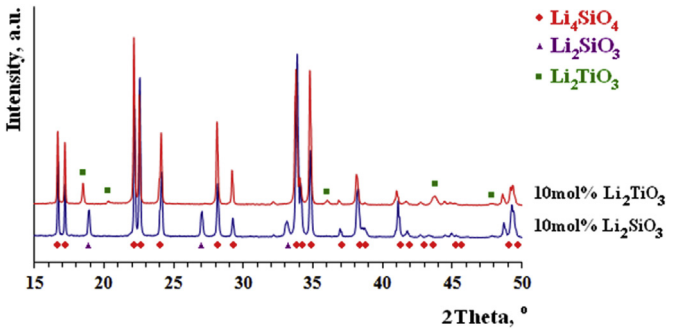

Fig. 1. p-XRD patterns of the reference Li_4SiO_4 pebbles with 10 mol% Li_2SiO_3 and the modified Li_4SiO_4 pebbles with 10 mol% Li_2TiO_3 before irradiation.

Therefore, it has been assumed that the colour of the modified Li_4SiO_4 pebbles might be attributed to the Pt or other metallic trace-impurities [42,43], yet this effect is not fully understood and requires additional analysis. It is not excluded that this observation may also be caused by some other effect, for example, the chemical reduction of Ti^{4+} ions during the fabrication process, which was described by T. Hoshino et al. [44].

4.1. Radiolysis of modified Li_4SiO_4 pebbles with additions of TiO_2 at room temperature

The formation and accumulation of paramagnetic RD and RP in the reference and the modified Li_4SiO_4 pebbles after irradiation with accelerated electrons (E = 5 MeV) up to 24 MGy absorbed dose at 300–345 K were analysed by ESR spectroscopy. The obtained ESR spectra of the reference and the modified pebbles before and after irradiation are shown in Fig. 3A and B.

In the ESR spectra of the reference and the modified Li_4SiO_4 pebbles before irradiation, the ESR signals were not detected, except for the signal of the standard with g-factor 1.9800 (Fig. 3A). The ESR spectra of the reference and the modified pebbles before irradiation are similar and thus they were not included in Fig. 3B, C and D.

In the ESR spectra of the reference Li_4SiO_4 pebbles with 10 mol% Li_2SiO_3 after irradiation, the formation of four signals with similar g-factors (from 2.040 to 2.002) was observed (Fig. 3A). These signals were attributed to E' centres (singlet, $g = 2.002 \pm 0.003$, $\Delta H = 0.8 \pm 0.1$ mT), HC_2 centres (anisotropic singlet, $g_1 = 2.006 \pm 0.003$, $\Delta H_1 = 0.4 \pm 0.1$ mT, $g_2 = 2.017 \pm 0.003$ and $\Delta H_2 = 0.7 \pm 0.1$ mT) and probably peroxide radicals ($g = 2.040 \pm 0.003$, $\Delta H = 1.8 \pm 0.1$ mT), which have been detected and described in the previous experiments [45]. The ESR signal of Li_n particles (narrow singlet, $g = 2.0025$, $\Delta H < 10^{-2}$ mT [17,46,47]) or F^+ centres (broad multiplet, $g = 2.003$ [46]) were not detected. It has been assumed that the ESR signal of Li_n particles cannot be observed due to the particle aggregation or overlapping with other signals, whereas the signal of F^+ centres is too broad to be analysed.

However, in the ESR spectra of the modified Li_4SiO_4 pebbles with 10–30 mol% Li_2TiO_3, the formation of two main groups of the first derivative signals was detected (Fig. 3B). The first group consists of four signals with g-factors from 2.037 to 2.004, while the

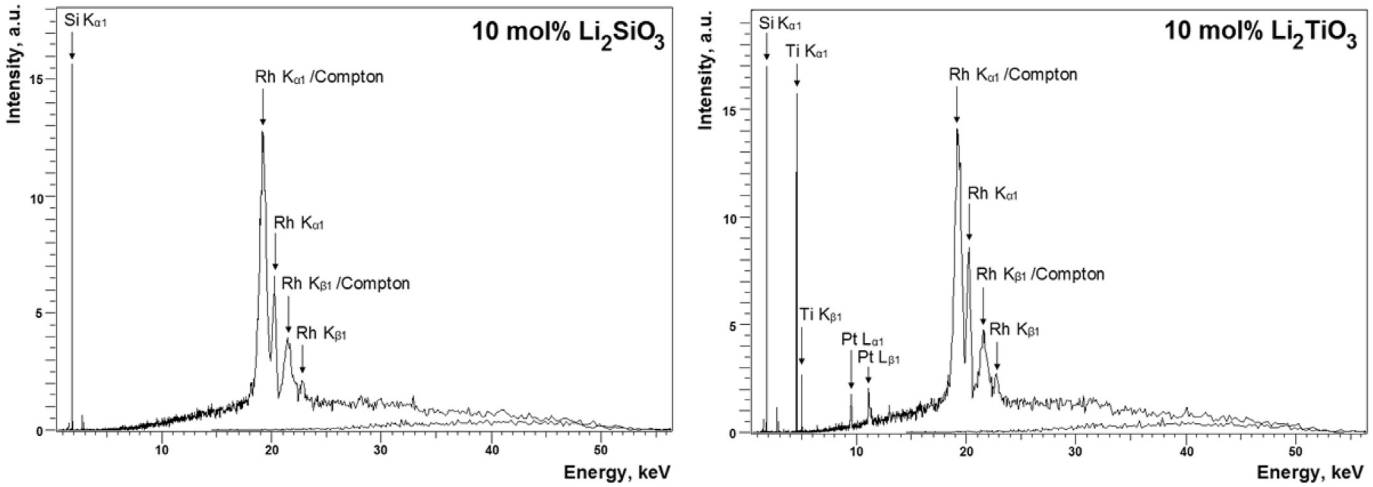

Fig. 2. XRF spectra of the reference Li_4SiO_4 pebbles with 10 mol% Li_2SiO_3 (left) and the modified Li_4SiO_4 pebbles with 10 mol% Li_2TiO_3 (right) (the pebbles are milled in powder; Rh lines are from excitation source).

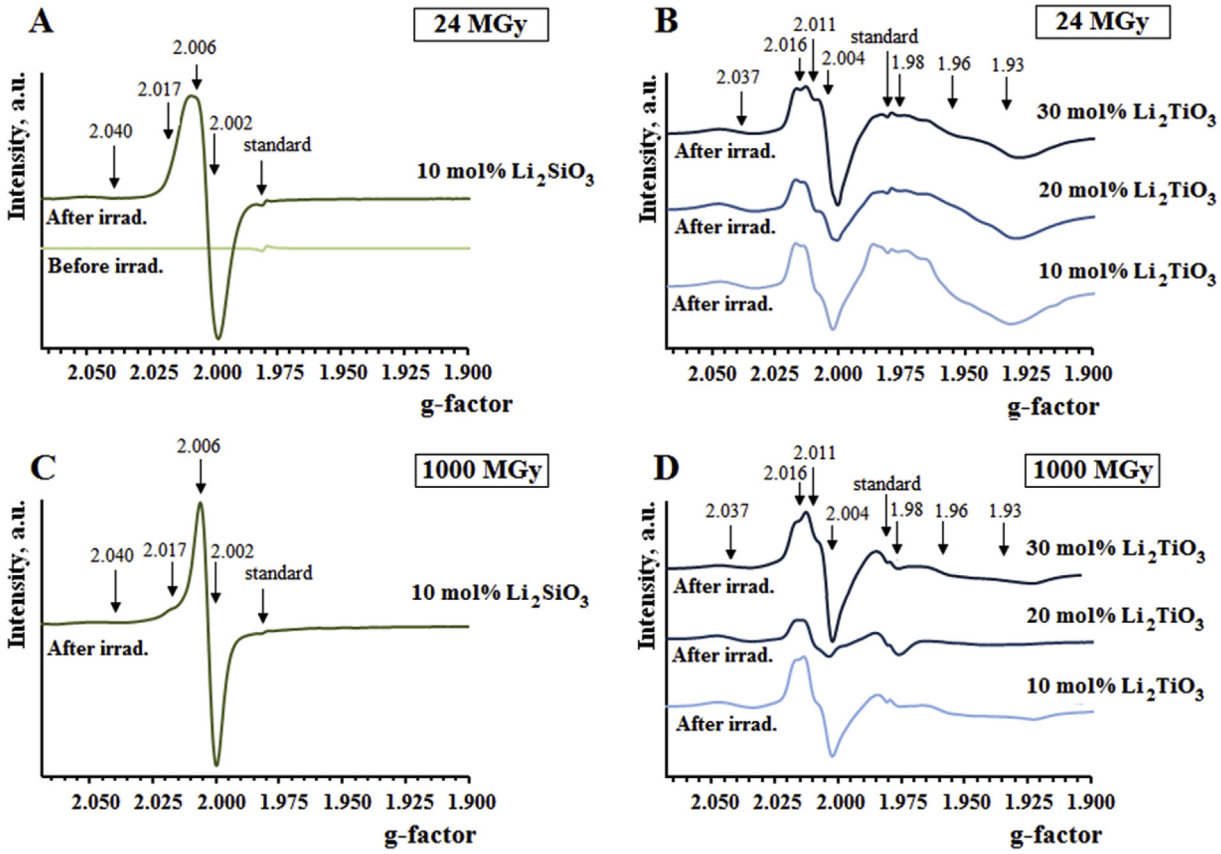

Fig. 3. ESR spectra of the reference Li_4SiO_4 pebbles with 10 mol% Li_2SiO_3 (A, C) and the modified Li_4SiO_4 pebbles with 10–30 mol% Li_2TiO_3 (B, D) before and after irradiation with accelerated electrons (E = 5 MeV) up to 24 MGy absorbed dose at 300–345 K (A, B) and up to 1000 MGy absorbed dose at 380–560 K (C, D).

second group of three signals is observed from 1.98 to 1.93.

The signals of the first group in the ESR spectra of the modified Li_4SiO_4 pebbles have similar shape, g-factor and linewidth to the signals, which are formed in the reference Li_4SiO_4 pebbles, "pure" Li_4SiO_4 [45], Li_2SiO_3 [19] and Li_2TiO_3 ceramic [29]. Therefore, the ESR signal with a g-factor of 2.004 ± 0.003 (ΔH = 0.9 ± 0.1 mT) might be attributed to E' centres (SiO_3^{3-}/TiO_3^{3-}). The two ESR signals with g-factor 2.011 ± 0.003 (ΔH = 0.8 ± 0.2 mT) and 2.016 ± 0.003 (ΔH = 0.4 ± 0.1 mT) could be assigned to HC_2 centres (SiO_4^{3-}/TiO_3^{-}). The ESR signal with g-factor 2.037 ± 0.003 (ΔH = 2.2 ± 0.2 mT) is most likely attributed to peroxide radicals (≡Si–O–O•).

The second group of signals (g_1 = 1.98 ± 0.01, $\Delta H_1 \approx$ 1 mT, g_2 = 1.96 ± 0.01, $\Delta H_2 \approx$ 3 mT, g_3 = 1.93 ± 0.01 and $\Delta H_3 \approx$ 3 mT) in the ESR spectra of the modified Li_4SiO_4 pebbles is broad, complex and un-characteristic for the reference pebbles. Previously Y.M. Kim and P.J. Bray [48], V. Grismanovs et al. [29] and P. Lombard et al. [49]

reported the formation of ESR signals with a similar g-factor and shape in Li_2TiO_3 and other alkali titanates containing ceramics after irradiation and related them to Ti^{3+} ion trapped-electron centres. However, it has also been reported that signals of Ti^{3+} centres are thermally unstable and broad signals in the ESR spectra practically disappear after thermal treatment up to 323 K [29,48]. Therefore, it is not excluded that some of these broad, complex and uncharacteristic signals may also be assigned to the paramagnetic metallic trace-impurities, for example, Pt^{3+} and Pt^{+} ions [50]. The Pt trace-impurities in the modified pebbles before irradiation were detected by XRF and SEM-EDS. For this reason, all of them were entitled as *unidentified RD* in the following text.

The total concentration of paramagnetic RD and RP was calculated using the double integration method of the first derivative ESR signals and by comparison with the standard signal. The total concentration of the accumulated paramagnetic RD in the reference and the modified Li_4SiO_4 pebbles, after irradiation up to 24 MGy absorbed dose at 300–345 K, is shown in Fig. 4.

The Li_2TiO_3 phase has a smaller decomposition degree and radiation chemical yield of RD than Li_2SiO_3 [25], and thus could increase the radiation stability of the modified Li_4SiO_4 pebbles. However, the obtained preliminary results do not confirm this suggestion, and by replacing Li_2SiO_3 with equal molar amounts of Li_2TiO_3 in the Li_4SiO_4 pebbles, the total concentration of paramagnetic RD slightly increases. Nevertheless, the modified Li_4SiO_4 pebbles show good radiation stability and the initial radiation chemical yield is under 0.5 defects per 100 eV.

As suggested above in the literature review, the formation of RD and RP in the ceramics mainly proceeds close to the structural defects: point defects (vacancies, topological and interstitial defects) and bulk defects (open and closed pores, cracks or inclusions). Therefore, it has been assumed that the slight increase of the total concentration of paramagnetic RD in the modified Li_4SiO_4 pebbles in comparison with the reference pebbles could be linked to the structural defects, which may have formed during the fabrication process. The slight differences of the modified pebbles with 20 mol% Li_2TiO_3 in comparison to two other modified pebbles might be related to a different pebble microstructure or chemical composition.

4.2. Microstructural changes and phase transitions in modified Li_4SiO_4 pebbles after irradiation with high absorbed doses at elevated temperatures

Under action of accelerated electrons up to 5000 MGy absorbed dose at 380–990 K, a rapid colour change in the reference and the modified Li_4SiO_4 pebbles was observed. The reference pebbles became “black”, whereas the modified pebbles turned blue-grey. Similar effects have also been observed and described for lithium oxide *(dirty yellow/black)* [47,48], Li_2TiO_3 with 5 mol% TiO_2 *(dark grey)* [51], Li_4SiO_4 *(dark brown)*, Li_2SiO_3 *(grey/blue)* and SiO_2 *(brown)* after irradiation. Therefore, colour changes of the pebbles after irradiation are attributed to the formation and accumulation of optically active RD or RP, such as F^+ centres, Li_n particles etc.

After irradiation with accelerated electrons up to 5000 MGy absorbed dose, major changes in the phase composition of the reference and the modified Li_4SiO_4 pebbles were not detected by p-XRD (Fig. 5) and FT-IR spectroscopy. Due to the high absorbed dose, the formation and accumulation of characteristic RP, such as Li_2SiO_3 or SiO_2, which feature disilicate bonds (≡Si–O–Si≡), were expected. However, due to the small radiolysis degree of Li_4SiO_4 and Li_2TiO_3 and the detection limits of both methods, major changes were not observed.

The microstructures of the reference and the modified Li_4SiO_4 pebbles at etched cross-sections before and after irradiation are shown in Fig. 6. The chemical composition of the pebbles is given in the upper row. In the reference pebbles at the etched cross-section, the Li_4SiO_4 phase is displayed in dark grey colour with inclusions of smaller, light grey grains of Li_2SiO_3. Whereas in the modified pebbles, light grey grains of Li_2TiO_3 are very small and homogeneously distributed as inclusions in the Li_4SiO_4 phase, which appears dark-grey. As suggested above, the modified pebbles with 20 mol% Li_2TiO_3 have a slightly different microstructure compared to the two other modified pebbles, which may have formed during the melting process.

During the irradiation with accelerated electrons up to 5000 MGy absorbed dose at 380–990 K, the microstructure of the reference and the modified Li_4SiO_4 pebbles is only slightly changed, besides the agglomeration of pores.

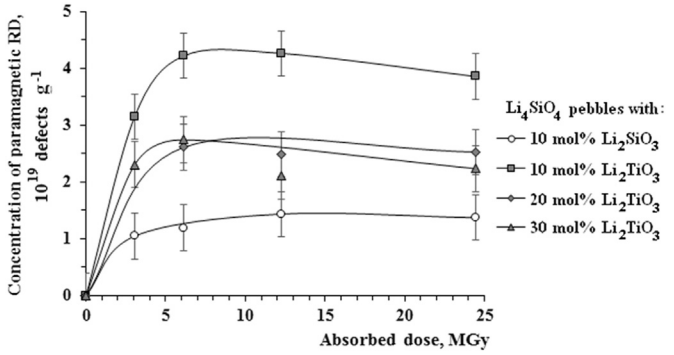

Fig. 4. The total concentration of the accumulated paramagnetic RD in the reference Li_4SiO_4 pebbles with 10 mol% Li_2SiO_3 and the modified pebbles with 10–30 mol% Li_2TiO_3 after irradiation with accelerated electrons (E = 5 MeV) up to 24 MGy absorbed dose at 300–345 K.

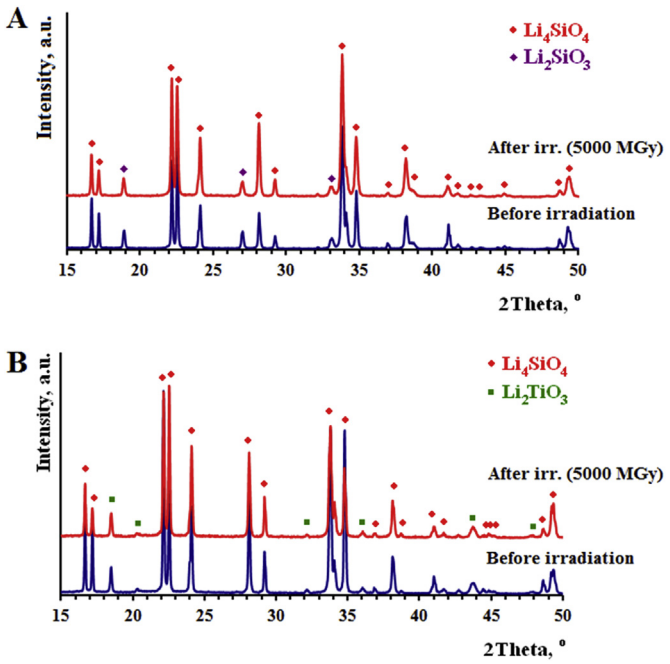

Fig. 5. p-XRD patterns of the reference Li_4SiO_4 pebbles with 10 mol% Li_2SiO_3 (A) and the modified Li_4SiO_4 pebbles with 10 mol% Li_2TiO_3 (B) before and after irradiation with accelerated electrons (E = 5 MeV) up to 5000 MGy absorbed dose at 380–670 K temperature.

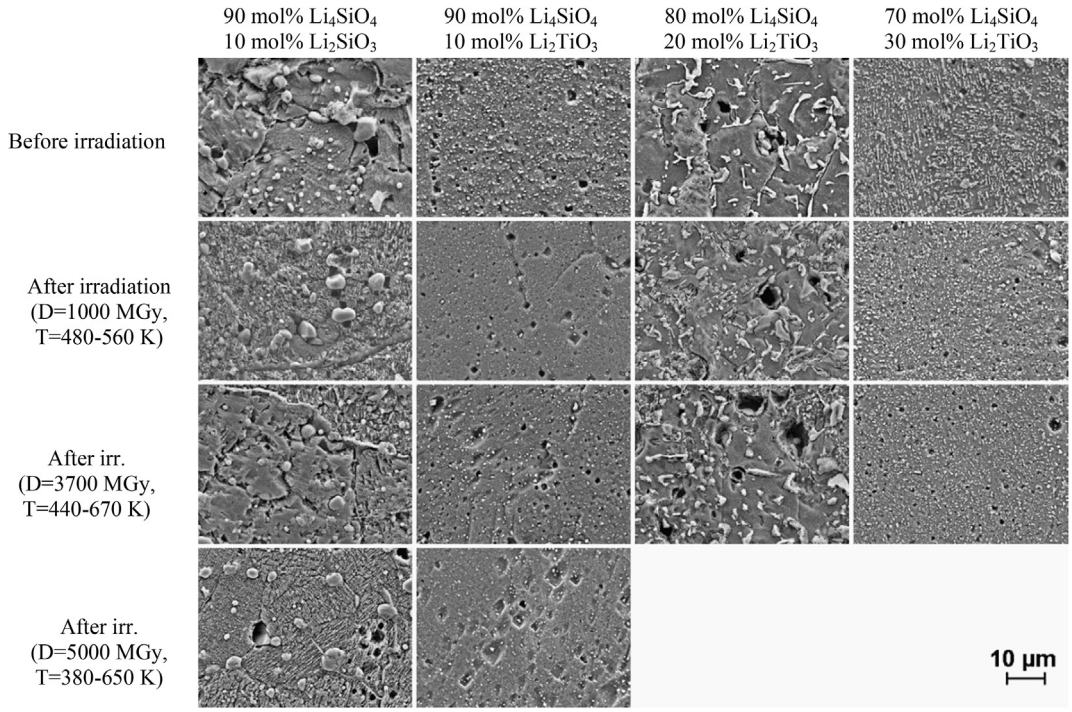

Fig. 6. Microstructure of the reference Li_4SiO_4 pebbles with 10 mol% Li_2SiO_3 and the modified Li_4SiO_4 pebbles with 10–30 mol% Li_2TiO_3 at etched cross-section before and after irradiation with accelerated electrons (E = 5 MeV) up 1000, 3700 and 5000 MGy absorbed dose at 380–670 K temperature.

4.3. Analysis of accumulated RD in modified Li_4SiO_4 pebbles with additions of TiO_2 after irradiation with high absorbed doses at elevated temperatures

Using ESR spectroscopy, it has been determined that after irradiation up to 5000 MGy absorbed dose at 380–730 K, the reference and the modified Li_4SiO_4 pebbles accumulated similar paramagnetic RD as in the pebbles, which were irradiated up to 24 MGy absorbed dose at 300–345 K (Fig. 3A and B). The ESR spectra of the reference and the modified pebbles after irradiation up to 1000 MGy absorbed dose at 380–560 K are shown in Fig. 3C and D.

Under action of accelerated electrons up to 1000 MGy absorbed dose at 380–560 K, mainly signals of E' centres and quite small signals of HC_2 centres and possibly peroxide radicals were observed in the ESR spectra of the reference Li_4SiO_4 pebbles (Fig. 3C). The concentration of HC_2 centres and peroxide radicals decreases, due to the secondary and third stage reactions of the radiolysis or recombination processes. In the ESR spectra of the modified pebbles, signals of both groups – E' centres, HC_2 centres, possibly peroxide radicals and *unidentified RD* (most likely Ti^{3+} centres or caused by impurities) were detected (Fig. 3D). However, the ESR signal intensity of *unidentified RD* significantly decreases in comparison with the modified pebbles, which were irradiated up to 24 MGy absorbed dose at 300–345 K.

The total concentration of accumulated paramagnetic RD in the reference and the modified Li_4SiO_4 pebbles after irradiation up to 5000 MGy absorbed dose at 300–730 K is shown in Fig. 7.

The obtained results clearly show that after irradiation at 380–730 K, the concentration of accumulated paramagnetic RD in the reference and the modified Li_4SiO_4 pebbles significantly decreases in comparison to pebbles, which were irradiated at 300–345 K (Fig. 7A). Also, by replacing Li_2SiO_3 with equal molar amounts of Li_2TiO_3 in the modified pebbles, the concentration of paramagnetic RD slightly decreases after irradiation at 380–730 K. It is assumed that *unidentified RD* in the modified pebbles are thermally un-stable at temperatures higher than 380 K and thus could influence thermally stimulated recombination processes during irradiation at 380–730 K. A dependence of the absorbed dose after irradiation between 380 K and 730 K was most likely not observed due to the influence of the different average irradiation temperature (Fig. 7B).

After irradiation at 630–730 K, only one quite small ESR signal ($g \approx 2.0030$, $\Delta H \approx 0.5$ mT) was detected for the modified Li_4SiO_4 pebbles. It is assumed, that this ESR signal could be associated with electron type RD and RP, such as E' centres or Li_n particles, which have a size smaller than 1 μm. In contrast to these measurements, the localisation of paramagnetic RD practically ends during irradiation up to 875–990 K and in the ESR spectra of the modified Li_4SiO_4 pebbles no characteristic signals were detected besides very small signals of metallic trace-impurities, like Mn^{2+}, Fe^{3+} etc.

4.4. Thermal stability of accumulated RD in modified Li_4SiO_4 pebbles with additions of TiO_2

The “black” and blue-grey colour of the irradiated reference and the modified Li_4SiO_4 pebbles practically disappears after thermal treatment up to 1023 K, most likely due to thermally stimulated recombination processes of optically active RD and RP or other transformations of them. After thermal treatment, the irradiated reference pebbles became practically white, whereas the modified pebbles turned white or dark grey.

The annihilation of paramagnetic RD in the reference and the modified Li_4SiO_4 pebbles up to 753 K is shown in Fig. 8. During thermal treatment up to 633 K, up to 98% of the accumulated RD in the pebbles were annihilated, due to recombination processes. It has also been detected that the concentration of *unidentified RD* (most likely Ti^{3+} centres or caused by impurities) in the modified pebbles already changes slightly at 483 K and recombination is practically complete at 573 K (Fig. 9). In the ESR spectra, after thermal treatment up to a temperature of 753 K, only one quite

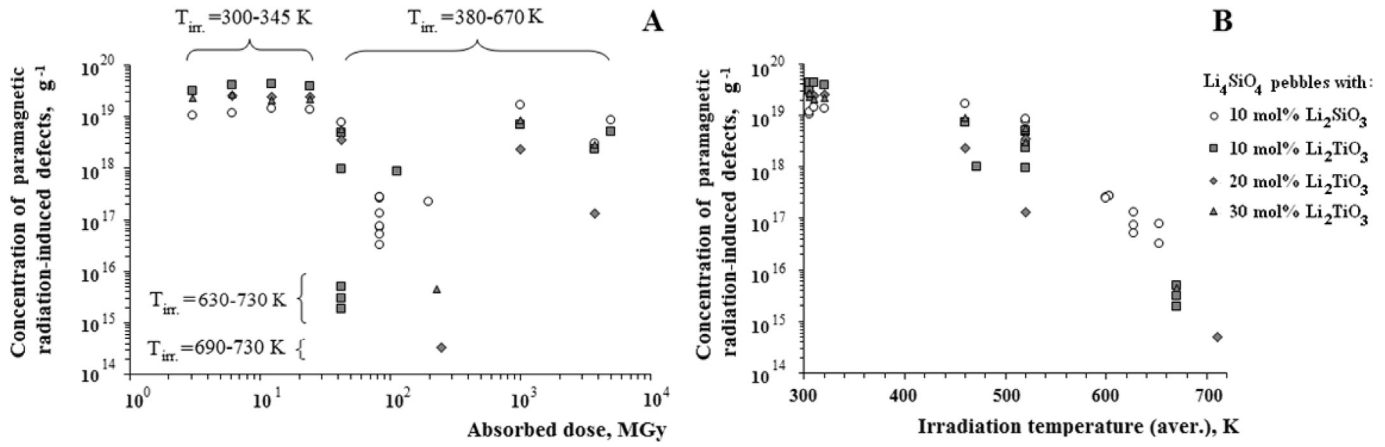

Fig. 7. The concentration of paramagnetic RD in the reference Li_4SiO_4 pebbles with 10 mol% Li_2SiO_3 and the modified Li_4SiO_4 pebbles with 10–30 mol% Li_2TiO_3 after irradiation with accelerated electrons (E = 5 MeV) up to 5000 MGy absorbed dose at 300–730 K as a function of the absorbed dose (A) and average irradiation temperature (B).

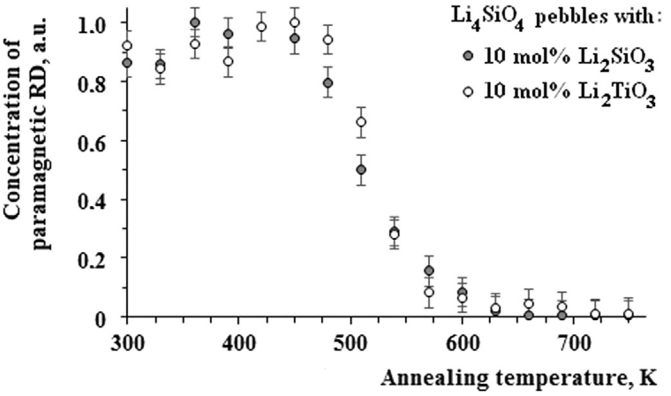

Fig. 8. The annihilation of paramagnetic RD in the irradiated (accelerated electrons, E = 5 MeV, D = 5000 MGy, T = 380–650 K, dry argon) reference Li_4SiO_4 pebbles with 10 mol% Li_2SiO_3 and the modified Li_4SiO_4 pebbles with 10 mol% Li_2TiO_3.

narrow signal (g = 2.0032, ΔH = 0.08 mT) was detected.

The narrow ESR signal in the spectra of the reference and the modified Li_4SiO_4 pebbles only disappears after thermal treatment

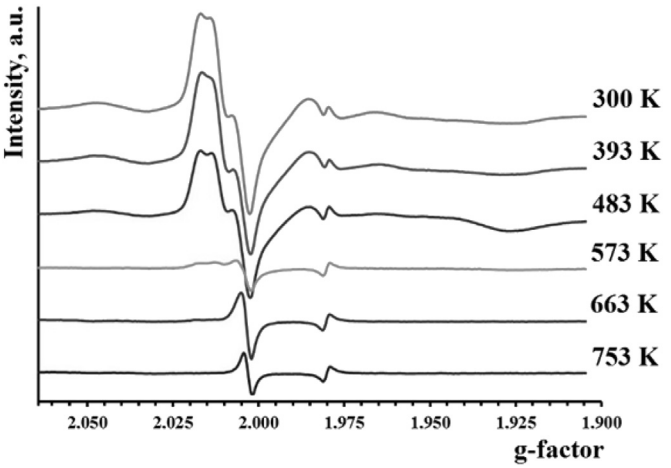

Fig. 9. The ESR spectra of the irradiated (accelerated electrons, E = 5 MeV, D = 5000 MGy, T = 380–650 K) modified Li_4SiO_4 pebbles with 10 mol% Li_2TiO_3 before and after thermal treatment up to 753 K.

up to 1023 K. Therefore, it has been assumed that this ESR signal could be associated with Li_n particles. However, to confirm the hypothesis additional research is required.

To supplement the results of ESR spectroscopy, the TSL glow curves and TSL spectra of the reference and the modified Li_4SiO_4 pebbles after irradiation were measured. The TSL glow curves of the pebbles after irradiation up to 5000 MGy absorbed dose at 380–650 K are shown in Fig. 10.

The obtained TSL data (Fig. 10A) correlates with the results of the ESR spectroscopy (Fig. 7A). The intensity of the TSL curves decreases replacing Li_2SiO_3 with equal molar amounts of Li_2TiO_3 in the Li_4SiO_4 pebbles after irradiation at 380–730 K. The obtained TSL glow curve of the reference pebbles contains at least three maxima at 420–430 K, 500–515 K and 545–560 K (Fig. 10B), whereas, in the modified pebbles only two maxima at 430–460 K and 480–495 K were detected (Fig. 10C). The TSL optical spectra of the reference and the modified pebbles indicate only one maximum close to 2.6 eV. The correlation between results of the ESR spectroscopy and TSL technique was observed in the reference pebbles (Fig. 10D) and the modified pebbles (Fig. 10E).

The obtained TSL results correlates also with results, which were previously reported by E. Feldbach et al. [52], M. Gonzalez and V. Correcher [32,33]. Previously, in the TSL glow curves maxima between 400 K and 600 K were detected in "pure" Li_4SiO_4 and Li_2TiO_3 ceramic. In the TSL optical spectra of Li_4SiO_4 ceramic two maxima around 2.8 and 3.8 eV were detected, while in the spectra of Li_2TiO_3 ceramic maxima around 1.8 and 2.9 eV were measured. It has been assumed, that the maxima around 1.8 and 3.8 eV in the TSL optical spectra of the modified Li_4SiO_4 pebbles were most likely not detected, due to the slow heating rate (0.1 K s^{-1}).

The activation energy of the recombination process was estimated by the shift of the peak in TSL curves at the different heating rates – 0.5, 1 and 2 K s^{-1}. The activation energy (E_a) of the recombination processes in the reference and the modified Li_4SiO_4 pebbles was determined to be about 60–100 kJ mol^{-1}. Previously, M. Oyaidzu et al. [26] and Y. Nishikawa et al. [19] on the basis of the ESR results calculated that the activation energy for the annihilation of E' centres in neutron irradiated Li_2TiO_3 (E_a = 41 kJ mol^{-1}), Li_2SiO_3 (E_a = 60 kJ mol^{-1}) and Li_4SiO_4 (E_a = 54 kJ mol^{-1}). Slight differences between the calculated activation energy from TSL and ESR results could be caused by the method of calculation or type of ionizing radiation, which was suggested by S. Suzuki et al. [53].

Summarising all the above-mentioned results, it can be

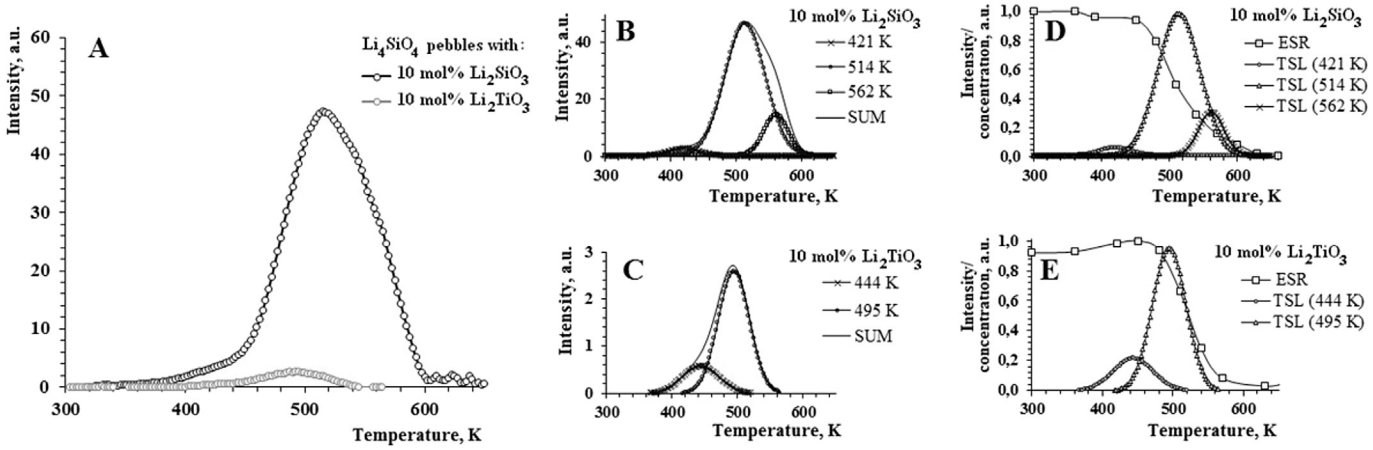

Fig. 10. The TSL glow curves (2 K s^{-1}) of the reference and the modified Li_4SiO_4 pebbles after irradiation with accelerated electrons, up to 5000 MGy absorbed dose at 380–650 K (A), the TSL glow curves with separated maximums (B, C), the combined results of ESR spectroscopy and TSL technique (D, E).

concluded that the modified Li_4SiO_4 pebbles have comparably good radiation stability with the reference pebbles. Therefore, the results suggest that the combination of Li_4SiO_4 and Li_2TiO_3 does not significantly deteriorate the radiation stability and that such mechanically advantageous breeder pebbles can be used as a tritium breeding ceramic for the HCPB TBM. However, all the above-mentioned results also clearly confirm the necessity to further study the radiation effects in the modified pebbles, which will occur under the operation conditions of the HCPB TBM.

5. Conclusions

In this research, the analysis of RD and RP formation and accumulation in the modified Li_4SiO_4 pebbles with 10–30 mol% Li_2TiO_3 as a second phase was made for the first time in order to estimate and compare the radiation stability. By using ESR spectroscopy, it was determined that in the modified pebbles, several paramagnetic species of electron and hole type RD and RP are formed and accumulated, such as E' centres (SiO_3^{3-}/TiO_3^{3-}), HC_2 centres (SiO_4^{3-}/TiO_3^{-}) etc. It was found that by replacing Li_2SiO_3 with an equal molar amount of Li_2TO_3 in the Li_4SiO_4 pebbles, the concentration of the paramagnetic RD is slightly increased after irradiation with accelerated electrons (E = 5 MeV) up to 24 MGy absorbed dose at 300–345 K. Nevertheless, the modified pebbles have good radiation stability and the initial radiation chemical yield of RD is below 0.5 defects per 100 eV.

After irradiation up to 5000 MGy absorbed dose at 300–990 K, major changes in the phase composition and microstructure of the modified Li_4SiO_4 pebbles were not observed by using p-XRD, SEM and FT-IR spectroscopy. The obtained results clearly show that the irradiation temperature has a significant impact on the radiolysis of the modified pebbles. The *unidentified RD* (most likely Ti^{3+} ion trapped-electron centres or caused by impurities) are thermally unstable and fully recombine at a temperature of 570 K. During irradiation up to 875–990 K, the localisation of paramagnetic RD in the modified pebbles practically ends.

Summarising the results, it can be concluded that the modified Li_4SiO_4 pebbles with 10–30 mol% Li_2TiO_3 as a second phase have comparable radiation stability with the reference pebbles. Therefore, the modified pebbles have the potential to combine the advantages of Li_4SiO_4 and Li_2TiO_3 within one single tritium breeding ceramic.

Acknowledgements

The authors greatly acknowledge the technical and experimental support of Liga Avotina, Elina Pajuste, Andris Lescinskis and Raimonds Poplausks (Institute of Chemical Physics, University of Latvia). The experimental support of Aleksejs Zolotarjovs (Institute of Solid State Physics, University of Latvia) is gratefully acknowledged.

This research of the Baltic-German University Liaison Office is supported by the German Academic Exchange Service (DAAD) with funds from the Foreign Office of the Federal Republic Germany. The research was done in frames of project "Investigation of changes of physico-chemical properties of fusion reactor functional materials under influence of high-energy radiation". The research was part-funded by Ministry of Education and Science (Republic of Latvia), project EURATOM No. 11-11/ES12. The views and opinions expressed herein do not reflect those of the Baltic-German University Liaison Office and Ministry of Education and Science.

References

[1] Y. Poitevin, et al., Fusion Eng. Des 85 (2010) 2340–2347.
[2] F. Dobran, Prog. Nucl. Energ 60 (2012) 89–116.
[3] Y. Poitevin, L.V. Boccaccini, G. Dell'Orco, E. Diegele, R. Lasser, J.-F. Salavy, J. Sundstrom, M. Zmitko, Fusion Eng. Des 82 (2007) 2164–2170.
[4] M. Zmitko, Y. Poitevin, L.V. Boccaccini, J.-F. Salavy, R. Knitter, A. Moslang, A.J. Magielsen, J.B.J. Hegeman, R. Lasser, J. Nucl. Mater 417 (2011) 678–683.
[5] L.M. Giancarli, et al., Fusion Eng. Des 87 (2012) 395–402.
[6] R. Knitter, P. Chaudhuri, Y.J. Feng, T. Hoshino, I.-K. Yu, J. Nucl. Mater 442 (2013) S420–S424.
[7] R. Knitter, M.H.H. Kolb, U. Kaufmann, A.A. Goraieb, J. Nucl. Mater 442 (2013) S433–S436.
[8] R. Knitter, B. Alm, G. Roth, J. Nucl. Mater 367–370 (2007) 1387–1392.
[9] R. Knitter, B. Lobbecke, J. Nucl. Mater 361 (2007) 104–111.
[10] M.H.H. Kolb, M. Bruns, R. Knitter, S. van Til, J. Nucl. Mater 427 (2012) 126–132.
[11] J. Tiliks, G. Kizane, A. Vitins, E. Kolodinska, J. Tiliks Jr., I. Reinholds, J. Nucl. Mater 386–388 (2009) 874–877.
[12] S. Yamamoto, et al., J. Nucl. Mater 283–287 (2000) 60–69.
[13] S. van Til, A.V. Fedorov, A.J. Magielsen, Fusion Eng. Des 87 (2012) 885–889.
[14] Q. Zhou, Y. Mou, X. Ma, L. Xue, Y. Yan, J. Eur. Cera. Soc. 34 (2014) 801–807.
[15] J.E. Tiliks, G.K. Kizane, A.A. Supe, A.A. Abramenkovs, J.J. Tiliks, V.G. Vasiljev, Fusion Eng. Des 17 (1991) 17–20.
[16] A. Abramenkovs, J. Tiliks, G. Kizane, V. Grishmanovs, A. Supe, J. Nucl. Mater 248 (1997) 116–120.
[17] J. Tiliks, G. Kizane, A. Vitins, G. Vitins, J. Meisters, Fusion Eng. Des 69 (2003) 519–522.
[18] K. Noda, T. Nakazawa, Y. Ishoo, K. Fukai, H. Matsui, D. Vollath, H. Watanabe, Mater. Trans. 34 (1993) 1150–1154.
[19] Y. Nishikawa, M. Oyaidzu, A. Yoshikawa, K. Munakata, M. Okada,

M. Nishikawa, K. Okuno, J. Nucl. Mater 367–370 (2007) 1371–1376.
[20] E. Carella, T. Hernandez, Physica B 407 (2012) 4431–4435.
[21] K. Moritani, H. Moriyama, J. Nucl. Mater 258–263 (1998) 525–530.
[22] E. Carella, T. Hernandez, Fusion Eng. Des 90 (2015) 73–78.
[23] K. Moritani, S. Tanaka, H. Moriyama, J. Nucl. Mater 281 (2000) 106–111.
[24] E. Carella, T. Hernandez, B. Moreno, E. Chinarro, Nucl. Mater. Energy 3–4 (2015) 1–5.
[25] J. Tiliks, G. Kizane, A. Abramenkovs, A. Supe, J. Tiliks Jr., V. Vasiljev, H. Werle, Fusion Tech. 1992 (1993) 1523–1527.
[26] M. Oyaidzu, et al., J. Nucl. Mater 329–333 (2004) 1313–1317.
[27] T. Nakazawa, A. Naito, T. Aruga, V. Grismanovs, Y. Chmi, A. Iwase, S. Jitsukawa, J. Nucl. Mater 367–370 (2007) 1398–1403.
[28] T. Nakazawa, V. Grismanovs, D. Yamaki, Y. Katano, T. Aruga, Nucl. Instr.. and Meth.. in Phys. Res. B 206 (2003) 166–170.
[29] V. Grismanovs, T. Kumada, T. Tanifuji, T. Nakazawa, Rad. Phy. Chem. 58 (2000) 113–117.
[30] E. Carella, M. Leon, T. Sauvage, M. Gonzalez, Fusion Eng. Des 89 (2014) 1529–1533.
[31] E. Carella, M. Gonzalez, Energy Procedia (2013) 26–33.
[32] M. Gonzalez, V. Correcher, J. Nucl. Mater 445 (2014) 149–153.
[33] V. Correcher, M. Gonzalez, Nuclear Instruments and Methods in Physics Research B 326 (2014) 86–89.
[34] G. Piazza, A. Erbe, R. Rolli, O. Romer, J. Nucl. Mater 329–333 (2004) 1260–1265.
[35] O. Leys, C. Odemer, U. Maciejewski, M.H.H. Kolb, R. Knitter, Pract. Metallogr. 50 (2013) 196–204.
[36] D.A.H. Hanaor, M.H.H. Kolb, Y. Gan, M. Kamlah, R. Knitter, J. Nucl. Mater 456 (2015) 151–161.
[37] M. Gonzalez, E. Carella, A. Morono, M.H.H. Kolb, R. Knitter, Fusion Eng. Des 98–99 (2015) 1771–1774.
[38] T. Hoshino, K. Tsuchiya, K. Hayashi, M. Nakamura, H. Terunuma, K. Tatenuma, J. Nucl. Mater 386–388 (2009) 1107–1110.
[39] M.H.H. Kolb, R. Knitter, U. Kaufmann, D. Mundt, Fusion Eng. Des 86 (2011) 2148–2151.
[40] J. Matejicek, Acta Polytech. 53 (2013) 197–212.
[41] H. Kashimura, M. Nishikawa, K. Katayama, S. Matsuda, M. Shimozori, S. Fukada, T. Hoshino, Fusion Eng. Des 88 (2013) 2202–2205.
[42] M.J. O'Malley, H. Verweij, P.M. Woodward, J. Solid State Chem. 181 (2008) 1803–1809.
[43] G. Piazza, J. Reimann, E. Gunther, R. Knitter, N. Roux, J.D. Lulewicz, J. Nucl. Mater 307–311 (2002) 811–816.
[44] T. Hoshino, K. Sasaki, K. Tsuchiya, K. Hayashi, A. Suzuki, T. Hashimoto, T. Terai, J. Nucl. Mater 386–388 (2009), 1098–1011.
[45] A. Zarins, G. Kizane, A. Supe, R. Knitter, M. Kolb, J. Tiliks Jr., L. Baumane, Fusion Eng. Des 89 (2014) 1426–1430.
[46] F. Beuneu, P. Vajda, G. Jashierowicz, Phys. Rev. 55 (1997) 11263–11269.
[47] P. Vajda, F. Beuneu, Phys. Rev. 53 (1991) 5335–5340.
[48] Y.M. Kim, P.J. Bray, J. Chem. Phys. 53 (1970) 716–723.
[49] P. Lombard, N. Ollier, B. Boizot, J. Non-Cryst. Solids 357 (2011) 1685–1689.
[50] J.R. Katzer, G.C.A. Schuit, J.H.C. Van Hooff, J. Catal. 59 (1979) 278–292.
[51] Y. Chikhray, et al., J. Nucl. Mater 386–388 (2009) 286–289.
[52] E. Feldbach, A. Kotlov, I. Kudryavtseva, P. Liblik, A. Maaroos, I. Martinson, V. Nagrnyi, E. Vasilchenko, Nucl. Instr. Meth. B 250 (2006) 159–163.
[53] S. Suzuki, M. Kobayashi, R. Kurata, W. Wang, T. Fujii, H. Yamana, K. Feng, Y. Oya, K. Okuno, Fusion Eng. Des 85 (2010) 2331–2333.

Fusion Engineering and Design 89 (2014) 1426–1430

Contents lists available at ScienceDirect

Fusion Engineering and Design

journal homepage: www.elsevier.com/locate/fusengdes

Influence of chemisorption products of carbon dioxide and water vapour on radiolysis of tritium breeder

Arturs Zarins[a,*], Gunta Kizane[a], Arnis Supe[a], Regina Knitter[b], Matthias H.H. Kolb[b], Juris Tiliks Jr.[a], Larisa Baumane[a]

[a] University of Latvia, Institute of Chemical Physics, Kronvalda Boulevard 4, LV-1010 Riga, Latvia
[b] Karlsruhe Institute of Technology, Institute for Applied Materials (IAM-WPT), 76021 Karlsruhe, Germany

HIGHLIGHTS

- Chemisorption products affect formation proceses of radiation-induced defects.
- Radiolysis of chemisorption products increase amount of radiation-induced defects.
- Irradiation atmosphere influence radiolysis of lithium orthosilicate pebbles.

ARTICLE INFO

Article history:
Received 19 August 2013
Received in revised form 9 December 2013
Accepted 8 January 2014
Available online 31 January 2014

Keywords:
Tritium breeder
Lithium orthosilicate pebbles
Radiolysis
Chemisorption products

ABSTRACT

Lithium orthosilicate pebbles with 2.5 wt% excess of silica are the reference tritium breeding material for the European solid breeder test blanket modules. On the surface of the pebbles chemisorption products of carbon dioxide and water vapour (lithium carbonate and hydroxide) may accumulate during the fabrication process. In this study the influence of the chemisorption products on radiolysis of the pebbles was investigated. Using nanosized lithium orthosilicate powders, factors, which can influence the formation and radiolysis of the chemisorption products, were determined and described as well. The formation of radiation-induced defects and radiolysis products was studied with electron spin resonance and the method of chemical scavengers. It was found that the radiolysis of the chemisorption products on the surface of the pebbles can increase the concentration of radiation-induced defects and so could affect the tritium diffusion, retention and the released species.

1. Introduction

Lithium orthosilicate pebbles (0.25–0.63 mm) with 2.5 wt% excess of silica are the European Union's reference tritium breeding material for the Helium Cooled Pebble Bed (HCPB) Test Blanket Modules (TBMs) [1–3]. Pebbles with lithium orthosilicate as main phase have appropriate tritium breeding parameters, i.e. good tritium release behaviour, high melting point and lithium density [3]. Beside the main task to produce and release tritium, the pebbles also must be able to withstand the harsh conditions as expected in the TBMs over the long time of operation [3]. In the HCPB TBMs tritium breeding material will be exposed to an intense neutron flux ($\Phi \leq 10^{18}$ neutrons m^{-2} s^{-1}), a high magnetic field (H = 7–10 T) and temperature (T = 573–1193 K) [1,2].

The most promising method for the lithium orthosilicate pebble fabrication is a melt-based process [3–8]. For the synthesis, lithium hydroxide and silica are used as raw materials [4,6,8]. The 2.5 wt% excess of silica is added to increase mechanical stability of the pebbles [3]. The mixture of raw materials is heated to about 1723 K and the then formed liquid is sprayed in dry air, to obtain pebbles [6–8]. Due to the excess of silica (Eq. (1)) and the rapid quenching, the resulting product has two phases – lithium orthosilicate as the main and lithium orthodisilicate as the minor phase [6–8]. After annealing at 1243 K in air, lithium orthodisilicate phase decomposes (Eq. (2)) and pebbles mainly consist of 90 mol% lithium orthosilicate and 10 mol% lithium metasilicate [6–8].

$$10LiOH + 3SiO_2 \rightarrow Li_4SiO_4 + Li_6Si_2O_7 + 5H_2O \uparrow \quad (1)$$

$$Li_6Si_2O_7 \rightarrow Li_4SiO_4 + Li_2SiO_3 \quad (2)$$

Latest analysis of the pebbles surface [7] showed that after annealing in air also carbon dioxide may accumulate and is only released at temperatures >773 K [8]. The carbon dioxide mainly accumulates as chemisorption product, i.e. lithium carbonate (Eq. (3)) [9]. Traces of lithium carbonate on the surface of the pebbles were observed in depths less than 1 μm [7]. The formation

* Corresponding author. Tel.: +371 67033883.
E-mail addresses: arturs.zarins@lu.lv, arturs.zarins.lukf@gmail.com (A. Zarins).

0920-3796/$ – see front matter © 2014 Elsevier B.V. All rights reserved.
http://dx.doi.org/10.1016/j.fusengdes.2014.01.005

of lithium carbonate probably occurs due to a too slow cooling rate after annealing or contact with air at storage stage.

$$Li_4SiO_4 + CO_2 \rightarrow Li_2CO_3 + Li_2SiO_3 \quad (3)$$

The chemisorption process of carbon dioxide can be catalyzed by air humidity (Eqs. (4) and (5)) [10]. Therefore small amounts of lithium hydroxide and absorbed water may also accumulate on the surface of the pebbles.

$$Li_4SiO_4 + H_2O \rightarrow 2LiOH + Li_2SiO_3 \quad (4)$$

$$2LiOH + CO_2 \rightarrow Li_2CO_3 + H_2O \quad (5)$$

The lithium carbonate and hydroxide are radiation unstable compounds [11] and may affect the formation of radiation-induced defects (RD) and radiolysis products (RP) during neutron and other type irradiation. The importance and role of RD and RP on the tritium diffusion and retention has been established [12–15]. Most crucial are electron type RP, i.e. colloidal lithium, which can interact with tritium and may disturb tritium diffusion and decrease its retention [15]. The colloidal lithium forms at the radiolysis of the lithium orthosilicate (Eq. (6)) as result of coagulation of the electron type RD [15].

$$Li_4SiO_4 \xrightarrow{\text{Ionizing radiation}} 2Li + Li_2SiO_3 + 0.5O_2 \quad (6)$$

The aim of this study is to estimate the influence of the chemisorption products of water vapour and carbon dioxide on the radiolysis of the lithium orthosilicate pebbles. In addition, nanosized powders were used to determine and investigate the factors which can influence the formation and radiolysis of chemisorption products.

2. Experimental

2.1. Fabrication of ceramic specimens

The lithium orthosilicate pebbles (screened to 0.45–0.56 mm), together with nanosized powders with three different compositions were selected for investigation (Table 1). The nanosized powders were used due to their high surface area and smaller grain size compared to the pebbles. The increased surface area increases the amount of chemisorption products [8,11].

The pebbles were produced by a melt-spraying method at Schott AG (Mainz, Germany) [4–8] and were annealed at 1243 K for 168 h in air.

The nanosized "pure" lithium orthosilicate powder was produced by plasma synthesis [16] at Institute of Inorganic Chemistry (Riga Technical University, Latvia). For the synthesis, lithium carbonate and silica were selected as raw materials. To eliminate residues of raw materials, the obtained powder was annealed at 890 K in air. The formation of 2 mol% lithium metasilicate phase can be explained by un-stoichiometry of the raw materials.

The 3 mol% (2 wt%) excess of silica was added to the "pure" powder. The mixture of both powders was homogenized by milling for 3 h in a ball mill and then annealed at 920 K for 3.5 h in air. The excess of silica was added to obtain similar composition as in the pebbles.

2.2. Preparation and irradiation of samples

The lithium orthosilicate pebbles were encapsulated in quartz tubes either with dry argon or air and were irradiated by accelerated electrons (Table 1). Irradiation was performed with the linear electron accelerator ELU-4 (Salaspils, Latvia), up to 4 h per day.

To understand the processes, which may occur during one of the irradiation cycles (up to 4 h) in air, the nanosized powders were used instead of the pebbles. The irradiation type practically do not influence the formation of RD and RP [17], and thus gamma rays instead of accelerated electrons were used, due to smaller dose rate and lower irradiation temperature. The electron flux of the linear electron accelerator was converted to gamma rays by a tungsten plate.

The nanosized lithium orthosilicate powders with three different compositions were irradiated by gamma rays at room temperature in air (Table 1), to investigate the formation and radiolysis of the chemisorption products. The dose rate and absorbed dose was reduced, to avoid formation of RP to the chemisorption products [18]. In order to identify RD of the chemisorption products, lithium carbonate and hydroxide powders were irradiated (D = 56 kGy, $T \approx 300$ K) as well. To investigate the thermal stability of RD, the irradiated nanosized powders were thermally treated up to 620 K for 30 min in air.

To simulate the processes, which may occur on the surface of the pebbles during one of the irradiation cycles, the nanosized lithium orthosilicate powder with 6 mol% of lithium metasilicate phase was thermally pre-treated (T = 570 K, t = 4 h) and then irradiated with gamma rays (D = 56 kGy, $T \approx 300$ K) in air.

2.3. Methods of characterization

The chemical composition of the ceramic specimens was analyzed by qualitative powder X-ray diffractometry (p-XRD), thermogravimetric analysis (TGA) and Fourier transformed infrared spectroscopy (FT-IR). The surface area and grain size were investigated by BET adsorption and by scanning electron microscopy (SEM), respectively. The accumulated RD and RP were analyzed with electron spin resonance (ESR) and with the method of chemical scavengers (MCS) [15–17].

The p-XRD patterns were obtained by a Bruker D8 (10–60° 2Θ, CuKα, λ = 0.15418 nm), the FT-IR spectra by a Perkin Elmer Spectrum Two (450–4000 cm^{-1}, pressed in KBr pellets) and the TGA curves by a Seiko EXTAR 6300 (290–1270 K, 2–10 K min^{-1}, dry argon and air). The ESR spectra were recorded by a Bruker BioSpin X-band radiospectrometer (300–400 mT, 30 dB, 9.83 GHz) operating at 100 kHz field modulation in room temperature. The grain size of the nanosized powders was analyzed with a Hitachi S-4800 SEM.

The MCS is based on the difference of red-ox properties of the hole and electron type RD and RP in acid containing solvents [15]. The irradiated ceramic specimens were dissolved in 0.1 M sulphuric acid solution with 1 M ethanol, to analyze the total amount of the electron type RD and RP, and with 1 M sodium nitrate, to analyze the amount of the electron type RP. In the acidic solutions the generated gaseous molecular hydrogen was obtained [17] and analyzed by gas chromatography.

3. Results and discussion

3.1. Radiolysis of lithium orthosilicate pebbles at elevated temperature in dry argon

Using MCS, it has been determined that after irradiation up to 11 GGy absorbed dose at 550–590 K in dry argon, lithium orthosilicate pebbles accumulated both simple and multi-electron centres. Up to 95% are multi-electron centres. Multi-electron centres consist of colloidal lithium aggregates, whereas simple centres – localized electrons in oxygen vacancies, so called F^+ and F° centres, and E′ centres (ion-radical SiO_3^{3-}) [17]. The estimated radiation chemical yield (5.1×10^{-5} localized electrons per 100 eV) and the decomposition degree (0.15 mol%) were much smaller than determined in previous studies [15–17], most likely due to the high absorbed dose and elevated irradiation temperature.

Table 1
Characterization of the investigated lithium orthosilicate ceramic specimens and irradiation conditions.

Parameter	Lithium orthosilicate pebbles	Nanosized lithium orthosilicate powders		
		"Pure"	With 3 mol% silica	With 6 mol% lithium metasilicate
Chemical composition	90 mol% Li_4SiO_4 10 mol% Li_2SiO_3	98 mol% Li_4SiO_4 2 mol% Li_2SiO_3	95 mol% Li_4SiO_4 2 mol% Li_2SiO_3 3 mol% SiO_2	92 mol% Li_4SiO_4 8 mol% Li_2SiO_3
Grain size	10 μm [11]	200–300 nm	200–400 nm	300–600 nm
Specific surface area ($m^2\,g^{-1}$)	0.20–0.25	23 ± 2	22 ± 2	17 ± 2
Irradiation conditions	Accelerated electrons, E = 5 MeV, D = 0.7–11 GGy, P = 88 MGy h^{-1}, T = 550–590 K, dry argon and air	Gamma rays, D = 7–56 kGy, P = 14 kGy h^{-1}, $T \approx 300$ K, air		

In the ESR spectra of the pebbles, which were irradiated in dry argon, only one signal (g = 2.001, ΔH = 1 mT) was observed (Fig. 1). It was attributed to the paramagnetic E′ centres, which have been investigated and characterized in previous experiments [11,15,17]. Presumably, the signal of colloidal lithium (g = 2.0025, $\Delta H \leq 10^{-2}$ mT [15]) in the ESR spectra cannot be observed due to aggregation, and the signal of F^+ centres is too broad to be analyzed.

The E′ centres together with HC_2 centres (ion-radical SiO_4^{3-}), are the primary stage electron and hole type RD of the lithium orthosilicate (Eqs. (7) and (8)) [17]. However due to the second and third stage reactions of the radiolysis [17], the concentration of the E′ centres is quite small (10^{15} radicals g^{-1}), in contrast, HC_2 centres practically do not accumulate.

$$SiO_4^{4-} \xrightarrow{\text{Ioniz. radiat.}} SiO_4^{3-}(HC_2\ \text{centre}) + e^- \quad (7)$$

$$SiO_4^{4-} + e^- \xrightarrow{\text{Ioniz. radiat.}} SiO_3^{3-}(E'\ \text{centre}) + O^{2-} \quad (8)$$

3.2. Influence of air on radiolysis of lithium orthosilicate pebbles at elevated temperature

Using air instead of dry argon as irradiation atmosphere of the lithium orthosilicate pebbles, not only signals of the E′ centres were observed in the ESR spectra, but also two symmetric signals (g = 2.193 and g = 1.898) with 50.2 mT splitting and two signals with g-factor 2.008 and 2.014 (Fig. 1). The signals with g-factor 2.008 and 2.014 were attributed to the HC_2 centres, whereas the two symmetric signals were attributed to atomic hydrogen.

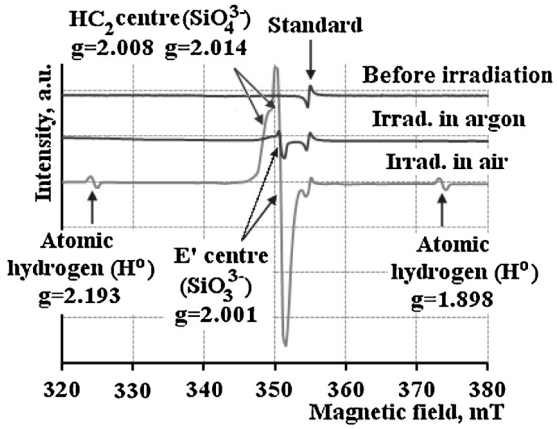

Fig. 1. ESR spectra of the lithium orthosilicate pebbles before and after irradiation (D = 11 GGy, T = 550–590 K) in dry argon and air.

In a previous study [11] the formation of atomic hydrogen was related to the radiolysis of the chemisorption products of water vapour (Eq. (9)). However the increase of the RD concentration (from 10^{15} to 10^{17} radicals g^{-1}) and the decomposition degree (from 0.15 to 1.5 mol%) as well as the formation of HC_2 centres was not completely understood.

$$LiOH \xrightarrow{\text{Ioniz. radiat.}} LiO^{\bullet} + H^{\bullet} \quad (9)$$

In this research it has been suggested that these effects could be related to the radiolysis of the chemisorption products of water vapour (Eq. (10)) and carbon dioxide (Eq. (11)), which may form during the irradiation in air.

$$2LiOH \xrightarrow{\text{Ioniz. radiat.}} 2Li + H_2O + 0.5O_2 \quad (10)$$

$$Li_2CO_3 \xrightarrow{\text{Ioniz. radiat.}} 2Li + CO_2 + 0.5O_2 \quad (11)$$

Up to 70% of RD localize in a 50 μm subsurface layer of the pebbles, due to intrinsic structural defects [12,15]. The radiolysis of the chemisorption products on the surface of the pebbles could influence the formation processes of RD and so a rapid increase of the RD concentration and decomposition degree could be detected.

The formation and radiolysis of the chemisorption products during the irradiation could be influenced by several factors: irradiation temperature and time, absorbed dose and dose rate, chemical composition and surface area of the pebbles etc. [8–11,15–18]. Therefore to understand the processes, which may occur during one of the irradiation cycles ($D \approx 350$ MGy, $t \approx 4$ h, T = 550–590 K) in air, the influence of the irradiation atmosphere, the chemical composition and the irradiation temperature on the radiolysis of the pebbles were investigated separately.

The formation of RD and RP in the lithium orthosilicate pebbles take place in three main stages. After irradiation with the absorbed dose >10–20 MGy at 400–600 K mainly colloidal lithium forms, due to the coagulation of the electron type RD [15]. To avoid the formation of colloidal lithium and to accumulate mainly primary stage RD, the dose rate and absorbed dose was reduced (from 350 MGy to 56 kGy).

3.3. Influence of air atmosphere on radiolysis of lithium orthosilicate powder at room temperature

To increase the surface area and thus the amount of chemisorption products, the nanosized powders were selected for further investigations instead of the pebbles.

The "pure" lithium orthosilicate powder showed impurities of lithium carbonate and hydroxide before irradiation. In the p-XRD patterns traces of additional signals were observed (Fig. 2A). In

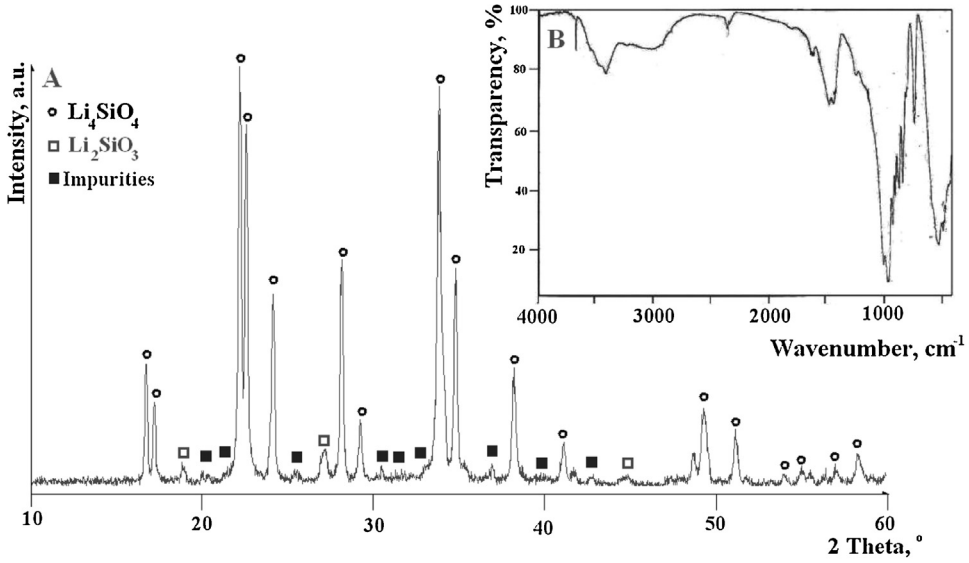

Fig. 2. p-XRD pattern (A) and FT-IR spectrum (B) of the "pure" lithium orthosilicate powder before irradiation.

the FT-IR spectrum bond vibrations of C—O (1400–1500 cm^{-1}) and O—H (2800–3500 cm^{-1}) were detected (Fig. 2B). By TGA a mass loss up to 2 wt% was observed during heating to 1073 K, which was unambiguously assigned to desorption of water (T = 420–570 K) and carbon dioxide (T = 670–870 K) [8]. The formation of the chemisorption products most likely occur during the fabrication or storage stage.

After irradiation up to 4 h (D = 56 kGy) at room temperature ($T \approx 300$ K) in air, major changes in the TGA curves, p-XRD patterns and FT-IR spectrum were not observed. Yet, due to the short irradiation time and the small absorbed dose, significant changes in the "pure" lithium orthosilicate powder were not expected [17].

However, in the ESR spectrum of the powder, seven signals were detected after irradiation (Fig. 3). Five of them are identical to the signals which were observed in the ESR spectrum of the pebbles (Fig. 1) and were identified as signals of atomic hydrogen, HC_2 and E′ centres, respectively. The formation of atomic hydrogen was attributed to the radiolysis of the lithium hydroxide. Whereas the interpretation of the two remaining signals with g-factors 2.026 and 2.036 is more complicated.

In the ESR spectrum of the pebbles the formation of these two signals were not observed, most likely due to high absorbed dose. In irradiated "pure" silicates these signals were often attributed to peroxide radicals ($\equiv Si-O-O^{\bullet}$) or HC_2 centres [13,17]. Yet in the ESR spectra of irradiated lithium hydroxide and carbonate powders signals with similar g-factors were observed [19]. This suggests that the origins of these signals could not be only peroxide radicals or HC_2 centres, but also paramagnetic RD of the chemisorption products. Due to that, both of them were marked as un-identified.

Other ESR signals, which could be related to RD of the chemisorption products, like, ion-radicals CO_2^- (g = 2.0006), CO_3^- (g = 2.0036) and CO_3^{3-} (g = 2.00415) [19], in the spectrum were not observed, most likely due to overlapping with signals of the E′ and HC_2 centres.

3.4. Influence of excess of silica on radiolysis of lithium orthosilicate powder at room temperature in air

After adding 3 mol% (2 wt%) excess of silica and subsequent homogenization by milling, the resulting lithium orthosilicate powder shows a rapid decrease of the RD concentration – up to 40% (Fig. 4). The silica practically does not influence the surface area and the grain size, thus the decrease of RD concentration could be related to the chemical properties of silica. In the homogenization process silica most likely accumulate on the surface of the

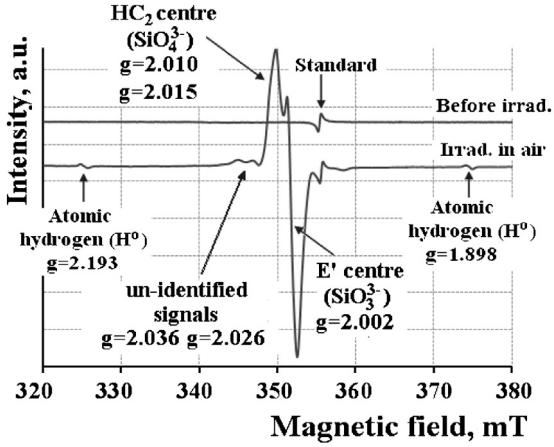

Fig. 3. ESR spectra of the "pure" lithium orthosilicate powder before and after irradiation (D = 56 kGy, $T \approx 300$ K) in air.

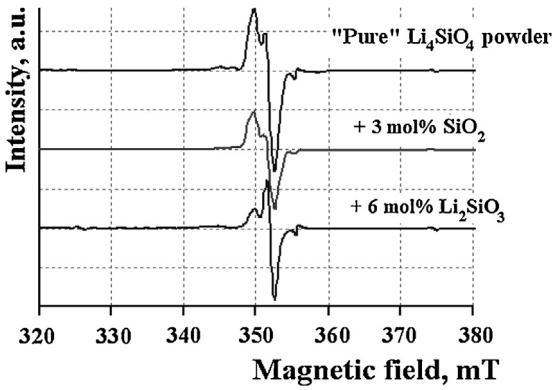

Fig. 4. ESR spectra of the "pure" lithium orthosilicate powder, with 3 mol% of silica and with 6 mol% of lithium metasilicate phase after irradiation (D = 56 kGy, $T \approx 300$ K) in air.

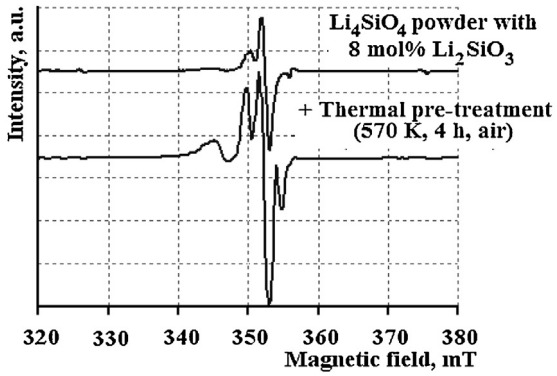

Fig. 5. ESR spectra of the irradiated (D = 56 kGy, $T \approx$ 300 K, air) lithium orthosilicate powder with 6 mol% lithium metasilicate before and after thermal pre-treatment (T = 570 K, t = 4 h) in air.

lithium orthosilicate grains and so possibly disturb the formation of chemisorption products.

After annealing up to 920 K in air, silica on the surface of the grains reacts with the lithium orthosilicate (Eq. (12)) [20,21] and the surface area decreases from 22 to 17 $m^2\ g^{-1}$, probably due to particle agglomeration. The formed 6 mol% lithium metasilicate phase also decrease the RD concentration – up to 25% (Fig. 4). The decrease of RD concentration was attributed both to a change of the contact surface area with air and the properties of lithium metasilicate [17,22].

$$Li_4SiO_4 + SiO_2 \xrightarrow{CO_2 \text{ and } H_2O} 2Li_2SiO_3 \quad (12)$$

3.5. Influence of irradiation temperature on radiolysis of lithium orthosilicate powder in air

To simulate the processes, which may occur on the surface of the pebbles during one of the irradiation cycles, the nanosized lithium orthosilicate powder with 6 mol% lithium metasilicate phase was used for further experiments.

The MSC and ESR results suggest that at elevated temperature the atomic hydrogen recombines at 320 K, HC_2 centres at 400–550 K, un-identified RD at 420–520 K and E′ centres at 450–650 K. Besides that, investigations by TGA in air, suggest that simultaneously with thermally stimulated recombination of RD, the formation of the chemisorption of water vapour and carbon dioxide may occur up to 420 K [21]. At higher temperature both gases are released in two steps: first occurs desorption of water (T = 420–573 K) and then carbon dioxide (T = 670–920 K) [21]. On basis of these results it has been sugested that at 550–590 K in air, besides recombination of RD, on the surface of the pebbles mainly the formation and radiolysis of the chemisorption products of carbon dioxide occurs.

After thermal pre-treatment at 570 K for 4 h in air, using TGA, it has been determined that the lithium orthosilicate powder contained up to 12 wt% of water vapour and carbon dioxide. Due to the radiolysis of the chemisorption products, an increase of RD concentration – up to 50%, was detected after irradiation (Fig. 5). The obtained results confirm that the chemisorption products increase not only the concentration of E′ centres, but also the amount of HC_2 centres and un-identified RD.

The obtained results clearly correlate with the data of the lithium orthosilicate pebbles, which were irradiated up to 11 GGy at 550–590 K in air (Fig. 1). These results also confirm the suggestion that the chemisorption products, due to the formation up to 420 K and radiolysis, can increase the concentration of the hole and electron type RD and the decomposition degree of the pebbles.

4. Conclusions

In this study the influence of the chemisorption products of water vapour and carbon dioxide (lithium hydroxide and carbonate) on the radiolysis of the lithium orthosilicate pebbles was investigated. It was concluded that the radiolysis of the chemisorption products can significantly affect the formation of the hole and electron type RD on the surface of the pebbles. It was found that the chemisorption products can increase the concentration of RD and the decomposition degree of the pebbles. Due to the radiolysis of the chemisorption products on the surface of the pebbles and increase of RD concentration, tritium diffusion could be affected.

Processes were described, which may occur on the surface of the pebbles during irradiation in air. It was determined that the formation and radiolysis of the chemisorption products on the pebbles depend on the chemical composition of the surface and the irradiation temperature. The excess of silica, due to the chemical properties, can disturb the formation of the chemisorption products and so could decrease the concentration of RD. Whereas at elevated irradiation temperature, due to the formation of the chemisorption products up to 420 K from air, the concentration of RD can significantly increase.

Acknowledgments

This study was carried out in cooperation with Institute of Inorganic Chemistry (Riga Technical University) and Faculty of Chemistry (University of Latvia). Research was financed by Ministry of Education and Science (Republic of Latvia), project EURATOM No. 11-11/ES12.

References

[1] M. Zmitko, Y. Poitevin, L. Boccaccini, J.-F. Salavy, R. Knitter, A. Möslang, et al., J. Nucl. Mater. 417 (2011) 678–683.
[2] L.M. Giancarli, M. Abdou, D.J. Campbell, V.A. Cnuyanov, M.Y. Ahn, M. Enoeda, et al., Fus. Eng. Des. 87 (2012) 395–402.
[3] R. Knitter, P. Chaudhuri, Y.J. Feng, T. Hoshino, I.-K. Yu, J. Nucl. Mater. 442 (2013) S420–S424.
[4] R. Knitter, B. Löbbecke, J. Nucl. Mater. 361 (2007) 104–111.
[5] R. Knitter, M.H.H. Kolb, U. Kaufmann, A.A. Goraieb, J. Nucl. Mater. 442 (2013) S433–S436.
[6] M.H.H. Kolb, R. Knitter, U. Kaufmann, D. Mundt, Fus. Eng. Des. 86 (2011) 2148–2151.
[7] M.H.H. Kolb, M. Bruns, R. Knitter, S. Van Tils, J. Nucl. Mater. 427 (2012) 126–132.
[8] R. Knitter, B. Alm, G. Roth, J. Nucl. Mater. 367–370 (2007) 1387–1392.
[9] K. Essaki, K. Nakagawa, M. Kato, H. Uemoto, J. Chem. Eng. Jpn. 37 (2004) 772–777.
[10] K. Essaki, M. Kato, H. Uemoto, J. Mater. Sci 40 (2005) 5017–5019.
[11] A. Zarins, A. Supe, G. Kizane, R. Knitter, L. Baumane, J. Nucl. Mater. 429 (2012) 34–39.
[12] G. Kizane, J. Tiliks, A. Vitins, J. Rudzitis, J. Nucl. Mater. 329–333 (2004) 1287–1290.
[13] Y. Nishikawa, M. Oyaidzu, A. Yoshikawa, K. Munakata, M. Okada, M. Nishikawa, et al., J. Nucl. Mater. 367–370 (2007) 1371–1376.
[14] G. Kizane, J. Tiliks, A. Vitins, J. Tiliks Jr., J. Rudzitis, Fus. Eng. Des. 75–79 (2005) 897–901.
[15] J. Tiliks, G. Kizane, A. Vitins, G. Vitins, J. Meistars, Fus. Eng. Des. 69 (2003) 519–522.
[16] J. Tiliks, G. Kizane, A. Vitins, B. Lescinskis, Proceedings CBBI-13, 2005, pp. 140–142.
[17] J.E. Tiliks, G.K. Kizane, A.A. Supe, A.A. Abramenkovs, J.J. Tiliks, V.G. Vasiljev, Fus. Eng. Des. 17 (1991) 17–20.
[18] S. Murali, V. Natarajan, R. Venkataramani, Pushparaja, M.D. Sastry, Appl. Radiat. Isot. 55 (2001) 253–258.
[19] E. Herrera, F. Urena-Nunez, A. Delfin Loya, Appl. Radiat. Isot. 63 (2005) 241–246.
[20] T. Tang, Z. Zhang, J.B. Meng, S.L. Luo, Fus. Eng. Des. 84 (2009) 2124–2130.
[21] J. Ortiz-Landeros, L. Martinez-dlCruz, C. Gomez-Yanez, H. Pfeiffer, Thermochim. Acta 515 (2011) 73–78.
[22] J. Ortiz-Landeros, M.E. Contreras-Garcia, G. Gomez-Yanez, H. Pfeiffer, J. Solid State Chem. 184 (2011) 2257–2262.

Journal of Nuclear Materials 429 (2012) 34–39

Contents lists available at SciVerse ScienceDirect

Journal of Nuclear Materials

journal homepage: www.elsevier.com/locate/jnucmat

Accumulation of radiation defects and products of radiolysis in lithium orthosilicate pebbles with silicon dioxide additions under action of high absorbed doses and high temperature in air and inert atmosphere

A. Zarins [a], A. Supe [a], G. Kizane [a,*], R. Knitter [b], L. Baumane [a]

[a] Laboratory of Radiation Chemistry of Solids, Institute of Chemical Physics, University of Latvia, Kronvalda Bulvaris 4, LV-1010 Riga, Latvia
[b] Karlsruhe Institute of Technology, Institute for Applied Materials (IAM-WPT), POB 3640, 76021 Karlsruhe, Germany

ARTICLE INFO

Article history:
Received 10 July 2011
Accepted 13 May 2012
Available online 26 May 2012

ABSTRACT

One of the technological problems of a fusion reactor is the change in composition and structure of ceramic breeders (Li_4SiO_4 or Li_2TiO_3 pebbles) during long-term operation. In this study changes in the composition and microstructure of Li_4SiO_4 pebbles with 2.5 wt% silicon dioxide additions, fabricated by a melt-spraying process, were investigated after fast electron irradiation (E = 5 MeV, dose rate up to 88 MGy h^{-1}) with high absorbed dose from 1.3 to 10.6 GGy at high temperature (543–573 K) in air and argon atmosphere. Three types of pebbles with different diameters and grain sizes were investigated. Products of radiolysis were studied by means of FTIR and XRD. TSL and ESR spectroscopy were used to detect radiation defects. SEM was used to investigate structure of pebbles. Experiments showed that Li_4SiO_4 pebbles with a diameter of 500 μm had similar radiation stability as pebbles with diameter <50 μm which were annealed at 1173 K for 128 h in argon and air atmosphere. As well as determined that lithium orthosilicate pebbles with size 500 (1243 K 168 h) and <50 μm (1173 K 128 h) have a higher radiation stability in air and argon atmosphere than pebbles with size <50 μm (1073 K 1 h). Degree of decomposition $\alpha_{10.56}$ of the lithium orthosilicate pebbles at an absorbed dose of 10.56 GGy in air atmosphere is 1.5% and 0.15% at irradiation in dry argon. It has been suggested that changes of radiation stability of lithium orthosilicate pebbles in air atmosphere comparing with irradiated pebbles in argon atmosphere is effect of chemical reaction of lithium orthosilicate surface with air containing – H_2O and CO_2 in irradiation process. As well as it has been suggested that silicon dioxide – lithium metasilicate admixtures do not affect formation mechanism of radiation defect and products of radiolysis in lithium orthosilicate pebbles.

1. Introduction

Lithium orthosilicate pebbles with 2.5 wt% silicon dioxide additions (Li_4SiO_4 + 2.5 wt% SiO_2) with diameters ranging from 250 to 630 μm fabricated by a melt-spraying process have been selected as one of possible breeder materials for the European Helium Cooled Pebble Bed (HCPB) blanket [1,2]. One of the technological problems of a fusion reactor is the change in composition and structure of ceramic breeder pebbles (Li_4SiO_4 or Li_2TiO_3) during long-term operation [3]. Our previous investigations [4] have shown that the concentration of products of radiolysis can reach a few percent during the exposure of lithium orthosilicate blankets to the ionizing radiation. Radiolysis of lithium containing ceramics may lead to changes of micro-particles' surface properties, and as a result, to deterioration of the tritium thermo-extraction parameters, mechanical and thermo-physical properties of ceramics [4]. Moreover, accumulation of radiation defects and products of radiolysis may cause significant changes in the mechanism of radiolysis at high doses and, accordingly, influence tritium release and retention. In addition, small concentration of impurities strongly affects the lithium orthosilicate radiolysis [4].

It must be highlighted that all previous research of radiolysis of lithium orthosilicate was done with "pure" lithium orthosilicate in the range of small absorbed doses (up to 1 GGy) and samples were irradiated at room temperature [4]. Thus the first aim of our research was to estimate the influence of silicon dioxide additions on radiation stability of lithium orthosilicate pebbles, formation of radiation defects and products of radiolysis under action of high (up to 10.6 GGy) absorbed doses of accelerated electrons, high temperatures (up to 578 K) and different atmospheres (air and argon atmosphere). These parameters of irradiation were selected according to the operating conditions of a fusion reactor, in which the blanket materials will be exploited at high temperature of 900–1100 K, under action of high magnetic field 7–10 T and intense neutron radiation of 2.4 MW m^{-2} or 10^{18} neutrons m^{-2} s^{-1} [1,2,5,6].

* Corresponding author. Address: University of Latvia, Institute of Chemical Physics, Kronvalda Blvd. 4, LV-1586, Riga, Latvia. Tel./fax: +371 67033883.
E-mail address: gunta.kizane@lu.lv (G. Kizane).

0022-3115/$ - see front matter © 2012 Published by Elsevier B.V.
http://dx.doi.org/10.1016/j.jnucmat.2012.05.028

Table 1
Characteristics of the investigated pebbles.

No.	Pebble size (μm)	Grain size (μm)	Annealing temperature (K)	Annealing time (h)	Excess of SiO_2, (wt%)
#1	<50	1	1073	1	2.5
#2	<50	5	1173	128	2.5
#3	500 ± 50	10	1243	168	2.5

In the melt-spraying process pebbles with a size from 10 to 1000 μm can be produced and only 50 wt% of all pebbles were with diameter 250–630 μm [7]. At the same time approximately 40% of pebbles were with the diameter less than 250 μm. From economical point of view it would be reasonable to consider use of these pebbles as filler material to reduce space between pebbles with diameter 250–630 μm (packing factor for mono-sized particles is in the range of 63–64% [8]) in the HCPB. Thus second aim of this study was to estimate radiation stability of small pebbles (<50 μm) and compare with the stability of pebbles of 250–630 μm diameter.

To achieve both aims of research three different types of Li_4SiO_4 pebbles (Table 1) with 2.5 wt% silicon dioxide additions were synthesised with the melt-spraying process. Changes in the composition and microstructure of the Li_4SiO_4 pebbles before and after irradiation were investigated by means of electron spin resonance (ESR), thermally stimulated luminescence (TSL), X-ray diffraction (XRD), Fourier transform infrared spectroscopy (FTIR) and chemical methods.

2. Experimental

Lithium orthosilicate pebbles with 2.5 wt% silicon dioxide additions (Li_4SiO_4 + 2.5 wt% SiO_2) were fabricated by a melt-spraying process in a semi-industrial scale facility at Schott AG, Mainz, Germany [9]. For our experiments two type lithium orthosilicate pebbles with diameter <50 μm and 500 μm were selected. While larger pebbles (500 μm) crystallize during cooling, pebbles with diameters smaller than 50 μm solidify amorphously [10]. Pebbles with a diameter of about 500 μm were annealed in order to obtain a homogeneous microstructure. Additionally, pebbles of the same fabrication campaign but with diameters of less than 50 μm were heat treated at different temperatures to achieve crystallization and a microstructure with different mean grain sizes. Characteristics of the investigated samples are summarised in Table 1.

Irradiation of pebbles was performed in quartz tubes in both air and dry argon atmosphere with accelerated 5 MeV electrons at 560 ± 20 K by means of the ELU4 accelerator (Salaspils, Latvia). The dose rate of 24.4 kGy/s was calculated from measured electron flux.

The ESR spectra of the radiation-induced free radicals where recorded by a Bruker BioSpin X-band radiospectrometer operating at 100 kHz field modulation. The XRD spectra were measured by a Bruker D5005 spectrometer (source: Cu Kα, λ = 0.15418 nm, anode current = 40 mA, voltage = 40 kV). FTIR spectroscopy was performed by means of an AVATAR 330 FTIR Thermo Nicolet and BRUKER EQUINOX55 spectrometers. TSL was measured at a heating rate of 2 K/s. The microstructure of the pebbles was investigated at etched cross-sections by field emission scanning electron microscopy (FE-SEM, ZEISS, SUPRA 55).

3. Results and discussion

3.1. Scanning electron microscopy

The microstructure of lithium orthosilicate pebbles with silicon dioxide additions after annealing at etched cross-sections is shown in Fig. 1. The different grain sizes of the samples before irradiation can be seen in the upper row. In samples #2 and #3 lithium orthosilicate is displayed in dark-grey with smaller, light-grey grains of lithium metasilicate as inter- or intra-crystalline inclusions. Because of the small grain size, lithium metasilicate cannot be detected in sample #1. In sample #2 the grains seem to be only loosely connected, and some of the pebbles were already destroyed during

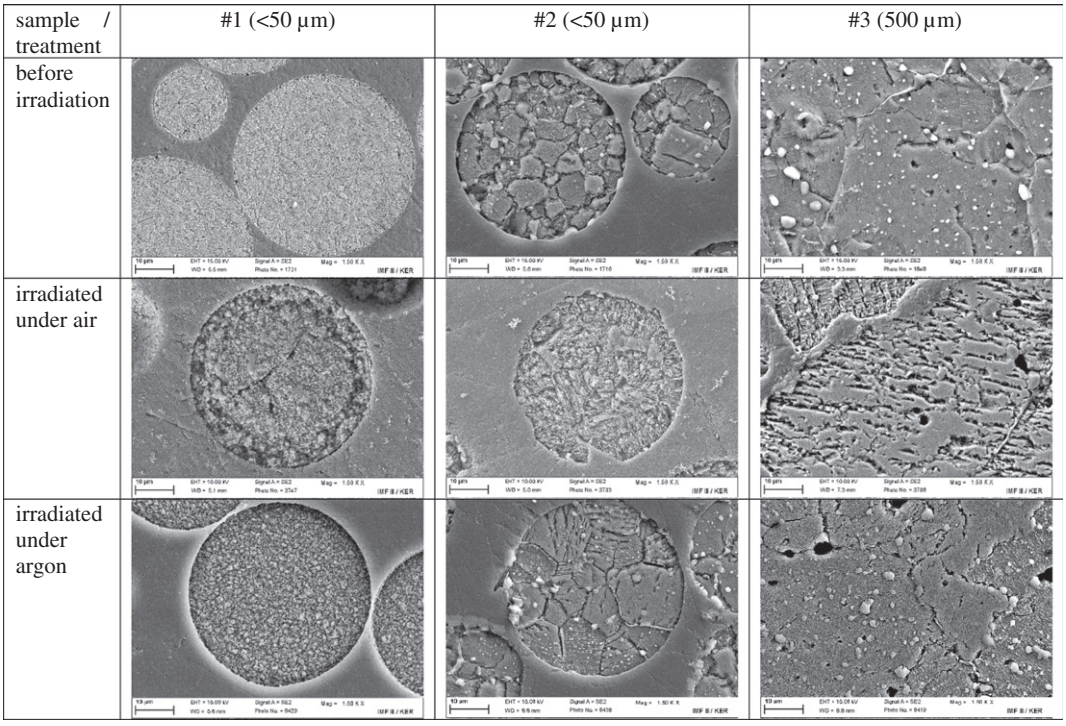

Fig. 1. Microstructure of pebbles at etched cross-sections before and after irradiation with an absorbed dose of 10.56 GGy.

grinding and polishing. This may be caused by an improper heat treatment during crystallization of the previously amorphous pebbles. After irradiation in air, all samples exhibit a fissured microstructure, and the smaller pebbles (samples #1 and #2) nearly appear to be disintegrated (middle row of Fig. 1). Different phases are hardly distinguishable by SEM. But after irradiation in argon, the samples are nearly unchanged (lower row in Fig. 1). The small pebbles seem to exhibit a slightly more porous microstructure with more gaping grain boundaries, but there is hardly any difference in the microstructure of the large pebbles compared to the unirradiated material. The second phase, lithium metasilicate, can also be detected as inter- or intra-crystalline inclusions in samples #2 and #3. As lithium orthosilicate is easily etched with a mixture of water and ethanol in only a few seconds, the preparation of cross-sections is subject to fluctuations. Especially lithium orthosilicate with small grain sizes is rapidly etched too much, so that the appearance of cross-sections may display a corrosion effect and therefore has to be regarded with suspicion. Nevertheless, the samples irradiated under air atmosphere appear to be chemically eroded by possible reactions with air, containing H_2O and CO_2.

3.2. Electron spin resonance spectroscopy

ESR spectra of all investigated samples of pebbles after irradiation with doses up to 10.56 GGy exhibit at least three different lines with *g*-factors of 2.001, 2.011 and 2.016. Those spectra are similar to the ones previously reported for irradiated "pure" Li_4SiO_4 [11] and can be interpreted as superposition of signals from so-called E′ and HC_2 centres (ion radicals SiO_3^{3-} and SiO_4^{3-}, respectively). Ion radical SiO_3^{3-} (HC_2 centre) in ESR spectra is presented with 2 lines ($g_{\perp} = 2.009$ and $g_{\parallel} = 2.016$) due to anisotropy of the *g*-factor. A very weak and board multiplex signal was also observed at ESR spectra of irradiated sample #1. This signal can be attributed to electrons localised in anion or oxygen vacancy (so called F^+ centres). ESR spectra of all three samples irradiated in air atmosphere with a dose of 10.56 GGy contain two symmetric lines with 50.2 mT splitting, typical for localised hydrogen atoms. Beside this, several unidentified lines possibly due to impurities were observed at ESR spectra of samples irradiated with a dose of 10.56 GGy in air atmosphere. Concentrations of stabilised paramagnetic centres in pebbles irradiated with doses from 1 to 5 GGy are in the range of 10^{15}–10^{16} radicals g^{-1} and slightly increase with increasing absorbed dose. Concentration of free radicals stabilised in samples irradiated in dry argon with absorbed doses of less than 2 GGy are significantly higher than in case of samples irradiated in air atmosphere. For samples irradiated in dry argon an increase of the absorbed dose higher than 5 GGy cause a decrease of radicals' concentration. On the other hand, a surprisingly high concentration of stabilised paramagnetic centres (10^{17}–10^{19} radicals g^{-1}) was observed in samples irradiated with a dose of 10.56 GGy in air atmosphere (see Table 2). Thus, in irradiated pebbles the same radiation defects are stabilized that were previously detected in "pure" Li_4SiO_4, but the concentration of stabilized free radicals at doses from 1 to 5 GGy is approximately 2 times higher (ESR measurements of "pure" Li_4SiO_4 irradiated with a dose of 10.56 GGy were not made previously) [11].

3.3. Thermally stimulated luminescence

TSL curves of irradiated lithium orthosilicate pebbles are also similar to the ones previously reported for irradiated "pure" Li_4SiO_4 [11] and contain three maxima at temperatures of 395 ± 25, 438 ± 12 and 500 ± 50 K. In the high temperature region the fourth

Table 2
Characteristics of ESR spectra.

Sample	Atmosphere, dose (GGy)	Radical	*g*-Factor	Splitting (mT)	Concentration, 10^{16} radicals g^{-1}
#1	Air, 1.32	E′	2.0013	None	0.002
		HC2	2.0154; 2.0093	None	0.080
		F^+	2.0022	Unresolved	0.009
#1	Air, 2.64	E′	2.0026	None	0.03
		HC2	2.0157; 2.0108	None	0.07
#1	Air, 5.28	E′	2.0013	None	0.09
		HC2	2.0156; 2.0095	None	0.07
#1	Argon, 5.28	E′	2.00	None	0.9
		HC2	2.015; 2.008	None	9.4
#1	Air, 10.56	E′	2.0011	None	2250
		HC2	2.0154; 2.0069	None	5
		H	2.0023	50.2	1
#1	Argon, 10.56	E′	2.0012	None	25.1
		HC2	2.015; 2.0075	None	1.4
		F^+	2.0022	Unresolved	1
#2	Air, 1.32	E′	2.0018	None	0.02
		F^+	2.0022	Unresolved	0.01
#2	Air, 2.64	E′	2.00	None	0.5
#2	Air, 5.28	E'	2.001	None	2.5
		HC2	2.015; 2.0065	None	0.1
#2	Air, 10.56	E′	2.0015	None	6.5
		HC2	2.015; 2.0085	None	0.4
		H	2.002	50.2	0.1
#2	Argon, 10.56	E′	2.001	None	0.04
		HC2	2.015; 2.0075	None	0.04
#3	Air, 1.32	E′	2.001	None	0.09
		HC2	2.015; 2.005	None	0.01
#3	Air, 2.64	E′	2.001	None	0.03
#3	Air, 5.28	E′	2.001	none	0.39
		HC2	2.015; 2.005	none	0.02
#3	Argon, 5.28	E′	2.001	None	0.3
		HC2	2.015; 2.008	None	0.05
#3	Air, 10.56	E′	2.0013	None	39
		HC2	2.0138; 2.0079	None	12
		H	2.002	50.2	1
#3	Argon, 10.56	E′	2.001	None	0.4

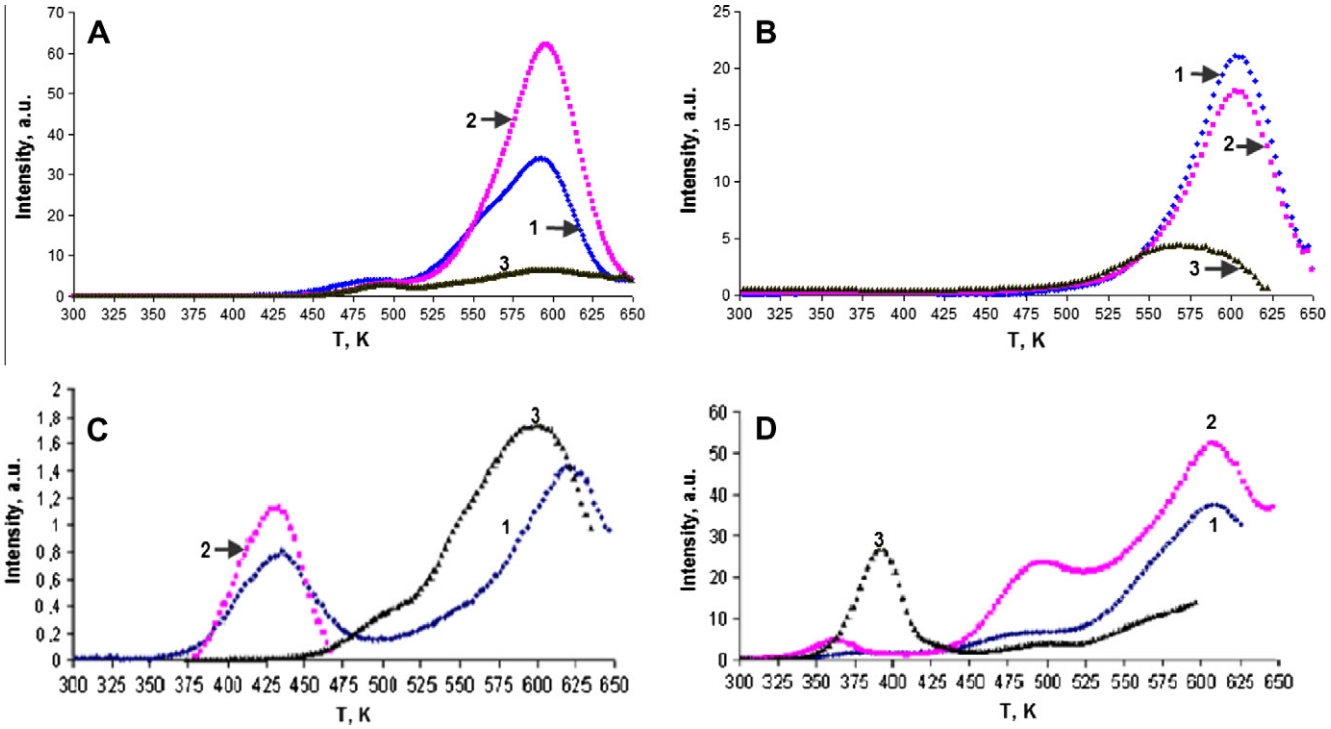

Fig. 2. TSL curves of lithium orthosilicate pebbles after irradiation with doses of 2.64 (A and C) and 10.56 (B and D) GGy in dry argon (A and B) and air (C and D) atmosphere (numbering of curves corresponds to numbers of investigated samples given in Table 1). Curve 3C is decreased 30 times, curve 2D is decreased 3 times.

maximum is observed at 612 ± 38 K (see Fig. 2). The maximum at 500 ± 50 K is unstable and disappears within 60 days after irradiation. The TSL intensity of samples irradiated in dry argon is significantly higher than that for samples irradiated in air atmosphere. In TSL curves of pebbles irradiated in argon the intensities of the maximum in the high temperature region (612 ± 38 K) are higher by factor 10–100 than intensities of other maxima. This may be due to the high temperature (up to 587 K) of irradiation. Beside this, in case of samples irradiated in argon the intensities of the first three maxima (395, 438 and 500 K) strongly decrease with the increasing of absorbed dose, but at the high irradiation doses ($D > 5$ GGy) only the fourth maximum (at 612 K) can be observed. On the other hand in TSL curves of samples irradiated in air atmosphere relatively high intensities of low-temperature peaks (at 400, 440 and 500 K) were observed at dose 10.56 GGy. It might be assumed that this effect is caused by high concentration of impurities (Li_2O, LiOH, Li_2CO_3 and other products of radiolysis) in irradiated samples. An explanation of this phenomenon can only be made after further investigation of post-irradiation processes in irradiated lithium orthosilicate pebbles with silicon dioxide additions. TSL optical spectra of all investigated samples indicate a maximum at 3.5 eV. Only TSL optical spectra of pebbles irradiated with a dose less than 1 GGy have a maximum at 2.9 eV. Both these maxima have previously been observed in TSL and radioluminescence spectra of "pure" Li_4SiO_4 [11]. The luminescence band with the maximum at 3.5 eV is due to exited states of SiO_4^{4-} anions (so called "L-centres", [4]). The origin of the luminescence band with a maximum at 2.9 eV is not yet clear, but it is assumed that it is due to excited states of electrons localised in structure defects (so called "F^+-centres"). Light absorption spectra registered by means of light diffuse refraction spectroscopy have a maximum at 3.0 eV (415 nm).

3.4. X-ray diffraction and Fourier transform infrared spectroscopy

Fig. 3 exemplarily displays the XRD spectra of sample #1 and #3 before and after irradiation at 10.56 GGy. While for sample #3 no change in the phase composition, not even after the irradiation in air could be detected by XRD, the diffraction diagram of sample #1 after irradiation in air exhibits significant amounts of impurities. Due to the large amount of phases, only LiOH, $LiOH{\cdot}H_2O$ and traces of Li_2CO_3 could be verified, however, traces of lithium oxide cannot be ruled out. In samples #1 and #2 irradiated in air atmosphere, a significant increase of the initial concentration of Li_2SiO_3 as well as characteristic lines for LiOH and Li_2CO_3 were detected with both mentioned methods. As the specific surface area of samples #1 and #2 is 1000 times higher than of sample #3, surface reactions with H_2O and CO_2 are significantly increased in samples with a smaller pebble size. Unfortunately it was not possible to determine the concentration of products of radiolysis by means of XRD or FTIR spectroscopy. According to FTIR spectroscopy, in all three samples irradiated in air with a dose of 10.56 GGy the concentration of Li_2SiO_3 formed during irradiation is approximately 1 wt% or 4.5 mol%. On the other hand, the concentration of metasilicate in samples irradiated in argon is practically unchanged. Therefore the degree of radiolysis for samples irradiated in argon atmosphere was determined by means of chemical method, described earlier [4,12]. The obtained concentrations of colloidal lithium and other reducing products of radiolysis and radiation defects were equal to 4.4×10^{19}, 1.2×10^{19}, and 3.1×10^{19} radicals g^{-1} for samples Nos. #1, #2 and #3, respectively. As can be seen from Fig. 1, the microstructure of pebbles irradiated in argon is virtually identical to the microstructure of the corresponding unirradiated sample (except sample #1, where small changes can be observed).

3.5. Discussion

Three different types of Li_4SiO_4 pebbles with 2.5 wt% silicon dioxide additions were investigated – two samples of small pebbles with diameter <50 μm (annealed at 1073 K for 1 h and 1173 K for 128 h) and standard pebbles with diameter 500 ± 10 μm (annealed at 1243 K for 168 h), which were synthesised with melt-spraying process and annealed at different

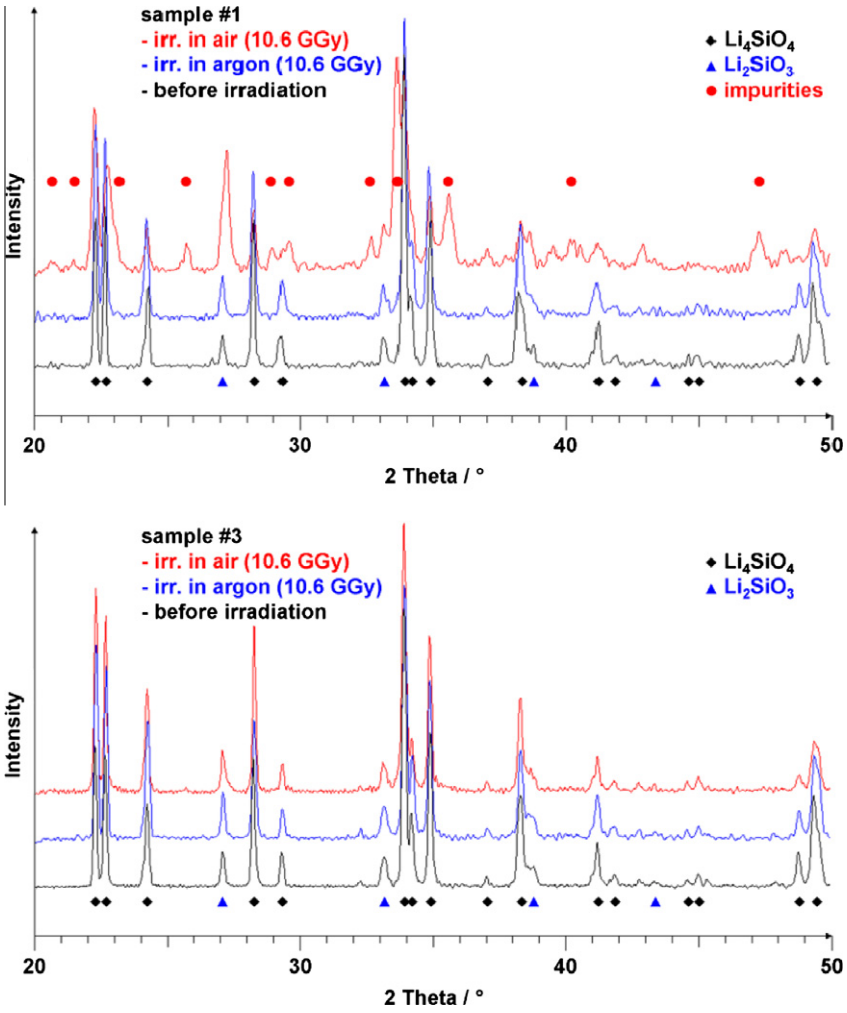

Fig. 3. XRD spectra of sample #1 (top) and sample #3 (below) before and after irradiation with an absorbed dose of 10.56 GGy.

temperature and different time in order to understand radiation stability. All three types of pebbles have a main crystalline phase, lithium orthosilicate (~90%), and a second minor phase, lithium metasilicate (~10%). In the same time only pebbles with a diameter <50 μm (annealed at 1073 K for 1 h) and 500 ± 10 μm (annealed at 1243 K for 168 h) have a homogeneous structure. In pebbles with diameter <50 μm (annealed at 1173 K for 128 h) the grains are only loosely connected.

Under action of accelerated electrons (5 MeV) high absorbed dose (10.56 GGy) and high temperature (560 K) in inert atmosphere structure of all three types of lithium orthosilicate pebbles is nearly unchanged. In both small pebbles (<50 μm) hardly any difference in the microstructure is visible compared to the large (500 ± 10 μm) pebbles. In irradiated Li_4SiO_4 pebbles in inert atmosphere new phases which can be detected with XRD do not form, but at the same time radiation defects form in lithium orthosilicate pebbles – ion radicals SiO_3^{3-} and SiO_4^{3-} and trapped electron in oxygen vacancy and products of radiolysis – colloidal lithium and Li_2SiO_3. Thus it can be concluded that silicon dioxide additions – lithium metasilicate, do not affect formation mechanism of radiation defect and products of radiolysis in lithium orthosilicate pebbles. Similar to the results reported for the chemical methods, FT-IR and XRD for irradiated Li_4SiO_4 pebbles with 2.5 wt% SiO_2 additions are in a good agreement with the assumption that radiolysis of Li_4SiO_4 can be described by the following summary equation:

$$Li_4SiO_4 \rightarrow 2Li + Li_2SiO_3 + 1/2O_2.$$

Total concentration of ion radicals in small lithium orthosilicate pebbles (<50 μm, 1073 K for 1 h) is 27.5×10^{16} radicals g^{-1}, but in larger pebbles (500 μm, 1243 K for 168 h) only 0.4×10^{16} radicals g^{-1}. Thus it can be concluded that pebbles with diameter <50 μm which are annealed at 1073 K for 1 h are radiation unstable comparing with pebbles with diameter 500 μm in air atmosphere.

In same time it should be highlighted that under action of accelerated electrons in small pebbles (<50 μm) which are annealed at 1173 K for 128 h total concentration of radiation defects reduces to 0.08×10^{16} radicals g^{-1}. Thus concentration of ion radicals is much more less than in pebbles with diameter 500 μm.

Thus it can be concluded that pebbles with diameter <50 (1173 K 128 h) and 500 μm (1243 K 168 h) have similar radiation stability in argon atmosphere., but pebbles with diameter <50 μm (1073 K 1 h) – has less stability. These results of small pebbles (<50 μm, 1073 K 1 h) can be explained by structural defects which form at melting-spray synthesis, but thermal treating of these pebbles at 1173 K temperature for 128 h reduces concentration of structural defects and increases radiation stability of pebbles.

Both high absorbed dose (10.56 GGy) and high temperature (560 K) changes radiolysis of lithium orthosilicate pebbles with SiO_2 admixes under action of air atmosphere – in all three types of pebbles more or less structure has been changed after irradiation. As well as comparing in air atmosphere irradiated pebbles with argon atmosphere irradiated pebbles observes higher concentration of radiation defects and products of radiolysis. Total

concentration of ion radicals 0.4×10^{16} radicals $g^{-1}$is much more less, for the largest pebbles (500 ± 10 μm) irradiated in argon atmosphere as for pebbles irradiated in air atmosphere. In this case total concentration of ion radicals increases substantially up to 52×10^{16} radicals g^{-1}. Fast change of radiation stability of lithium orthosilicate pebbles can be explained by chemical reaction of lithium orthosilicate with air containing substances – H_2O and CO_2 in irradiation process [13–15]:

$$Li_4SiO_4 + H_2O \leftrightarrow 2LiOH + Li_2SiO_3 \quad \text{or} \quad Li_4SiO_4 + CO_2 \leftrightarrow Li_2CO_3 + Li_2SiO_3.$$

This suggestion confirms the results of the spectra of FT-IR and XRD of irradiated pebbles in air atmosphere. Traces of LiOH, Li_2CO_3 and lithium metasilicate can be observed. Similarly, the formation of water chemisorption products in lithium orthosilicate pebbles with silicon dioxide additions indicates atomic hydrogen which can be observed in ESR spectra of pebbles, irradiated in air atmosphere [13]:

$$\equiv Si{-}OLi + H{-}OH \leftrightarrow \equiv Si{-}OH + Li{-}OH$$

$$LiOH \leftrightarrow LiO^{\cdot} + {}^{\cdot}H \text{ or } \equiv Si{-}OH \leftrightarrow \equiv Si{-}O^{\cdot} + {}^{\cdot}H$$

Water and carbon dioxide chemisorption products – lithium hydroxide and lithium carbonate are radiation unstable compounds and admixing of these compounds can affect radiation stability changes of lithium orthosilicate pebbles in air atmosphere under action of high absorbed doses and high temperature.

Formation of LiOH and Li_2CO_3 may significantly be increased by surface reactions, especially for pebbles with small diameters and large surface areas [15]. Specific surface of small pebbles (<50 μm) is ~100 times higher than for pebbles with "normal" diameter (500 μm). By that in small pebbles (<50 μm) under irradiation in air atmosphere changes of structure and composition are grater than in pebbles with "normal" diameter (500 μm).

For example the total concentration of ion radicals in small pebbles (<50 μm) annealed 1073 K for 1 h is 22.56×10^{18} radicals g^{-1}, but for large pebbles with diameter 500 μm (annealed 1243 K for 168 h) is only 0.52×10^{18} radicals g^{-1}. At same time the total concentration of radiation defects in small pebbles which are annealed at 1173 K for 128 h is considerably smaller – 0.07×10^{18} radicals g^{-1}. Thus it can be concluded that pebbles with diameter <50 μm (1073 K 1 h) in air atmosphere are radiation unstable but pebbles with diameter <50 (1173 K 128 h) and 500 μm (1243 K 168 h) in air atmosphere are more radiation stable.

It highlighted that the degree of decomposition $\alpha_{10.56}$ of the lithium orthosilicate matrix at an absorbed dose of 10.56 GGy calculated from estimated concentration of radiolytic lithium metasilicate is approximately equal to 1.5% for irradiation in air atmosphere and 0.15% for irradiation in dry argon. This is significantly lower than the value $\alpha_{10.56} \approx 5\%$ calculated on base of empiric equation [4]:

$$\alpha_D(\%) \approx 5 \times 10^{-2} \cdot D^{0.5}$$

where D is absorbed dose, MGy.

Comparison of the obtained data of investigated pebbles allow to conclude that the lithium orthosilicate pebbles (Li_4SiO_4 + 2.5 wt% SiO_2) with size 500 μm (1243 K 168 h) and <50 μm (1173 K 128 h) have a higher radiation stability in air and argon atmosphere than pebbles with size <50 μm (1073 K 1 h), but comparison of the obtained date for pebbles with a diameter of 500 μm, which represent the potential material for the European test blanket module, have similar radiation stability with pebbles with diameter <50 μm which are annealed at 1173 K for 128 h in argon and air atmosphere.

4. Conclusions

Lithium orthosilicate pebbles (Li_4SiO_4 + 2.5 wt% SiO_2) with size 500 μm (1243 K 168 h) and <50 μm (1173 K 128 h) have a higher radiation stability in air and argon atmosphere than pebbles with size <50 μm (1073 K 1 h). Li_4SiO_4 pebbles with a diameter of 500 μm have similar radiation stability with pebbles with diameter <50 μm which are annealed at 1173 K for 128 h in argon and air atmosphere. Radiation stability of Li_4SiO_4 pebbles depend on both diameter that is connected with grain size and thermal treatment temperature. The degree of decomposition $\alpha_{10.56}$ of the lithium orthosilicate pebbles with silicon dioxide addition at an absorbed dose of 10.56 GGy in air atmosphere is 1.5% and 0.15% for irradiation in dry argon. It has been suggested that changes of radiation stability of lithium orthosilicate pebbles in air atmosphere comparing with irradiated pebbles in argon atmosphere is effect of chemical reaction of lithium orthosilicate surface with air containing substances – H_2O and CO_2 in irradiation process. It has been suggested that silicon dioxide – lithium metasilicate admixtures do not affect the formation mechanism of radiation defect and products of radiolysis in lithium orthosilicate pebbles.

References

[1] M. Zmitko, Y. Poitevin, L. Boccaccini, J.-F. Salavy, R. Knitter, A. Möslang, A.J. Magielsen, J.B.J. Hegeman, R. Lässer, J. Nucl. Mater. 417 (2011) 678–683.
[2] Y. Poitevin, L.V. Boccaccini, M. Zmitko, I. Ricapito, J.-F. Salavy, E. Diegele, F. Gabriel, E. Magnani, H. Neuberger, R. Lässer, L. Guerrini, Fusion Eng. Des. 85 (2010) 2340–2347.
[3] A. Zarins, A. Supe, G. Kizane, R. Knitter, I. Reinholds, A. Vitins, V. Tilika, A. Actins, L. Baumane, Sci. J. Riga Tech. Univ. Mater. Sci. Appl. Chem. 22 (2010) 100–104.
[4] J.E. Tiliks, G.K. Kizane, A.A. Supe, A.A. Abramenkovs, J.Y. Tiliks, V.G. Vasiljev, Fusion Eng. Des. 17 (1991) 17–20.
[5] A. Vītiņ, G. Ķizāne, J. Tīliks, J. Tīlks Jr., Fusion Eng. Des. 82 (2007) 2341–2346.
[6] Y. Poitevin, L.V. Boccaccini, A. Cardella, L. Giancarli, R. Meyder, E. Diegele, R. Lasser, G. Benamati, Fusion Eng. Des. 75–79 (2005) 741–749.
[7] R. Knitter. P. Risthaus, in: R. Knitter (Ed.), Proceedings of the 12th International Workshop on Ceramic Breeder Blanket Interactions, CBBI-12, Wissenschaftliche Berichte, FZKA 7078, 2004, p. 129.
[8] J. Reimann, R. Knitter, G. Piazza, New compilation of the material data base and the material assessment report, Technical Report, 2005.
[9] R. Knitter, B. Löbbecke, J. Nucl. Mater. 361 (2007) 104–111.
[10] R. Knitter, B. Alm, G. Roth, J. Nucl. Mater. 367–370 (2007) 1387–1392.
[11] A. Abramenkovs, J. Tiliks, G. Kizane, S. Tanaka, A. Supe, V. Grishmanov, Fusion Technol. Lisbon 2 (1996) 1507.
[12] J. Tīliks, G. Ķizāne, A. Vītiņš, B. Leščinskis, Nanostructured ceramic blanket materials, in: A. Ying, P. Calderoni (Eds.), Proceedings of the 13th International Workshop on Ceramic Breeder Blanket Interactions, Fusion Science and Technology Center, University of California, Los Angeles, CA, USA, 2006, p. 140.
[13] J. Ortiz-Landeros, L. Martínez-dlCruz, C. Gómez-Yáñez, H. Pfeiffer, Thermochimica Acta 555 (2011) 73–78.
[14] M. Kato, S. Yoshikawa, K. Nakagava, J. Mater. Sci. Lett. 21 (2002) 485–487.
[15] T. Okumura, Y. matsukura, K. Gotou, K. Oh-ishi, J. Ceram. Soc. Jpn. 116 (12) (2008) 1283–1288.